**PHD**

# An investigation into the role of iron homeostasis during the pathogenic and mutualistic interactions of Photorhabdus

Watson, Robert James

*Award date:*
2007

*Awarding institution:*
University of Bath

# An investigation into the role of iron homeostasis during the pathogenic and mutualistic interactions of *Photorhabdus*

Robert James Watson

For the degree of Doctor of Philosophy

University of Bath
Department of Biology and Biochemistry

September 2007





ProQuest LLC
789 East Eisenhower Parkway
P.O. Box 1346
Ann Arbor, MI 48106-1346

# Table of contents

**Chapter 2**

## Abstract

*Photorhabdus* spp. is a genus of bacteria found colonising the gut of a specialised stage of the nematode, *Heterorhabditis*, called the infective juvenile (IJ). The IJ is a free-living stage of the nematode that seeks out and infects insect larvae. Once inside the insect the IJs release *Photorhabdus* into the hemolymph where the bacteria rapidly proliferate, killing the insect within 48-72h. The nematodes grow and reproduce in the insect cadaver by feeding on the *Photorhabdus* biomass. *Photorhabdus* participates in both pathogenic and mutualistic interactions within its natural lifecycle and this study set out to identify the role of iron within the lifecycle. The importance of iron acquisition has been demonstrated for many important pathogens, however its role in beneficial interactions has not been so well studied. This study has shown that *exbD* mediated iron uptake is responsible for full virulence and symbiosis in *P. temperata* K122 and is required for virulence in *P. luminescens* TT01. However the TT01 *exbD* mutant was able to support nematode growth and development suggesting that the requirement for iron uptake was different in different bacteria-nematode complexes. Genes predicted to be involved in iron acquisition were identified in the sequenced genome of TT01 and these genes were deleted. However none of these mutants had any defect on either pathogenicity or mutualism. Nonetheless the addition of low levels of the iron chelator 2,2'-dipyridyl to the growing *Photorhabdus* bacteria resulted in a complete absence of nematode growth and development suggesting that iron levels are critical for nematode development. Proteomic analysis of *Photorhabdus* grown under these conditions has revealed the presence of iron regulated proteins which are potentially involved in the interaction with the nematode.

## Publications

**Watson, R.J., Spencer, G.V., Joyce, S.A. and Clarke, D.J.** 2005 The *exbD* gene of *Photorhabdus temperata* is required for full virulence in insects and symbiosis with the nematode *Heterorhabditis*. Molecular Microbiology 56(3), 763–773.

**Joyce, S.A., Watson R.J. and Clarke, D.J.** 2006 The regulation of pathogenicity and mutualism in *Photorhabdus*. Current Opinion in Microbiology. 9(2), 127-132.

## Abbreviations

| | |
|---|---|
| °C | Degrees Celsius |
| µl | Microlitre |
| Amp | Ampicillin |
| CAMP | Cationic antimicrobial peptides |
| CAS | Chrome Azurol S |
| Cfu | Colony forming unit |
| Cm | Chloramphenicol |
| CTAB | Cetyl Trimethyl Ammonium Bromide |
| DIP | 2,2'-dipyridyl |
| DNA | Deoxyribosenucleic acid |
| dNTP | Deoxynucleotide 5'-triphosphate |
| EMB | Eosin methylene blue |
| $Fe^{2+}$ | ferrous iron |
| $Fe^{3+}$ | ferric iron |
| Fig. | Figure |
| g | Gram |
| GFP | Green fluorescent protein |
| h | Hour |
| IJ | Infective Juvenile |
| Km | Kanamycin |
| Kv | Kilovolts |
| K122 | *P. temperata* K122 Rif |
| LB | Luria-Bertani medium |
| $LT_{50}$ | Lethal time for 50% insect death |
| M | Molar |
| mFd | Microfarad |
| mg | Milligram |
| ml | Millilitre |
| mM | Millimolar |
| mm | Millimetre |
| NCBI | National Center for Biotechnology Information |

| | |
|---|---|
| NRPS | Non ribosomal peptide synthase |
| OD | Optical density |
| ORF | Open reading frame |
| O/N | Overnight culture |
| PBS | Phosphate buffered saline |
| PCR | Polymerase Chain Reaction |
| pH | $-\log_{10}[H^+]$ |
| PPTase | 4'phosphopantetheinyl transferase |
| Rif | Rifampicin |
| Rpm | Revolutions per minute |
| SDS | Sodium dodecyl sulphate |
| TAE | Tris-acetate-EDTA |
| Tf | Transferrin |
| Tn | Transposon |
| TT01 | *P. luminescens* TT01 Rif |
| UV | Ultra violet |
| V | Volts |
| ybt | Yersiniabactin siderophore |

## Acknowledgements

Firstly, I would like to thank my supervisor Dr David Clarke for his continued support through the entire duration of my PhD. I must also thank him for the opportunity he gave to me as a young graduate in order to fulfil my ambitions to gain a PhD. I would also like to thank everyone in the Clarke Lab (Catherine, Helen, Hilton, Jane, Yahui, Lionel, Itamar, Anat), both past and present for their support, advice and encouragement. A big thank you must go to Susie who helped me through many scientific quandaries and for her help and advice.

I would also like to thank my parents, Colin and Lynda who without their continued support over the many years I would have been unable to undertake this degree. I must also mention my Sister who has shown great enthusiasm for all of my scientific quests and for the opportunity to talk to her school class, the children were really inspiring.

Lastly, and certainly not least, a massive thank you must go to my wife Rebecca. They say behind every good man is a good woman and that is certainly the case here. Her unabated support over the last 4 years has been immense and I owe her a huge gratitude.

I would also like to thank the University of Bath and the BBSRC as their facilities and funding over the last 3 years has enabled me to carry out my research.

# Chapter 1

# An investigation into the role of iron homeostasis during the pathogenic and mutualistic interactions of *Photorhabdus*

## 1.1 General Introduction

### 1.1.1 *Photorhabdus*

*Photorhabdus*, is a genus of Gram-negative bacteria from the family Enterobacteriaceae (Poinar *et al.*, 1980). Notably *Photorhabdus* is the only known bioluminescent genus of bacteria that does not have a marine origin. Several species of *Photorhabdus* have been identified by molecular analysis: *Photorhabdus luminescens*, *Photorhabdus temperata* and *Photorhabdus asymbiotica* (Fischer-Le Saux et al., 1999). *P. luminescens* and *P. temperata* have been identified as possessing complex lifecycles that involve pathogenic interactions with insect larvae and symbiotic interactions with nematodes from the family *Heterorhabditis*. *P. asymbiotica* is an emerging human pathogen that was originally identified as the causative agent of infections of humans in Australia, the USA and the Far East (Akhurst *et al.*, 2004; Farmer *et al.*, 1989; Gerrard *et al.*, 2004; Weissfeld *et al.*, 2005). *P. asymbiotica* was considered not to have an interaction with a nematode partner (hence the name) however, a nematode partner was recently identified for *P. asymbiotica* implying that all of the *Photorhabdus* species are involved in a complex lifecycle with *Heterorhabditis* nematodes (Gerrard *et al.*, 2006).

### 1.1.2 Life cycle

The lifecycle begins and ends with *Photorhabdus* bacteria colonising the gut of the non-feeding infective juvenile (IJ) stage of the *Heterorhabditis* nematode (Fig. 1.1). Infective juveniles are a specialised stage of the nematode designed for survival and dispersal in the soil. The IJs seek out and infect susceptible insect larvae by either directly penetrating the cuticle or gaining access though

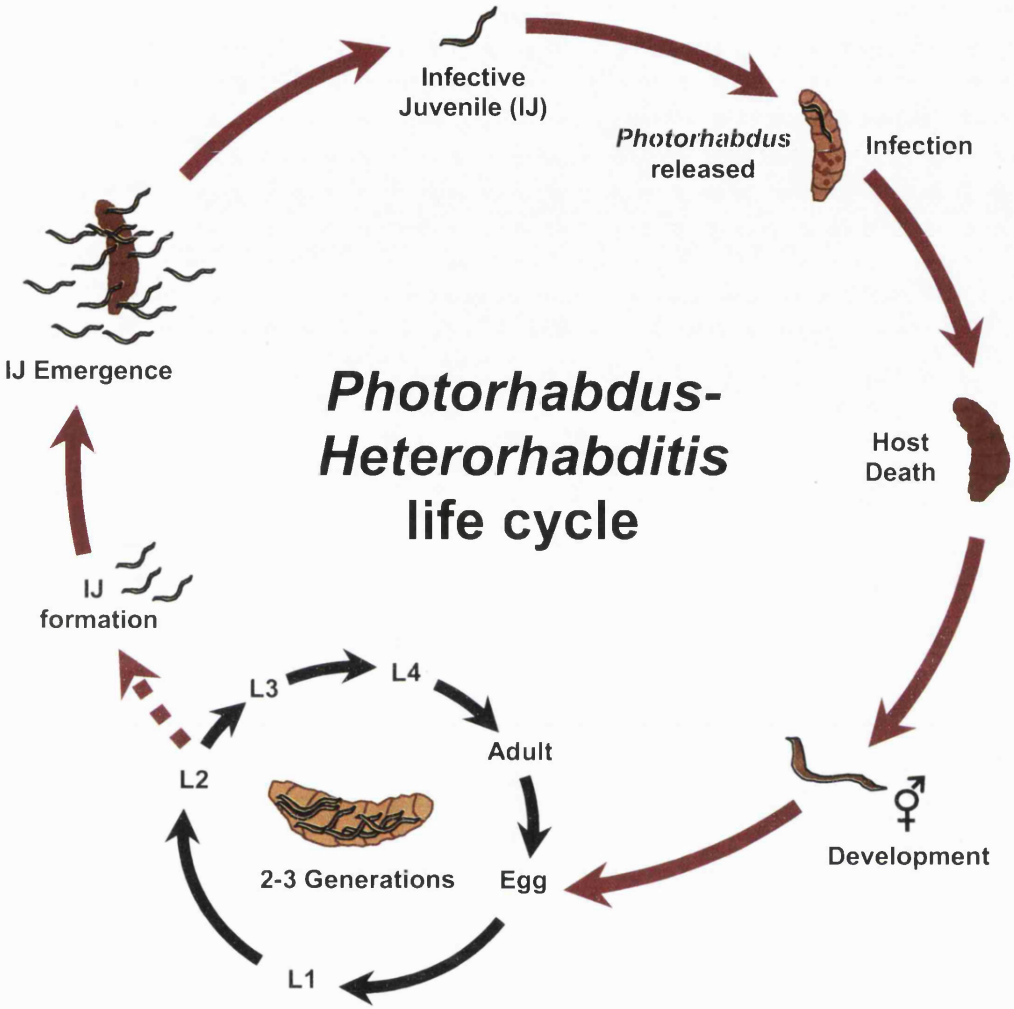


**Figure 1.1.** The *Photorhabdus-Heterorhabditis* lifecycle.

natural openings such as the spiracles, mouth or anus. Upon entry into the insect the IJ migrates to the insect hemolymph (blood) where the *Photorhabdus* bacteria are regurgitated (Ciche and Ensign, 2003). Death of the insect occurs within 48-72 h following the exponential growth of the *Photorhabdus*. At this stage (i.e. post-insect death) the insect has been bioconverted into a nutrient soup containing a high density of *Photorhabdus* biomass. This bioconversion is facilitated by the secretion of proteases and other tissue degrading enzymes by the bacteria (Daborn *et al.*, 2001). The IJ nematode develops into a self-fertile hermaphrodite nematode in a process known as recovery. The hermaphrodites lay eggs and these eggs develop through the larval L1-L4 stages into male and female adults by feeding on the *Photorhabdus* biomass in the insect cadaver. Nematode reproduction continues for two or three generations until the nematodes have fully exploited the host resources. At this point the developing L2 larvae are stimulated to undergo an alternative development pathway to form the IJ nematodes. Crucially the *Photorhabdus* must recolonise the IJ nematode gut before the mouth and anus become sealed and the IJs emerge from the cadaver in search of a new host. *Heterorhabditis* nematodes which are free of *Photorhabdus* are unable to kill insect larvae demonstrating the strict interdependence of these two partners (Han and Ehlers, 2000). The colonised IJs then disperse through the soil in search of a new host to infect (for recent reviews see (Goodrich-Blair and Clarke, 2007; Joyce *et al.*, 2006)).

Under optimal conditions in the laboratory the lifecycle of the *Photorhabdus-Heterorhabditis* complex, from infection to emergence, takes approximately 3 weeks and a single IJ infecting the insect results in several hundred thousand IJs emerging from the insect host after the life-cycle is complete. Therefore, it is clear there is a highly evolved and successful mutualistic interaction between *Photorhabdus* and *Heterorhabditis*.

### 1.1.3 Pathogenicity

Once inside the hemolymph, *Photorhabdus* must evade the insect immune system and multiply rapidly to kill the insect larvae. The innate immune system of the insect consists of both cellular and humoral responses that are stimulated

upon recognition of invading micro-organisms by host recognition receptors (Lemaitre and Hoffmann, 2007). Cellular immunity includes the circulation of blood cells (hemocytes) in the insect blood system (hemolymph) that recognise invading microbes and recruit other haemocytes to encapsulate the offending organsim. The capsule is melanised by the action of the phenoloxidase enzyme that is released from the haemocytes. The micro-organism is trapped in the blackened melanised capsule and is removed from circulation (Kanost *et al.*, 2004; Lemaitre and Hoffmann, 2007). Phagocytosis is a component of the cellular response and plasmatocytes in *Drosophila* are responsible for the engulfing and disposal of microbial pathogens (Lemaitre and Hoffmann, 2007). The humoral response includes the production of a wide range of cationic antimicrobial peptides (CAMP) by the insect fat body that can target a wide range of microbes and can permeabilise bacterial membranes (Imler and Bulet, 2005; Nappi and Ottaviani, 2000). Therefore, insects possess a complex immune system which *Photorhabdus* must overcome. *Photorhabdus* are highly virulent with some strains exhibiting $LD_{50}$ values of just 1 bacterium per insect (Clarke and Dowds, 1995). This level of virulence is remarkable given that the insect innate response is able to clear an infection of $>10^6$ cfu of *E. coli* (Goodrich-Blair and Clarke, 2007). Therefore, it would be expected that *Photorhabdus* is able to avoid detection by the insect immune system or can secrete effectors in order to suppress it. *Photorhabdus* appears to favour the latter approach as the immune system of *Manduca sexta* insects has been shown to up regulate genes encoding microbial recognition proteins upon injection of *Photorhabdus* bacteria into the hemolymph (Eleftherianos *et al.*, 2006). Recently a stilbene antibiotic produced by *Photorhabdus* has been discovered which is able to inhibit the phenoloxidase response of the immune system and a *Photorhabdus* mutant which is unable to produce the antibiotic is severely attenuated in the insect host (Eleftherianos *et al.*, 2007). *P. luminescens* also encodes a functional type three secretion system (TTSS) which secretes a homologue of YopT from *Y. pestis*, LopT. YopT protects *Y. pestis* by inhibiting phagocytosis by macrophages and *Photorhabdus* LopT has also been shown to prevent phagocytosis by insect immune cells, although a TTSS mutant is not affected in *Photorhabdus* virulence (Brugirard-Ricaud *et al.*, 2005). *In silico* analysis of the *P. luminescens* TT01 genome has also revealed many toxin encoding regions (Duchaud *et al.*, 2003). Several of

these toxins have been studied including the Tc toxin complex (Blackburn *et al.*, 1998; Waterfield *et al.*, 2001), Mcf toxins (Daborn *et al.*, 2002; Dowling *et al.*, 2004; Waterfield *et al.*, 2003), and Txp40 toxin (Brown *et al.*, 2006). These toxins have been shown to act by targeting the midgut cells of the insect and Mcf1 has been shown to induce apoptosis of the midgut epithelium and insect phagocytes (Dowling *et al.*, 2007). Therefore, these toxins may further act to depress the immune response of the insect and allow *Photorhabdus* growth. *Photorhabdus* has also been shown to produce two further toxins, PirA and PirB which were not toxic when expressed individually, however when expressed or mixed together they show insecticidal activity against *Galleria mellonella* insect larvae (Waterfield *et al.*, 2005). *Photorhabdus* has been shown to secrete hemolysin that is an extracellular toxic protein that can cause cell lysis. Transcription of the hemolysin operon, *phlBA* was observed in insect hemolymph before death, however a *phlA* mutant was fully virulent. Therefore PhlA is not a major virulence factor under the conditions studied (Brillard *et al.*, 2002). A protease has also been investigated for its role in *Photorhabdus* virulence. The PrtA protease was found to be expressed late in insect infection just before insect death and purified PrtA protease was not toxic to insects. Together this data has led the authors to suggest that PrtA is not a major virulence factor and may be involved in bioconversion of the insect host instead (Bowen *et al.*, 2003; Daborn *et al.*, 2001). Moreover toxin activity appears to be redundant in *Photorhabdus* due to the fact that, despite the high number of potential toxins encoded in the genome, no single toxin appears to be essential for pathogenicity.

All of these virulence factors must be co-ordinately expressed in order to elicit a successful pathogenic attack against the insect larvae. The PhoP-PhoQ two-component regulatory system has been identified as essential for *Photorhabdus* virulence (Derzelle *et al.*, 2004b). This signalling pathway was shown to regulate $Mg^{2+}$ dependent modifications in lipopolysaccharides (LPS) and control gene expression from the *pbgPE* locus required for the synthesis and incorporation of 4-aminoarabinose into the 4'-terminal phosphate of lipid A (Derzelle *et al.*, 2004b). Interestingly a mutant with an insertion in the *pbgE1* gene was severely attenuated for virulence in *G. mellonella* insect larvae (Bennett and Clarke,

2005). Therefore, it appears that the pathogenicity defect of the *ΔphoP* mutant is due to the inability to sense the environment and activate transcription of the *pbgPE* operon. Modification of LPS is involved in adaptation to the innate immune response and both of these mutants show increased sensitivity to CAMPs (Bennett and Clarke, 2005; Derzelle *et al.*, 2004b). Quorum sensing has also been implicated in virulence and disruption of *luxS*, encoding the gene responsible for the production of AI-2, resulted in decreased virulence against *Spodoptera littoralis* insects (Krin *et al.*, 2006). The *luxS* mutant was shown to be altered in the expression of 221 genes compared to the wild type the genes and pathways that were depressed in this mutant are; biofilm formation, the cytotoxic protein CcdB, insecticidal toxin *tcdA1*, phage related proteins and resistance to oxidative stress (Krin *et al.*, 2006). However, with such a large number of genes which show altered expression levels the exact reasons for the virulence attenuation remain to be discovered. Interestingly in *E. coli* a *luxS* mutant is altered for cellular metabolism which affects the production of AI-3, a signalling molecule that has been shown to be required for virulence gene expression in *E. coli* and consequently leads to decreased virulence (Walters *et al.*, 2006). Therefore, a *luxS* mutation may cause many pleiotropic effects.

### 1.1.4 Nematode growth and development

After the insect has been killed *Photorhabdus* must be able to support nematode growth and development. *Photorhabdus* exploits the nutrients in the insect cadaver and produces bacterial biomass on which the nematodes feed and develop. The essential nature of the *Photorhabdus* for nematode growth and development has been demonstrated by infecting *G. mellonella* insect larvae with axenic *Heterorhabditis* nematodes. The nematodes were unable to kill the insect and they could not develop beyond the L1 stage i.e. the nematodes were able to use their internal lipid reserves to recover from the IJ into a hermaphrodite which laid eggs that hatched but could not continue to develop (Han and Ehlers, 2000). *Heterorhabditis* nematodes can be readily grown *in vitro* on lawns of *Photorhabdus* bacteria that have been cultured on nutrient agar plates that are supplemented with a source of cholesterol. The nematodes can also be grown,

with limited success, in liquid medium inoculated with *Photorhabdus* (Strauch and Ehlers, 1998). The relationship between the bacteria and nematode is highly specific and growth and development of the nematode will only normally occur with its cognate *Photorhabdus* partner or a very close relative (Gerrard *et al.*, 2006; Gerritsen and Smits, 1997; Gerritsen *et al.*, 1998). This suggests that the nutrients required by the developing nematodes must be provided by the *Photorhabdus* biomass. During stationary phase growth, *Photorhabdus* produces two crystalline inclusion proteins encoded by the *cipA* and *cipB* genes which appear to play an important role in nematode nutrition and can account for up to 40 % of the total cell protein content (Bowen and Ensign, 2001). Deletion of either *cipA* or *cipB* resulted in a strain which could no longer support nematode growth and development, however these mutants also showed pleiotropic effects, such as loss of bioluminescence which has made the exact role of these proteins unclear (Bintrim and Ensign, 1998). In support of the role of the Cip proteins in nutrition, expression of either CipA or CipB from *E. coli* was able to enhance the growth and development of *Steinernema* nematodes (You *et al.*, 2006). The nutritional value of the *Photorhabdus* is not the only important factor in mediating nematode growth and development. Nematodes will only develop on viable *Photorhabdus* which suggests that an active component is required to establish nematode growth and development (Glazer, I and Clarke, D.J. Unpublished data). The requirement for viable *Photorhabdus* suggests that a signal or series of signals may be needed to ensure nematode development (Strauch and Ehlers, 1998). Characterisation of *P. luminescens* culture supernatants has revealed at least 2 compounds which promote nematode recovery, however the exact nature of these 'food' signals remain to be determined (Aumann and Ehlers, 2001). Interestingly a transposon insertion in the *ngrA* gene of *Photorhabdus luminescens* NC19 resulted in a strain that was unable to support the recovery of the IJ into fertile hermaphrodites (Ciche *et al.*, 2001). The *ngrA* gene encodes a 4'phosphopantetheinyl transferase (PPTase) which is essential for the production of small bioactive molecules including the catechol siderophore photobactin and the stilbene antibiotic (Ciche *et al.*, 2001; Gehring *et al.*, 1997). In a follow-up investigation photobactin was shown to play no role in the nematode recovery and growth deficiency (Ciche *et al.*, 2003). Therefore, the possibility remains that a molecule, which relies on the PPTase

encoded by *ngrA,* is required as a signal to initiate nematode growth and development. A potential target for these signals has been identified by deletion of the ASJ chemosensory neuron from *Heterorhabditis* IJs by laser ablation. Removal of this neuron prevents IJ recovery when grown on *Photorhabdus* bacteria (Hallem *et al.*, 2007). The ASJ receptors have previously been identified as necessary for nematode recovery in *C. elegans* and the human parasitic nematode *Strongyloides stercoralis* (Ashton *et al.*, 2007; Bargmann and Horvitz, 1991). Therefore, the signals produced by *Photorhabdus* may act through the ASJ chemosensory neurons in *Heterorhabditis.*

Nematode growth and development takes place after the insect has died. Therefore, the post-exponential growth phase of *Photorhabdus* is associated with mutualism (ffrench-Constant *et al.*, 2003). It is notable that during post-exponential growth *Photorhabdus* produces a number of phenotypes and activities such as bioluminescence, antibiotic secretion, pigmentation, lipase and protease activity that, therefore, might be associated with mutualism. These phenotypes are called the primary-specific factors or symbiosis factors (see Section 1.1.6 below). The transcriptional repressor, HexA, appears to co-ordinately repress the expression of these symbiosis factors during exponential growth (Joyce and Clarke, 2003). Interestingly a HexA mutant is also significantly attenuated in virulence suggesting that HexA may play an important role in the regulation of the transition between pathogenicity and mutualism (Joyce and Clarke, 2003; Joyce *et al.*, 2006).

### 1.1.5 Nematode colonisation

At the end of the nematode growth and development *Photorhabdus* bacteria need to successfully colonise the gut of the developing IJ population to ensure their continued transmission to a new host and the successful propagation of the lifecycle. Relatively little is known about this aspect of *Photorhabdus-Heterorhabditis* interaction, however one locus has been identified which is essential for colonisation of the nematode gut. A mutation in the *pbgE1* gene of *P. luminescens* resulted in a strain that could not colonise the nematode gut. This mutant was unable to synthesise O antigen in its LPS and the mutant was shown

to be more susceptible to the CAMP, polymyxin B and was unable to grow under acid stress (Bennett and Clarke, 2005).

Whilst the growth and development of a specific nematode will only occur on a few closely related species of *Photorhabdus*, recolonisation is even more stringent with only the cognate partner being able to colonise the IJ gut (Han and Ehlers, 1998). For example mixing two closely related strains of *Photorhabdus* will result in only the cognate strain being able to re-colonise the nematode. Very little is known about how this degree of specificity is achieved. Recently a study used microarrays to look for differences in the genomes of different strains of *Photorhabdus*: *P. temperata* X1Nach associated with *H. megidis* nematodes and both *P. luminescens* TT01 and *P. temperata* C1 that are associated with *H. bacteriophora* nematodes. The purpose of this study was to identify regions of DNA that were unique to each species and in this way identify regions of genomic DNA that confer specificity to the nematode – bacteria interaction. This study revealed 31 loci which are missing from X1Nach compared to TT01 which suggests that these regions may be involved in the specific interaction with *H. bacteriophora* nematodes (Gaudriault *et al.*, 2006) These loci include potential fimbrial operons which may be involved in controlling the specific interaction between *Photorhabdus* and the nematode.

### 1.1.6 Phenotypic variation

*Photorhabdus* can be cultured in two distinct forms, the primary variant and the secondary variant. The primary variant is characterised by the expression of specific phenotypes including pigmentation and bioluminescence which occur during post-exponential growth i.e. primary-specific factors (Table 1.1). The secondary variant, in contrast, is characterised by the lack of, or the extremely reduced expression of, these phenotypes (Table 1.1) (Boemare and Akhurst, 1988). Both the primary and secondary variants are equally pathogenic when injected into insect larvae (Bleakley and Nealson, 1988); however only the primary variant is able to support nematode growth and development. The fact that these primary variant phenotypes appear to be expressed post exponentially and that they are repressed in the non-symbiotic secondary variant has led to

them being termed 'symbiosis factors' (ffrench-Constant *et al.*, 2003). Proteomic analysis of the primary and secondary variants, using 2-D polyacrylamide electrophoresis, has identified 32 membrane proteins and 54 cytoplasmic proteins that had altered abundance between the different variants, therefore providing a list of potentially important proteins controlling the interaction of the *Photorhabdus* with its nematode partner (Turlin *et al.*, 2006).

The co-ordinated repression of the production of the primary specific factors in the secondary variant led to the hypothesis that there was a repressor protein expressed in the secondary variant that was responsible for repressing the primary variant characteristics (O'Neill *et al.*, 2002). Indeed it has been shown that the secondary variant appears to be maintained by the high-level expression of the *hexA* gene in the secondary variant during exponential and stationary phase growth. A mutation in the *hexA* gene of the secondary variant of *P. temperata K122* restored the expression of the majority of the primary variant phenotypes and this derepression was also associated with the ability of the secondary variant *hexA* mutant to support nematode growth and development (Joyce and Clarke, 2003).

**Table 1.1**. Phenotypes of the primary and secondary variants of *Photorhabdus*

| Phenotype | Primary variant | Secondary variant |
|---|---|---|
| Bioluminescence | +++ | + |
| Colony morphology | Convex, mucoid | Flat, non-mucoid |
| Protease production | +++ | - |
| Lipase production | +++ | - |
| Pigmentation | +++ | - |
| Antibiotic production | +++ | - |
| Catalase production | +++ | - |

Another player in phenotypic variation is the *ner* gene. This locus was identified when DNA was transformed from the secondary variants into the primary variants to discover any genetic regions that may be responsible for the

secondary phenotype. Overexpression of *ner* in primary variant cells results in the conversion of the cell to a secondary variant, however deletion of *ner* has no effect on phenotypic variation and the *ner* region was shown to be exactly the same in both primary and secondary variants (O'Neill *et al.*, 2002). Interestingly overexpression of *ner* does not affect *hexA* expression which suggests that either *ner* is acting downstream of *hexA* or there are 2 pathways involved in the control of phenotypic variation (Joyce and Clarke, 2003).

Secondary variants can be isolated after prolonged culturing of primary variant cells and it is formally possible that the secondary variant is just an artefact from prolonged growth in the laboratory. However, the identification of the regulatory proteins discussed above suggest that this is a regulated phenomenon in *Photorhabdus*. Moreover it was recently shown that a two-component signalling pathway, AstRS, is involved in regulating the timing of phenotypic variation. Therefore, a deletion of *astR*, encoding the response regulator of the pathway, results in a mutant that undergoes phenotypic variation seven days earlier than the wild type (Derzelle *et al.*, 2004a) Proteomic analysis has revealed that the AstRS pathway positively regulates the expression of 10 proteins including 3 universal stress proteins UspA, UspB and UspC. Therefore, one possibility is that the AstRS pathway may prevent phenotypic variation by protecting the cell from stress (Derzelle *et al.*, 2004a; Joyce *et al.*, 2006). The timing of phenotypic variation suggests that it will occur towards the end of the life-cycle in the insect cadaver. Moreover it has been shown that, following nutrient starvation, secondary variant cells were able to initiate growth much faster than primary variant cells when re-exposed to nutrients. This suggests that the secondary variants may be better adapted to survival in the harsh environmental conditions outside of the insect cadaver (Smigielski *et al.*, 1994). Therefore, one possible model for the role of phenotypic variation is that, once the new generation of IJs have left the insect cadaver carrying their primary variant symbionts, the remaining biomass in the insect cadaver can undergo phenotypic variation in preparation for life without the nematode i.e. as a free-living bacterium in the soil.

## 1.2 Iron

### 1.2.1 Iron in biological systems

It has been suggested that iron acquisition is probably the most important factor for a pathogen to be able to survive and proliferate inside its host (Ratledge and Dover, 2000). Most aerobic bacteria have an absolute requirement for iron, as it possesses essential functions required for the reduction of oxygen, for the synthesis of ATP, the reduction of ribotide precursors of DNA, for the formation of haem, and for other essential metabolic purposes (Neilands, 1995). Only a specialised few bacteria such as *Lactobacilli* spp. have actually managed to replace the essential iron-containing ribotide reductase with an enzyme using adenosylcobalamin as the radical generator (Reichard, 1993). It is the potential for redox cycling that has ensured that iron plays an essential role in almost all living organisms including as a key component of the electron transport chain. Although iron is such an essential component of life, too much free iron is actually damaging to cells because of its ability to catalyse the Fenton reaction (Fig. 1.2) resulting in the production of reactive hydroxyl radicals. Interestingly a recent study has shown that all bacteriocidal antibiotics stimulate the production of hydroxyl radicals that contribute to cell death (Kohanski *et al.*, 2007). Therefore, iron levels must be tightly regulated in order to maintain the intracellular iron concentration between desirable limits (Escolar *et al.*, 1999).

Iron is the most abundant transition metal on Earth, however the solubility of iron is extremely low at physiological pH in aerobic environments, therefore the bioavailability of iron is poor (Clarke *et al.*, 2001). Ferric iron hydroxide ($Fe(OH)_3$)is the major form of iron under aerobic conditions at pH 7, and this molecule only has a solubility of $1.4 \times 10^{-9}$ M under these conditions (Chipperfield and Ratledge, 2000). At these concentrations the level of iron

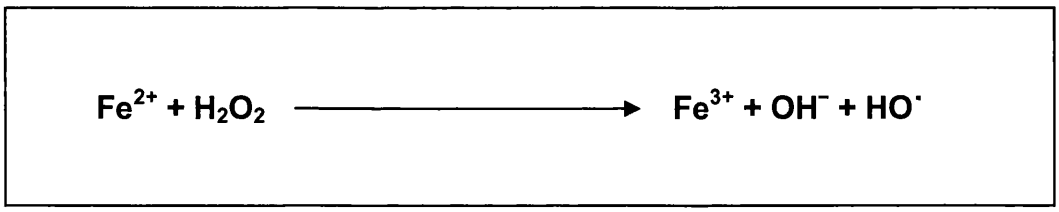


**Figure 1.2.** The Fenton reaction produces the highly damaging and reactive hydroxyl radical ($HO^{\cdot}$)

available is well below the $10^{-7}$ to $10^{-5}$ M required for optimal bacterial growth (Andrews *et al.*, 2003). Therefore, both hosts and pathogens have overcome the problem of iron solubility by complexing iron to molecules that make the iron more soluble. In humans and other higher vertebrates iron is complexed with high affinity binding proteins in the host such as the glycoprotein transferrin (Tf). Transferrins are single chain glycoproteins of molecular weight 80,000 that are characterised by having two similar, but not identical, binding sites for iron (Ratledge and Dover, 2000). Tf is never fully saturated with iron and this plays an important role in providing spare capacity to 'mop up' any surplus ions that may arise in blood or fluids (Raymond *et al.*, 2003). The strategy of withholding iron from pathogenic bacteria has long been identified as being of key importance in host defence mechanisms (Payne, 1993; Weinberg, 1993) and injecting iron compounds into an animal host can significantly enhance the virulence of a wide range of bacterial pathogens (Griffiths, 1999). Therefore, it is likely that pathogenic bacteria are limited in their capacity for multiplication *in vivo* due to the iron-withholding defence mechanism of the infected host (Payne, 1993; Weinberg, 1993). However, it is clear that bacteria have developed mechanisms that enable them to acquire iron from various host sources as they are still able to multiply in the host (Ratledge and Dover, 2000).

### 1.2.2 Bacterial iron acquisition

#### 1.2.2.1 Siderophores

Siderophores are specific, high affinity, low molecular weight ferric ($Fe^{3+}$) binding agents that are produced and secreted by many, but not all, micro-organisms in response to iron limitation. Siderophores act to solubilise iron from

the surrounding milieu and deliver the iron to the bacteria (Fig. 1.3). Siderophores function simply by having a much greater affinity for iron than the host iron-binding molecules such as ferritin, Tf and lactoferrin (Ratledge and Dover, 2000). Siderophores also have the ability to bind iron from insoluble salts including ferric hydroxide, which is the manner whereby siderophore-producing micro-organisms are able to acquire iron from laboratory growth medium (Ratledge and Dover, 2000). Siderophore production must be tightly regulated as surplus iron can be toxic to cells due to the generation of free radicals and, as there is no evidence for iron secretion mechanisms, regulation must be controlled at the level of uptake (Bagg and Neilands, 1987; Crosa, 1997).

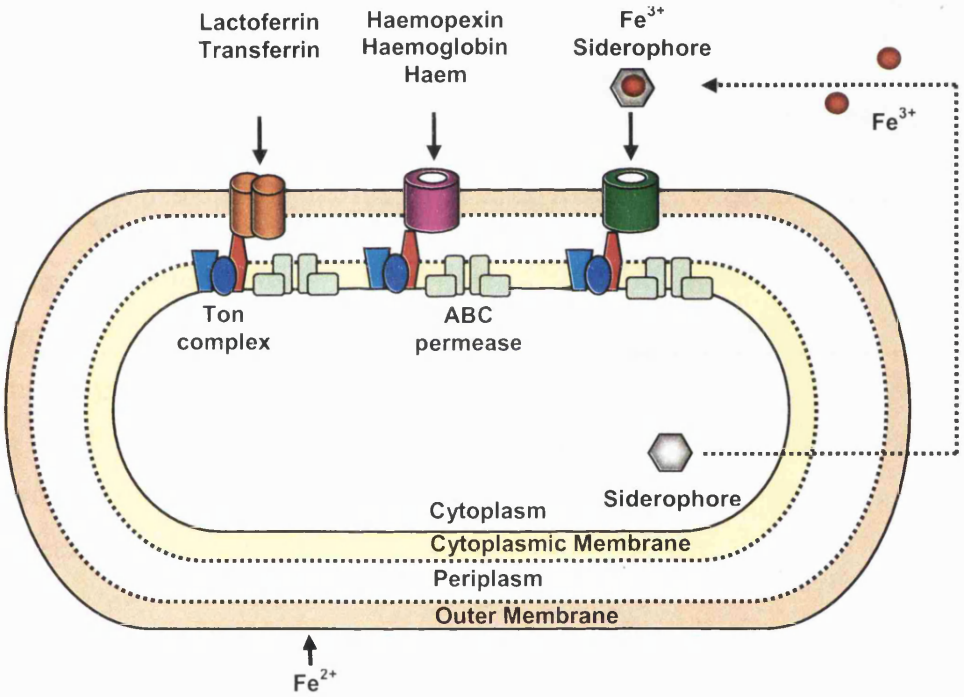


**Figure 1.3.** TonB-dependent ferric iron uptake systems in Gram-negative bacteria.

There are three main groups of siderophores that have been determined by their metal binding functionality (Raymond and Dertz, 2004). These three groups are the catecholates, hydroxamates and hydroxycarboxylates (Fig. 1.4). Enterobactin is one of the most well studied catecholate siderophores produced by *E. coli* and other bacteria. This family of siderophores is synthesised by non-ribosomal peptide synthases (NRPS) and the steps in the assembly of enterobactin have

been well characterised. Synthesis of enterobactin consists of two parts; a) chorismate is converted into 2,3-dihydroxybenzoate by EntA, EntB and EntC and b) the formation of enterobactin from 2,3-dihydroxybenzoate by EntD, EntE and EntF (Fig. 1.5). Some strains of *Photorhabdus* make an enterobactin like siderophore called photobactin (Ciche *et al.*, 2003) (Fig. 1.5).

Many bacteria are able to produce multiple siderophores and indeed some bacteria have evolved the ability to acquire siderophores produced by other bacteria therefore reducing the energetic costs of siderophore production when an iron-containing siderophore is available in the environment. It is logical that the ability to use multiple siderophores would be advantageous for optimal iron acquisition under the different conditions encountered by a bacterium. Enterobactin is inactivated by the albumin in human serum and therefore this would be an ineffective siderophore for iron acquisition in the blood. However aerobactin (a hydroxamate siderophore) which is also produced by *E. coli,* is not affected by serum albumin (Raymond and Dertz, 2004). Remarkably some pathogenic bacteria have managed to modify enterobactin to produce a siderophore called salmochelin which avoids inhibition by the mammalian immune system (Fischbach *et al.*, 2006). Aerobactin has also been shown to bind iron well under acidic conditions, whilst catechol siderophores such as enterobactin are unstable under these conditions and lose the complexed iron (Valdebenito *et al.*, 2005).

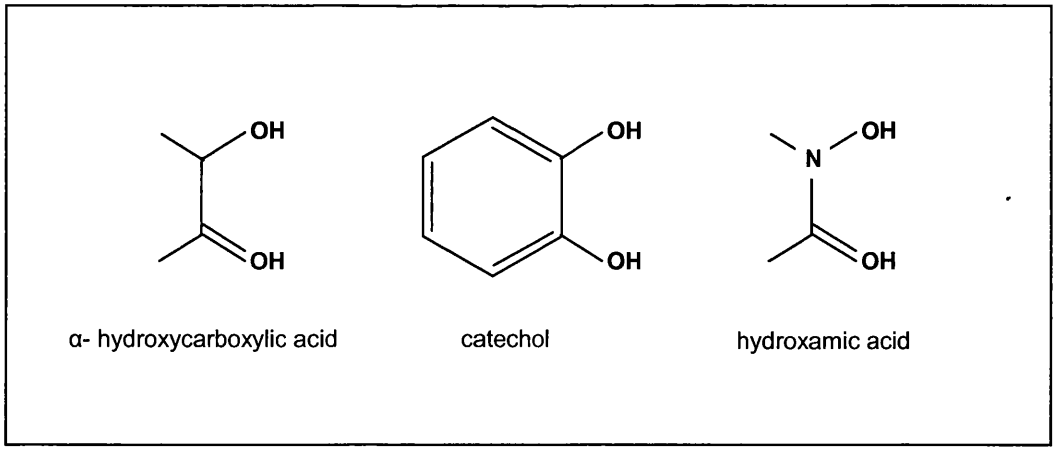


**Figure 1.4.** The chemical structure of metal binding of the three broad groups of siderophores.

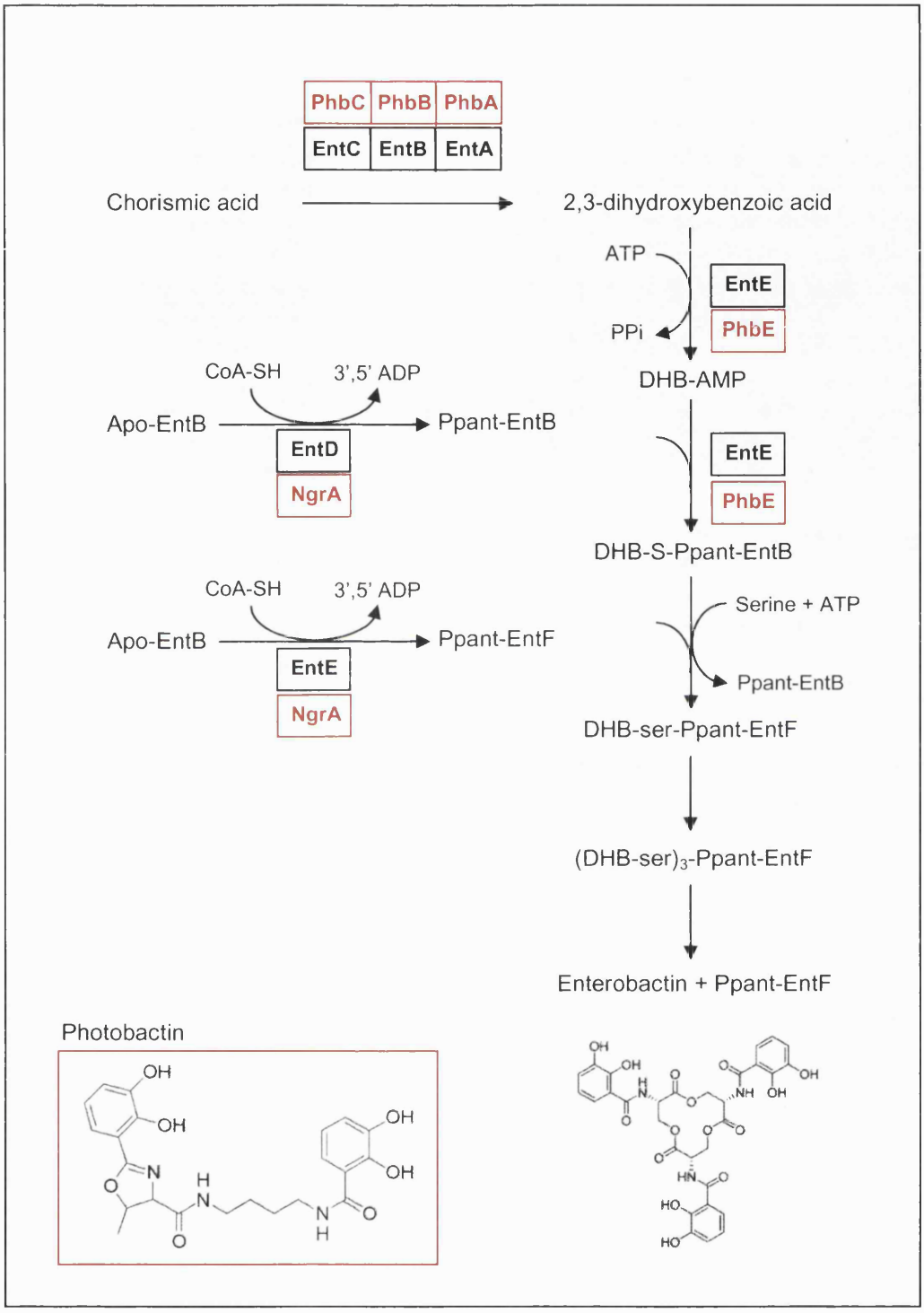


**Figure 1.5.** Enterobactin biosynthesis in *E. coli*. Genes identified with a homologue in *P. luminescens* NC19 have been listed and highlighted in red. Adapted from (Ratledge and Dover, 2000).

The importance of siderophore production and utilisation varies across a wide range of bacteria. For example *N. meningitidis* the major organism causing meningitis, does not produce any siderophores implying that siderophore production is not required for virulence (Perkins-Balding *et al.*, 2004). Nonetheless it would be expected that siderophores would be beneficial during infection and the inability to produce and/or transport siderophores has severely affected the virulence of several important pathogens including *Y. pestis* (Bearden *et al.*, 1997), *P. aeruginosa* (Meyer *et al.*, 1996) and the marine bacterium *Vibrio vulnificus* (Litwin *et al.*, 1996) which causes septicaemia and serious wound infections.

Interestingly although the biosynthesis of siderophores is reasonably well characterised, the process of siderophore secretion into the environment remains largely unresolved. ExiT was identified as a potential ABC transporter by homology analysis in *M. smegmatis* and inactivation of *exiT* by a transposon insertion lead to a significant decrease in exochelin siderophore efflux (Zhu *et al.*, 1998). However, there was no detectable intracellular build up of exochelin and although the authors speculate this could be due to feedback control on production, the excretion defect could be due to the lack of exochelin production rather than a defect in export. However more recent advances are suggesting some of the mechanisms by which siderophores may be excreted including export via large major facilitator superfamily (MFS) membrane bound transporters (Grass, 2006).

1.2.2.2 Siderophore Receptors

Having gone to the expense of producing complex siderophore molecules to acquire essential iron from the environment the bacterium must be able to selectively recapture the secreted siderophore from the environment. As the siderophores are generally present in the environment at low concentrations and they are too big to enter the cell by diffusion the siderophores must be captured with high efficiency. This role is fulfilled by specialised surface siderophore receptors that translocate the siderophore into the periplasm. These receptors are generally only expressed in response to iron limitation as some infectious agents

such as colicins and bacteriophages have evolved to parasitise bacteria by binding to outer membrane siderophore receptors (Cascales *et al.*, 2007; Lazdunski *et al.*, 1998). The crystal structures of several outer membrane receptors, including the enterobactin receptor FepA (Buchanan *et al.*, 1999), the ferrichrome receptor FhuA (Ferguson *et al.*, 1998; Locher *et al.*, 1998), the ferric dicitrate receptor FecA (Ferguson *et al.*, 2002; Yue *et al.*, 2003), the pyochelin receptor FptA (Cobessi *et al.*, 2005) and the pyoverdine receptor FpvA (Wirth *et al.*, 2007) have been solved revealing that these receptors are composed of two structural domains, a β-barrel and a plug domain which fits inside the barrel. This plug domain moves in order to permit transfer of the substrate i.e. siderophore into the periplasm (Wandersman and Delepelaire, 2004). This movement is an energy-dependent process and in Gram-negative bacteria the provision of energy appears to be fulfilled by the TonB energy-transducing system. In Gram-positive cells the lack of an outer membrane means that active transport across the cytoplasmic membrane can be driven by ABC transporters that are coupled to siderophore receptors (Andrews *et al.*, 2003).

#### 1.2.2.3 The TonB system

Molecules below a threshold size of approximately 600 Da can cross the outer membrane of Gram-negative bacteria by diffusion though the channels formed by porins (Nikaido, 1994). However this excludes important molecules such as siderophores and vitamin $B_{12}$ and therefore, these molecules must be transported by membrane transporters. There are no usual sources of energy such as ATP at the outer membrane consequently the energy for transport across the outer membrane of iron loaded siderophores must be transferred from the inner membrane to the outer membrane receptor. This energy transduction is achieved by a complex of proteins (TonB, ExbB, ExbD) that are localised in the cytoplasmic membrane (Postle and Larsen, 2004) (Fig. 1.6.). In *E. coli* the TonB complex is encoded by a single *tonB* gene and an operon encoding *exbB* and *exbD* and transcription from these loci is regulated by the iron concentration of the environment (Higgs *et al.*, 2002).

TonB has been shown to interact with outer membrane receptors in a small region in the N-terminus of the receptor called the TonB-box. Several studies have shown that mutations in this region abolish interaction of TonB with the outer membrane receptor, but that complementary mutations in the C-terminus of TonB could restore the activity (Barnard *et al.*, 2001; Cadieux *et al.*, 2000; Heller *et al.*, 1988).

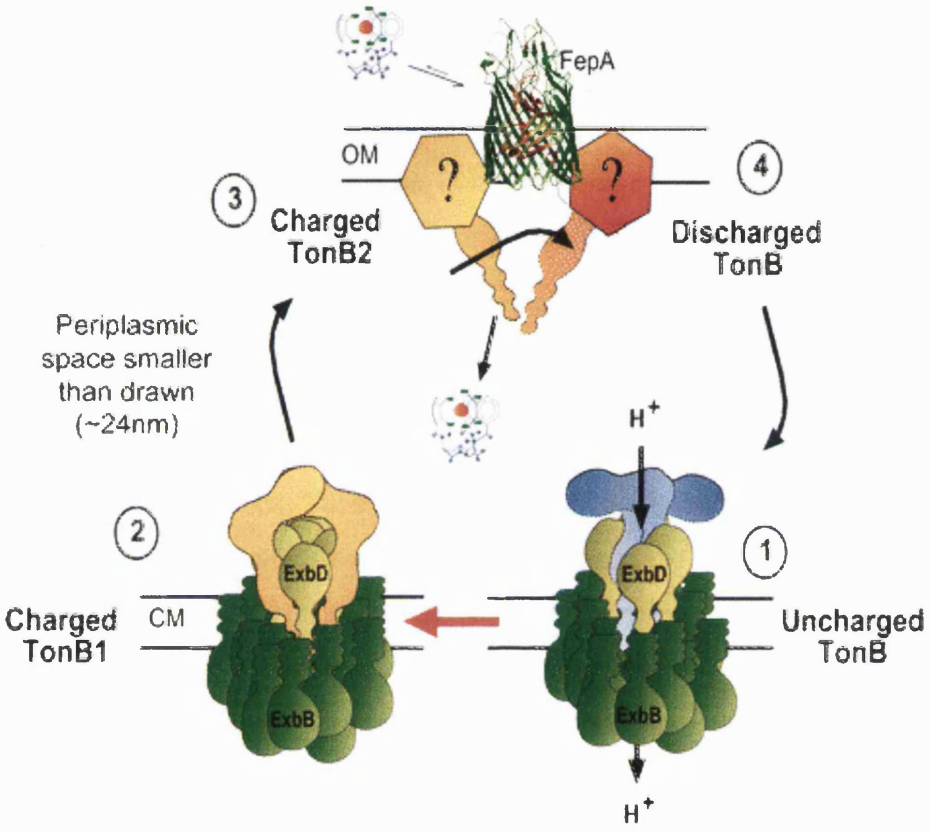


**Figure 1.6.** Shuttling model of TonB transfer from the cytoplasmic membrane to the outer membrane. Energy is harvested from the proton gradient in the CM by the ExbB-ExbD energy harvesting complex (1). The energy is stored as a conformational change in TonB which is present as a dimer (2). TonB shuttles to the outer membrane and the conformationally-stored potential energy is transferred to a ligand bound TonB-dependent outer membrane transporter (3). The stored energy is released from TonB and the ligand is transferred into the periplasm. Discharged TonB is recycled back to the CM for re-use (4).Reproduced from Postle and Larsen, 2007.

Crystal structures have recently been obtained for TonB interacting with FhuA and for TonB interaction with the vitamin $B_{12}$ receptor BtuB (Pawelek *et al.*, 2006; Shultis *et al.*, 2006). These studies identified several residues that appeared to be important for interaction of TonB with the outer membrane receptor.

However substitutions at key residues identified in these crystal structures did not affect TonB activity. Further analysis revealed a deletion of 7 residues of TonB (S157 to Y163) to be essential for initial contact with the outer membrane receptor (Vakharia-Rao *et al.*, 2007).

The exact mechanism of the transfer of energy from the cytoplasmic membrane to the outer membrane still remains unsolved, however a shuttling model has been proposed whereby ExbB and ExbD are the energy-harvesting complex (predicted by their similarity to the MotAB stator motor proteins in the flagella apparatus) that reside in the cytoplasmic membrane and energise TonB before it is released for interaction with the outer membrane receptor. However this model would involve diffusion of TonB across the periplasmic space of approximately 240 angstroms and its cycling between the cytoplasmic and outer membranes (Postle and Larsen, 2007; Zhai *et al.*, 2003) (Fig. 1.6). The evidence for this model has been the identification of the TonB protein at both the inner and outer membrane during purification (Larsen *et al.*, 2003). More recent modelling data appears to suggest that TonB can interact with the outer membrane receptor and pass energy to the outer membrane receptor mechanistically over a large distance (Gumbart *et al.*, 2007). Intriguingly the outer membrane receptor was shown to unwind to a maximum extension of ~200 angstroms, therefore it does appear that it may be possible for the receptor to 'reach' across to TonB (Fig. 1.7).

In *E. coli* there are more TonB dependent membrane receptors at any one time compared to the availability of the TonB system, therefore there is competition for the energy translocation complex (Kadner and Heller, 1995). Interestingly some bacteria encode multiple TonB systems. *Pseudomonas syringae* (Buell *et al.*, 2003) has been identified as possessing five potential *tonB-exbB-exbD* loci, four of which are closely linked to putative receptor genes (Wandersman and Delepelaire, 2004). *Vibrio cholerae* possesses two *tonB-exbB-exbD* loci, termed 1 and 2, which carry out both redundant and specific functions (Seliger *et al.*, 2001). Both systems are able to transport hemin and the siderophores vibriobactin and ferrichrome. However TonB1 is specific for schizokinen siderophore transport and TonB2 is required for enterobactin transport (Seliger *et al.*, 2001). Although encoding multiple copies of the TonB system could alleviate

the problem of TonB supply it appears that some of these extra copies are in fact specific for certain transport mechanisms. Other systems with partially redundant functions have also been identified in some bacteria e.g. the Tol-Pal system (TolQ and TolR) in *E. coli* that can, partially at least, compensate for mutations in ExbB and ExbD (Postle and Kadner, 2003).

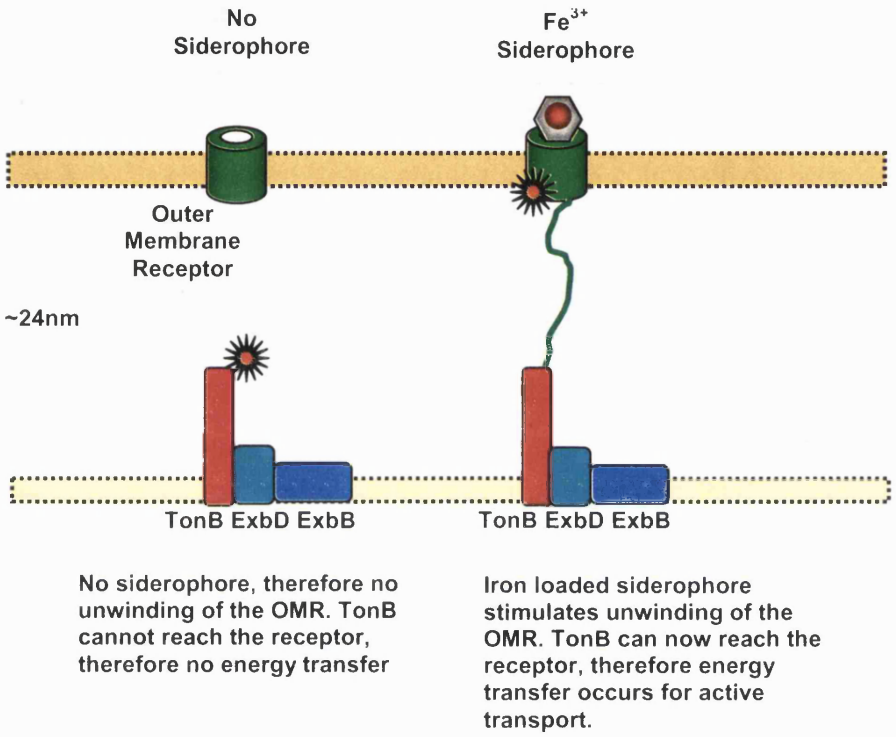


**Figure 1.7.** Proposed model of energy transfer from the TonB system to the outer membrane receptor. When the siderophore binds to the outer membrane receptor (green) the receptor unwinds revealing more of its structure. TonB has been shown to interact with the outer membrane receptor at up to 20 nm (Gumbart *et al.*, 2007) therefore if the receptor was able to unwind to this distance upon ligand binding energy transfer would be achieved (orange star). In this situation TonB (red) would not dissociate from the TonB-ExbB-ExbD complex.

However what is apparent is that the majority of the active iron transport systems that utilise outer membrane receptors rely on the TonB system for their function as iron acquisition mechanisms (Fig. 1.3). TonB is required for iron uptake via

siderophores and therefore a mutation in TonB (ExbB or ExbD) in pathogenic strains of bacteria would be expected to reduce their pathogenic potential by starving the bacterium for iron. Certainly this is the case for *Shigella dysenteriae* where TonB was found to be essential for intracellular growth (Reeves *et al.*, 2000)

The TonB system not only provides energy for the transport of siderophores. Vitamin $B_{12}$ is captured at the outer membrane and is transported by the BtuB receptor in the outer membrane in a TonB dependent manner (Gudmundsdottir *et al.*, 1989; Hufton *et al.*, 1995). Colicins are proteins produced by some bacteria that can kill closely related strains and the group B colicins have been shown to enter bacteria via TonB-dependent receptors (Cascales *et al.*, 2007). Other molecules that utilise the TonB system for the active uptake of compounds into the cell includes the transport of nickel via the TonB system in *Helicobacter pylori* under acidic conditions. The TonB-dependent FrpB4 outer membrane receptor was responsible for transporting iron under normal pH but was involved in transporting nickel at low pH (Schauer *et al.*, 2007). The plant pathogen *Xanthomonas campestris* pv. *campestris* (Xcc) has been identified as a bacterium that can transport sucrose via a TonB-dependent outer membrane receptor (Blanvillain *et al.*, 2007). Therefore, these findings are demonstrating alternative roles for TonB-dependent receptors under different environmental conditions. However it remains to be seen if these are widespread features or if they are limited to a specialised few bacteria.

#### 1.2.2.4 Alternative TonB-dependent uptake systems

Although siderophores are a major method of iron acquisition, bacteria also employ several alternative TonB-dependent mechanisms for the active acquisition of iron (Fig. 1.3). When a pathogen finds itself within a host there are a range of iron sources that can be scavenged. For example, in humans, the proteins that are required for the delivery of iron around the body for incorporation into iron-sulphur proteins or for redox reactions can be a direct target for these pathogens. Therefore, bacteria can remove iron from transferrin and lactoferrin by utilising these proteins directly. *N. meningitidis* does not

produce siderophores but, rather, this bacterium produces transferrin-binding outer membrane receptors, TbpA and TbpB (DeRocco and Cornelissen, 2007). The iron is stripped from the host transferrin and is transported into the cytoplasm by an ABC transporter. The importance of the transferrin receptors has been shown in the closely related *N. gonorrhoeae* where a deletion of these two proteins prevented infection of human males (Cornelissen *et al.*, 1998). Lactoferrin is a source of iron in serum and lactoferrin binding proteins are expressed by some bacteria at the cell surface which act to liberate iron from lactoferrin (Wandersman and Delepelaire, 2004). In *N. meningitidis* lactoferrin is captured and transported by the LbpA and LbpB proteins and insertional inactivation of *lbpA* revealed that LbpA is essential for iron acquisition from transferrin *in vitro* (Bonnah and Schryvers, 1998; Perkins-Balding *et al.*, 2004).

Haem is another potential source of iron for invading pathogens and several bacteria have evolved mechanisms to utilise this molecule. Haem is rarely found as a free compound and is usually found as a component of haemoglobin, haptoglobin-haemoglobin and haemopexin. Some strains of bacteria can use haem as an iron source by producing outer membrane receptors that can bind haem directly. Other bacteria secrete hemophores which are specialised extracellular proteins found in Gram-negative bacteria that acquire haem from the environment and are captured by specific outer membrane receptors (Wandersman and Delepelaire, 2004).

1.2.2.5 Transport across the cytoplasmic membrane

Transport of iron into the cytoplasm of Gram-negative bacteria not only requires the translocation of iron across the outer membrane, but also requires the transport of iron across the cytoplasmic membrane. This is achieved by ABC (ATP-binding cassettes) permeases that consist of a periplasmic binding protein coupled to an inner membrane complex that is energised by hydrolysis of ATP (Fig. 1.3). Interestingly the specificity of the ABC permease for the transport of substrates is much lower than that of the outer-membrane receptors. There are almost 9 times the number of TonB-dependent outer membrane receptors compared to ABC permeases in *P. aeruginosa* (Koster, 2001). FhuD is an *E. coli*

siderophore periplasmic binding protein that is able to bind ferrichrome, coprogen, rhodotorulic acid, ferrioxamine A/B/C and aerobactin (Wandersman and Delepelaire, 2004). Therefore, FhuA is an outer membrane receptor that is specific for its cognate siderophore whilst FhuD is more promiscuous and allows the ABC permease to transport a wider range of iron containing molecules.

1.2.2.6 TonB independent uptake systems

Not all iron acquisition strategies require the TonB system in order to transport iron into the cell. The predominant ferric ($Fe^{3+}$) uptake systems are TonB-dependent however, at acidic pH or low oxygen tensions the ferrous form ($Fe^{2+}$) of iron becomes more readily available as it is much more soluble under these conditions. Therefore, bacteria have evolved several mechanisms for the TonB independent transport of ferrous iron (Fig. 1.8). These transport systems have been shown to play a key role in the virulence of some important bacterial pathogens. The Yfe system, encoded by the *yfeABCDE* operon, was discovered in *Y. pestis* and consists of YfeA, a periplasmic binding protein, YfeB an ATP hydrolase, YfeC and YfeD, a heterodimeric permease and YfeE, a putative inner membrane protein of unknown function. This locus encodes an ABC transport system, that is able to restore growth, under iron limiting conditions, to an enterobactin-defective *E. coli* strain (Bearden *et al.*, 1998). *Y. pestis* mutants lacking yersiniabactin siderophore (Ybt) are completely avirulent when introduced into a host via a subcutaneous route which mimics the flea bite. This system is not required during the latter stages of the disease and *Y. pestis* $Ybt^-$ mutants are fully virulent if introduced intravenously. The *yfe* system has also been shown to be essential for full virulence of *Y. pestis* when introduced via the intravenous route of infection (Bearden and Perry, 1999). The *yfeAB* mutation resulted in a reduced transport of radioactively-labelled manganese as well as iron (Bearden and Perry, 1999). Interestingly several homologues of the *yfe* system have been identified which also show a dual ferrous iron and manganese

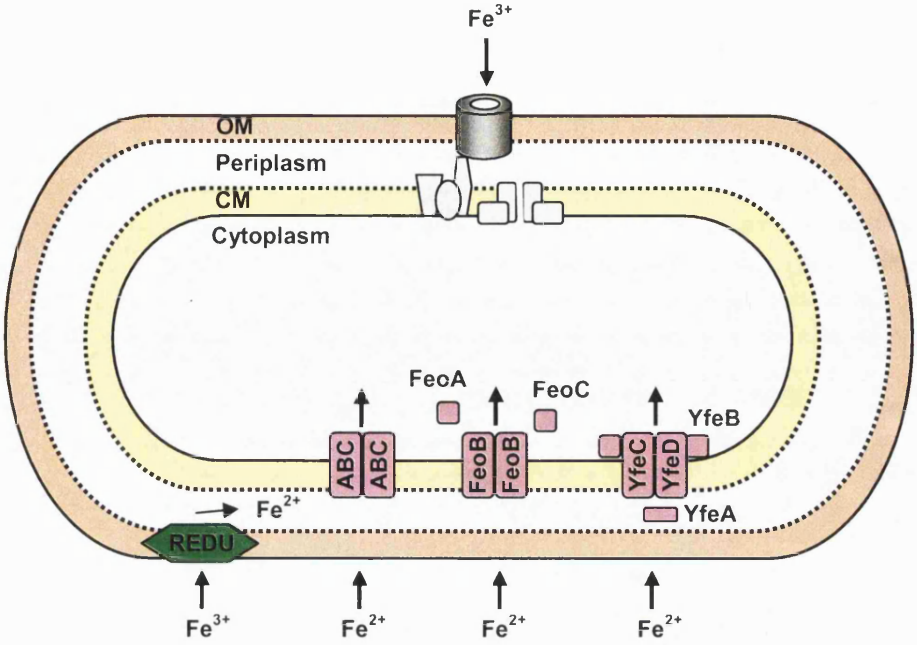


**Figure 1.8.** Ferrous iron transport systems in bacteria. Ferrous iron can be transported directly from the environment via an ATP dependent transport system (pink) or ferric iron can be reduced to ferrous iron by the action of ferric reductases (green) for transport by the ABC transport systems.

transport role (Boyer *et al.*, 2002; Runyen-Janecky *et al.*, 2006; Sabri *et al.*, 2006). The SitABCD homologue from an avian pathogenic *E. coli* transports iron and manganese and is responsible for maintaining resistance to hydrogen peroxide, but only in a *mntH* manganese transport mutant (Sabri *et al.*, 2006). Interestingly a *sitA* mutant of *Sinorhizobium meliloti* shows an increased sensitivity to oxidative stress and these defects can be complemented by the addition of manganese (Davies and Walker, 2007). However, in *Y. pestis* neither a mutation in *mntH,* (encoding a manganese transporter) nor a *mntH yfeAB* double mutant showed any intracellular growth defects suggesting that the main role for the Yfe transporter during virulence of *Y. pestis* is the transport of iron (Perry *et al.*, 2007). Therefore, it appears that the YfeABCD system and its homologues can transport both ferrous iron and manganese but that its specificity or dependence for each ion may depend on the strain or host under investigation. Ferrous iron can also be transported by the Feo transporter which has also been

shown to play an important role in the ability of *E. coli* K-12 strains to colonise the mouse intestine (Stojiljkovic *et al.*, 1993). The Feo system is comprised of the FeoABC proteins which are believed to act in the cytoplasmic membrane (FeoB) and in the cytoplasm (FeoA) to elicit transport of ferrous iron into the cytoplasm (Cartron *et al.*, 2006) (Fig. 1.8). The role of FeoC may be as a transcriptional regulator of the *feoABC* genes (Cartron *et al.*, 2006). Interestingly some bacteria also possess ferric reductases which are able to reduce ferric iron to ferrous iron which can allow the import of iron via a ferrous uptake route (Fig. 1.8.) (Ratledge and Dover, 2000).

### 1.2.3 Iron storage

When iron is present in greater quantities than is required for growth bacteria utilise ferritins and bacterioferritins for the storage of this valuable resource. Ferritin, a major iron storage protein is found in both eukaryotes and prokaryotes and, in *E. coli,* this protein is encoded for by the *ftnA* gene. Ferritin has the remarkable ability to store up to 2000-3000 iron atoms within its structure (Andrews *et al.*, 2003). Many bacteria also possess a haem-containing ferritin called bacterioferritin (Andrews *et al.*, 2003). These reserves act as a source of iron when exogenous supplies are limiting. However, bacterioferritin can also act to detoxify reactive oxygen species, thereby providing a protective role as well as a storage role (Bou-Abdallah *et al.*, 2002). The Dps protein has also been shown to be an iron storage protein that can provide protection against oxidative stress in *E. coli.* Dps appears to act in a similar way to bacterioferritins whereby $Fe^{2+}$ is oxidised within the protein to $Fe^{3+}$ by the action of $H_2O_2$ thereby avoiding the production of free radicals by the Fenton reaction (Zhao *et al.*, 2002).

### 1.2.4 Regulation of iron acquisition

The whole process of iron acquisition and storage must be tightly controlled in order to maintain iron levels between tolerable limits. In many Gram-negative bacteria iron homeostasis this process is regulated by the ferric uptake regulator protein, Fur. Fur is a global regulator and it has been estimated as to be

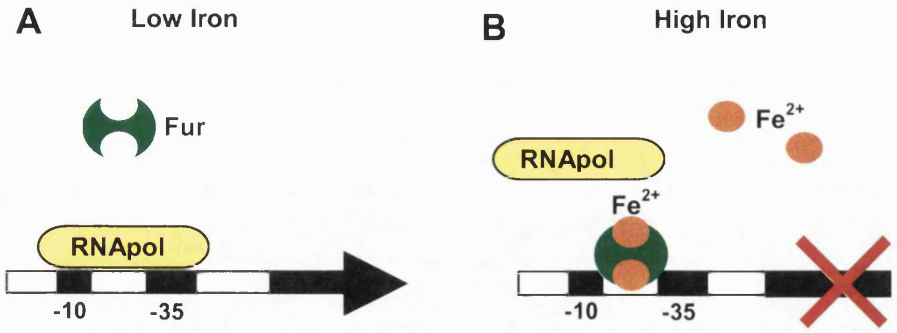


**Figure 1.9.** Mechanism of Fur regulation. When iron is low (A) the Fur protein cannot bind to DNA therefore the promoter is free to bind and the genes are transcribed. When intracellular levels of iron increase the ferrous iron binds to Fur leading to a conformational change that allows the Fur protein to bind to the DNA. Fur binding blocks the RNA polymerase from binding, therefore the genes are not transcribed.

responsible for the regulation of more than 90 genes in *E. coli* (de Lorenzo *et al.*, 2004). In many Gram-positive bacteria there appears to be a similar protein, DxtR, that has been identified as an iron-dependent repressor (de Lorenzo *et al.*, 2004). Fur represses the expression of genes when the level of internal $Fe^{2+}$ increases to a threshold level that allows $Fe^{2+}$ to interact directly with the Fur protein. Once ferrous iron is bound to Fur it is able to bind to DNA and repress gene expression. Most Fur binding sites are present within the -10 to -35 regions of the respective promoters therefore blocking promoter binding by RNA polymerase (Fig. 1.9). This results in genes being switched off when the level of iron is high. When iron levels are low the ferrous iron does not bind to Fur and the genes are de-repressed. This simplistic view of Fur regulation was held for many years. However the control of iron acquisition genes in response to iron deprivation has recently become more complex and Fur has been shown to positively regulate the expression of at least 9 genes in *E. coli* (Andrews *et al.*, 2003). These genes include genes involved in iron storage i.e. *ftnA* and *bfr*. Therefore under conditions of high ferrous iron the expression of *ftnA* and *bfr* increases and this is dependent on Fur. This Fur-dependent positive regulation appears to be due to the presence of a small 90nt RNA called RyhB. RyhB is itself negatively regulated by Fur so that under conditions of high $Fe^{2+}$ the level of *rhyB* decreases. This leads to an increase in the stability of the *ftnA* and *bfr* mRNA (amongst others) resulting in increased expression of these genes (Masse

and Gottesman, 2002). It is perhaps not surprising that Fur also regulates genes in addition to those directly involved in iron acquisition e.g. primary metabolism and oxidative stress. Therefore it appears that iron can act as an environmental signal.

### 1.2.5 Iron as a signal

The coordinate expression of bacterial genes is regulated by the ability of the bacteria to sense their environment. Fur plays a major role in the global expression of genes in response to iron perturbations, however some siderophores have also been implicated in signalling. The siderophore is able to confer a signal to the inside of the cell where extra cytoplasmic function (ECF) sigma factors are stimulated. Most ECF sigma factors are found in association with membrane-bound anti-sigma factors. Therefore the role of the signal is to cause release of the ECF sigma factor. The ECF sigma factor is then able to bind to the RNA polymerase and direct the complex to transcribe genes involved in iron acquisition. The ferric dicitrate system found in *E. coli* is the most comprehensively studied example and the ability of the outer membrane receptor to transduce a signal appears to depend on the presence of an N terminal extension in the receptor (Koebnik, 2005). FecI is the iron-starvation ECF sigma factor that binds RNA polymerase and directs transcription of the *fecABCDE* genes upon release from the anti-sigma factor FecR (Fig. 1.10.). This system is activated by binding of ferric citrate to the TonB-dependent outer membrane receptor FecA. Interestingly, in addition to controlling genes involved in iron acquisition, this system has been utilised for the regulation of virulence factors. Pyoverdine is a siderophore produced by *P. aeruginosa* that is able to regulate the production of iron acquisition genes and the expression of genes encoding endoprotease and endotoxin A virulence factors (Vasil, 2007).

Iron is a key nutrient and bacteria have developed many sophisticated mechanisms to maintain the levels of iron required for growth. The vast number of these systems underlies the importance of iron for the proliferation of bacteria.

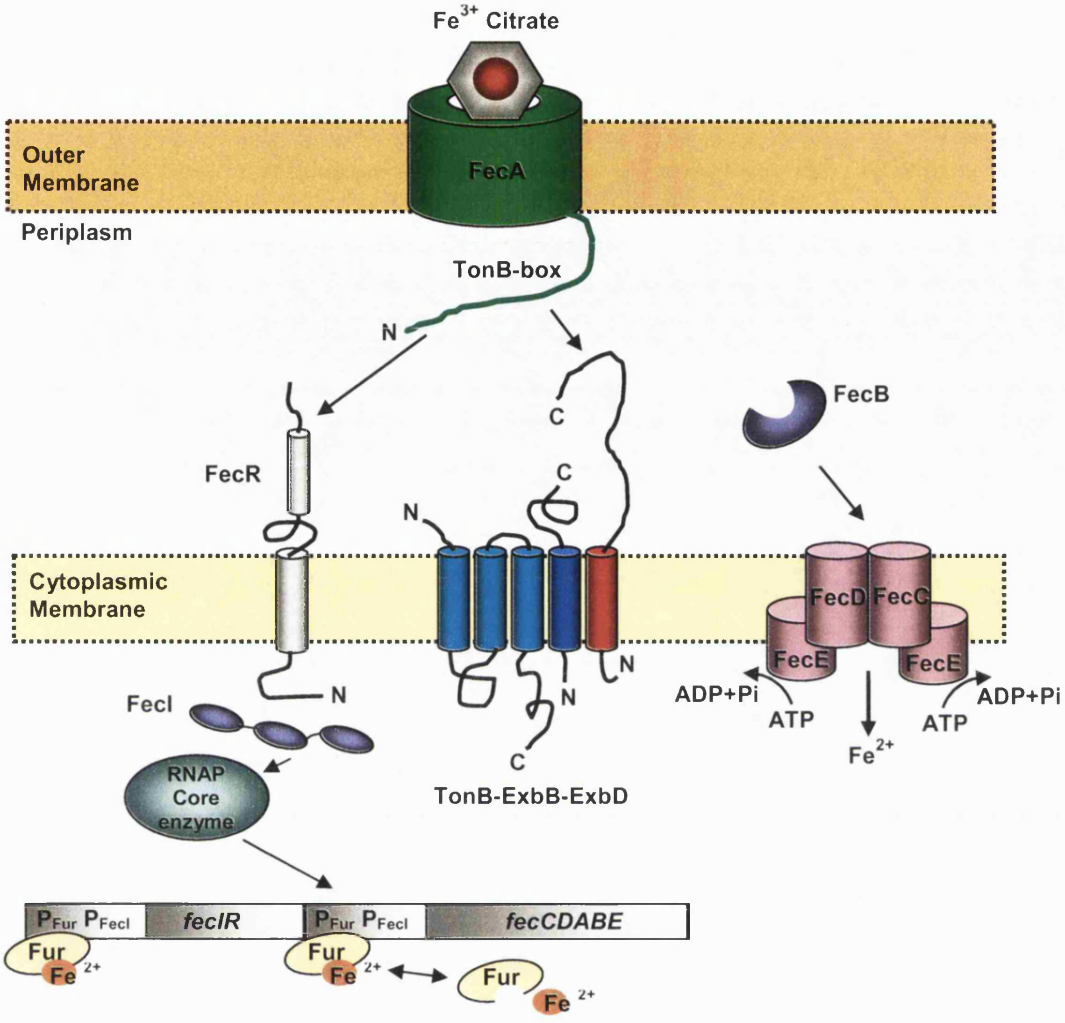


**Figure 1.10.** Ferric citrate transport in Gram-negative bacteria. Adapted from (Braun *et al.*, 2004)

### 1.2.6 Iron in pathogenicity and mutualism

Iron is a key element for all forms of life, not least for bacteria. The subject of iron and its importance in human infections dates back over a century where the detrimental effects of administering iron to tuberculosis patients had been observed (Trousseau, 1872). Injection of iron compounds into animal hosts has been shown to significantly enhance the virulence of a wide range of bacterial pathogens (Griffiths, 1999). Furthermore, the deletion of iron acquisition systems in many bacterial pathogens has rendered them unable to cause disease or severely limited in their capacity to do so. The importance of iron in beneficial symbiotic interactions has been less well studied. The *glnD* gene was identified in *V. fischeri* as important for squid light organ persistence and a transposon insertion in this gene resulted in a strain that was unable to produce wild type levels of siderophore and was less able to grow under iron limiting conditions. However this mutant was also affected in nitrogen utilisation, therefore the exact role of iron within this system remains to be precisely defined (Graf and Ruby, 2000). The *Rhizobium leguminosarum tonB* gene was identified as essential for import of vicibactin siderophore and for wild type levels of growth on haem or under iron limited conditions. Despite these phenotypes the mutation in *tonB* did not interfere with symbiotic $N_2$ fixation in pea nodules (Wexler *et al.*, 2001). Furthermore a *tonB* mutant of *Xenorhabdus nematophila* was fully able to colonise the *Steinernema* nematode, however this mutant was not tested for insect virulence (Martens *et al.*, 2005). Compared to the number of studies into iron homeostasis in pathogenic bacteria the number of studies in mutualists is relatively small, therefore as *Photorhabdus* is both a pathogen and a mutualist the lifecycle offers us a remarkable opportunity to ask complex questions about iron homeostasis in both pathogenicity and mutualsim.

## 1.3 Aims and Objectives

Nutritional interplay between prokaryotes and eukaryotes has been shown to be a major mechanism ensuring the maintenance of beneficial associations or defining the outcome of infection. Therefore, the role of an essential nutrient, iron, will be investigated in *Photorhabdus.* The aim of this project is to define the role of iron homeostasis systems during the interaction between *Photorhabdus* and its two different invertebrate hosts. To address this question iron homeostasis mutants of *Photorhabdus* will be created and studied for their ability to participate in the life-cycle. This study will identify iron homeostasis mechanisms that are important for pathogenic, mutualistic or both interactions.

# Chapter 2

# Materials and Methods

## 2.1 Bacterial strains, plasmids and growth conditions.

Strains and plasmids used in this study are listed in Table 2.1. *Photorhabdus temperata* K122, *Photorhabdus luminescens* subsp. *laumondii* TT01 and *E. coli* strains were routinely cultured in Luria-Bertani (LB) broth or on LB agar and were incubated at 30°C (for *Photorhabdus*) or 37°C (for *E. coli*). When required antibiotics were added at the following final concentrations: kanamycin (Km) 50 μg/ml, ampicillin (Amp) 100 μg/ml, chloramphenicol (Cm) 20 μg/ml, tetracycline (Tet) 15 μg/ml and rifampicin (Rif) 100 μg/ml.

**Table 2.1.** Bacterial Strains and plasmids used in this study

| Strain or plasmid | Genotype | Reference |
|---|---|---|
| ***Photorhabdus*** | | |
| *P. temperata* K122 Rif | Spontaneous Rif$^R$mutant of wild-type | (Joyce and Clarke, 2003) |
| *P. luminescens* TT01 Rif | Spontaneous Rif$^R$mutant of wild-type | (Bennett and Clarke, 2005) |
| BMM401 | K122 *phbC*::Km | This study |
| BMM415 | K122 *phbF*::Km | This study |
| BMM416 | K122 *phuD*::Km | This study |
| BMM417 | K122 *exbD*::Km | This study |
| BMM429 | TT01 Δ*rpoS* | Y.Wei. Unpublished |
| BMM430 | TT01 Δ*exbD* | This study |
| BMM431 | TT01 Δ*yfeABCD* | This study |
| BMM432 | TT01 Δ*feoAB* | This study |
| BMM433 | TT01 Δ*exbD* Δ*yfeABCD* | This study |
| BMM434 | TT01 Δ*exbD* Δ*feoAB* | This study |
| BMM435 | TT01 Δ*feoAB* Δ*yfeABCD* | This study |
| BMM436 | TT01 Δ*exbD* Δ*feoAB* Δ*yfeABCD* | This study |
| BMM437 | TT01 Δ*ftnA* | This study |
| BMM438 | TT01 Δ*ppxAB* | This study |
| BMM439 | TT01 Δ*plu4231* | This study |
| BMM440 | TT01 Δ*plu4231* Δ*ppxAB* | This study |
| ***E. coli*** | | |
| S17-1(λ*pir*) | lysogenised with λ*pir*, replication of *ori* R6K | Laboratory stock |

| | | |
|---|---|---|
| K12 JM109 | F' *traD36 proA$^+$B$^+$ lacI$^q$ Δ(lacZ)M15/ Δ(lac-proAB) glnV44 e14$^-$ gyrA96 recA1 relA1 endA1, thi hsdR17* | New England Biolabs |
| EC100 | F$^-$ *mcrA Δ(mrr-hsdRMS-mcrBC) Ø80dlacZ ΔM15* ΔlacX74 *recA1 endA1 araD139* Δ*(ara, leu)7697galU galK* λ*- rpsL nupG* | Epicentre |
| EC100D *pir*-116 | F$^-$ *mcrA Δ(mrr-hsdRMS-mcrBC) Ø80dlacZ ΔM15* ΔlacX74 recA1 *endA1 araD139* Δ*(ara, leu)7697galU galK* λ*- rpsL nupG pir-*116 (DHFR) | Epicentre |
| **Plasmids** | | |
| pBR322 | *ori* colE1, Amp$^R$ Tet$^R$ | Laboratory stock |
| pLOF-Km | *ori* R6K, mob RP4, Amp$^R$, Km$^R$ | (Herrero *et al.*, 1990) |
| pBAD24 | *ori* colE1, Amp$^R$, p*araBAD* | (Guzman *et al.*, 1995) |
| pBMM700 | pBAD24, p*araBAD-exbB* Amp$^R$ | This study |
| pBMM701 | pBAD24, p*araBAD-exbD* Amp$^R$ | This study |
| pBMM702 | pBAD24, p*araBAD-exbBD* Amp$^R$ | This study |
| pCIITn7 K-a | Conjugative mini-Tn*7* delivery Km$^R$ | (Redford and Welch, 2006) |
| pUX-BF13 | Tn*7* transposase *(in trans)* helper | (Bao *et al.*, 1991) |
| pDS132 | *R6K ori, mobRP4, Cat, sacB* | (Philippe *et al.*, 2004) |
| pBMM429 | pDS132 plus flanking *rpoS* region Cm$^R$ | This study |
| pBMM429KI | pDS132 plus complete *rpoS* region Cm$^R$ | This study |
| pBMM430 | pDS132 plus flanking *exbD* region Cm$^R$ | This study |
| pBMM431 | pDS132 plus flanking *yfeABCD* region Cm$^R$ | This study |
| pBMM432 | pDS132 plus flanking *feoAB* region Cm$^R$ | This study |
| pBMM437 | pDS132 plus flanking *ftnA* region Cm$^R$ | This study |
| pBMM438 | pDS132 plus flanking *ppxAB* region Cm$^R$ | This study |
| pBMM439 | pDS132 plus flanking *plu4231* region Cm$^R$ | This study |
| pSU2007 | Derivative of R388. GFP, TRA$_W$, IncW, Tp$^R$ Km$^R$ | (Martinez and de la Cruz, 1988) |

## 2.2 Overnight cultures

A single colony of the required bacterial strain was picked from an LB agar plate using a loop and was resuspended in 3 ml of LB broth with appropriate antibiotics in a 30 ml Universal container. The culture was incubated in a shaking water bath at the appropriate temperature overnight.

## 2.3 Nematode cultures

Nematode cultures were maintained by passage through *Galleria mellonella* (Greater Wax Moth) larvae. The nematode strains used in these studies were *Heterorhabditis downesi* K122 (the cognate partner of *P. temperata* K122)

(Stock *et al.*, 2002) or *Heterorhabditis bacteriophora* TT01 (the cognate partner of *P. luminescens* TT01). To infect insect larvae 1000 surface sterilised IJ nematodes were applied in 1 ml PBS to an 8.5 cm Whatman filter circle in a 9 cm Petri dish. Ten *Galleria mellonella* were placed onto the filter paper and the larvae were incubated at 25°C. Insect death occurred after 2-3 days and 14 days post-infection the cadavers were removed and nematodes recovered by placing the cadavers on a White trap (White, 1927) (Fig. 2.1). The White trap is constructed using a 9 cm Petri dish with the lid of a 5.5 cm Petri dish placed in the centre of the larger dish. A 5.5 cm Whatman filter paper is placed within the lid of the 5.5 cm Petri dish lid. PBS is then put into the apparatus to moisten the filter paper and create a moat of PBS in the larger Petri dish. The insect cadavers are then placed into the smaller Petri dish lid and incubated at 25°C. The IJ nematodes leave the cadavers and enter the moat of PBS. The IJs were then transferred to 25 $cm^3$ tissue culture flasks and were stored at 4°C until required.

**Figure 2.1.** White trap with infected insect cadavers placed in the centre and IJ nematodes visible to the eye as milky white texture in the PBS.

## 2.4 Phenotypic characterisation of *Photorhabdus*

### 2.4.1 Growth curves

Overnight cultures were prepared from individual colonies for each strain to be analysed. Cultures were diluted to an $OD_{600}$ of 0.05 in fresh LB medium and

were incubated at 30°C with shaking at 200 rpm. Samples were removed at appropriate time points for $OD_{600}$ measurements using a Spectronic Unicam Helios Gamma spectrophotometer.

### 2.4.2 Siderophore production

*Photorhabdus* strains to be tested were grown overnight and adjusted to an $OD_{600}$ of 1 before 5 µl was spotted onto CAS agar. The CAS solution was prepared by dissolving 60.5 mg chrome azurol S in 50 ml distilled water. This was mixed with 10 ml iron (III) solution (1 mM $FeCl_3.6H_2O$, 10 mM HCl) and the solution was then added slowly, with stirring, to 72.9 g CTAB dissolved in 40 ml distilled water (Schwyn and Neilands, 1987). The resulting 100 ml of CAS solution was autoclaved and transferred into 50 ml sterile Falcon tubes wrapped in foil for storage. This CAS solution was then added in a 1 in 10 ratio to stock molten LB agar before pouring. Approximately 30 ml of blue agar was poured in each 9 cm Petri dish. The plates were incubated at 30°C for 48 h before the orange halos surrounding the *Photorhabdus* colonies were measured.

### 2.4.3 Antibiotic production

*Photorhabdus* strains to be tested were grown overnight and adjusted to an $OD_{600}$ of 1 with fresh LB broth before 5 µl was spotted onto LB agar plates with a minimum of 10 mm between spots. These plates were incubated for 48 h at 30°C. Soft agar (LB broth with 0.75 % added agar) was prepared and cooled to which 1 ml of *Micrococcus luteus* was added per 100 ml. This mixture was then poured over the plate until the spots of *Photorhabdus* were completely covered and the plates left to cool. These plates were incubated for a further 48 h at 30°C and antibiotic production was scored as a zone of inhibition of *M. luteus* growth surrounding the *Photorhabdus* colony.

**Table 2.2** Agar composition

| Agar | Composition per litre $dH_2O$ | | Use |
|---|---|---|---|
| **LB agar (Merck)** | LB Powder (Merck) | 25 g | Routine Culture |
| | Containing: | | |
| | Peptone from casein | 10 g | |
| | Yeast extract | 5 g | |
| | Sodium chloride | 10 g | |
| | Agar (Merck) | 15 g | |
| **Lipid agar** | Nutrient Agar (Oxoid) | 25 g | Symbiosis assays |
| | Yeast extract (BD) | 5 g | |
| | $MgCl_2.6H_2O$ (Fisher) | 2 g | |
| | Corn syrup (Karo) | 10 g | |
| | Cod Liver Oil (Seven Seas) | 5 ml | |
| **Sucrose LB agar** | Tryptone (BD) | 10 g | Directed Knock Out |
| | Yeast extract (BD) | 5 g | |
| | Sucrose (Fisher) | 10 g | |
| | Agar (Merck) | 15 g | |
| **Magnesium LB agar (MgLB)** | Tryptone (BD) | 10 g | Conjugations |
| | Yeast extract (BD) | 5 g | |
| | NaCl (Fisher) | 5 g | |
| | 1M $MgCl_2$ (Fisher) | 1 ml | |
| **CAS agar** | CAS solution 1:10 LB Agar | | Siderophore production |
| **EMB agar** | EMB Powder (Merck) | 36 g | Dye uptake |
| **NBTA** | Nutrient agar (Oxoid) | 28 g | Dye uptake |
| | Bromothymol Blue | 25 mg | |
| | 2,3,5 tetrazolium salt | 30 mg | |
| **BTB** | Nutrient agar (Oxoid) | 28 g | Dye uptake |
| | Bromothymol Blue | 25 mg | |
| **TTC** | Nutrient agar (Oxoid) | 28 g | Dye uptake |
| | 2,3,5 tetrazolium salt | 30 mg | |
| **MacConkey agar No.3** | MacConkey powder (Oxoid) | 51.5 g | Dye uptake |
| **Lipase agar (LIA)** | Nutrient agar (Oxoid) | 28 g | Lipase production |
| | Tween 80 (BDH) | 5 ml | |
| **Protease agar (PIA)** | Nutrient Broth (Oxoid) | 1 g | Protease production |
| | Gelatine (Fisher) | 20 g | |
| | *D*-Glucose (Fisher) | 0.5 g | |
| | Agar (Merck) | 15 g | |
| | pH to 7.2 | | |
| **Soft agar** | LB Powder (Merck) | 25 g | Antibiotic and general overlays |
| | Agar (Merck) | 7.5 g | |

### 2.4.4 Bioluminescence

Colonies of *Photorhabdus* were analysed for light production using the UVP Epi Chemi II Darkroom system set to measure chemiluminescence. The plates were exposed for approximately 5 minutes and images were printed using the Sony Digital Graphic Printer (UP-D890). Bioluminescence was qualitatively scored relative to the wild type. Bioluminescence produced by liquid cultures of *Photorhabdus* was quantitatively monitored by placing duplicate 100 µl aliquots of culture into a black 96 well plate and light production was analysed using the TECAN Genios microplate reader set to measure luminescence.

### 2.4.5 Dye uptake

Dye uptake media was prepared according to the instructions in Table 2.2. Overnight cultures were diluted to an $OD_{600}$ of 1 before 5 µl of each culture was placed onto EMB and NBTA agar. Where required, strains were also tested on BTB, TTC and MacConkey agar. Plates were incubated at 30°C for 48 h before dye uptake was scored.

### 2.4.6 Catalase

Overnight cultures of *Photorhabdus* were diluted to an $OD_{600}$ of 1 before a 10 µl aliquot was added to 10 µl of 3 % $H_2O_2$ on a glass slide. Catalase was scored as the ability of the culture to produce bubbles of $O_2$ gas relative to the wild type control.

### 2.4.7 Lipase

Lipase production was assayed on LIA plates which comprise nutrient agar with 0.5 % v/v Tween 80. Lipase activity was measured by a white halo of precipitate surrounding the *Photorhabdus* colony.

### 2.4.8 Protease

Overnight cultures of the strains of interest were diluted to an $OD_{600}$ of 1 before 5 µl of each culture was placed onto the surface of the PIA agar. Protease activity was scored as a halo of clearing of the opaque medium surrounding the *Photorhabdus* colony.

### 2.4.9 Streptonigrin assay

Cells were grown overnight in LB broth at 28°C and 100 µl of the cell suspension was spread onto the surface of a freshly prepared LB agar plate. Small (13 mm) discs of filter paper (Whatman) were soaked with 50 µl of streptonigrin (400 µg/ml). Therefore each disc contained 20 µg of streptonigrin and the discs were placed on the surface of the LB agar plate. After incubation at 28°C for 48 h the radius of the zone of growth inhibition surrounding the filter disc was measured.

### 2.4.10 Hydrogen peroxide disc assay

The *Photorhabdus* strains of interest were grown in overnight cultures and were diluted to an $OD_{600}$ of 4 and 1 ml aliquots of this standardised culture was then added to 100 ml of cooled soft agar. Approximately 20 ml of this solution was then poured over LB agar plates and was allowed to set. Individual 13 mm Whatman filter discs soaked with 50 µl fresh 30 % (v/v) hydrogen peroxide were added to the centre each of the plates and the plates were incubated at 30°C for 24-48 h before the zone of growth inhibition surrounding the disc was measured.

## 2.5 Transposon Mutagenesis

Mutants in *P. temperata* K122 were generated using the Tn*5* transposon present on the pLOF-Km plasmid (Herrero *et al.*, 1990). Mutants were isolated by conjugating pLOF-Km from *E. coli* S17-1 into *P. temperata* K122 Rif and selecting for $Rif^R$ $Km^R$ exconjugants.

## 2.6 Conjugation of *Photorhabdus*

Overnight cultures were prepared of the *Photorhabdus* strain to be conjugated (i.e. recipient) and the *E. coli* S17-1 strain containing the plasmid for conjugation (i.e. donor). Following overnight growth 50 ml fresh MgLB broth (LB broth supplemented with 1 mM $MgCl_2$) was inoculated 1:100 with the *Photorhabdus* overnight culture in a 250 ml conical flask. Two hours later the donor *E. coli* was inoculated 1:100 into fresh MgLB broth. Both of these cultures were incubated with shaking at 30°C until an $OD_{600}$ of 0.5 was reached. At this point 4 ml of *Photorhabdus* was removed from the culture and spun down at 8,000 rpm, washed gently twice with 1 ml MgLB before the cells were resuspended in 200 µl MgLB broth. At the same time 1 ml of *E. coli* was removed from the culture, spun down at 8,000 rpm, washed gently twice with 1ml MgLB before the cells were finally resuspended in 100 µl MgLB broth. The two washed suspensions were then combined together and mixed gently and the entire 300 µl was pipetted onto the centre of an MgLB agar plate without antibiotics. The culture was then incubated overnight at 30°C. Exconjugants were recovered from the agar plate by applying 3 ml MgLB broth directly to the plate and resuspending the bacteria with a sterile spreader. The resulting bacterial suspension was removed from the agar with a pipette into a 15 ml Falcon tube. 10, 50, 100 and 200 µl of this mixture was then transferred onto fresh selective medium (containing Rif and Km) and spread over the surface of the agar. The rest of the mixture was immediately frozen at -80°C with 20 % (v/v) (final concentration) glycerol for further use. The plates were then incubated at 30°C for 48 to 72 h until the appearance of colonies.

## 2.7 Triparental mating conjugation

To insert Tn*7* into the chromosome of *Photorhabdus,* cultures of *Photorhabdus* (the recipient), *E. coli* S17-1 strain containing the pCIITn*7*K-a plasmid (the donor) and *E. coli* carrying the helper plasmid pUXBF13 (the helper) were grown overnight. Conjugation was carried out as described in Section 2.6 except that, after washing and resuspension, the strains were mixed as

200 µl:100 µl:100 µl (recipient:donor:helper) and the resulting 400 µl was pipetted onto the centre of an MgLB agar plate without antibiotics. After overnight culture at 30°C exconjugants were then recovered from the agar plate by applying 3 ml MgLB broth directly to the plate and resuspending the bacteria with a sterile spreader. The resulting bacterial suspension was removed from the agar with a pipette into a 15 ml Falcon tube. 10, 50, 100 and 200 µl of this mixture was then transferred onto fresh kanamycin rifampicin selective medium and spread over the surface of the agar. Colonies were then re-streaked onto Rif Km plates to ensure the colonies were pure and onto Rif Amp plates to ensure no growth which indicates the successful loss of the ampicillin resistant pUXBF13 helper plasmid. The Tn*7* transposon inserts specifically between the *glmS* and *rpmE* genes in Gram-negative bacteria (Fig. 2.2) Primers RJW122 and RJW123 were used to identify successful insertions by colony PCR.

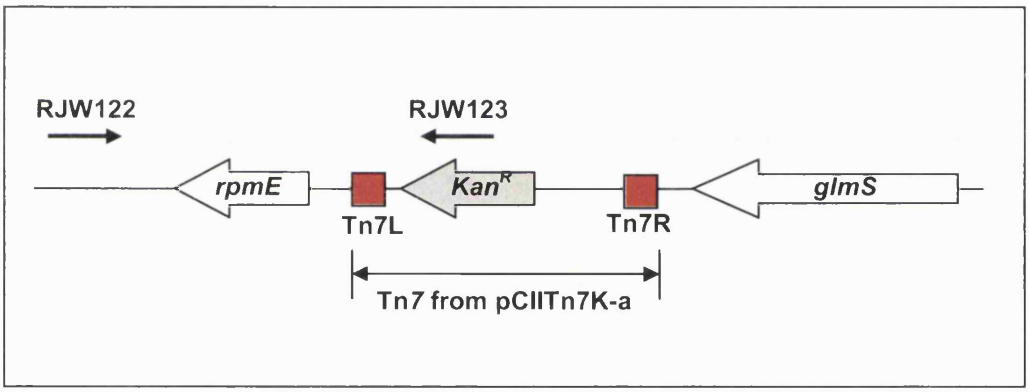


**Figure 2.2** Location of the Tn*7* transposon insertion from pCIITn7K-a. Primers RJW122 and RJW123 for identifying successful insertions also shown.

## 2.8 Polymerase chain reaction (PCR)

PCR was performed with GoTaq (Promega), Pfu (Promega) or KOD (Merck) according to manufacturer's instructions. Unless otherwise stated PCR's were performed with the following reaction conditions; 5min at 95°C; 30 cycles: 1 min at 95°C, 1 min at 55°C, 3 min at 72°C; 7 min 72°C. Colony PCR was

performed by resuspending a single colony in 100 µl sterile water and using 1 µl of this mixture as the template for PCR. PCR products were visualised by electrophoresis on 1 % (w/v) TAE (4.84 g Tris, 1.14 ml acetic acid, 2 ml EDTA pH 8.0 per litre) agarose gels containing 5 µg/ml ethidium bromide in 1x TAE buffer. 1 kb DNA ladder (Promega) was used according to manufacturers instructions and the gels were run at 80 v for 1 hour before the DNA was visualised in a UVP BioDoc-it UV transiluminator.

## 2.9 DNA purification

### 2.9.1 Plasmid DNA

Plasmid DNA was extracted using the Wizard® Plus SV Minipreps DNA Purification System (Promega) or QIAprep Spin Miniprep Kit (Qiagen) according to the manufacturers supplied instructions

### 2.9.2 PCR clean up

DNA was recovered from PCR using the QIAquick PCR Purification Kit (Qiagen) according to the manufacturers supplied instructions.

### 2.9.3 Recovery of DNA from agarose gels

Gel bands were excised from TAE agarose gels and the DNA was extracted using the QIAquick Gel Extraction Kit (Qiagen) according to the manufacturers supplied instructions.

## 2.10 DNA modification

Restriction digestions and ligation reactions were performed according to the manufacturers instructions (NEB and Promega). All DNA was visualised on 1 % TAE agarose gels unless otherwise stated.

## 2.11 Extraction of genomic DNA

Genomic DNA was extracted from the *Photorhabdus* strains of interest using methods adapted from standard procedures (Wilson, 1992). Therefore 3 ml of the *Photorhabdus* strain of interest was grown overnight in a 30 ml universal and the cells were harvested by centrifugation and the supernatant discarded. The pellet was resuspended by repeated pipetting in 567 µl TE buffer (10 mM Tris, 1 mM EDTA, pH 8) and was then transferred into a 1.5 ml eppendorf. 30 µl of 10 % (w/v) SDS and 3 µl of 20 mg/ml proteinase K was added to give a final concentration of 100 µg/m proteinase K in 0.5 % SDS. The sample was mixed thoroughly and incubated at 37°C for 1h. At this point, 100 µl of 5 M NaCl was added and the solutions were mixed thoroughly before 80 µl of preheated CTAB/NaCl solution (10 % (w/v) CTAB in 0.7 M NaCl) was added. The mixture was mixed thoroughly and incubated at 65°C for 10 minutes. An equal volume of 0.7 to 0.8 ml chloroform/isoamyl alcohol (24:1) was added, the solution was mixed and the aqueous and organic phases were separated by centrifugation 13,000 rpm for 5 minutes. The top aqueous layer was removed with care so as not to disturb the white interface layer and transferred into a fresh eppendorf. An equal volume of phenol/chloroform/isoamyl alcohol (25:24:1) was added and the solution was mixed thoroughly. The sample was centrifuged again at 13,000 rpm for 5 minutes. The aqueous supernatant was transferred to a fresh eppendorf and 0.6 volumes of isopropanol was added to precipitate the nucleic acids. The sample was stored at -80°C to aid precipitation for 2-3 h or overnight. The DNA was pelleted by centrifuging the sample at 13,000 rpm for 10 minutes and the pellet was washed with 70% ethanol. The pellet was allowed to air dry before 100 µl sterile water was added to resuspend the DNA. The integrity of the genomic DNA was analysed by agarose gel electrophoresis

## 2.12 Mapping of Tn*5* insertions

Genomic DNA isolated from mutant strains containing Tn*5* insertions was digested with EcoRV (NEB) overnight and was purified by ethanol precipitation. At the same time pBR322 was digested with EcoRV to create compatible sites

for cloning and the vector was dephosphorylated using Calf Alkaline Phosphatase (Promega) to reduce vector re-ligation. Various concentrations of vector and total genomic DNA fragments were ligated together and the resulting ligation mixture was electroporated into EC100 *E. coli* (Epicentre). The transformation mixture was plated onto selective medium using the Km resistance gene present on the Tn*5* transposon as a selective marker (see Fig. 2.3). Therefore, colonies that were Amp Km resistant were selected for overnight growth and plasmid purification. Recovered plasmid DNA was restricted with EcoRV and run on an agarose gel estimate the insert size. Plasmid DNA was sent for sequencing with the pBR-F and pBR-R primers designed at the ends of the pBR322 vector in addition to the Tn5R4 primer designed at one end of the transposon (see Table 2.3 for primer sequences).

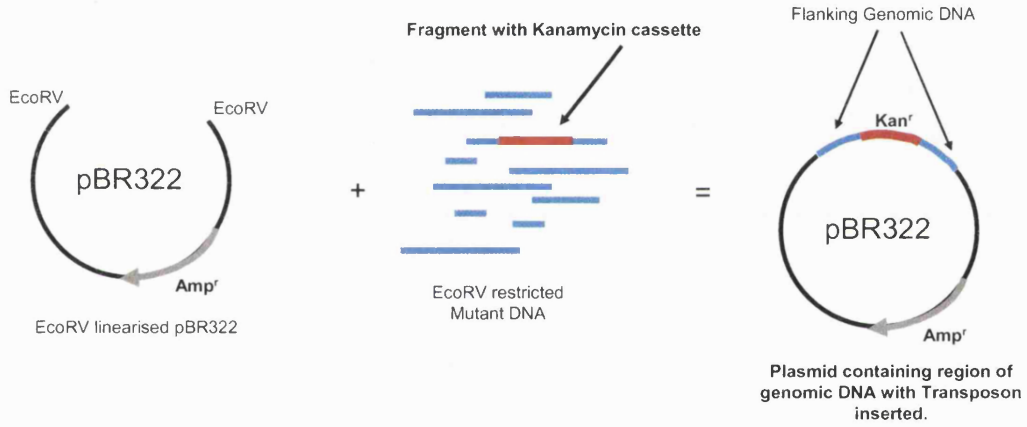


**Figure 2.3** Schematic of the cloning procedure of genomic DNA flanking the transposon insertion

## 2.13 EZ::TN Mutagenesis

Transposon mutagenesis of K122 K12A11 cosmid DNA was carried out using the EZ::TN <TET-1> insertion kit according to the manufacturer's instructions (Epicentre Technologies). The reaction mixture was electroporated into *E. coli* JM109 and the mixture plated onto tetracycline agar to select for successful transposon insertions. Colonies were sent to the University of Bath sequencing

service for preparation and sequencing using the supplied TET-1 FP-1 forward primer and TET-1 RP-1 reverse primer.

## 2.14 Transformation

### 2.14.1 Electroporation of *Photorhabdus*

Electrocompetent cells were prepared by inoculating *Photorhabdus* into 200 ml LB broth from an overnight culture to give an $OD_{600}$ 0.05. *Photorhabdus* was incubated with shaking at 30°C until the culture reached early exponential phase ($OD_{600}$ 0.2) and the culture was then placed on ice for 90 minutes. Cells were then harvested by centrifugation for 10 minutes at 4000 rpm and 4°C. The pellet was resuspended in 200 ml ice cold 1 mM HEPES pH 7.0, 5 % (w/v) sucrose. Cells were harvested again by centrifugation as above and were resuspended in 100 ml, 20 ml and finally 2 ml ice cold 1 mM HEPES pH 7.0, 5 % Sucrose. At this stage 50 µl of the washed cells were combined with 100 ng good quality DNA in an eppendorf on ice before transferring into a pre chilled 2 mm gap electroporation cuvette. The cells were then electroporated at 2.1 kV, 100 Ohms, 25 mFd using the Biorad Micropulser electroporator. Immediately after shocking 1 ml of pre-warmed (30°C) LB broth was added to the cuvette to resuspend the transformed bacteria and the mixture was transferred to a 15ml round-bottomed Falcon tube and incubated with shaking at 30°C for 3 hours. Various dilutions were then plated onto selective media and incubated at 30°C.

### 2.14.2 Electroporation of *E. coli*

EC100 or EC100D *pir*-116 cells were purchased from Epicentre and were used according to manufacturers instructions or cells were prepared from cultures before use. *E. coli* S17-1 or K12 JM109 was grown as an overnight culture and was inoculated 1:100 fresh 500 ml LB. The cells were grown at 37°C with shaking at 200 rpm until mid-exponential phase $OD_{600}$ of 0.5 to 0.7. The cells were harvested by centrifugation at 4,000 rpm for 20 min at 4°C. The supernatant was discarded and the cell pellet was gently resuspended in 500 ml ice-cold

sterile $H_2O$. The cells were harvested again by centrifugation at 4,000 rpm for 20 min at 4°C. The supernatant was discarded and the cell pellet was gently resuspended in 250 ml ice-cold sterile $H_2O$. The cells were harvested again by centrifugation at 4,000 rpm for 20 min at 4°C. The supernatant was discarded and the cell pellet was gently resuspended in 8 ml ice-cold sterile 15 % (v/v) glycerol. The cells were harvested one final time by centrifugation at 4,000 rpm for 20 min at 4°C. The supernatant was discarded and the cell pellet was gently resuspended in a final volume of 800 µl ice-cold sterile 15 % (v/v) glycerol. Aliquots of 50 µl were prepared and used immediately and further aliquots were stored at -80°C until required. Following preparation of fresh cells or defrosting of purchased cells 1-5 µl DNA was mixed with 50 µl cells before electroporation in pre-chilled 2 mm gap cuvettes at 2.5 kV, (setting EC1) using the Biorad Micropulser electroporator. 1 ml pre-warmed LB was added to the cuvette and the cells were gently resuspended before the mixture was transferred to a sterile 14 ml round bottomed tube and was incubated with shaking at 37°C for 1 hour. Aliquots were then spread onto selective media.

## 2.15 Complementation of BMM417 *exbD*::Km

To construct pBMM700 the *exbB* gene from *P. temperata* K122 was amplified using Pfu DNA polymerase (Promega) and the oligonucleotide primers RJW001 and RJW002. The amplification was performed as follows 2 min at 92°C; 35 cycles: 1 min at 92°C, 1 min at 56°C, 6 min at 72°C; 5 min 72°C. RJW001 contains a NcoI restriction site and RJW002 contains a XbaI site to facilitate positional cloning into the pBAD24 vector (Guzman *et al.*, 1995). Therefore *exbB* expression was under the control of the L-arabinose inducible *araBAD* promoter. In the same way pBMM701 (containing the ORF for the *exbD* gene) was constructed using RJW003 and RJW004 and pBMM702 (containing the ORFs for *exbB* and *exbD*) was constructed using RJW001 and RJW004. The plasmids were transformed into *Photorhabdus* by electroporation.

## 2.16 Construction of directed knock out mutants

The directed knock out of *Photorhabdus* genes was performed using a 3 step PCR technique modified from a method used in *Sinorhizobium meliloti* (Ferrieres *et al.*, 2004). Genomic fragments of ~600 bp corresponding to the region immediately upstream and downstream of the gene for deletion were amplified using gene specific primers (Table 2.3) and the KOD Polymerase (Merck) (Fig. 2.4.). Primer sets 1 and 2 were used to amplify the upstream region and primer sets 3 and 4 used to amplify the downstream region. The amplification was performed using standard conditions: 5 min at 95°C; 30 cycles: 1 min at 95°C, 1 min at 60°C, 1 min at 72°C; 7 min 72°C. Primers 2 and 3 are designed with homologous overlapping sequences and this facilitates the annealing of the upstream and downstream fragments together leaving only the 3 bp start codon of the gene along with the 3 bp stop codon, therefore only 6 nucleotides remain of the gene in the knock out fragment. The 600 bp upstream and downstream fragments were then PCR purified to remove any primers and equal quantities of each product were used in the second step primerless PCR step. The primerless PCR has only 10 cycles and was designed to allow the two fragments to anneal at the overlapping homologous region to provide a template for the final step PCR. The amplification was performed as follows: 5min at 95°C; 10 cycles: 1 min at 95°C, 1 min at 50°C, 1 min at 72°C; 7 min 72°C. In the final step 10 µl of the PCR from step 2 was used as a template for amplification using Primers 1 and 4 (Fig. 2.4.). The amplification was performed as follows: 5min at 95°C; 30 cycles: 1 min at 95°C, 1 min at 60°C, 1 min at 72°C; 7 min 72°C. The fragment was gel purified following the step 3 PCR to remove any contaminating fragments. Primer 1 incorporates an SphI site and Primer 4 incorporates a SacI site to allow directional cloning of the fragment into pDS132. The pDS132 plasmid contains the gene for resistance to Cm, the *sacB* gene for negative selection and also contains the RP4 ori that is dependent on the λpir protien for plasmid replication (Philippe *et al.*, 2004).

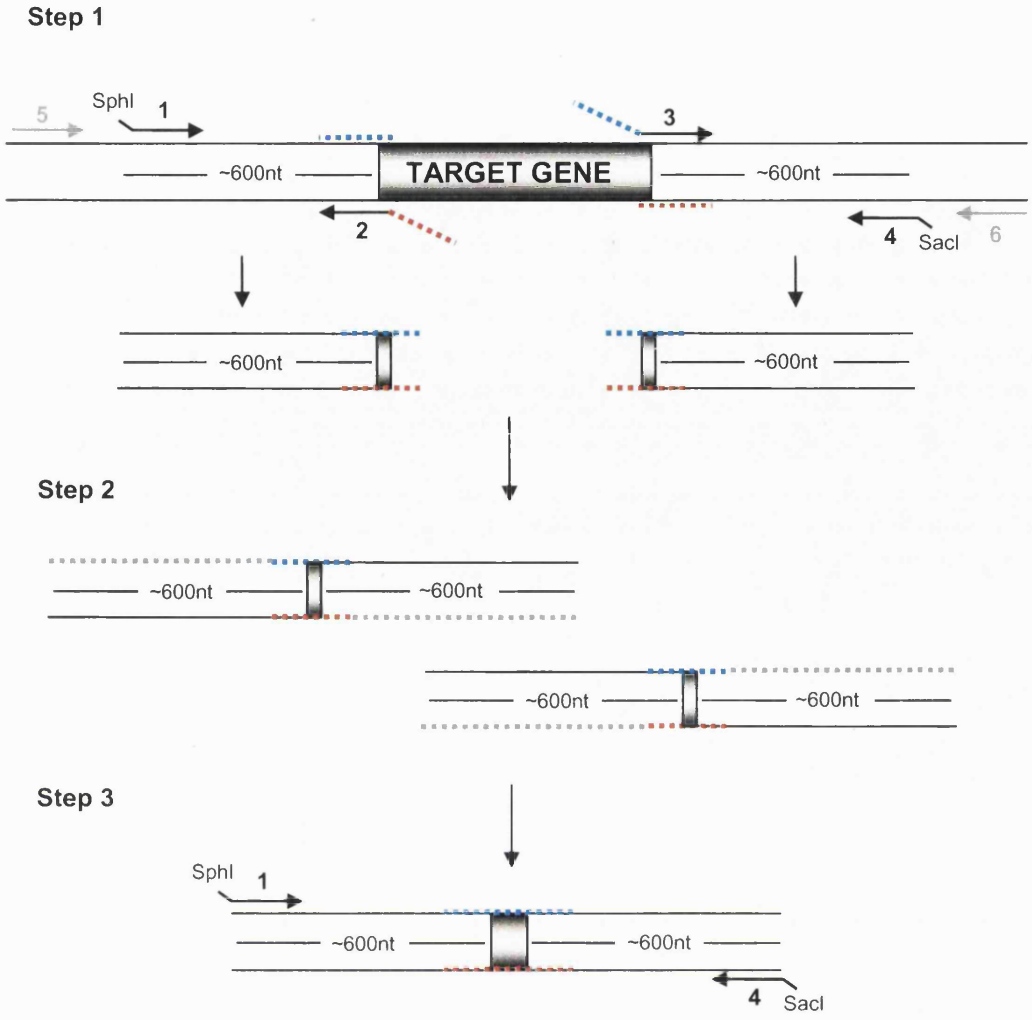


**Figure 2.4.** Schematic of the construction of the knock out fragment. Approximately 600 bp of DNA upstream and downstream of the gene is amplified using primer sets 1+2 and 3+4. Complementary regions in Primers 2 and 3 allow the two fragments to be fused together at step 2 in a primerless PCR. Finally in step 3 Primers 1 and 4 are used to amplify the entire KO fragment which was then cloned into pDS132. Primers 5 and 6 are outside of the 600 bp regions and are used for screening of mutants for the appropriate genotype.

**Table 2.3** Oligonucleotides used in this study

| Oligo | Sequence 5' to 3' | Detail |
|---|---|---|
| RJW001 | TATTTACCATGGCGAAAGGTAATTCACTGCTAAAT | 5' cloning of *exbB* |
| RJW002 | AATAATCTAGATCACCTTGCCTTGCTATTTGCCAAATCCAG | 3' cloning of *exbB* |
| RJW003 | TATTTACCATGGCAATGCGTCTTAATGAAAATTTGGAC | 5' cloning of *exbD* |
| RJW004 | AATAATCTAGATCACTAACCCGATGAAACCGCTTCCATTCC | 3' cloning of *exbD* |
| RJW115 | TTATGCATGCGGTGATTGCTTCTGTTATTACTT GG | Directed KO of *exbD* |
| RJW116 | GAATCAGTGACAATTACATAAGTCACCTTGTCTTG | Directed KO of *exbD* |
| RJW117 | CAAGGTGACTTATGTAATTGTCACTGATTCTTCC | Directed KO of *exbD* |
| RJW118 | TTATGAGCTCGCCAACCAATTTGCCTCTGCCCTAC | Directed KO of *exbD* |
| RJW122 | CCATCTCCCTTTGTTAGTGAC | Tn7 insertion identification |
| RJW123 | GGTTGTATTGATGTTGGACG | Tn7 insertion identification |
| RJW130 | GGTTCAGCATTGGCTGATACAGC | Identification of *exbD* KO |
| RJW131 | GCCAATTGAAAATGTAACTCGC | Identification of *exbD* KO |
| RJW132 | TTATGCATGCGTCAAGTTCACAATAACAATGTCTG | Directed KO of *ppxAB* |
| RJW133 | GGCTTTTTTATTCACATTTATATATATCC | Directed KO of *ppxAB* |
| RJW134 | GGATATATATAAATGTGAATAAAAAAGCC | Directed KO of *ppxAB* |
| RJW135 | TTATGAGCTCGCCATCACAGTAATACAGGTTGTGC | Directed KO of *ppxAB* |
| RJW140 | GCACACTTACTGAAATGTCAGG | Identification of *ppxAB* KO |
| RJW141 | CCACCACATCATAATATCG | Identification of *ppxAB* KO |
| RJW155 | TTATGCATGCGCTCATAGAGAACTATGTGACTGG | Directed KO of *ftnA* |
| RJW156 | GAATTAATTCCATTTCATTACATAATAGATACTCC | Directed KO of *ftnA* |
| RJW157 | GTATCTATTATGTAATGAAATGGAATTAATTCACC | Directed KO of *ftnA* |
| RJW158 | TTATGAGCTCCGTGAAGCGACAAAGAACATACAGC | Directed KO of *ftnA* |
| RJW163 | TTATGCATGCGCAAAGGAATCGATACTAAAGC | Directed KO of *plu4231* |
| RJW164 | CTAATCATTTTCACATTGATATATACCTTTCATGG | Directed KO of *plu4231* |
| RJW165 | GGTATATATCAATGTGAAAATGATTAGCAGGG | Directed KO of *plu4231* |
| RJW166 | TTATGAGCTCGACATTTCCTTGTTAAATGACATGC | Directed KO of *plu4231* |
| RJW167 | TTATGCATGCCGTAGTAAAAGCGGGTGATATCG | Directed KO of *feoAB* |
| RJW168 | GCTAATCATTTTCAATTCCTACATATGACCTTCCG | Directed KO of *feoAB* |
| RJW169 | CGGAAGGTCATATGTAGGAATTGAAAATGATTAGC | Directed KO of *feoAB* |
| RJW170 | TTATGAGCTCCCAAAACGCTTCTCTTAGAAGATGC | Directed KO of *feoAB* |
| RJW171 | TTATGCATGCGGTTATCAATACCTGCCAGATGC | Directed KO of *yfeABCD* |
| RJW172 | CCCTTTTTGTTACATAAATTCAAACC | Directed KO of *yfeABCD* |
| RJW173 | GGTTTGAATTTATGTAACAAAAAGGGTTATATCTG | Directed KO of *yfeABCD* |
| RJW174 | TTATGAGCTCGGTGTTGAAGTTTGTTACTTATAGC | Directed KO of *yfeABCD* |
| RJW175 | GGATTTCAAGATGGATTGC | Identification of *ftnA* KO |
| RJW176 | CCTTGTTCACTACACCATGC | Identification of *ftnA* KO |
| RJW181 | GCTTATACTAATACAGCTATCC | Identification of plu4231 KO |
| RJW183 | GCTCATCATATCTGAATCTGAGC | Identification of plu4231 KO |
| RJW184 | GGTTTAGTTCATATCTCTTCG | Identification of *feoAB* KO |
| RJW186 | CGAATGCAAGAGGTTAAACG | Identification of *feoAB* KO |
| RJW187 | CGATCTGCATTAAAAGTACG | Identification *yfeABCD* KO |
| RJW189 | GCTTGGTCATCCAGCGAAGC | Identification *yfeABCD* KO |
| RJW190 | TAATTAAGCTTCGTCAATGGGTGCGGCTGATAGC | pBMM4291.8 cloning of *rpoS* + 800bp *nlpD* |
| RJW191 | TATAAGCTTGCCAAACTATTCAACAATTAAGTACG | pBMM4291.8 cloning of *rpoS* + 800bp *nlpD* |
| RJW205 | TAATTACTAGTCGTCAATGGGTGCGGCTGATAGC | pCIITn7K-a cloning of *rpoS* + 800bp *nlpD* |
| RJW206 | TATACTAGTGCCAAACTATTCAACAATTAAGTACG | pCIITn7K-a cloning of *rpoS* + 800bp *nlpD* |
| RJW207 | TATTTATCTAGAGATTCTCAATCAACTAATGC | *rpoS* knock-in complementation |
| RJW208 | TAAATAGCATGCTTATTGACGCGTCGTTTAGG | *rpoS* knock-in complementation |
| RJW216 | GCAGACTTTGAGGACCGGTAGTAGC | Identification of *rpoS* KO/KI |

| | | |
|---|---|---|
| RJW218 | GTGACACAACTCTCAATTATTTTCG | Identification of *rpoS* KO/KI |
| pBR-F | GTCATCCTCGGCACCGTCACCCTGG | Sequencing of isolated DNA in pBR322 |
| pBR-R | CCAAAGCGGTCGGACAGTGCTCCGAG | Sequencing of isolated DNA in pBR322 |
| Tn5R4 | CCGTTGCGCTGCCCGGATTACAGCC | Sequencing of isolated DNA from Tn5 transposon |
| ExbDFor | CTGCGTAAATCGGGC | Colony blot probe |
| ExbDRev | ACGCAGAATTTTTGATTTCAT | Colony blot probe |
| HB015 | GTTATGAGCCATATTCAACG | Southern blot Kan probe |
| HB016 | TCGAGCATCAAATGAAACTGC | Southern blot Kan probe |
| rpoS knockout 1 | TATTTAGCATGCGATTCTCAATCAACTAATGC | Directed KO of *rpoS* |
| rpoS knockout 2 | GCCAAACTATTCAACAATTACATAAGCTGCCCC | Directed KO of *rpoS* |
| rpoS knockout 3 | GGGTAGGGGCAGCTTATGTAATTGTTGAATAG | Directed KO of *rpoS* |
| rpoS knockout 4 | TAAATAGAGCTCTTATTGACGCGTCGTTTAGG | Directed KO of *rpoS* |
| TET1 FP1 | GGGTGCGCATGATCCTCTAGAGT | Sequencing EZ:TN TET |
| TET1 RP1 | TAAATTGCACTGAAATCTAGAAATA | Sequencing EZ:TN TET |

Sequences underlined are restriction sites.

The fragment and vector were ligated together and was electroporated into EC100D *pir*-116 (Epicentre) and positive clones were selected on LB Cm agar. These clones were then selected and plasmid DNA extracted for restriction digestion confirmation of successful knock out insert ligation. Clones confirmed as containing the correct size insert were then transformed into *E. coli* S17-1λpir by electroporation and successful clones were then selected for conjugation into *Photorhabdus* (see section 2.6) Exconjugants were selected on Rif Cm agar indicating a successful single cross over where the entire plasmid had integrated into the genome. Several of these colonies were re-streaked onto fresh Rif Cm agar plates to ensure the purity of the *Photorhabdus* strain. Several colonies were selected for overnight growth in MgLB broth with no selection to encourage the vector to recombine out of the genome (Fig. 2.5). Various dilutions of the overnight cultures were plated onto LB agar containing 0.2 % sucrose to counter select for strains which still contained the plasmid. Colonies that were able to grow on sucrose agar were then replica plated onto sucrose agar and LB Cm agar to ensure only colonies with the correct profiles were selected ($Suc^R$ $Cm^S$) for colony PCR screening. The colony PCR was performed with the following reaction conditions: 10 µl Promega GoTaq green buffer, 2 µl 25 mM $MgCl_2$, 1 µl 25 mM dNTP's. 1 µl 100 pmol/µl upstream primer 5, 1 µl 100 pmol/µl downstream primer 6, 33.5 µl $H_2O$, 1 µl colony template, 0.5 µl GoTaq

polymerase. The amplification was performed as follows: 5 min at 95°C; 30 cycles: 1 min at 95°C, 1 min at 55°C, 3 min at 72°C; 7 min 72°C. Successful gene knock out strains were identified by a reduced sized PCR product compared to the wild type with Primers 5 and 6 (Fig. 2.5).

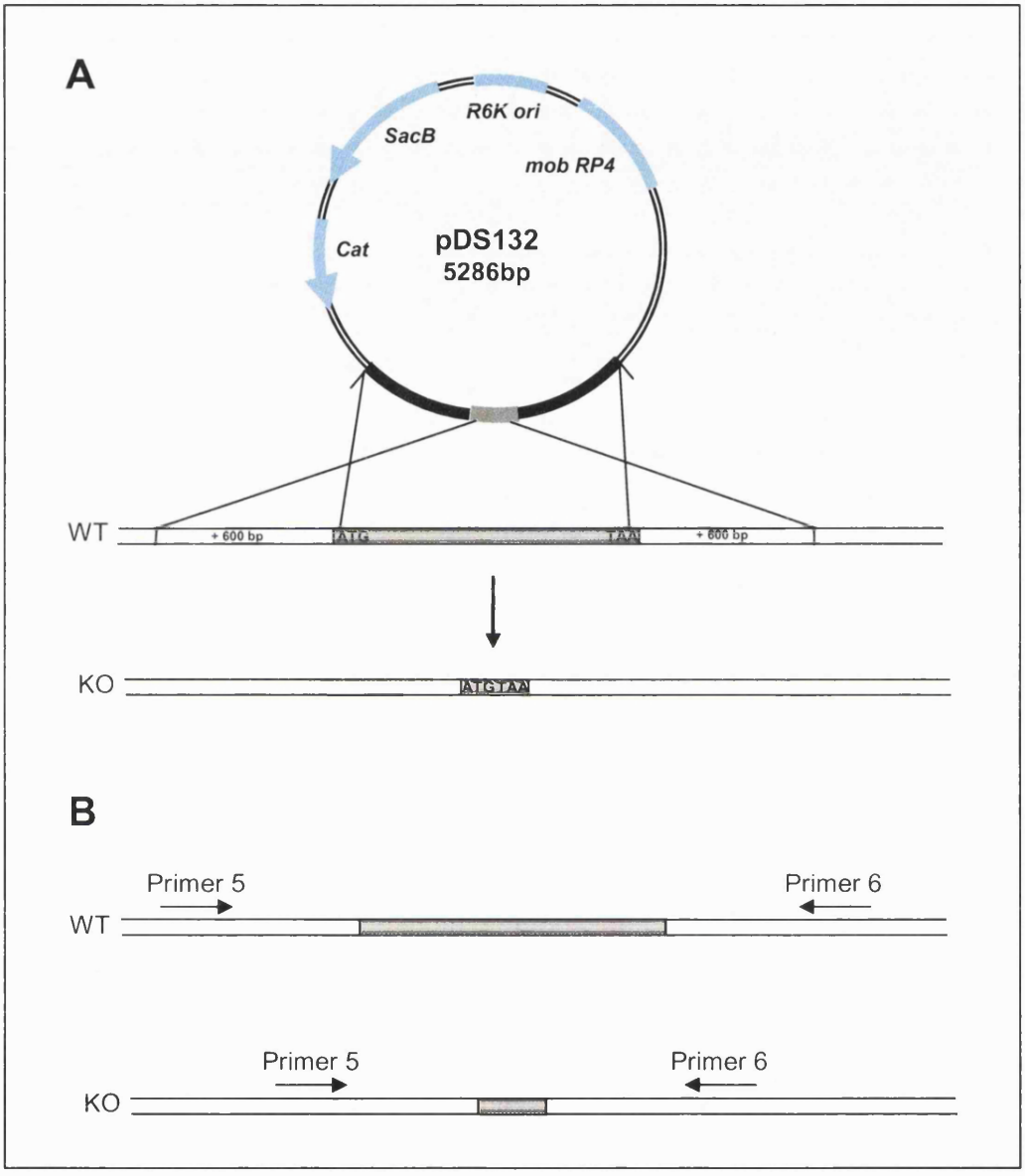


**Figure 2.5.** Schematic of the directed knock out procedure in *Photorhabdus*. A. The knock out fragment was cloned into pDS132 and the plasmid transferred into *Photorhabdus* by conjugation. Allelic exchange results in the production of both knock out alleles (KO) and wild type alleles (WT). B. Knock out (KO) mutants can be distinguished from wild type (WT) by the size of the PCR fragment using Primers 5 and 6.

## 2.17 Pathogenicity Assays

### 2.17.1 Virulence of *Photorhabdus* by injection

The *Photorhabdus* strains to be tested were grown overnight and 1 ml was harvested by centrifugation at 13,000 rpm for 1 minute and the bacteria were washed twice in PBS. The $OD_{600}$ was taken and the strain was resuspended in PBS to a final $OD_{600}$=1, an optical density that is equivalent to 2 x $10^8$ cfu/ml (Clarke, 1993). The cell suspension was diluted to a final concentration of $10^4$ cfu/ml and an aliquot of 10 µl (containing 100 cfu) was injected directly into each of 10 *G. mellonella* larvae from a 100 µl Hamilton syringe and the infected larvae were incubated at 25°C. Insects were monitored at regular intervals and death was assessed by whether larvae responded to gentle prodding with plastic forceps. The $LT_{50}$ was calculated as the time taken for 50 % of the insect larvae to die by taking the average of three readings from individual graphs of the data.

### 2.17.2 *Photorhabdus In vivo* growth rate

To determine the *in vivo* bacterial growth rate of K122, BMM417 and BMM417/pBMM702 100 cfu of the appropriate bacterial strain was injected into each of 50 *G. mellonella* larvae. At regular time intervals 5 insect larvae were surface sterilised with 100 % ethanol, placed in 10 ml LB in a sterile universal and homogenised using 4 mm sterile glass beads. The homogenate was then diluted and aliquots were spread on LB agar plates with the appropriate antibiotic selection. In this way the viable count of the bacteria at each time point was determined during infection of the insect larvae. The data points for each bacterial strain were then analysed using Excel and the slope of the best-fit line through the data points was used to calculate the growth rate of the bacteria.

### 2.17.3 Infection of insects by *Heterorhabditis*

IJ nematodes isolated from symbiosis assays were surface sterilised by washing with 0.4 % (w/v) hyamine and 3 washes with sterile PBS. The IJs were counted

in 5 µl aliquots and the sterilised nematodes were diluted to give 1000 nematodes per ml and 1 ml of this suspension was placed onto an 8.5 cm Whatman filter disc in a Petri dish. 10 *Galleria mellonella* insect larvae were added and the plate was incubated at 25°C. Insects were monitored at regular intervals and death was assessed by whether larvae responded to gentle prodding with plastic forceps. If required the insects were placed on White traps after 14 days to recover the IJs.

## 2.18 Symbiosis assays

### 2.18.1 Surface sterilisation

Infective juvenile (IJ) nematodes greater then 3 weeks old isolated from insect infection stocks were surface sterilised in 0.4 % (w/v) hyamine (Sigma-Aldrich) for 15 minutes and were washed three further times in sterile PBS to remove any traces of hyamine.

### 2.18.2 Nematode growth and development

*In vitro* symbiosis assays were performed using lipid agar plates (Dunphy and Webster, 1989) (see Table 2.2). Lipid agar was inoculated with 50 µl from an overnight culture of the appropriate bacteria spread in a Z formation and incubated at 30°C for 72 h before 50 surface sterilised IJ nematodes were added. The plates were sealed with parafilm and were further incubated at 25°C. Nematode growth and development was monitored over 21 days using a Nikon SMZ1500 stereo light microscope. IJ nematodes were recovered at the end of the symbiosis assay by washing the lid of the Petri dish with sterile PBS and the IJ nematodes were transferred to a 25 $cm^3$ tissue culture flask for further use or storage at 4°C.

### 2.18.3 Colonisation of *Heterorhabditis* by *Photorhabdus*

IJ nematodes recovered from the symbiosis assays were surface sterilised and individual IJ nematodes were selected under the microscope and transferred into 100 µl PBS in a 1.5 ml eppendorf. The IJ was homogenised for 1 minute using a

pellet pestle and motor (Kontes) and 50 µl of the homogenate was spread onto the surface of a single LB agar plate and incubated at 30°C for 72 h. The level of *Photorhabdus* colonisation of the nematode was determined by counting the number of CFU multiplied by 2. For each strain tested 10 individual IJs were crushed and the homogenate plated unless otherwise stated.

## 2.19 Determination of whole-cell total iron content

Bacteria were grown on the appropriate lipid agar plates for 72 h at 28°C and the bacterial biomass was recovered by scraping the bacteria off the surface of the plate. This biomass was transferred to a 15 ml centrifuge tube and was resuspended in 15 ml sterile PBS. The cell pellet was harvested by centrifugation at 4,000 rpm for 15 minutes and the supernatant discarded. The harvested bacteria were washed twice in PBS containing 0.5 mM EDTA to remove any surface contaminating divalent cations. The bacterial pellet was snap frozen in liquid nitrogen and freeze-dried overnight and the dry weight of the collected cells was recorded. The dry pellet was then resuspended in 4 ml of 30 % nitric acid and heated to 85°C overnight. The cleared solution was then analysed for total iron content using the atomic adsorption spectroscopy service at the University of Reading.

## 2.20 Southern hybridisation (Sambrook et al., 1989)

A volume of the mutant DNA, at a concentration of 40 µg used for the hybridisation was restricted with 60 units of EcoRV restriction enzyme. RNase (1 µg/ml) was present in the reaction to remove any contaminating RNA present. 1 % TAE agarose gels were prepared and 20 µl of each mutant DNA was added into the wells, along with one lane of molecular weight marker and 2 µl of 1 in 100 diluted kanamycin probe as a control. The gels were run at 80 v for approximately 1 hour, and photos were taken ensuring that the ruler was included for band size identification. The gels were then placed in an appropriate amount of denaturing solution (1.5 M NaCl, 0.5 M NaOH) in a dish on a tilting table for 30 minutes. The solution was discarded and a further volume of denaturing solution added for 15 minutes. The denaturing solution was discarded and a

volume of neutralisation solution (1 M TRIS pH 7.4, 1.5 M NaCl) was added and left on the tilting table for 30 minutes. This solution was then discarded and a fresh volume of neutralising solution added for a further 15 minutes. The treated gels were then transferred to nitrocellulose membrane (Hybond-$N^+$, Amersham Pharmacia) by capillary hybridisation overnight using a Southern blotting technique based on capillary transfer using 20x SSC (175.3 g NaCl, 88.2 g $Na_3Ci$ /l pH7.0). The membranes were exposed to UV to cross link the DNA to the membrane in the crosslinker @ 1200 Joules. The membrane was prehybridised for 1 hour in Church solution (1 mM EDTA pH 8.0, 0.25 M sodium phosphate buffer pH 7.2, 7 % (w/v) SDS) at 60°C. A radioactive probe corresponding to the kanamycin cassette from the Tn*5* transposon was prepared using the random labelling method and $\alpha^{32}P$ dATP with primers HB015 and HB016. The probe was allowed to hybridise to the membrane for 12-14 hours. The membrane was washed once with 2x SSC for 20 minutes at 55°C. The solution was discarded and the membrane was washed with 0.2x SSC, 0.5 % SDS for 20 minutes at 60°C. The membranes were then exposed to film for various lengths of time to give optimum exposure.

## 2.21 Colony hybridisations

A cosmid bank was transferred in duplicate onto two LB amp plates at identical sites. The plates were incubated at 37°C overnight. A 9 cm circular nitro-cellulose filter was placed on top of the colonies. The filter absorbed the liquid from the top of the plate and the position of the first colony was marked with a pencil. The filter was then removed carefully and applied, with tweezers to the following solutions in Petri dish lids, taking care not to allow any solution on top of the filter. The filters were floated on top of the drops of liquid in the Petri dish lids for the required amount of time (Fig. 2.6). Once the filters had been passed through the washes the filter was carefully blotted underneath to remove excess liquid and the filters were exposed to UV at 1200 Joules to crosslink the DNA to the membrane. The membranes were then incubated in a hybridisation bottle with 15 ml of pre-warmed Church solution for 1 hour at 65°C. The probe was then added to the hybridisation bottle and hybridisation was performed

overnight. A radioactive probe corresponding to an internal fragment of *exbD* was prepared using primers ExbDFor and ExbDRev by the random labelling method and α32P dATP. Following pre-hybridisation and probing the fluid was discarded and the membrane was washed with 2x SSC 0.5 %, SDS at 60°C. The filters were then wrapped in plastic and were exposed to autoradiograph film for the desired length of time.

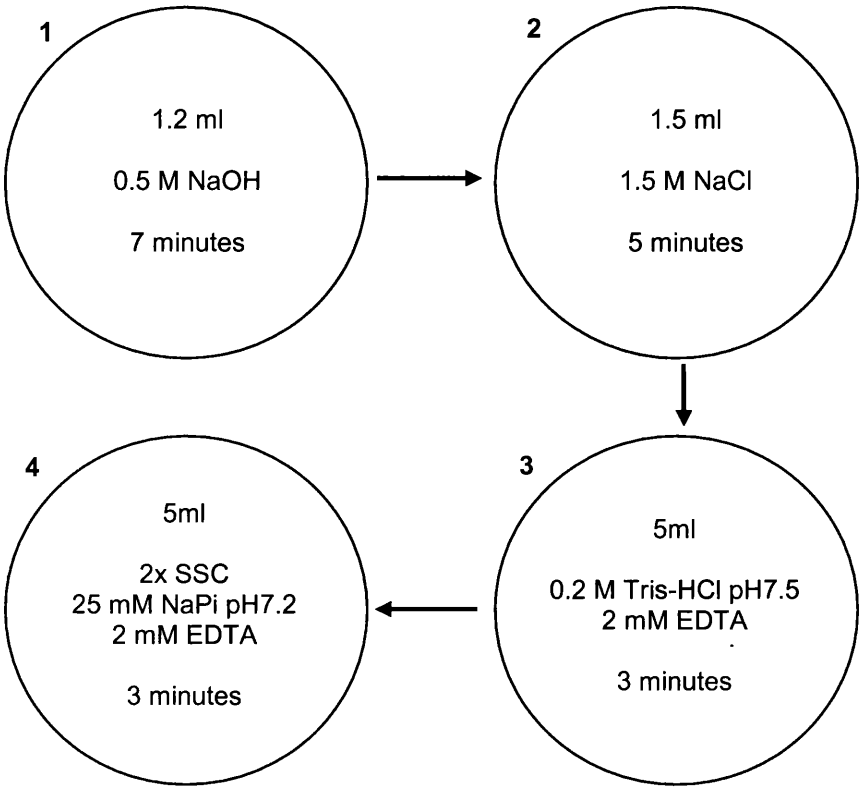


**Figure 2.6** Schematic of the washing steps and incubation times for colony blots.

# Chapter 3

# Identification and characterisation of siderophore mutants in *Photorhabdus*.

## 3.1 Introduction

Part of this work has been published in Molecular Microbiology 2005.
**Watson, R.J., Spencer, G.V., Joyce, S.A. and Clarke, D.J.** The *exbD* gene of *Photorhabdus temperata* is required for full virulence in insects and symbiosis with the nematode *Heterorhabditis*. Molecular Microbiology 56(3), 763–773.

*Photorhabdus* has a complex lifestyle switching from an insect pathogen to a symbiont of nematodes. Not only does the *Photorhabdus* kill the insect host, but it converts the insect into *Photorhabdus* biomass which the nematodes use as food to grow and develop before finally the *Photorhabdus* recolonise the gut of the specialised infective juvenile (IJ) stage nematodes. It is likely that regulation of gene expression will play a role in controlling the interactions between *Photorhabdus* and its invertebrate hosts and this chapter set out to identify the role of a key nutrient, iron, in the lifecycle of *Photorhabdus*.

Iron is an essential element in many living organisms as it forms a core part of many metabolic enzymes. Ratledge and Dover (2000) suggest that the acquisition of iron may be the major determinant whether a micro-organism can establish an infection. Therefore the role of iron homeostasis in the regulation of interactions between *Photorhabdus* and its eukaryotic hosts was investigated.

Iron can exist in two forms, ferrous ($Fe^{2+}$) and ferric ($Fe^{3+}$), with most of the iron present in the environment in the oxidised ferric form due to the presence of oxygen. Ferric iron is almost insoluble under aerobic conditions therefore iron generally exists in biological systems complexed to proteins which increase solubility for transport and usage. Bacteria have evolved specialist mechanisms to acquire this iron from the environment, and one of the major ways they achieve iron uptake is to produce, excrete and transport low molecular weight

molecules called siderophores. These molecules have a higher binding affinity for iron than environmental binding proteins resulting in the bacterial siderophores stealing the iron in order to deliver it back to the bacteria.

Siderophore production and its subsequent uptake has been shown to be essential for maintaining iron homeostasis in several organisms including *Y. pestis* (Bearden *et al.*, 1997), *P. aeruginosa* (Meyer *et al.*, 1996) and the marine bacterium *Vibrio vulnificus* (Litwin *et al.*, 1996). Therefore, in order to study *Photorhabdus* iron metabolism, random transposon mutants were created and screened for differences in siderophore production.

## 3.2 Results

### 3.2.1 Siderophores

Siderophores are low molecular weight compounds secreted by micro-organisms that bind iron with high affinity. In order to detect bacterial siderophore production a colorimetric assay can be performed (Schwyn and Neilands, 1987). Chrome Azurol S (CAS) is a dye that, when bound to iron, is a blue colour. However when a strong chelator is present, such as a siderophore, the colour changes from blue to orange as the iron is removed from the dye. When *P. temperata* K122 is grown on LB agar containing CAS (LB-CAS agar), an orange halo is produced around the colony following incubation for 48 h at 28°C indicating that under these conditions, siderophores are being produced (Fig. 3.1).

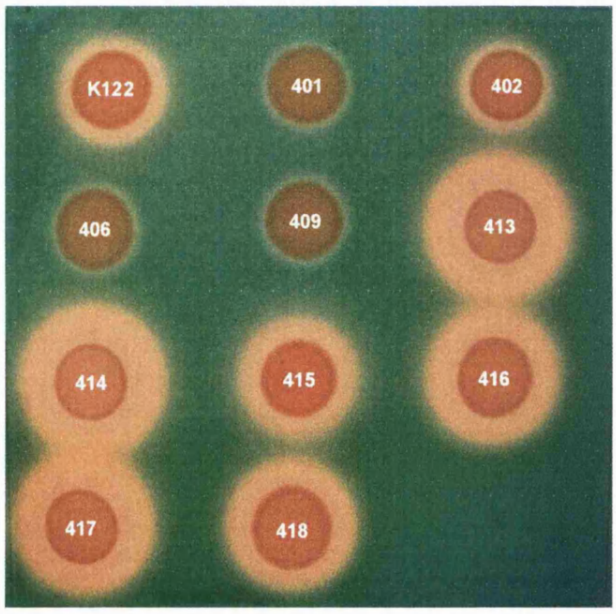


**Figure 3.1.** Siderophore production by K122 WT and all 10 transposon mutants. Overnight cultures were diluted to an OD 1 and 5 µl of each strain spotted onto LB-CAS agar. The plate was then incubated for 48 h at 28°C

### 3.2.2 Generation of siderophore mutants

In order to obtain strains of *P. temperata* that produced altered levels of siderophore a library of random transposon mutants was constructed using pLOF-Km as described in Materials and Methods. Approximately 600 independent transposon mutants were screened on LB-CAS agar for altered halo sizes (Spencer, 2001). In total 10 mutants were identified that showed altered siderophore production compared to the wild type (Fig. 3.1). Four of these mutants (BMM401, BMM402, BMM406 and BMM409) did not produce any siderophore (no halo on LB-CAS agar) and six mutants (BMM413-BMM418) produced an increased amount of siderophore (increased halo size on LB-CAS agar) (Fig. 3.1).

### 3.2.3 Identification of site of transposon insertion

Genomic DNA was isolated from each mutant and a Southern blot was performed using the kanamycin cassette as a probe, to confirm the presence of a single transposon insertion in each of the mutants (Fig. 3.2). Based on the fragment size differences the Southern blot appeared to suggest 5 genetically different mutants. The site of the transposon insertion was then identified by cloning the Km resistance cassette and flanking genomic DNA into pBR322, as described in Materials and Methods. The location of insertion was precisely mapped by DNA sequencing performed at the University of Bath sequencing service using primers pBR-F and pBR-R designed at the ends of pBR322 and primer Tn5R4 from the kanamycin cassette of the Tn*5* transposon. Homology analysis was performed on the sequences using the tblastx algorithm at the NCBI. The sequencing analysis revealed that several of the mutants identified had an insertion in the same gene. Therefore, BMM401, BMM402, BMM415, BMM416 and BMM417 were retained for further analysis (Table 3.1). BMM418 was discarded from any further analysis as the sequencing data revealed only pLOF-Km vector sequence.

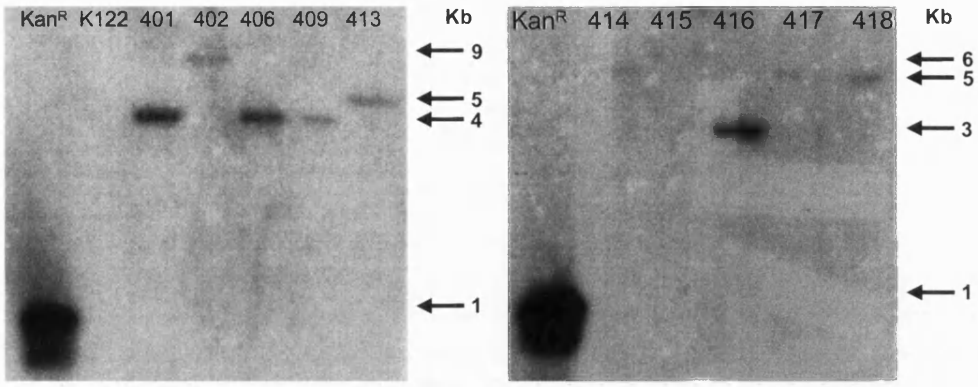


**Figure 3.2.** Southern blot analysis of genomic DNA from siderophore mutants. DNA was restricted with EcoRV enzyme and probed with a radioactive kanamycin probe complementary to the Km cassette on the Tn*5* transposon.

Three of the mutants, BMM401, BMM415 and BMM416 were identified as insertions in a siderophore locus that has been previously shown to be required for the production and uptake of the siderophore photobactin in *P.luminescens* NC19 (see Fig.3.3) (Ciche *et al.*, 2003). The insertion in the non-producing mutant BMM401 was identified to be in a gene, *phbC*, predicted to encode isochorismate synthase, a protein required for the production of the 2,3-dihydroxybenzoic acid moiety, a key molecule which is a characteristic for the catechol class of siderophores. In *P. luminescens* NC19 the *phbC* gene is immediately upstream from three genes, *phbE*, *phbB* and *phbA,* therefore it is possible that the expression of these genes has also been affected. These genes (*phbE, phbB and phbA*) show homology to *entE*, *entB* and *entA* respectively from *E. coli* where they are involved in production of the mature enterobactin molecule (Raymond *et al.*, 2003). The phenotype of BMM401 (*phbC*) (i.e. no siderophore production) suggests that photobactin is the major siderophore produced by *P. temperata* K122 under the conditions of the screen used in this study.

In BMM415 the insertion was identified in *phbF*, a gene predicted to encode a non-ribosomal peptide synthase (NRPS). It would be expected that this NRPS is involved in the production of the mature photobactin and it is possible that the mutation results in the production of an altered photobactin molecule that can still bind iron but is not recognised by the bacteria resulting in an overproduction phenotype.

Mutant BMM416 was identified as an insertion in *phuD*, a gene predicted to encode a permease that would be expected to be involved in the uptake of the photobactin-associated iron across the cytoplasmic membrane (Ciche *et al.*, 2003). In both BMM415 and BMM416 the siderophore hyper-producing phenotype may be due to defective siderophore uptake resulting in a build up of photobactin in the medium.

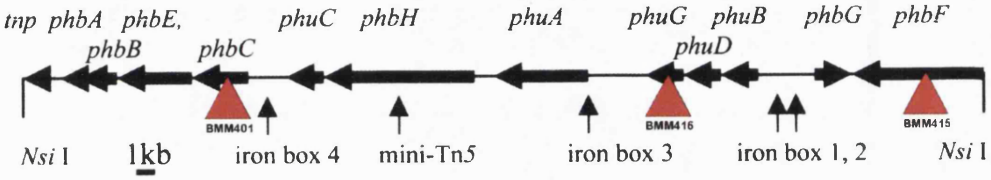


| Gene | Gene Length (bp) | Location | Direction | Product |
|---|---|---|---|---|
| *tnp* | 607 | 1..607 | - | putative transposase TnpA |
| *phbA* | 759 | 1107..1865 | - | putative 2,3-dihydro-2,3-dihydroxybenzoate dehydrogenase PhbA |
| *phbB* | 876 | 1867..2742 | - | putative 2,3-dihydro-2,3-dihydroxybenzoate synthase PhbB |
| *phbE* | 1644 | 2729..4372 | - | putative 2,3-dihydroxybenzoate-AMP-ligase PhbE |
| ***phbC*** | **939** | **4410..5348** | **-** | **putative isochorismate synthase PhbC** |
| *phuC* | 840 | 5870..6709 | - | ABC-transport protein PhuC |
| *phbH* | 3087 | 6809..9895 | - | nonribosomal peptide synthetase PhbH |
| *phuA* | 2061 | 10084..12144 | - | putative photobactin outer membrane receptor precursor PhuA |
| ***phuD*** | **969** | **12783..13751** | **-** | **putative cytoplasmic permease PhuD** |
| *phuG* | 1053 | 13843..14895 | - | putative cytoplasmic permease PhuG |
| *phuB* | 1041 | 14919..15959 | - | periplasmic binding protein PhuB |
| *phbG* | 1311 | 16360..17670 | + | putative photobactin biosynthesis protein PhbG |
| ***phbF*** | **3044** | **17733..20777** | **-** | **nonribosomal peptide synthetase PhbF** |

**Figure 3.3** Location of transposon insertions shown on the photobactin operon from *P. luminescens* NC19. Red triangles represent transposon insertions. Adapted from Ciche *et al.* (2003).

BMM402 was identified as a transposon insertion in *pfkA* which encodes 6-phosphofructokinase isozyme I which is an enzyme involved in the glycolysis and gluconeogenesis cycles. These pathways lead in to the phenylalanine, tyrosine and tryptophan biosynthesis pathways which produce chorismate. Chorismate is an essential starting component of many siderophores including enterobactin (Raymond *et al.*, 2003). Therefore it seems reasonable that the lack of photobactin siderophore production by BMM402 may be due to reduced availability of chorismate.

**Table 3.1** K122 Transposon Mutants.

| Mutant | CAS phenotype[a] | Gene disrupted | Encoded protein |
|---|---|---|---|
| BMM401 | No halo | *phbC*[b] | Isochorismate synthase |
| BMM402 | No halo | *pfkA* | Phosphofructokinase isozyme I |
| BMM406 | No halo | *phbC*[b] | Isochorismate synthase |
| BMM409 | No halo | *phbC*[b] | Isochorismate synthase |
| BMM413 | Hyper | *exbD* | ExbD |
| BMM414 | Hyper | *exbD* | ExbD |
| BMM415 | Hyper | *phbF*[b] | Non-ribosomal peptide synthase |
| BMM416 | Hyper | *phuD*[b] | ATP-dependent permease |
| BMM417 | Hyper | *exbD* | ExbD |
| BMM418 | Hyper | *N/A* | pLOFKm vector sequence only |

a: phenotype on LB-CAS agar
b: genes in the photobactin operon from *P. luminescens* NC19 (acc: AY042783).

The remaining mutant, BMM417, was isolated as a hyper-producer of siderophore (see Fig. 3.1). Characterisation of this mutant revealed that the transposon was inserted in a gene predicted to encode a protein with strong homology to ExbD from other Gram-negative bacteria. The transposon was inserted between nucleotides 369 and 370 of the 423bp open reading frame (ORF) predicted to encode ExbD. The insertion has been mapped towards the C terminus of the 141 amino acid protein between codon 123 and 124 (Arg123 and Lys124). ExbD is a component of the TonB complex (composed of TonB, ExbB and ExbD) that facilitates the uptake of siderophores and other molecules (e.g. vitamin $B_{12}$ and colicins) across the gram negative outer membrane (Postle and Larsen, 2007). Therefore an insertion in *exbD* may completely abolish or

severely reduce the active transport of molecules that rely on TonB-dependent outer membrane receptors resulting in a build up of siderophore in the media.

### 3.2.4 Phenotypic characterisation of siderophore mutants

To ensure the transposon insertions did not have pleiotropic effects the five selected mutants were all compared to the wild type K122 for pigmentation, colony morphology, bioluminescence, antibiotic production, lipase, protease and catalase production and dye absorption. In all cases the mutants showed a similar phenotype to wild type except for the altered level of siderophore production (Table 3.2).

**Table 3.2** Phenotypic tests on selected mutants

| Test | **K122** | **BMM401** | **BMM402** | **BMM415** | **BMM416** | **BMM417** |
|---|---|---|---|---|---|---|
| Siderophore production | ++ | - | - | ++++ | ++++ | ++++ |
| Pigmentation | Orange | Orange | Orange | Orange | Orange | Orange |
| Colony Morphology | Convex, mucoid | Convex, mucoid | Convex, mucoid | Convex, mucoid | Convex, mucoid | Convex, mucoid |
| Bioluminescence | +++ | +++ | +++ | +++ | +++ | ++++ |
| Antibiotics | +++ | +++ | +++ | +++ | +++ | +++ |
| Lipase | +++ | +++ | +++ | +++ | +++ | +++ |
| Protease | +++ | +++ | +++ | +++ | +++ | +++ |
| Catalase | +++ | +++ | +++ | +++ | +++ | +++ |
| Dye Uptake EMB | Purple | Purple | Purple | Purple | Purple | Purple |
| NBTA | Purple | Purple | Purple | Purple | Purple | Purple |
| BTB | Green | Green | Green | Green | Green | Green |
| TTC | Red | Red | Red | Red | Red | Red |

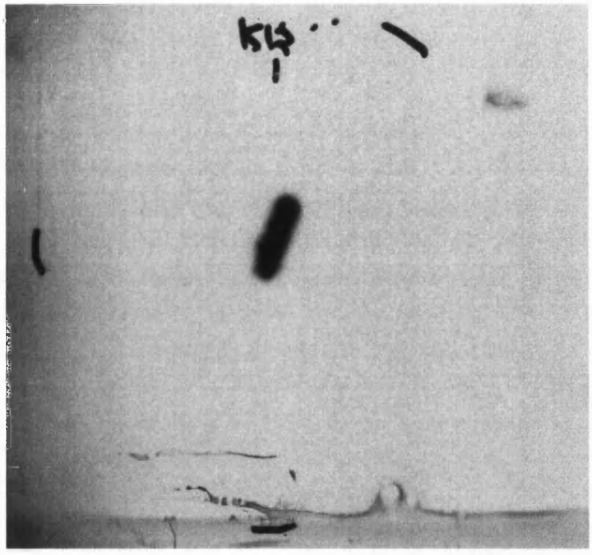

**Figure 3.4.** Colony blot of *P. temperata* K122 cosmid bank 12. Colony blots were probed with a radioactive *exbD* fragment probe and were exposed to autoradiograph film. Cosmid A11 was identified as positive for the *exbD* genomic region.

### 3.2.5 Identification of the genetic region surrounding *exbD*

The genome of *Photorhabdus temperata* K122 has not been sequenced, therefore in order to identify the genetic region around the transposon insertion in *exbD* (BMM417) a cosmid library of K122 chromosomal DNA was screened by colony hybridisation (see Materials and Methods), and in this way cosmid A11 was identified (Fig. 3.4). This cosmid was prepared for sequencing by inserting primer sites using the Epicentre EZ-TN <TET-1> Transposon insertion kit (see Materials and Methods). The cosmid was sent to the University of Bath sequencing service and the sequences assembled using the Lasergene SeqManII program. After preliminary analysis the *exbD* gene was found on a 5589 bp DNA contig. This sequence was submitted to GenBank with the accession number AY453591. The DNA surrounding the transposon insertion site in BMM417 revealed that, as expected, the *exbD* gene is found immediately downstream from the *exbB* gene and it is likely that these genes are co-transcribed, as is the case in other bacteria (see Fig. 3.7). Immediately upstream from *exbB* an ORF was identified with strong homology to *metC*, encoding cystathionine betalyase involved in amino acid metabolism and sulphur and nitrogen metabolism. Downstream from *exbD* an ORF (Pht001) predicted to encode a membrane protein with unknown function was identified. This gene is immediately

upstream from two further genes. The *attA* gene is predicted to encode an argininosuccinate lyase which is involved in arginine biosynthesis and *attC* is predicted to encode a phosphoribosylglycinamide formyltransferase involved in purine biosynthesis.

### 3.2.6 Pathogenicity of selected mutants

In order to identify any defects in the pathogenic interaction between *Photorhabdus* and the insect pathogenicity assays were performed with the five selected mutants (see Materials and Methods). As expected the injection of 100 cfu of wild type K122 resulted in the death of all the insects within 48 h (see Table 3.3). On the other hand, after 48 h, all of the insects injected with BMM417 were still alive. Even after 72 h only 30 % of the insects had been killed by BMM417 (Table 3.3). The remaining mutants BMM401, BMM402, BMM415 and BMM416 all killed the insects in the same time as the wild type K122 suggesting that photobactin is not required for pathogenicity (Table 3.3).

**Table 3.3** Pathogenicity tests on selected mutants.

| | 24h | 48h | 72h |
|---|---|---|---|
| K122 WT | 0 % | 100 % | 100 % |
| BMM401 | 0 % | 90 % | 90 % |
| BMM402 | 0 % | 100 % | 100 % |
| BMM415 | 0 % | 100 % | 100 % |
| BMM416 | 0 % | 100 % | 100 % |
| BMM417 | 0 % | 0 % | 30 % |

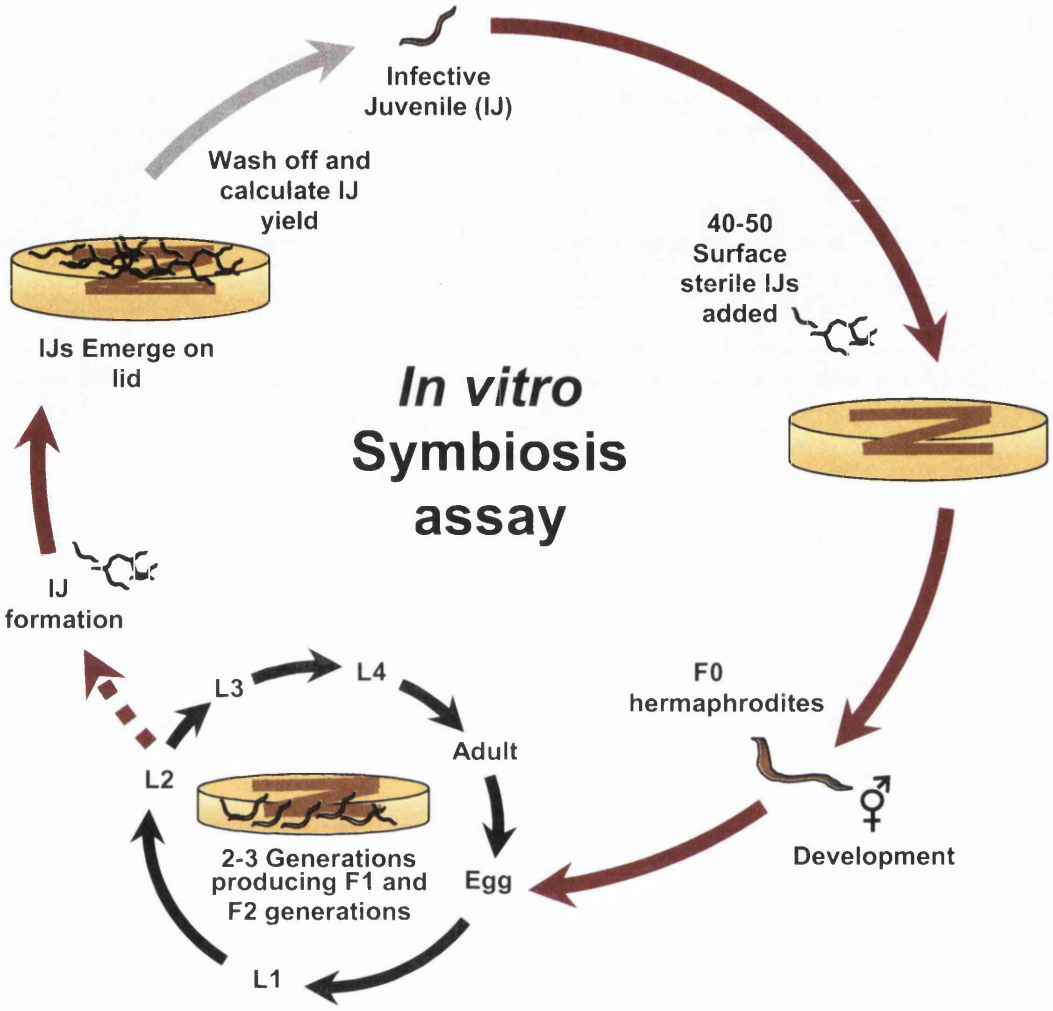


**Figure 3.5** *In vivo* symbiosis assay. *Photorhabdus* is streaked onto lipid agar in a 'Z' formation and is incubated at 30°C for 72 h. 40-50 surface sterilised IJ nematodes are then added and the plates sealed and incubated at 25°C for 21 days. Nematode growth and development is monitored using a stereo dissecting light microscope.

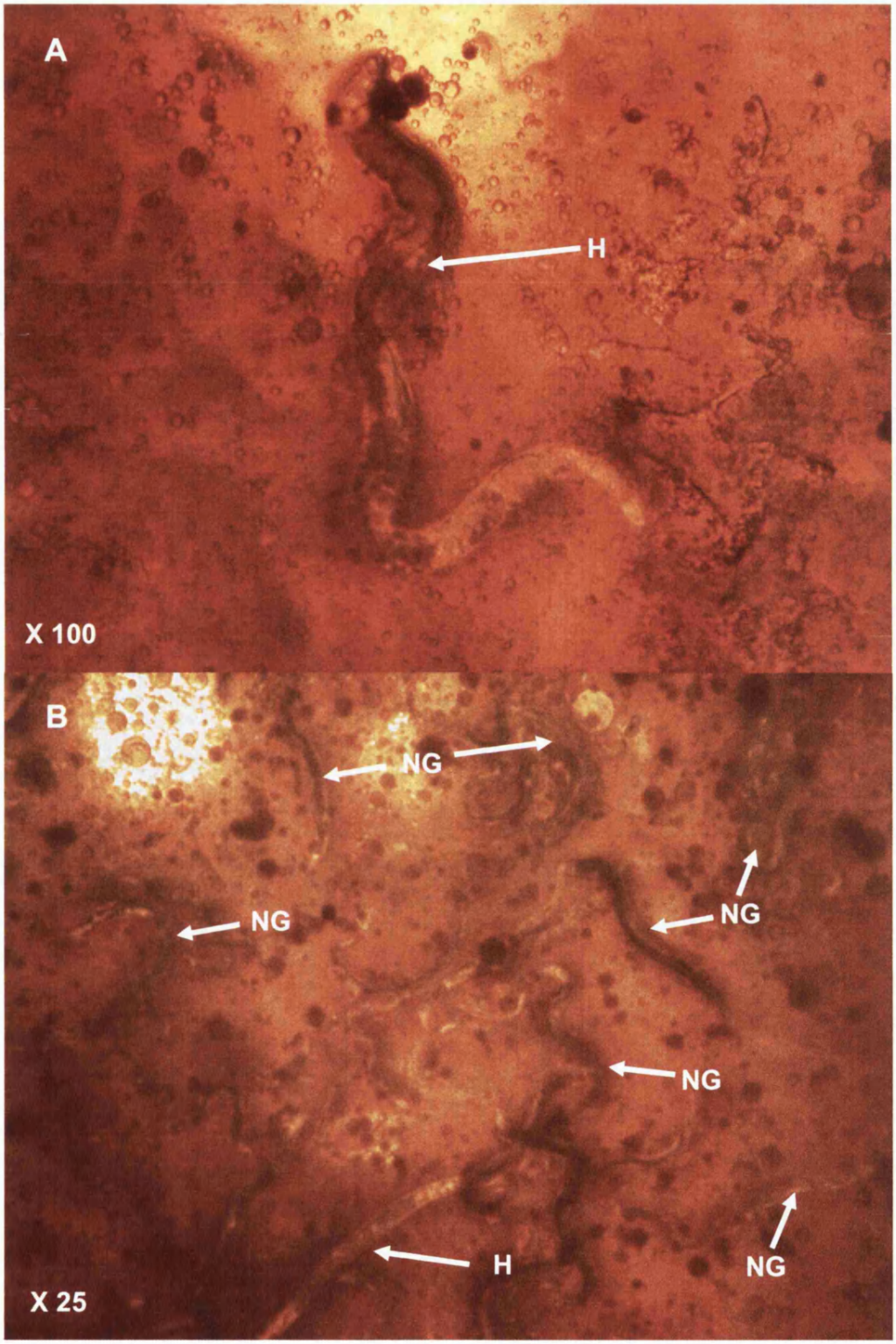


**Figure 3.6** Images of nematode development on lipid agar. **A**. Typical *H. downesi* hermaphrodite following 7 days incubation on lipid agar. **B**. First (F1) and second generation (F2) mixed population of nematodes typically seen after 14 days. Images were captured using a Nikon Coolpix 995 digital camera and a Nikon SMZ1500 stereo light microscope. H= hermaphrodite. NG = F1/F2 generations. Arrows highlighting examples of nematodes.

### 3.2.7 Symbiosis of selected mutants

The siderophore mutants were also tested for their ability to support nematode growth and development *in vitro*. All strains were put onto lipid agar and *in vitro* symbiosis assays were performed as described in Materials and Methods (Fig. 3.5). Interestingly BMM417 appeared to have a lighter pigmentation compared to all of the other strains (Fig. 3.14). In *Y. pestis* dark brown pigmentation is produced by the absorption of sufficient exogenous iron-containing haemin into the cell (Perry *et al.*, 1990). The haemin storage locus (*hms*) was able to restore pigmentation to a spontaneous *Y. pestis* pigmentation chromosomal deletion mutants (Pendrak and Perry, 1993). Therefore absorption of sufficient quantities of iron containing compounds has been shown to have a pigmentation phenotype in other bacteria. The symbiosis plates were observed under a light microscope for the recovery of IJ stage nematodes to hermaphrodites and nematode growth and development which is a measure of the success of the bacteria in promoting nematode reproduction (see Fig. 3.6). A further measure of the success of the bacteria to support nematode growth and development is the number of IJ nematodes produced at the end of the assay divided by the original number of IJs added and this metric is called the IJ yield.

**Table 3.4.** Symbiosis assays with selected mutants

| | IJ recovery to hermaphrodite[a] | Nematode growth and development[b] | IJ formation after 21 days |
|---|---|---|---|
| K122 WT | +++ | +++ | +++ |
| BMM401 | +++ | +++ | +++ |
| BMM402 | +++ | +++ | +++ |
| BMM415 | +++ | +++ | +++ |
| BMM416 | +++ | +++ | +++ |
| BMM417 | +++ | + | - |

a: Hermaphrodite nematodes were counted after 7 days
b: Nematode growth and development was scored as the presence of mixed populations at 14 days

Interestingly BMM417 (*exbD*) showed a defect in its ability to support nematode growth and development beyond the hermaphrodite stage. Indeed only these F0 stage hermaphrodites could be detected in the symbiosis plates. Finally after 21 days the IJs that had been produced on the symbiosis plates were washed from the lids and IJ yields were compared to wild type K122 (Table 3.4). All of the other mutants BMM401, BMM402, BMM415 and BMM416 were fully able to support all stages of symbiosis implying that the photobactin siderophore was not involved in the interaction with the nematode. However, no IJs were found on plates that contained BMM417 (Table 3.4). Therefore, it is clear that *exbD* is required for both pathogenicity and symbiosis of *P. temperata*

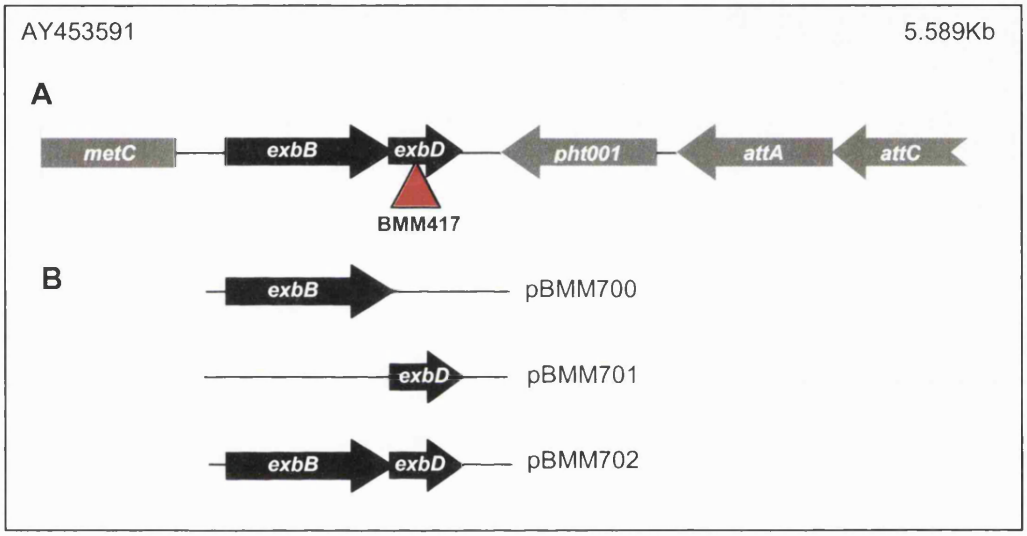


**Figure 3.7 A.** The *exbBD* locus in *P. temperata* K122.The site of transposon insertion in *exbD* is indicated and the 5.6 Kb DNA sequence has been deposited in Genbank (accession number AY453591). **B.** The inserts of the plasmids used to complement the BMM417 mutation are shown.

### 3.2.8 Complementation of the mutation in BMM417

To ensure that the siderophore hyper production phenotype of BMM417 was due to the insertion of the transposon into the *exbD* gene, several plasmids were constructed, pBMM700 (*exbB*), pBMM701 (*exbD*) and pBMM702 (*exbBexbD*) (Fig. 3.7). These plasmids are derived from pBAD24 and the expression of the cloned gene(s) is under the control of the arabinose inducible $P_{BAD}$ promoter (Guzman *et al.*, 1995). These plasmids were transformed into BMM417 and the level of siderophore production was observed on LB-CAS agar with or without

arabinose (Fig. 3.8). The presence of pBMM701 (*exbD*) in BMM417 rescued siderophore production to wild type levels when induced by arabinose and moderately reduced siderophore production without induction. This clearly demonstrates that the siderophore overproduction in BMM417 was due to the insertion in the *exbD* gene. In support of this it is clear that the presence of pBMM702, which expresses both the *exbB* and *exbD* genes, also restores the level of siderophore production in BMM417 to wild type levels. On the other hand the presence of pBMM700 (*exbB*) in BMM417 only reduced the level of siderophore slightly when induced by arabinose suggesting that the function of ExbB and ExbD may be partially redundant in TonB shuttling. pBMM702 (*exbBexbD*) is able to complement siderophore production levels to wild type without the requirement for induction, therefore pBMM702 in BMM417 was selected for any further complementation analysis as there was no requirement for addition of exogenous arabinose inducer.

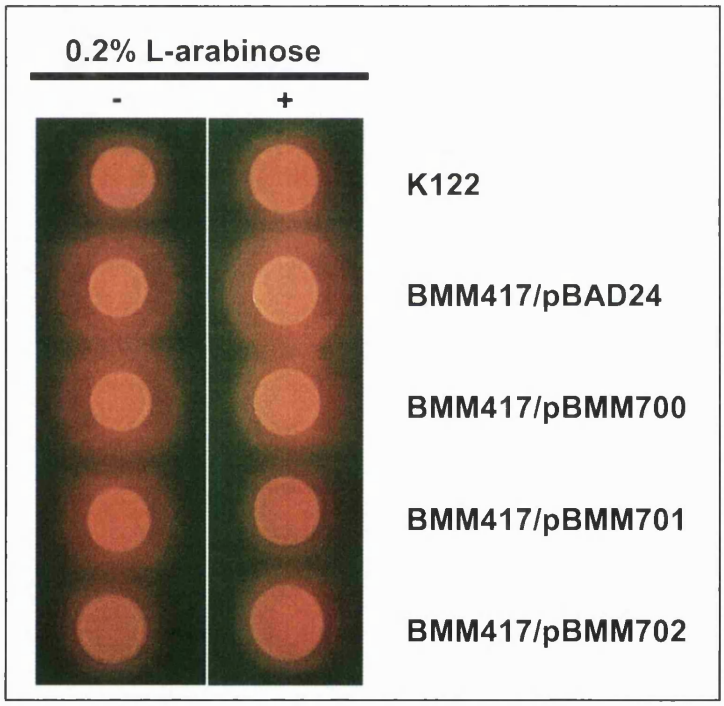


**Figure 3.8** Complementation of the siderophore hyper-production phenotype in BMM417. *Photorhabdus* K122 or BMM417 containing the different plasmids, as indicated, were grown overnight at 28°C in LB broth and, after adjusting the $OD_{600}$ of the culture to 1, 10 µl of cell suspension was spotted onto LB-CAS agar, with or without added L-arabinose, as indicated.

### 3.2.9 Iron acquisition by BMM417

It would be expected that BMM417 would be crippled for all TonB-dependent siderophore uptake systems. Therefore, this mutant should be affected in its ability to scavenge iron in an environment where iron is limiting. When BMM417 is grown in LB medium the growth rate is similar to that of the parental strain suggesting that free iron is not limiting in LB broth (Fig. 3.9). However when the free iron in LB is chelated by the addition of 100 µm 2,2'-dipyridyl (DIP), an $Fe^{2+}$ iron chelator, the growth rate of BMM417 is much reduced compared to the parental strain or BMM417/pBMM702 (Fig. 3.9). This suggests that BMM417 is unable to scavenge iron from low iron environments and this is dependent on the *exbD* gene as the plasmid pBMM702 can rescue the growth defect.

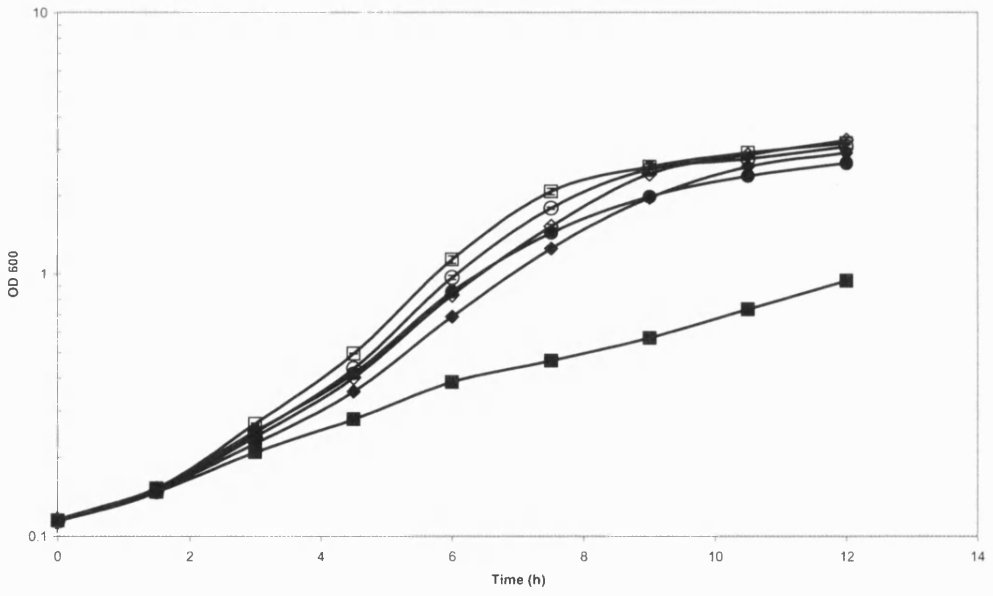


**Figure 3.9** The growth of BMM417 is sensitive to iron levels in the medium.
*P. temperata* K122 (diamonds), BMM417 (squares) and BMM417/pBMM702 (circles) was grown overnight in LB broth and inoculated (1:100) into fresh LB broth (open symbols) or LB broth supplemented with 100 µM DIP, a strong chelator of ferrous ($Fe^{2+}$) iron (filled symbols). Growth of the bacteria at 28°C was measured by following the $OD_{600}$ of the culture over time.

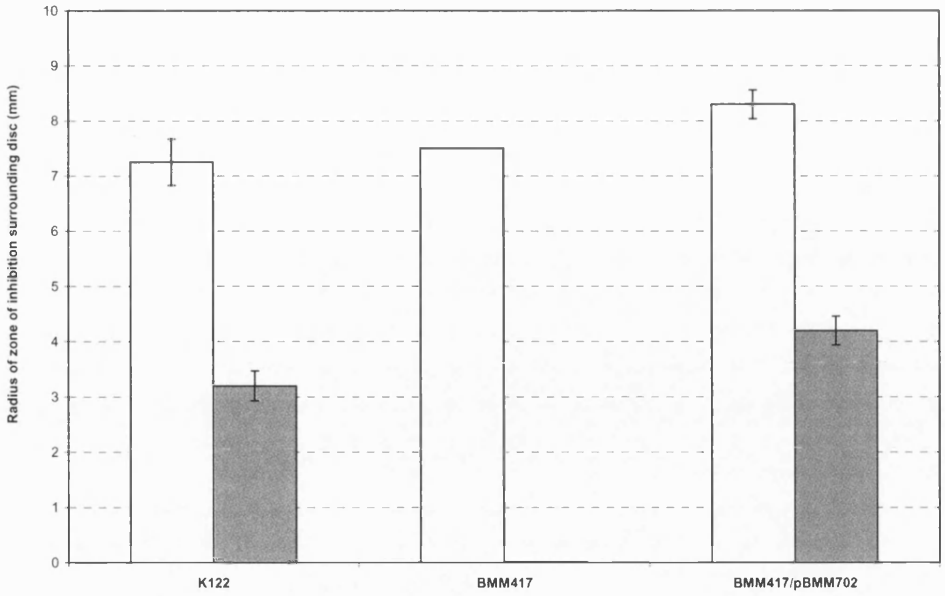


**Figure 3.10** Level of resistance of K122, BMM417 and BMM417/pBMM702 to the antibiotic streptonigrin. *Photorhabdus* was grown overnight at 30°C in LB broth and an aliquot was spread onto fresh LB agar plates (white columns) or LB agar plates supplemented with 100 μM DIP (grey columns). 13 mm filter paper discs containing 20 μg streptonigrin were placed on the surface of the agar and the plates were incubated at 30°C for 48 h. 5 plates were used for each strain and the average of the radius of the zone of growth inhibition surrounding the disc is presented. The error bars represent the standard deviation (S.D.).

The antibiotic streptonigrin can be used as an indicator of the levels of iron within a cell because it requires iron in order to be active. Therefore if iron levels are reduced the cell will be more resistant to streptonigrin (Yeowell and White, 1982). K122, BMM417 and BMM417/pBMM702 were cultured overnight in LB broth and an aliquot of the overnight culture was spread on LB media. A 13 mm Whatman filter disc was impregnated with 20 μg streptonigrin and placed in the centre of the plate and the plates were incubated at 30°C for 48 h before the radius of growth inhibition surrounding the disc was measured (Fig. 3.10) When the bacteria were grown on LB agar the radius of zone of antibiotic inhibition was similar for the wild type and BMM417, suggesting that when iron is present at excess concentrations in LB media it is readily available to all strains. When the iron in LB agar was chelated by the addition of 100 μM of DIP chelator K122 and BMM417/pBMM702 have a smaller halo (3.2 mm and 4.2 mm) compared to that observed in the absence of DIP (7.25 mm and 8.3 mm) indicating that these cells contain less iron. When BMM417 was grown under these iron chelated conditions this mutant appears to be completely resistant to

the streptonigrin antibiotic as BMM417 was able to grow right up to the streptonigrin disc. Therefore, when excess iron is removed from the LB agar by DIP chelator, the level of internal iron appears greatly reduced in BMM417 when compared to wild type cells (Fig. 3.10). These data are in agreement with the growth rate data (Fig. 3.9) and suggests that in low iron environments BMM417 is unable to scavenge for iron.

### 3.2.10 Pathogenicity of BMM417

Most organisms, including insects, maintain very low levels of free iron by the sequestration of iron by various host-produced proteins (Locke and Nichol, 1992). BMM417 clearly grows poorly in an environment where free iron is not readily available and it might be expected that BMM417 would be unable to grow when introduced into insect larvae. This poor growth could explain the reduced virulence of BMM417 and to test this, final instar larvae of the Greater Wax Moth, *Galleria mellonella* were injected with 100 cfu of either K122 or BMM417 and the insects were incubated at 28°C. As expected K122 killed the insects with an $LT_{50}$ of 54.5 h (Table 3.5). Interestingly, BMM417 also killed all of the injected insects but the $LT_{50}$ was 99.2 h. When BMM417 was complemented with the pBMM702 plasmid the $LT_{50}$ returned to a level similar to the parental strain (Table 3.5). Therefore, BMM417 is clearly less virulent than the wild type *P. temperata* K122 and this reduction is dependent on the *exbD* gene as pBMM702 can rescue the pathogenicity defect of BMM417.

**Table 3.5** $LT_{50}$ and *in vivo* doubling times of K122, BMM417 & BMM417/pBMM702.

| Strain | $LT_{50}$ (h) ± S.D.[a] | *In vivo* doubling time (h) ± S.D.[b] |
|---|---|---|
| K122 | 54.5 ± 2.2 (1.0) | 1.9 ± 0.3 (1.0) |
| BMM417 | 99.2 ± 7.8 (1.82) | 3.4 ± 0.4 (1.79) |
| BMM417/pBMM702 | 56.3 ± 1.0 (1.03) | 2.2 ± 0.3 (1.15) |

a: the values presented are the mean of 3 experiments ± standard deviation. The numbers in parentheses are the relative $LT_{50}$ values compared to K122.
b: the values shown are the mean of the doubling times calculated in three independent experiments ± standard deviation (S.D.). The values in parentheses are the relative doubling times compared to K122.

### 3.2.11 *In vivo* growth of BMM417

It has been shown previously that an $LT_{50}$ of *Photorhabdus* is closely correlated with the growth rate of the bacteria (Clarke and Dowds, 1995). To test whether the *in vivo* growth rate of BMM417 was slower than the parental strain, insects were injected with K122, BMM417 or BMM417/pBMM702, and the doubling times of these bacteria were monitored during growth in the insect larvae (see Materials and Methods). In this way the *in vivo* doubling time of K122 was calculated at 1.9 h (Table 3.5). This is similar to the doubling of the bacteria in LB broth ($t_d$=1.4h) indicating that *P. temperata* can grow very well in the insect. However, BMM417 has a calculated *in vivo* doubling time of 3.4 h, approximately twice that of the parental strain. This defect was complemented by the expression of *exbD* from pBMM702 (see Table 3.5). Therefore, *exbD* is required for normal bacterial growth *in vivo* and the growth of BMM417 is probably restricted by the limited availability of iron in the insect.

### 3.2.12 Exogenous iron in pathogenicity

BMM417 shows a slower *in vivo* growth rate and this can be complemented by expression of the *exbD* gene from pBMM702. This evidence suggests that iron uptake is important for *Photorhabdus* pathogenicity, however this is assuming that iron is the key molecule that is not being transported in BMM417. Many bacteria encode *exbD*-independent iron acquisition systems which allow iron uptake when there is sufficient iron in the environment. Therefore it seemed possible that the pathogenicity defect might be rescued by co-injection of high levels of iron with the bacteria. To determine the maximum concentration of iron that could be injected per insect without affecting insect viability 10 µl of various concentrations of $FeCl_3$ between 1 mM to 1 M were injected into *G. mellonella* larvae. The maximum concentration that did not cause insect death was 100 mM. To determine the final concentration of iron injected into the insect the volume of insect hemolymph was estimated. This was achieved by freeze drying 10 individual *Galleria* insect larvae to remove any water from the insects. Therefore

assuming that most of the water within the insect was present in the hemolymph the decrease in weight after freeze drying was used to approximate the hemolymph volume. In this way the average weight difference was calculated as 179.4 mg +/- 23 (S.D.) per insect. Therefore the approximate volume of hemolymph was calculated at 200 µl and the final concentration of $FeCl_3$ in the hemolymph after injection of 10 µl of a 100 mM $FeCl_3$ solution is calculated as approximately 5 mM. *G. mellonella* larvae were injected with 10 µl 100 mM $FeCl_3$ one hour before a further injection with each of the *Photorhabdus* strains. Insect death and $LT_{50}$ values were then calculated as described in Materials and Methods. When co-injected with iron BMM417 had a $LT_{50}$ of 46 h compared to K122 WT at 44 h. This compares to 96.5 h and 52 h respectively for the two strains without iron supplementation. Importantly co-injection of insects with the same concentration of NaCl does not alter the $LT_{50}$ (Table 3.6) and an alternative test showed that exogenous iron injection does not increase the susceptibility of the insects to non-pathogenic infections such as *E. coli* ZK2686 (data not shown). Therefore the addition of exogenous iron is able to rescue the $LT_{50}$ defect in BMM417 and this supports the hypothesis that an intact *exbD* gene is required for the efficient transport of iron into the *Photorhabdus*. Interestingly the $LT_{50}$ was reduced for wild type when exogenous iron was injected into the insects which suggests that wild type *P. temperata* K122 are limited for iron availability during infection.

**Table 3.6** Pathogenicity complementation by iron

| | $LT_{50}$ (h) ± S.D. | | |
|---|---|---|---|
| Strain | - $FeCl_3$ | + $FeCl_3$ | + NaCl |
| K122 | 52 ± 2.9 | 44 ± 2.8 | 51 ± 0.0 |
| BMM417 | 96.5 ± 12 | 46 ± 1.4 | 101.5 ± 9.2 |
| BMM401 | 58 ± 5.7 | 47 ± 1.4 | 52.5 ± 0.7 |

Insects were pre-injected with 10 µl 100 mM $FeCl3.7H_2O$ or NaCl 1 hour before injection with the *Photorhabdus* strain or with PBS as a control. 10 *Galleria mellonella* larvae were injected with 100 cfu of each strain and were incubated at 25°C. Death was assessed by checking for insect movement after gentle stimulation. Data presented is the mean of 2 experiments ± standard deviation (S.D.)

### 3.2.13 Symbiosis of BMM417

*P. temperata* is required for the growth and development of the nematode, *Heterorhabditis downesi*. The ability of the bacteria to support nematode growth and reproduction can be assayed *in vitro* facilitating the analysis of mutants that are affected for pathogenicity. Lipid agar plates were inoculated with K122, BMM417, BMM417/pBMM702 and BMM401. After 3 days incubation at 28°C, 40 surface-sterilised *H. downesi* IJs were added to the plates (Fig. 3.5). The plates were then incubated at 25°C and nematode development, growth and reproduction was monitored using a microscope. After 7 days nematode recovery from infective juvenile to hermaphrodite development was scored (Fig. 3.6), 7 to 20 days post-inoculation the development of first and second generation (F1 and F2) nematodes were observed (Fig. 3.6) and finally at 21 days or more the production of a new generation of IJs was monitored and an IJ yield (number of new IJs/ number of IJs in initial inoculum) was calculated by washing the new IJs from the lids of the symbiosis plates and recording the number collected.

**Table 3.7** Symbiosis success of nematodes grown on K122 strains

| Strain | % Nematode recovery to hermaphrodite° | Frequency of nematode growth and development* | Frequency of IJ production at 28 days** |
|---|---|---|---|
| K122 | 56 +/- 17 | 100 % | 60% |
| BMM417 | 67 +/- 20 | 0 % | 0% |
| BMM417/pBMM702 | 35 +/- 27 | 90 % | 50% |
| BMM401 | 52 +/- 11 | 100 % | 90% |

° % Nematode recovery was calculated as the number of hermaphrodites that were counted at 7 days divided by the original number of IJs applied (40) as an average of 10 plates +/- S.D.
* Frequency of nematode growth and development was measured following 14 days growth on lipid agar. Plates were scored as positive if F1-F2 generation nematodes were present or negative if only F0 hermaphrodites present.
** Frequency of IJ production was calculated by scoring plates as positive if IJs were detected on the lids of the plates or negative if no IJs were detected. Data is derived from 10 plates.

All of the strains were able to support nematode recovery to hermaphrodite nematodes after 7 days (Table 3.7). Observation of the symbiosis plates at 14 days post IJ addition where it would be expected that F1 and F2 nematode generations would be present revealed that the wild type K122, BMM417/pBMM702 and BMM401 had indeed supported the production of a

mixed population of male and female nematode progeny on the majority of plates (Table 3.7). However, BMM417 could only support development of F0 hermaphrodites and was unable to support nematode growth and reproduction (Table 3.7). Indeed all of the strains except for BMM417 were also able to support the production of an IJ yield after 28 days. The nematodes feed on the viable bacterial biomass to support their growth and development and one possible reason for the inability of BMM417 to support growth and development would be a reduction in either bacterial biomass or viability. Therefore the bacterial biomass was removed from lipid agar and was dried as described in Materials and Methods. The analysis revealed that there was a similar level of biomass produced by all of the strains (Fig. 3.11). Viability of BMM417 is the same as K122 WT as both strains produce a similar number of colonies when removed from lipid agar at the appropriate time (Fig. 3.12). Therefore biomass or viability defects can be discounted as the reason for the symbiosis defect of BMM417.

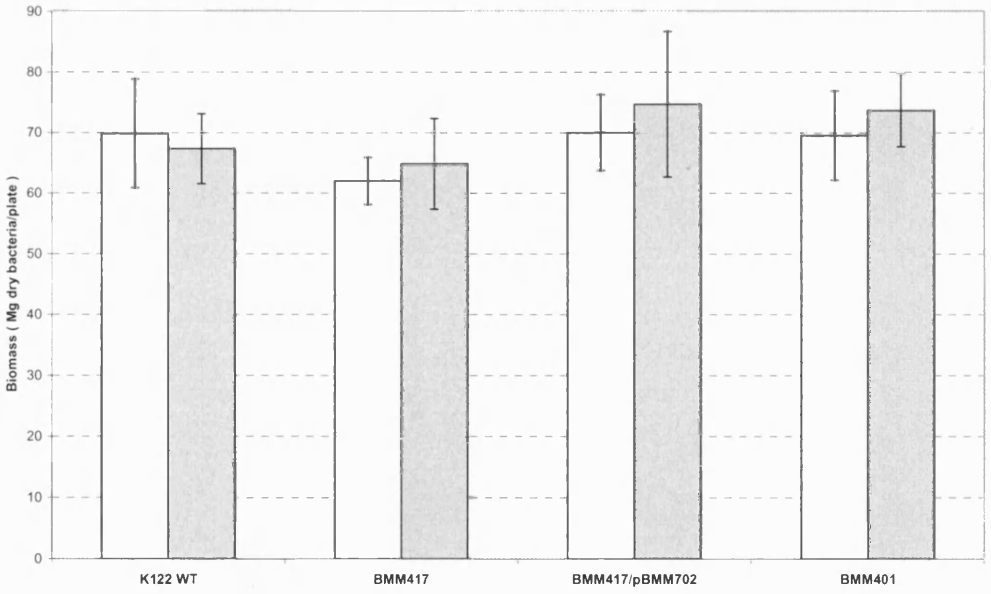


**Figure 3.11** Dry bacterial biomass. Bacteria removed from lipid agar plates either without iron (white bars) or with 100 µM iron ($FeCl_3$) supplementation (grey bars) after growth at 30°C for 72 h before bacteria removed and freeze dried until no further change in weight. Values are averages of 3 samples and error bars represent the standard deviation.

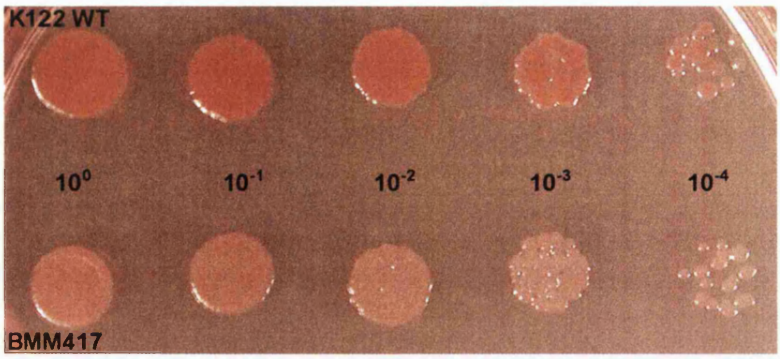


**Figure 3.12** Viability of bacteria removed from lipid agar after 5 days incubation at 30°C. 5 µl spots of a serial dilution on LB agar of K122 WT bacteria (Top) and BMM417 bacteria (Bottom) removed from lipid agar plates and resuspended in 10 ml PBS before diluting to an optical density of 1.

### 3.2.14 Iron content of BMM417

The nematodes feed on the bacterial biomass and therefore the inability of BMM417 to acquire iron in low iron environments may result in an iron nutrient defect that prevents nematode growth and development. The results using streptonigrin suggest that, on LB agar, the iron levels are similar in BMM417 and wild type. In order to establish the iron levels of bacteria in the symbiosis assay fresh lipid agar plates were seeded with K122, BMM417 and BMM417/pBMM702 and the bacteria was grown for 5 days at 30°C. At this time the bacteria were removed from the agar plates and prepared for atomic adsorption spectrometry as described in Materials and Methods. The total level of iron for K122 was calculated as 110.3 ng/mg dry weight of cells (Table 3.8). Interestingly BMM417 contains 30 % less iron than K122 and this reduction is complemented by pBMM702 carrying *exbD*. Therefore this decrease in iron content is *exbD*-dependent. It is possible that the decrease in iron content may be only due to the inability of BMM417 to transport the photobactin siderophore via the TonB-ExbB-ExbD system. Therefore BMM401 which cannot produce the photobactin siderophore (Table 3.1) was analysed for total iron content. Interestingly BMM401 and BMM417 show very similar levels of iron suggesting that the inability to use or produce photobactin is the cause of this reduction in cellular iron levels (Table 3.9). However BMM401 is able to support nematode growth and development suggesting that the reduction in iron levels observed in BMM417 is not responsible for the defect in nematode growth and reproduction.

**Table 3.8** Total iron content analysis of BMM417 and WT strains grown on lipid agar.

| Strain | Total iron (ng/mg dry weight) ± S.D.[b] |
|---|---|
| K122 | 110.3 ± 6.1 |
| K122/pBAD | 108.7 ± 10.5 |
| BMM417 | 76.9 ± 4.4 |
| BMM417/pBAD | 70.6 ± 7.0 |
| BMM417/pBMM702 | 120.0 ± 6.2 |

b: iron determinations were carried out in triplicate and values shown are the mean ± standard deviation

**Table 3.9** Total iron content analysis of strains including BMM401 grown on lipid agar.

| Strain | Total iron (ng/mg dry weight) ± S.D.[b] |
|---|---|
| K122 | 105.9 ± 4.3 |
| BMM417 | 70.1 ± 8.0 |
| BMM401 | 76.3 ± 4.3 |
| BMM417/pBMM702 | 114.6 ± 3.0 |

b:iron determinations were carried out in triplicate and values shown are the mean ± standard deviation

### 3.2.15 Exogenous iron in symbiosis

As BMM417 has been shown to be less able to scavenge iron under iron limiting conditions it seemed reasonable that the delivery of iron into the cell may have been altered in terms of both the quantity of iron and intracellular location. Many bacteria encode low affinity iron uptake systems therefore the ability of exogenous iron in the lipid agar was tested for its ability to restore symbiosis with BMM417. K122, BMM417 and BMM417/pBMM702 were cultured on lipid agar supplemented with 50 μM and 100 μM $FeCl_3$ or NaCl as a control. Interestingly the addition of 100 μM $FeCl_3$ (or 50 μM $FeCl_3$) resulted in a correction of the light pigmentation observed in BMM417 cells to a wild type darker pigmentation (Fig. 3.14). When IJ nematodes were inoculated onto non-supplemented lipid agar plates inoculated with BMM417 nematode growth and development occurred on only 1 plate out of a total of 18 plates used in

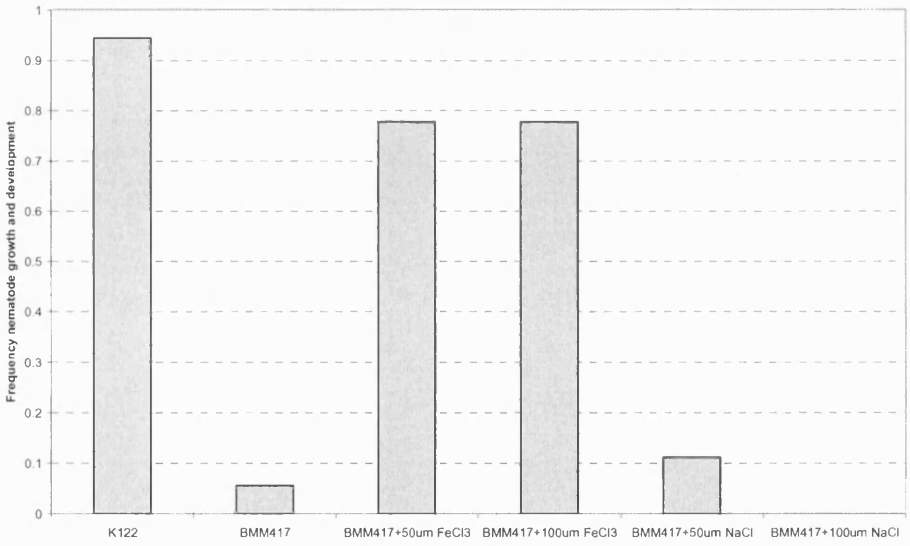


**Figure 3.13** Lipid agar plates, supplemented with either $FeCl_3$ or NaCl (at the indicated concentrations), were inoculated with BMM417 and incubated at 28°C for 72 h. Approximately 40 IJ nematodes were added to each of these plates and nematode growth and development was followed as described in Materials and Methods. For these experiments the presence of only F0 hermaphrodites 20 days after the addition of the IJs was scored negative for nematode growth and development whilst the presence of F2 generation nematodes was scored as positive for nematode growth and development. The frequency was calculated as the number of plates that scored positive for nematode growth and development divided by the total number of plates used in the experiment (n=18).

this experiment, i.e. a frequency of 0.055 (Fig 3.13). When either 50 μM or 100 μM $FeCl_3$ was added to the lipid agar, the IJs inoculated onto the bacterial biomass produced both F1 and F2 generations on the majority of the lipid agar plates tested (frequency 0.78). Importantly, when equivalent concentrations of NaCl were added to the lipid agar there was no rescue of nematode growth and development indicating the rescue is dependent on the addition of iron (Fig. 3.13). Certainly the complementation cannot be due to a change in bacterial biomass as all strains produced the same level of biomass even when supplemented with excess iron (Fig. 3.11) (ANOVA, $F = 0.93$, d.f. = 7, $P = 0.51$). Interestingly, although the nematodes were able to grow and reproduce on BMM417 supplemented with $FeCl_3$, these nematodes did not develop into IJs at the end of the assay, therefore it was not possible to calculate an IJ yield. The reason for this is unclear although it might suggest that, in addition to being a nutrient, iron may also be involved in regulating development in the nematode. Nonetheless it is clear that reduced iron levels in BMM417 are, at least partially responsible for the defect in ability of this mutant to support nematode growth and development.

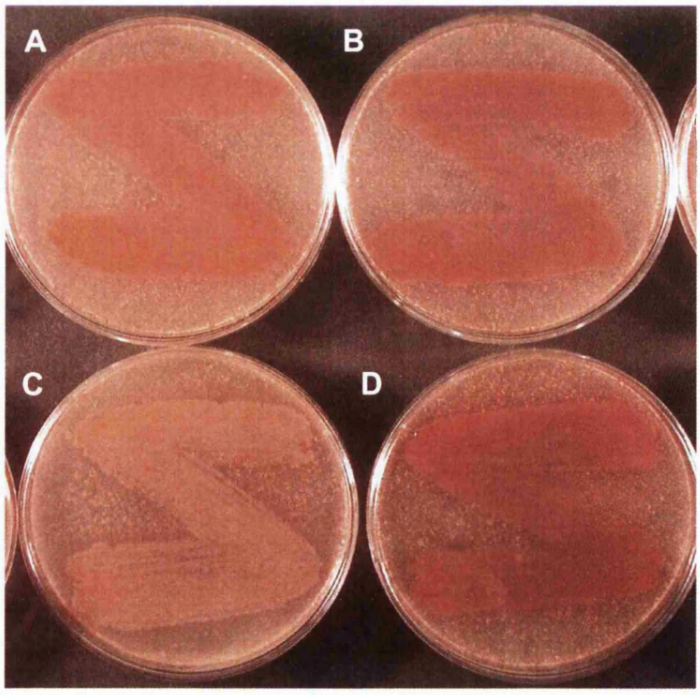


**Figure 3.14** *P. temperata* K122 grown on lipid agar. (A) Wild type grown without iron supplementation. (B) Wild type grown with 100 μM $FeCl_3$ (C) BMM417 grown without iron supplementation. (D) BMM417 grown with 100 μM $FeCl_3$. Plates were incubated at 30°C for 48 h.

## 3.3 Discussion

In this chapter five independent mutants were identified in *P. temperata* K122 that were affected in siderophore production. Three of the mutants; BMM401, BMM415 and BMM416 were identified in an operon predicted to encode the genes for the biosynthesis and uptake of the photobactin siderophore and a fourth mutant, BMM402 was identified which was probably involved in providing the precursors for siderophore synthesis. The fact that BMM401 did not produce any detectable siderophore on LB-CAS agar suggests that photobactin is the major siderophore produced when *P. temperata* is grown on these indicator plates. BMM401 was not affected in either pathogenicity or symbiosis and this is in agreement with a previous study that found no role for the photobactin siderophore in the lifecycle of *P. luminescens* NC19 (Ciche *et al.*, 2003)

One of the mutants identified, BMM417, showed a consistent defect in its ability to kill insect larvae and to support nematode growth and development. BMM417 was subsequently identified as a transposon insertion in the *exbD* gene. The ExbD protein is part of the TonB complex which is comprised of the TonB, ExbB and ExbD proteins which combine to form an energy transduction system. This TonB system is found in the cytoplasmic membrane of many Gram-negative bacteria where it utilises the proton motive force to induce conformational changes in TonB-dependent outer membrane receptors for the active uptake of molecules such as siderophores. Unsurprisingly, due to the incredibly important role of iron acquisition in infection a mutant in the TonB system regularly affects the virulence of a number of bacteria (Beddek *et al.*, 2004; Bosch *et al.*, 2002; Jarosik *et al.*, 1994; Pradel *et al.*, 2000; Reeves *et al.*, 2000; Stork *et al.*, 2004; Torres *et al.*, 2001; Tsolis *et al.*, 1996) .

A mutation in the *exbD* gene increases the $LT_{50}$ of *P. temperata* against *Galleria mellonella* to approximately twice that of the wild type. This increase in $LT_{50}$ correlates with a decrease in the *in vivo* growth rate. This suggests that the reduced pathogenicity of BMM417 is probably due to a reduced growth rate in the insect. Addition of excess iron into the insect host completely rescues the pathogenicity defect of BMM417 strongly suggesting that iron is the limiting

factor in growth when the *exbD* gene is inactive. However the possibility remains that the defect results from an inability to transport other nutrients that are dependent on the TonB complex for uptake into the bacteria. One of those nutrients is vitamin $B_{12}$, although analysis of the *P. luminescens* TT01 genome (not available at the start of this project) suggests that the complete *cob* and *cib* loci, encoding all of the genes necessary for the aerobic and anaerobic biosynthesis of vitamin $B_{12}$, are present in *Photorhabdus* (Duchaud *et al.*, 2003). BMM417 does grow in the insect, although with a slower growth rate, and eventually reaches cell densities within the cadaver that are equivalent to wild type levels suggesting that the *exbD* mutation does not completely prevent iron acquisition in the insect. Some bacteria employ multiple genes encoding for components of the TonB complex. Indeed *Vibrio cholerae* (Occhino *et al.*, 1998; Seliger *et al.*, 2001), *Vibrio anguillarum* (Stork *et al.*, 2004), *Actinobacillus pleuropneumoniae* (Beddek *et al.*, 2004) and *Pseudomonas aeruginosa* (Zhao and Poole, 2000) all encode two TonB systems that carry out both redundant and specific functions. However *in silico* analysis of the *P. luminescens* TT01 genome reveals that *Photorhabdus* has only one copy of *tonB*, *exbB* and *exbD*. There is also some evidence that the *tolQ* and *tolR* genes are capable of a certain degree of cross complementation in *exbBD* mutants of *E.coli* (Postle and Kadner, 2003) and homologues of these genes can be identified in the *Photorhabdus* genome. A final possibility is that TonB-independent iron uptake systems are present in *Photorhabdus*. The *yfeABCD* locus of *Y. pestis* encodes an ATP-dependent permease that transports inorganic iron (and manganese) into the cell independently of the TonB complex (Bearden *et al.*, 1998; Bearden and Perry, 1999; Janakiraman and Slauch, 2000; Perry *et al.*, 2003; Perry *et al.*, 2007) . The *yfe*-encoded iron uptake system is homologous to the Sit system encoded on *Salmonella* pathogenicity island 1 in *Salmonella enterica* serovar Typhimurium and both Yfe and Sit are required for the full virulence of their respective bacteria (Bearden and Perry, 1999; Janakiraman and Slauch, 2000). Analysis of the *P. luminescens* TT01 genome has revealed a copy of the *yfe* locus, however it has not been determined if this locus is present in *P. temperata* K122. There are also additional systems that have been identified in the TT01 genome including the Feo ferrous iron uptake system (Cartron *et al.*, 2006) which comprises the FeoABC proteins that can transport ferrous iron in the absence of TonB.

As *Photorhabdus* is the food source for the developing nematodes the nutritional value of the bacteria is extremely important. Nutrient provisioning is an essential interaction between some prokaryotes and eukaryotes. For example nitrogen fixation by *Rhizobium* bacteria converts inert $N_2$ gas in the atmosphere which is not directly available to plants into $NH_3$ which is essential for optimal plant growth in low nitrogen environments (Zahran, 1999). When humans are starved of iron this malnutrition can lead to anaemia which not only leads to poor health but also to disability and death. An estimated 50% of anaemia in the world is due to iron deficiency in the diet (Stoltzfus, 2003). The data presented here suggest the inability of BMM417 to support nematode growth and development is due to the inability to acquire sufficient iron. Exogenous iron in the media is able to rescue the nematode growth and development phenotype when BMM417 was the food source and this may be due to alternative iron acquisition systems that are active at these high external iron concentrations. Intriguingly the total iron levels of the *Photorhabdus* do not appear to play a direct role in symbiotic ability as both BMM401 and BMM417 show the same 30 % reduction in total iron contents, however BMM401 is fully virulent and symbiotic, whereas BMM417 has severe pathogenicity and symbiosis defects. The total iron analysis used provides the data for total iron content, but does not take into account how the iron was distributed within the bacteria. Therefore, iron may be present at similar levels between BMM401 and BMM417 but the iron may have been distributed completely differently between these two mutants. Interestingly *Y. pestis* needs sufficient quantities of haemin and the presence of the haemin storage locus (*hms*) in order to become pigmented. The pigmentation of BMM417 appeared reduced compared to K122, and the photobactin mutants, when grown on lipid agar and this may suggest a similar link between pigmentation and iron storage in *Photorhabdus*. Certainly the presence of 50 μM or 100 μM $FeCl_3$ in the lipid agar was able to increase the pigmentation of BMM417 and it is at these exogenous iron levels that symbiosis is reinstated. However it should be noted that this pigmentation increase was far above that of wild type and indeed even the pigmentation of wild type increased in the presence of exogenous iron. Therefore, it is possible that during iron uptake in low iron environments an

*exbD*-dependent uptake system is responsible for providing the iron to a specific bacterial iron storage protein, for example the pigmented molecule haem that can be accessed by the nematode. Some nematode worms, including *C. elegans*, cannot synthesise haem *de novo* and therefore require haem to be supplied in their diet. *C. elegans* can feed on *E. coli* bacteria and when *C. elegans* were put onto a synthetic food source which had been depleted for haem the worms arrested at the L4 stage of growth (Rao *et al.*, 2005). Therefore if the *Heterorhabditis* nematode is also unable to synthesise haem it would rely on haem being supplied by *Photorhabdus*. Gram-negative bacterial haem uptake is an *exbD*-dependent process, therefore it might be expected that BMM417 would be restricted in its ability to acquire haem from the environment. It is possible therefore that BMM417 is unable to support nematode growth and development due to an inability to provide sufficient exogenously acquired haem to the nematodes. Another explanation for the defect may be due to the inability of BMM417 to acquire an alternative siderophore which is essential for symbiosis. The transport of all siderophores would have been disrupted as the TonB energy transducing complex has been inactivated by the loss of *exbD*. An interesting consideration is the *ngrA* (no growth and reproduction) mutant described by Ciche *et al.* (2001) in *P. luminescens* NC19 that cannot support nematode growth and reproduction. The *ngrA* gene has strong homology to *entD* gene of *E. coli* which encodes the enzyme PPTase. The EntD enzyme is involved in the transfer of the PPT moiety from coenzyme A to EntB and EntF which are required for enterobactin siderophore synthesis in *E. coli* (Raymond *et al.*, 2003). In *Photorhabdus* the NgrA PPTase probably performs the same operation in the production of photobactin. This mutant also loses the ability to produce antibiotics, therefore suggesting the PPTase is involved in the production of other molecules as well as siderophores. Therefore it is possible that NgrA is involved in the production of an alternative siderophore that is essential for the symbiotic relationship between the bacteria and nematode.

All of the results suggest that ExbD-dependent iron acquisition is critical for normal pathogenicity and symbiosis in *Photorhabdus*. However iron acquisition via photobactin is dispensable under the conditions investigated although it is possible that another, as yet identified, siderophore is required. The iron

requirement could also be via a non-siderophore pathway, for example via haem uptake. The fact that providing excess exogenous iron can rescue both the pathogenicity and the nematode growth and development phenotypes suggests that these defects are due to iron limitation. However it appears that the overall level of iron in *Photorhabdus* is not critical for symbiosis with the nematode, although it may be the way in which the iron is acquired or stored that may be essential for the interplay between *Photorhabdus* and *Heterorhabditis*.

# Chapter 4

# An analysis of iron homeostasis genes in *Photorhabdus luminescens* TT01

## 4.1 Introduction

The previous chapter identified that the *exbD* gene was required for full virulence and symbiosis in *P. temperata* K122. The *exbD* gene encodes the ExbD protein which forms part of the energy transducing TonB complex, consisting of ExbB-ExbD-TonB. This complex provides energy to the outer membrane of Gram-negative bacteria for the active transport of molecules such as siderophores and vitamin $B_{12}$. To understand the exact nature of the *exbD* defect all aspects of iron homeostasis in *Photorhabdus* need to be investigated. The genome sequence of *Photorhabdus luminescens* TT01 became available in 2003 (Duchaud *et al.*, 2003) and this has enabled the identification of many predicted mechanisms for iron acquisition (Table 4.1). Working with the sequenced TT01 genome offers distinct advantages in genetic manipulation compared to working with the unsequenced *P. temperata* K122 strain. Therefore in order to try and identify the exact reasons why the *exbD* mutation in *P. temperata* K122 was causing the pathogenicity and symbiosis defects a directed knock out technique was developed in order to create directed mutants in *P. luminescens* TT01.

**Table 4.1.** Iron homeostasis genes in *P. luminescens* TT01

| Class | Gene(s) | plu ID | Description |
|---|---|---|---|
| Transport | *exbB, exbD* | plu3941, plu3940 | Components of the TonB membrane energy transduction system |
| | *tonB* | plu2485 | Component of the TonB membrane energy transduction system |
| | *feoA, feoB* | plu0209, plu0208 | Feo ferrous ($Fe^{2+}$) uptake system of *E. coli* |
| | *yfeA, yfeB, yfeC, yfeD* | plu2672 - plu2675 | Yfe ferrous ($Fe^{2+}$) uptake system of *Y. pestis* |
| | *fecI - fecE* | plu4444 - plu4450 | Iron (III) dicitrate transport system of *E. coli* |
| Siderophores | *plu2850 – plu2853* | plu2850 - plu2853 | Putative fericenterochelin siderophore uptake *Y. pestis* |
| | *plu4621, fhuE-fhuF* | plu4621 - plu4627 | Probable siderophore biosynthesis and uptake of enterobactin like siderophore |
| | *plu2315-plu2324* | plu2315-plu2324 | Yersiniabactin uptake of *Y. pestis* (high-pathogenicity island) |
| Haemin | *plu2631, hmuR – plu2637* | plu2631, plu2632-2637 | Haemin uptake (*hmu* locus of *Y. pestis*) |
| Iron storage | *ftnA* | plu2689 | nonhaem ferritin 1 |
| | *bfr* | plu4728 | Bacterioferritin |
| | *ppxA ppxB.* | plu4242, plu4243 | photopexins A and B |
| | *plu4230* | plu4230 | Some homology with *ppxAB* |
| | *plu4231* | plu4231 | High similarity with *ppxAB* |
| Iron regulation | *fur* | plu1327 | ferric uptake transcription regulator |

Adapted from Duchaud, E. *et al.* 2003

## 4.2 Results

### 4.2.1 Directed knock out of *exbD* in *P. luminescens* TT01

In order to investigate the exact nature of the defects observed with the *exbD* mutation it seemed prudent to transfer the *exbD* mutation into *P. luminescens* TT01 as the sequence was made available for this bacterium in 2003. To investigate the role of *exbD* in *P. luminescens* TT01 an allelic exchange procedure needed to be developed as successful directed deletions had not been created in *Photorhabdus* previously. The suicide vector pDS132 was selected as an improved vector to the widely used pCVD442 allelic exchange vector (Philippe *et al.*, 2004). The pDS132 vector had a region of DNA encoding an IS*1* element removed to reduce the occurrence of untargeted recombination. The DNA regions for recombination were 600 bp fragments of DNA from upstream and downstream of the gene to be removed with approximately 15 bp that are homologous between the two fragments (see Fig. 4.1). Fragment 1 was amplified using primers RJW115 and RJW116 and Fragment 2 was amplified using RJW117 and RJW118. The primers were designed so that the 3' end of Fragment 1 and the 5' end of Fragment 2 share a 30 bp homologous that can anneal during a second PCR to form a 1.2 kb fragment. A final PCR with the primers RJW115 and RJW118 amplifies this fragment to produce the 1.2 kb deletion fragment. The deletion fragment was gel purified and was ligated into the pDS132 plasmid before the deletion was constructed as described in Materials and Methods. Primers were designed to regions outside of the recombination region in the genome to allow PCR screening by size differentiation. The primers RJW130 and RJW131 were positioned at 1129 bp and 836 bp from the start and stop codons of *exbD* respectively. Therefore, the expected size of a PCR product from a knock out allele is 1971 bp whilst the size of a PCR product from the wild type is 2391 bp. The first screen provided 30 % success in identifying the expected knock-out (KO) allele. To confirm the KO allele of the selected mutant Δ*exbD* #4 colony PCR was performed with the primers used originally to construct the KO vector, RJW115 and RJW118 and primers RJW130 and RJW131. The

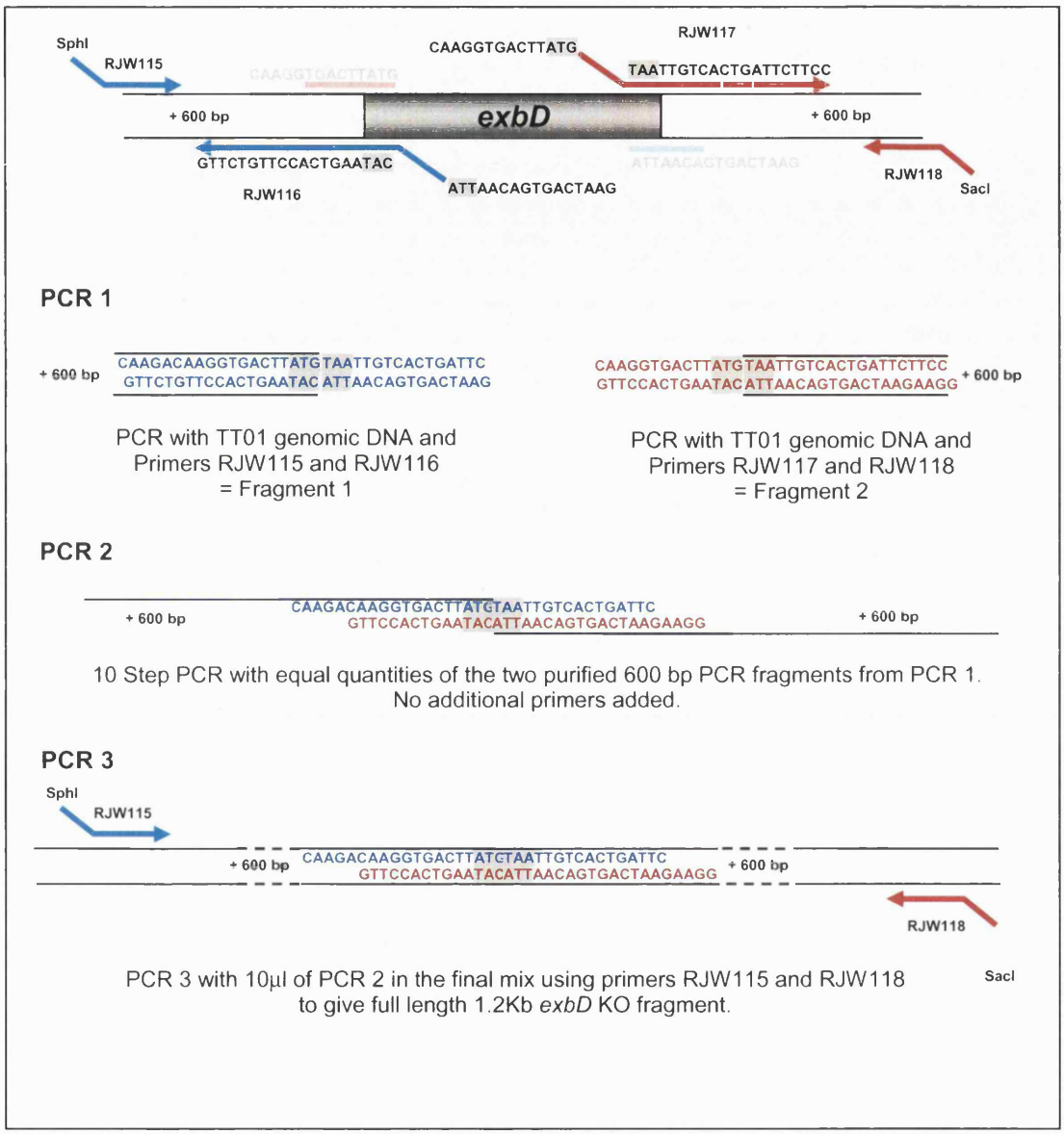


**Figure 4.1.** Schematic of the construction procedure for the knock out vector. The first step PCR produces two 600 bp fragments which are fused together in the second step. A final 3rd step PCR produces the full length fragment for cloning into pDS132.

amplified fragments for both sets of primers gave the KO allele in both cases confirming the deletion (Fig. 4.2). This mutant has been designated BMM430 and this strain contains a markerless deletion of the *exbD* gene. Deletion of the *exbD* gene results in a strain that cannot energise TonB in an efficient manner, therefore it would be expected that all of the TonB dependent receptors to be deficient in transport. It has been predicted that there are twelve such receptors present in the TT01 genome (Koebnik, 2005), therefore a mutation in *exbD* is expected to affect twelve TonB-dependent uptake pathways, the majority of which are dedicated to iron transport (Table 4.2).

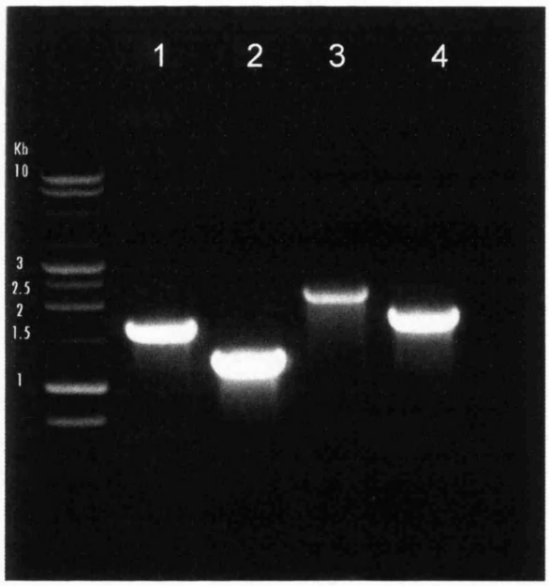


**Figure 4.2.** 1% agarose gel of Δ*exbD* #4 confirmatory PCR.
Lane 1 Wild Type and Lane 2 Δ*exbD* #4 amplified with RJW115+RJW118
Lane 3 Wild Type and Lane 4 Δ*exbD* #4 amplified with RJW130+RJW131

**Table 4.2.** TonB dependent receptors in *P.luminescens* TT01

| Gene | plu ID | Description |
|---|---|---|
| *plu0739* | plu0739 | Probable Outer Membrane Receptor |
| *hemR* | plu1238 | Haemin receptor precursor protein HemR |
| *plu2316* | plu2316 | Similar to the pesticin receptor precursor FuyA |
| *hmuR* | plu2632 | Haemin receptor precursor |
| *plu2715* | plu2715 | Similar to outer membrane siderophore receptor CjrC of *E.coli* |
| *plu2850* | plu2850 | Probable haemin/siderophore outer membrane receptor |
| *plu3513* | plu3513 | Similarities with haem receptor HasR |
| *plu3519* | plu3519 | Putative siderophore membrane receptor of ABC transport system |
| *plu3838* | plu3838 | Similar to outer membrane haemin receptor precursor |
| *fecA* | plu4446 | Iron(III) dicitrate outer membrane transporter precursor protein FecA |
| *fhuE* | plu4622 | FhuE receptor precursor (Outer-membrane receptor for ferric iron uptake) |
| *btuB* | plu4735 | Vitamin $B_{12}$ receptor precursor protein BtuB |

TonB-dependent receptors as identified by Koebnik, R. 2005 utilising 2 hidden Markov models based on the receptor plug domain and barrel domain.

### 4.2.2 Siderophore production of the *ΔexbD* mutant

Siderophore hyperproduction was one of the identifying phenotypes of the *exbD* mutant in *P. temperata* K122, therefore it might be expected that BMM430 would have the same phenotype. LB-CAS agar plate assays of BMM430 revealed that the level of siderophore production is the same as TT01 (Fig. 4.3). Therefore, it appears that BMM430 does not hyper produce any siderophore. In *P. temperata* K122 photobactin appears to be the major siderophore produced under the conditions tested (see Fig. 4.3 and Section 3.2.3). Interestingly, *in silico* analysis has revealed that there is no predicted photobactin operon in the TT01 genome although the TT01 genome does reveal several loci for the production and utilisation of other siderophores (Table 4.1)

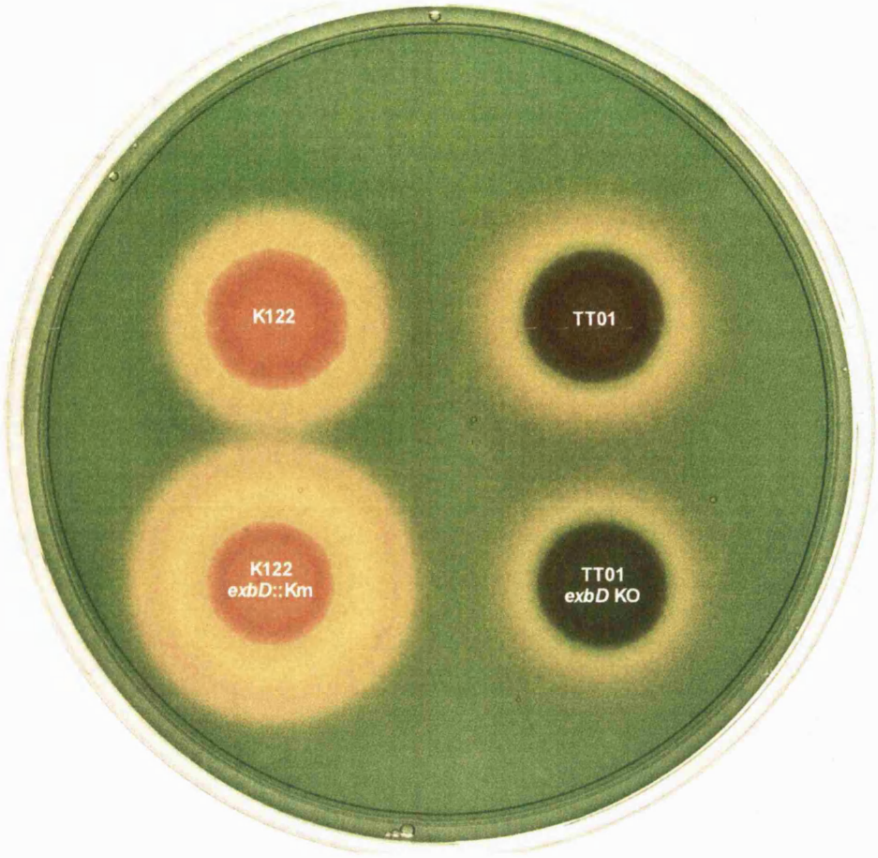


**Figure 4.3.** Siderophore production of K122, K122 *exbD*::Km (BMM417), TT01 and TT01 Δ*exbD* (BMM430). Overnight cultures were diluted to an OD of 1 before 10 µl was spotted onto LB-CAS agar and incubated at 30°C for 72 h.

### 4.2.3 Pathogenicity of the *ΔexbD* mutant

To compare the virulence of BMM430 to wild type TT01, 100 cfu of each strain was injected into 10 *G. mellonella* larvae and the insects were incubated at 25°C. As expected wild type TT01 killed all of the insects within 48 h. In contrast no insects injected with BMM430 died suggesting the *exbD* deletion resulted in a strain that was completely avirulent (data not shown). This avirulence may be due to the inability of the mutant to grow in the insect hemolymph (as seen with

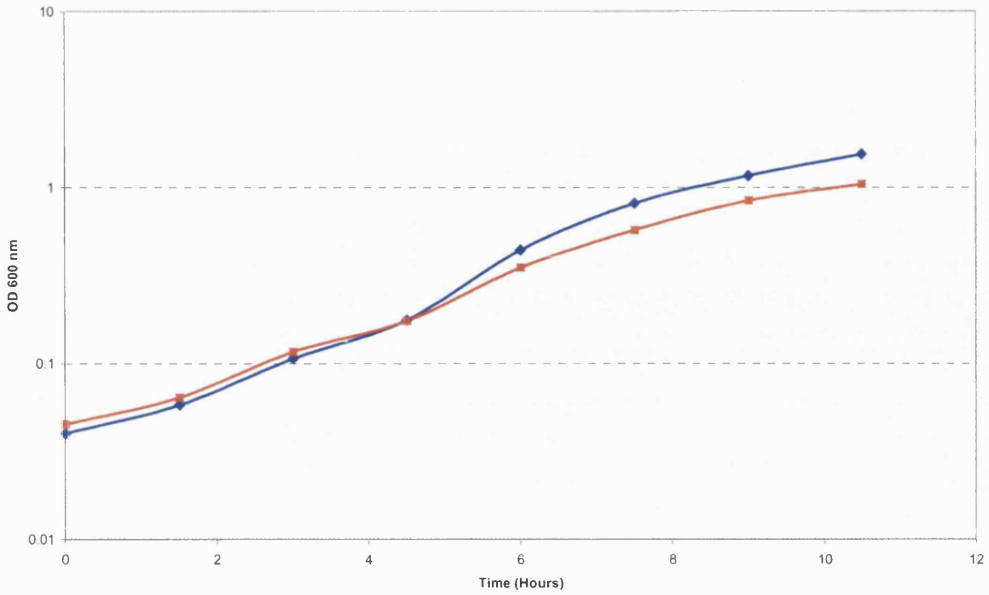


**Figure 4.4.** Growth of TT01 WT (diamonds) and BMM430 (Δ*exbD*) (squares) in Graces insect media. Strains were grown at 30°C with shaking at 200 rpm.

the *exbD* mutation in *P. temperata* ) although it is not possible to measure "no growth" directly. To approximate hemolymph conditions BMM430 was grown in Graces insect media, a synthetic media that is representative of *Anthera* hemolymph. In this medium the growth of BMM430 was decreased compared to the wild type (Fig. 4.4) suggesting that this mutant is less able to grow in an environment representative of the insect hemolymph. When BMM430 was grown in LB broth the growth rate was similar to the wild type however when 50 μM DIP chelator was added to chelate the ferrous iron BMM430 was not able to grow at the same rate which suggests that, as expected, BMM430 is less able to scavenge iron in a low iron environment (Fig. 4.5). However, a reduced growth rate was observed with the *exbD* mutant in *P. temperata* K122 but this mutant was still able to kill insects, albeit that it took twice as long as the wild type to kill. This may suggest that the mechanism of iron acquisition in BMM430 within the insect is different from the mechanism of iron acquisition within the medium.

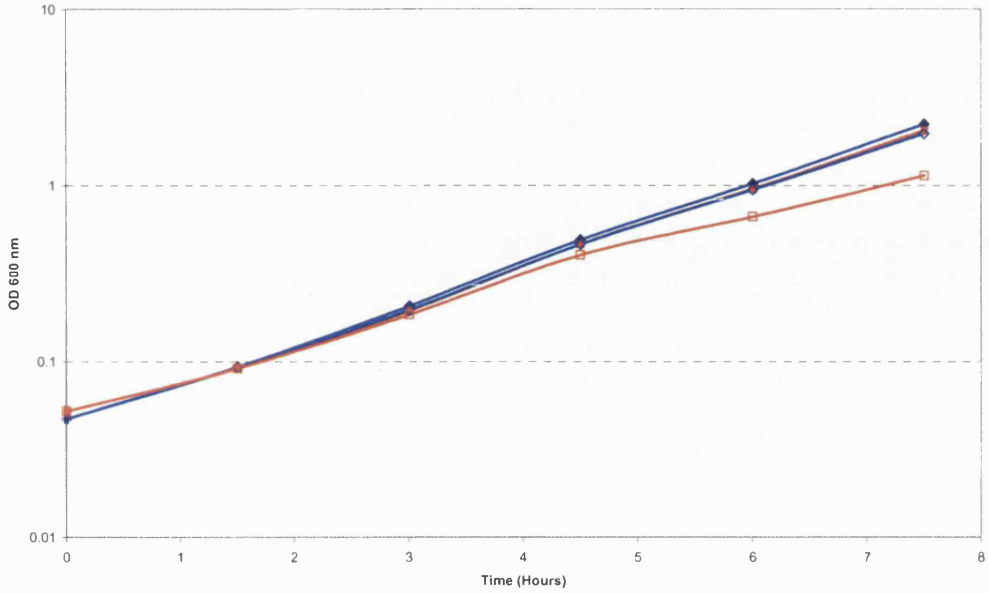


**Figure 4.5.** Growth of wild type TT01 (diamonds) and BMM430 (squares) in plain LB (closed symbols) or LB supplemented with 50 μM DIP (open symbols). Strains were grown at 30°C with shaking at 200 rpm.

### 4.2.4 Symbiosis of the *ΔexbD* mutant

The *P. temperata* K122 *exbD* mutant BMM417 was unable to support nematode growth and reproduction (see Section 3.2.13). To determine whether BMM430 had the same phenotype a symbiosis assay was performed with BMM430 and TT01 WT. This analysis revealed that BMM430 was fully able to support nematode growth and development and was also able to produce an IJ yield to a similar level to the wild type (Fig. 4.7). Nematode growth and development was clearly not arrested in the same way as observed with BMM417. BMM430 produced a large number of IJ nematodes after 21 days that were recovered from the lids of the symbiosis assay plates. The IJ nematodes were surface sterilised and crushed individually to determine the level of bacterial colonisation. The number of nematodes colonised and the level of individual colonisation was similar to wild type (Fig. 4.8 and 4.10). Interestingly when IJ nematodes that had been reared on BMM430 were used to infect *G. mellonella* insect larvae the insects died after a prolonged period of 8 days (data not shown). This was

unexpected as the Δ*exbD* mutant, BMM430, alone is non-pathogenic when injected at 100 cfu per insect (the nematode normally carries approximately 100 cfu/IJ see Fig. 4.10). However, the insects developed a black colouration and did not turn brick red as expected with a wild type infection and no IJs could be recovered when the insects were placed on White traps following 14 days incubation suggesting that the infection had not proceeded in the usual manner.

### 4.2.5 Alternative iron uptake systems in *P. luminescens* TT01

The deletion of the *P. luminescens* TT01 *exbD* gene did not cause a defect in the ability of the *Photorhabdus* to support the growth and development of *Heterorhabditis*. Therefore it seemed reasonable that alternative iron acquisition systems were active and able to provide the iron required for maintenance of the symbiotic interaction. In order to investigate this hypothesis, the TT01 genome was analysed for known *exbD*-independent iron acquisition systems. Two ferrous iron uptake systems the *feoAB* system and the *yfeABCD* system were identified that may play an important role in *Photorhabdus* iron acquisition (Table 4.1). The *feoAB* system was previously identified in *E. coli* where mutants in the *feo* locus were unable to colonise mouse intestines fully (Stojiljkovic *et al.*, 1993). The *yfeABCD* system was previously identified in *Y. pestis* where virulence was severely reduced in a Δ*yfeAB* mutant (Bearden and Perry, 1999). To test for the role of these genes in *Photorhabdus* a set of mutant strains were constructed; Δ*feoAB* (BMM432), Δ*yfeABCD* (BMM431), double mutants of Δ*feoAB* Δ*yfeABCD* (BMM435), Δ*exbD* Δ*yfeABCD* (BMM433) and Δ*exbD* Δ*feoAB* (BMM434) and a Δ*exbD* Δ*yfeABCD* Δ*feoAB* triple mutant (BMM436). These iron transport mutants were tested for their ability to grow on iron restricted media i.e. LB agar supplemented with increasing levels of DIP. As expected, all strains carrying the Δ*exbD* allele showed reduced growth compared to the wild type at concentrations of 100 μM DIP, confirming that *exbD* plays an important role in scavenging iron in TT01 (Fig. 4.6). In addition, the *yfeABCD* locus may

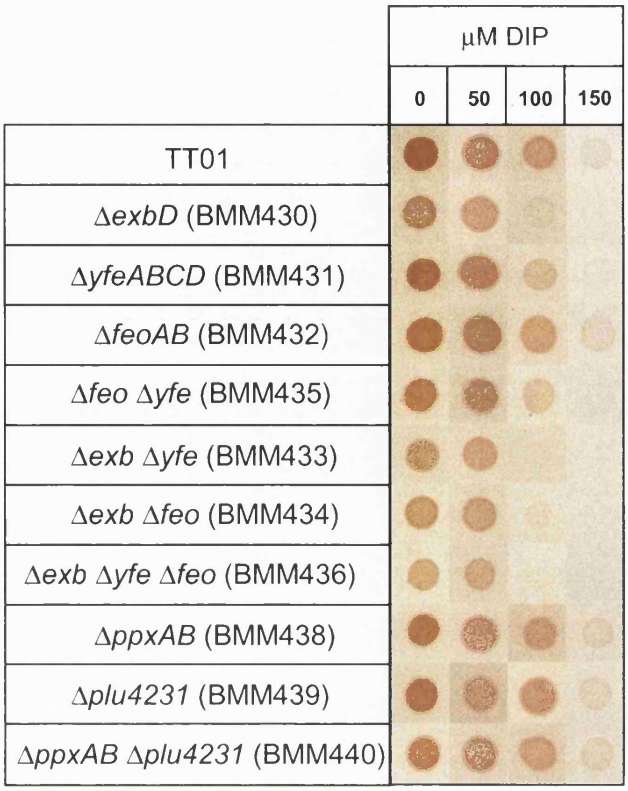


**Figure 4.6.** Growth of strains on LB agar with increasing quantities of DIP chelator. 10 μl spots of overnight culture diluted to $OD_{600}$ of 1 and were spotted onto LB agar and incubated at 30°C for 48 h.

also play an important role in iron scavenging as the Δ*yfeABCD* mutant did not grow as well as wild type in the presence of 150 μM DIP (Fig. 4.6). On the other hand, the *feoAB* mutant grew as well as wild type suggesting that this system does not play a significant role in iron scavenging under these conditions. The triple mutant Δ*exbD* Δ*yfeABCD* Δ*feoAB* would be expected to be crippled in both ferric and ferrous iron uptake and appeared to be the most affected for iron acquisition as there was no growth above 50 μM DIP (Fig. 4.6). These data reveal that when ferrous iron ($Fe^{2+}$) is removed from the LB agar *exbD*-mediated ferric iron acquisition ($Fe^{3+}$) is essential to maintain normal levels of *Photorhabdus* growth.

### 4.2.6 Pathogenicity of ferrous transport mutants

Ferrous ($Fe^{2+}$) iron is much more soluble under anaerobic conditions and may contribute a major source of iron in environments with low oxygen tensions e.g. certain niches within the insect host. Interestingly, the *yfeABCD* system is required for full virulence in *Y. pestis* and it is possible that different iron acquisition systems (TonB-dependent, FeoAB and YfeABCD) may be required during different stages of *Photorhabdus* pathogenicity. Therefore pathogenicity assays were performed by injecting 100 cfu of each *Photorhabdus* strain into *G. mellonella* larvae. The ferrous iron transport mutants, whether single mutants or multiple mutants, did not show any defect in pathogenicity, killing the insects in the same time as the wild type (Table 4.3). The Δ*feoAB* and Δ*yfeABCD* mutants combined with the Δ*exbD* strain were also tested for virulence, but as expected none of the insects died (data not shown). Therefore, ferrous iron acquisition does not appear to have a significant role in pathogenicity in *Photorhabdus*.

**Table 4.3.** % Insect death following injection of 100 cfu of each strain

| Sample | % Insect death at 50h |
|---|---|
| TT01 WT | 90% |
| Δ*feoAB* (BMM432) | 100% |
| Δ*yfeABCD* (BMM431) | 90% |
| Δ*yfeABCD* Δ*feoAB* (BMM435) | 100% |
| PBS Control | 0% |

10 insects were injected per strain. This analysis was performed once.

### 4.2.7 Symbiosis of ferrous transport mutants

BMM430, unlike the situation in *P. temperata* K122, showed no defect in its ability to support nematode growth and development (see Fig. 4.7). It was possible that in TT01 iron uptake is still important for symbiosis but other TonB-independent iron acquisition systems provided a level of iron uptake that was sufficient for nematode growth and development. Therefore the Δ*exbD*

Δ*yfeABCD* Δ*feoAB* triple mutant (BMM436) was tested in a symbiosis assay and surprisingly, no defects were detected in nematode growth and development. At the end of the symbiosis assays the IJ yield was measured to see how successful each bacterial strain had been at supporting nematode proliferation. The IJ nematodes were washed from the lids of the Petri dishes and counted which revealed a very similar number of IJs produced for all of the ferrous transport mutants, either as single locus mutations or in combination with Δ*exbD* (Fig. 4.7).

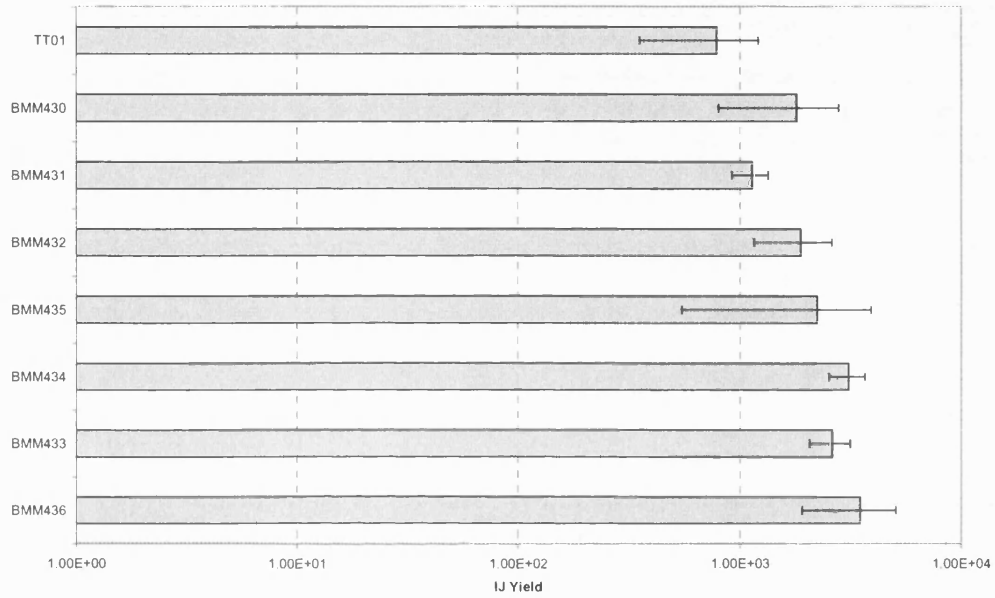


**Fig. 4.7.** IJ Yield from iron transport KO symbiosis assays. Values presented are an average of 5 plates. Error bars represent standard deviation.

### 4.2.8 IJ nematode colonisation

To ensure the symbiotic cycle had been completed and the IJ nematodes were colonised with *Photorhabdus* bacteria the IJs recovered from symbiosis assays were surface sterilised, crushed individually and the lysate was spread onto LB agar plates. In this way the population of colonising bacteria could be enumerated by counting colonies from the crushing following 72 h incubation at 30°C. Interestingly there appeared to be a defect in the ability of mutants containing the Δ*yfeA-D* allele to colonise the nematode (Fig. 4.8). Both the level (i.e. cfu/IJ) and frequency (i.e. number of nematodes colonised) of nematode

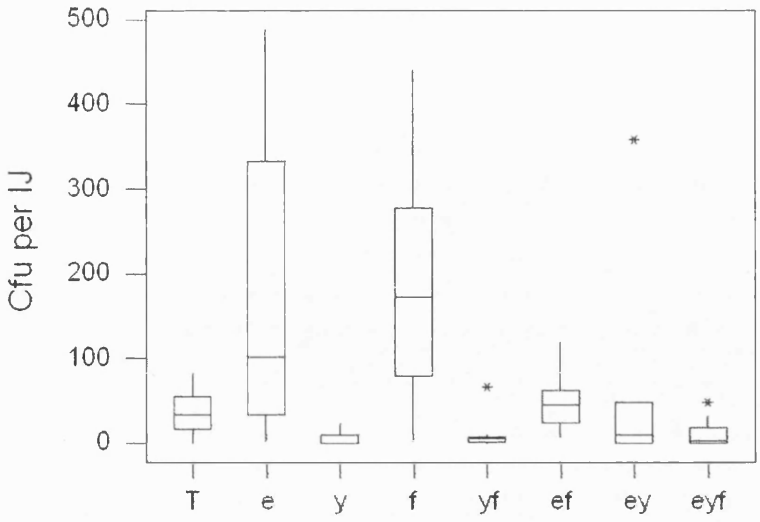


**Figure 4.8.** Colonisation of IJ nematodes with mutant bacteria. IJs were crushed and the lysate plated onto LB agar. Values are the average cfu per IJ from 10 IJs. Data are presented as a boxplot. The line within the box represents the mean value. The box extends to the first and third quartiles. The whiskers indicate the upper and lower limits and stars indicate outliers that are outside of these upper and lower limits. Strains carrying the Δ*yfe* allele were collectively significantly different from those not carrying the *yfe* mutation, Mann-Whitney P = <0.0001. T=TT01 WT e=BMM430 y=BMM431 f=BMM432 yf=BMM435 ef=BMM434 ey=BMM433 eyf=BMM436.

colonisation appeared severely reduced compared to the wild type (44% compared to 90% wild type frequency of colonisation and of the nematodes colonised, the mean cfu was 11 cfu for Δ*yfeABCD* (BMM431) and 42 cfu for wild type). These nematodes were also used to infect insects by moistening filter paper with PBS containing 1000 surface-sterilised IJ nematodes in a Petri dish to which 10 *G. mellonella* larvae were added. If the IJs grown on Δ*yfeABCD* mutant bacteria were affected in colonisation, as the data suggested, then this would be reflected in the number of insects killed i.e. the IJs containing the Δ*yfeABCD* mutant would kill significantly fewer insects and take longer to kill these insects than IJs containing the wild type bacteria. Surprisingly all of the insects were killed in the same time as wild type, suggesting a normal level of nematode colonisation in the Δ*yfeABCD* mutants (data not shown). Following 14 days incubation the IJ nematodes were recovered from the insect cadavers on White traps. The IJs were then crushed in single IJ crushes to determine the level of

colonisation following *in vivo* conditions. Once again the Δ*yfeABCD* mutant showed a severe decrease in the number of colonies recovered on LB agar compared to the wild type (data not shown). Therefore the IJ crushing results suggest that the Δ*yfeABCD* mutants are unable to colonise the IJ gut. On the other hand IJs carrying the Δ*yfeABCD* mutant were clearly able to kill the insect larvae. Therefore, it seemed reasonable that the Δ*yfeABCD* mutation was actually causing the mutants to be defective in growth on LB agar after passage through the nematode.

4.2.9 Δ*yfeABCD* shows a defect in growth from IJ nematodes.

Xu and Hulbert (1990) identified a growth defect of *Photorhabdus* on LB medium exposed to fluorescent light. They discovered that components of yeast extract are degraded by the action of fluorescent lights to produce up to 20 μM $H_2O_2$. Exposure to fluorescent light was correlated with a significant decrease in the plating viability of *Photorhabdus* (Xu and Hurlbert, 1990). Moreover pyruvate was identified as a compound that, when added to the LB agar, prevented the generation of $H_2O_2$ (Xu and Hurlbert, 1990). To test whether the addition of pyruvate altered the number of *Photorhabdus* recovered from nematodes colonised with wild type bacteria individual IJs were crushed and plated onto plain LB agar and LB agar supplemented with 0.1 % (w/v) pyruvate (Fig. 4.9.). Statistical analysis revealed no significant difference between these two sets of data (Mann-Whitney $P = 0.9696$).

Nematodes grown on the Δ*yfeABCD* mutant were crushed and the lysates were plated onto LB agar supplemented with 0.1 % (w/v) pyruvate. Remarkably, under these conditions, the level of colonisation by the Δ*yfeABCD* mutant was not significantly different from the wild type (Mann-Whitney $P = 0.4952$) (Fig. 4.9). This strongly suggests that the inability to recover Δ*yfeABCD* mutant bacteria from the IJ was indeed due to the toxic effects of $H_2O_2$ in the plating media. As the $H_2O_2$ build up is due to the breakdown of compounds in the yeast extract catalysed by fluorescent laboratory lights, the same result would be expected if the LB agar was incubated in the dark for 16 hours or more or if an

alternative compound was used to neutralise the $H_2O_2$ (Xu and Hurlbert, 1990). The inability of Δ*yfeABCD* bacteria to recover on LB agar does indeed appear to be due to $H_2O_2$-induced toxicity as LB medium incubated in the dark or supplemented with catalase (28U $ml^{-1}$) allowed Δ*yfeABCD* bacterial growth to the same level as with pyruvate (data not shown). Interestingly there was no difference in the ability of wild type TT01 bacteria recovered from IJs to grow on LB media exposed to light suggesting that this defect is associated with the Δ*yfeABCD* mutation. Therefore, colonisation of the nematode by the Δ*yfeABCD* mutant appears to render these bacteria more sensitive to the presence of $H_2O_2$ than the wild type TT01.

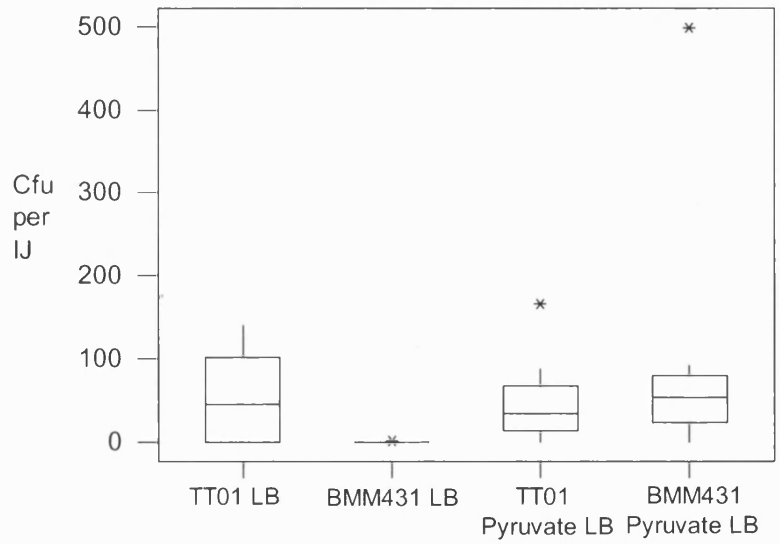


**Figure 4.9** Colonisation of IJ nematodes with TT01 or Δ*yfeABCD* (BMM431) mutant bacteria. Single nematodes were crushed and the lysate plated onto LB medium or LB medium supplemented with 0.1 % (w/v) pyruvate. Values are the average cfu per IJ from 10 IJs. Data is presented as a boxplot. The line within the box represents the mean value. The box extends to the first and third quartiles. The whiskers indicate the upper and lower limits and stars indicate outliers that are outside of these upper and lower limits.

Interestingly the *yfe* locus has also been implicated in manganese transport (Bearden and Perry, 1999) and free manganese ions can protect against reactive oxygen species by scavenging $H_2O_2$ and superoxide in complex with cellular ligands (Jakubovics and Jenkinson, 2001). Therefore, it seemed reasonable that the recovery defect observed with the Δ*yfeABCD* mutant (and linked to $H_2O_2$ sensitivity) could be due to a reduced ability to transport manganese. In order to investigate this possibility, cultures of Δ*yfeABCD* mutant and wild type were grown in LB broth cultures with or without added manganese chloride. These cultures were used to plate out serial dilutions onto LB agar that had been exposed to light or kept in the dark with or without pyruvate supplementation. Manganese supplementation did not rescue the light mediated defect and at higher concentrations (> 1 mM) caused growth cessation (data not shown). In an alternative approach, filter paper discs were soaked with 50 µl of 30 % (v/v) $H_2O_2$ and the discs were added to a soft agar overlay inoculated with the *Photorhabdus* strain to be tested. A clear halo surrounding the disc indicates the level of resistance to the $H_2O_2$ insult and the Δ*yfeABCD* mutant exhibited the same diameter halo (23.3 mm ± 1.5 mm) as the wild type at (23.7 mm ± 1.2 mm). Therefore the Δ*yfeABCD* mutant does not have an inherent increased sensitivity to $H_2O_2$. These data appear to suggest that the niche of the nematode gut induces specific physiological changes in the Δ*yfeABCD* mutant bacteria, perhaps related to $Mn^{2+}$ homeostasis, that do not occur during growth in LB broth cultures.

### 4.2.10 IJ nematode colonisation in the presence of pyruvate

Once the need to supplement the LB agar with 0.1% (w/v) pyruvate had been established single IJ nematode crushing was performed again following symbiosis assays. A comparison of the Δ*yfeABCD* and Δ*feoAB* ferrous transport mutants revealed no difference in the level of nematode colonisation, even when the mutations were combined. Interestingly even though the Δ*exbD* Δ*yfeABCD* and Δ*exbD* Δ*feoAB* double mutants appeared to have wild type levels of colonisation the triple mutant Δ*exbD* Δ*yfeABCD* Δ*feoAB* showed a decreased

level of colonisation suggesting under severe iron restriction colonisation may be affected (Fig. 4.10.).

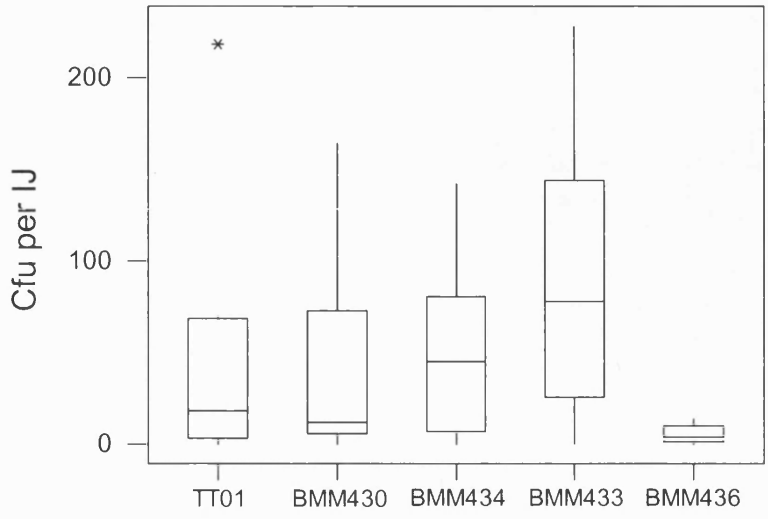


**Figure 4.10.** Colonisation of IJ nematodes with TT01 or iron uptake mutant bacteria. Single nematode crushing onto LB media supplemented with 0.1% (w/v) pyruvate. Values are the average cfu per IJ from 10 IJs. Data is presented as a boxplot. The line within the box represents the mean value. The box extends to the first and third quartiles. The whiskers indicate the upper and lower limits and stars indicate outliers that are outside of these upper and lower limits.

### 4.2.11 Iron storage proteins

Cells normally have iron reserves and excess iron that is not required immediately for essential bacterial processes must be stored safely in order to avoid oxidative damage. Therefore, it is possible that, these bacterial iron reserves serve as an important source of iron for the nematodes. *In silico* genome analysis revealed several genetic loci that were potentially involved in iron storage, based on homology with genes in *E.coli* and other bacteria (Table 4.1). The *ftnA* gene encodes for ferritin, a family of iron storage proteins that are widespread in nature. The next locus is *bfr*, a gene encoding for bacterioferritin, a bacterial-specific ferritin that contains haem. Of particular interest were the two genes, *ppxA* and *ppxB,* encoding proteins that are predicted to contain repeated motifs similar to the vertebrate haem-scavenging molecule haemopexin (Crennell

*et al.*, 2000). Therefore *Photorhabdus* possess an eukaryotic-like protein that is potentially involved in iron storage. The haemopexin motif may indicate a potential mechanism for the specific delivery of iron from the bacteria to the nematodes. In addition, blastp analysis of the TT01 genome using the PpxA and PpxB proteins revealed *plu4231* as a homologue of the *ppxA* and *ppxB* genes, and this ORF was included in the KO analysis. Unfortunately, despite repeated attempts, it was not possible to construct a deletion mutant in the *bfr* locus, suggesting that bacterioferritin may be essential to the cell.

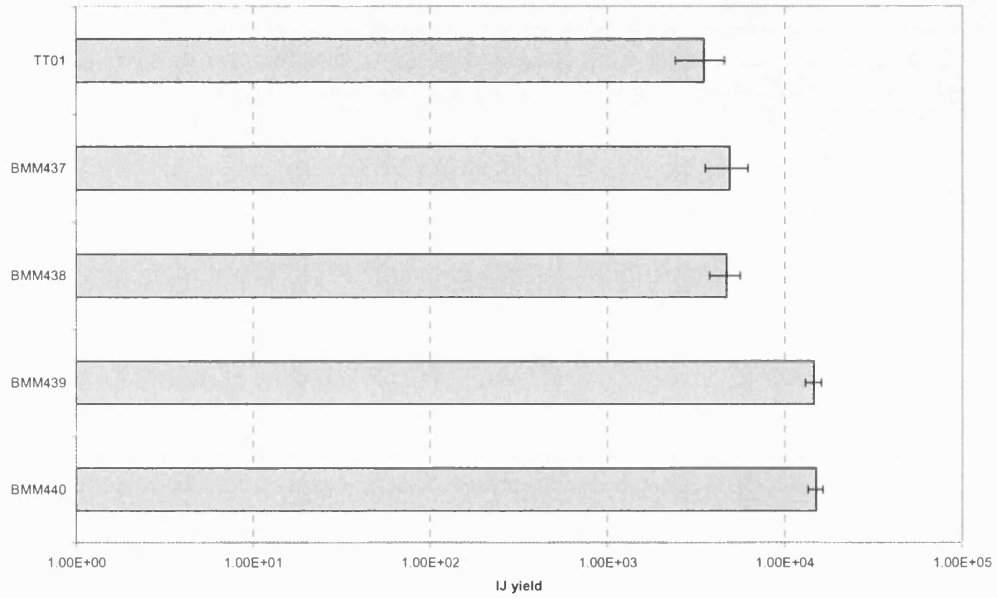


**Figure 4.11.** IJ yield for iron storage gene KO mutants. Values are an average of 5 plates. Error bars represent standard deviation. BMM437=Δ*ftnA* BMM438=Δ*ppxAB* BMM439=Δ*plu4231* BMM440=Δ*ppxAB* Δ*plu4231*

### 4.2.12 Symbiosis of iron storage mutants

The rationale is that the nematodes feed on the bacterial biomass in order to grow and develop and, therefore, the nematodes must acquire their iron requirement directly from the *Photorhabdus* bacteria. A reduction in the ability of the bacteria to acquire and/or store iron would be expected to reduce the ability of the *Photorhabdus* to support a large nematode population due to their lower nutritional value. It has been concluded that $Fe^{3+}$ uptake is essential for nematode growth on *P. temperata* K122 but neither $Fe^{3+}$ uptake nor $Fe^{2+}$ uptake appear to

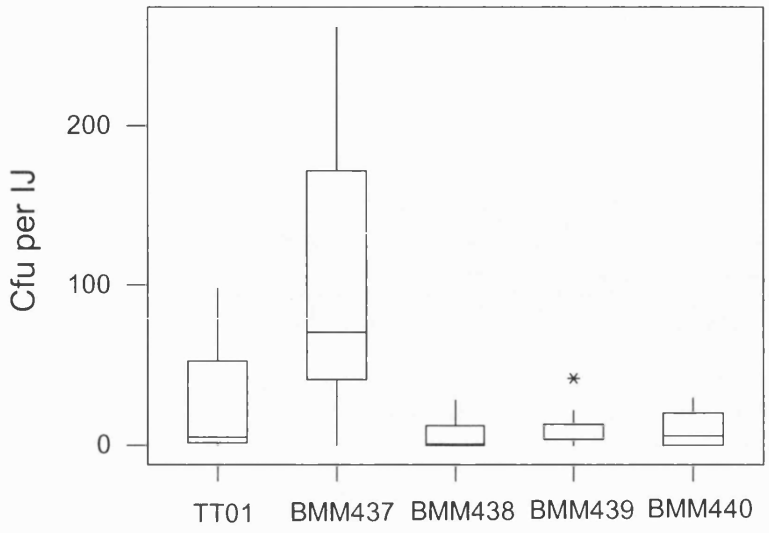


**Figure 4.12.** Colonisation of IJ nematodes with TT01 or iron storage mutant bacteria. Single nematode crushings onto LB media supplemented with 0.1% (w/v) pyruvate. Values are the average cfu per IJ from 10 IJs. Data is presented as a boxplot. The line within the box represents the mean value. The box extends to the first and third quartiles. The whiskers indicate the upper and lower limits and stars indicate outliers that are outside of these upper and lower limits. BMM437=Δ*ftnA* BMM438=Δ*ppxAB* BMM439=Δ*plu4231* BMM440=Δ*ppxAB* Δ*plu4231*

be important for growth on *P. luminescens* TT01. Therefore symbiosis assays were performed with all of the mutants constructed in genes encoding iron storage proteins to identify any role for these genes in nematode growth and development. IJ recovery to hermaphrodite and growth and development were all unaffected (data not shown) and IJ yields at 21 days were also very similar (Fig. 4.11). Individual IJ crushing revealed the Δ*ftnA* mutant to have an increased CFU count compared to the wild type but this was within 'normal' values seen during single IJ crushing assays (Fig. 4.12). The values for the *ppxAB* mutants appeared to be slightly reduced compared to the wild type (Fig. 4.12). Therefore the IJs retrieved from the symbiosis assay were subject to insect infection assays and the IJ nematodes were collected 14 days after insect death. Single IJ crushing of these nematodes from the *in vivo* assays revealed a similar level of colonisation between all strains suggesting no defect in the ability of the iron storage mutants to colonise IJ nematodes (Fig. 4.13).

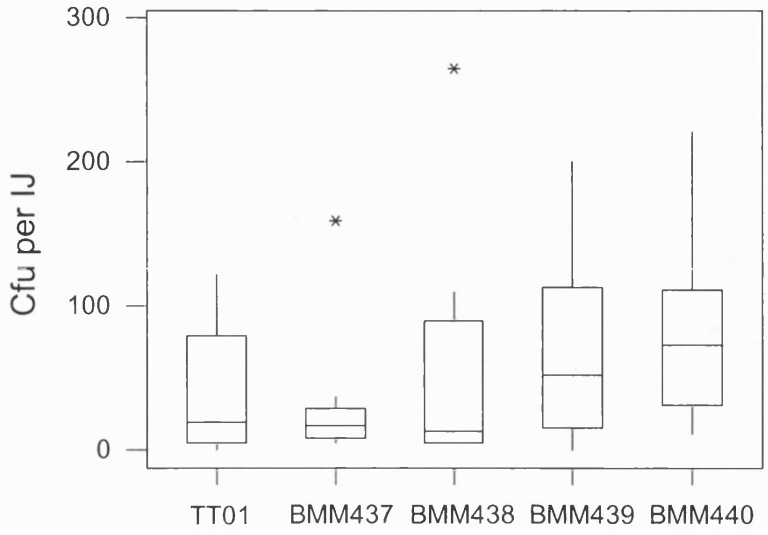


**Figure 4.13.** Colonisation of IJ nematodes with TT01 or iron storage mutant bacteria after *in vivo* infections. Single nematode crushings onto LB media supplemented with 0.1% (w/v) pyruvate. Values are the average cfu per IJ from 10 IJs. Data is presented as a boxplot. The line within the box represents the mean value. The box extends to the first and third quartiles. The whiskers indicate the upper and lower limits and stars indicate outliers that are outside of these upper and lower limits. BMM437=Δ*ftnA* BMM438=Δ*ppxAB* BMM439=Δ*plu4231* BMM440=Δ*ppxAB* Δ*plu4231*

### 4.2.13 Pathogenicity of the nematode-*Photorhabdus* complex

It is possible that intracellular iron stores may be required for rapid growth in an iron limited environment before siderophores and other iron scavenging mechanisms have been deployed, such as might be expected during the initial stages of infection. Therefore nematodes that were grown on the iron storage mutant strains were assayed for their ability to kill insect larvae. All of the IJ nematodes were able to kill *G. mellonella* insect larvae in the same time as the wild type (data not shown) confirming that a) the nematodes were colonised and b) the mutant bacteria appear to be fully virulent.

### 4.2.14 Iron regulation

Mutations in ferric iron uptake (*exbD*), ferrous iron uptake (*yfeABCD* and *feoAB*) and iron storage (*ppxAB*, *plu4231* and *ftnA*) all appeared to play no role in the symbiotic ability of *P. luminescens* TT01 to support nematode growth and development. The major regulator of iron genes in enteric bacteria is Fur, a protein that acts by repressing genes involved in iron acquisition (and other functions such as virulence) when iron is in excess. In environments where iron is limiting Fur is not complexed with $Fe^{2+}$ and Fur-regulated genes are de-repressed. Therefore a deletion of *fur* would create a state of constitutive de-repression of the Fur regulon. However no Δ*fur* mutant was identified after the screening of several hundred colonies over multiple independent conjugation attempts. An alternative method for producing *fur* mutants is to identify alleles that render cells resistant to high levels of manganese (Hantke, 1987). Despite several attempts on various concentrations of manganese no $Mn^{2+}$-resistant mutants were identified. Therefore it is possible that *fur* is an essential gene in TT01 as has been reported for other bacteria including *Burkholderia pseudomallei* (Loprasert *et al.*, 2000)

Recent data from microarray analysis in *Bacillus subtilis* revealed a significant overlap of 20 operons that were regulated in response to both a Δ*fur* mutation and iron starvation by treatment with DIP (Baichoo *et al.*, 2002). Therefore it seemed possible to phenocopy a *fur* mutation by adding DIP to the medium. Therefore DIP was added to lipid agar in increasing quantities up to a maximum of 200 μM, a concentration that resulted in the cessation of bacterial growth. Surface sterilised IJ nematodes were added following 72 h incubation of bacteria and were observed for symbiosis. A relatively low concentration of DIP, 50 μM, was sufficient to block recovery of the IJs to hermaphrodites. At this low level of chelator there did not appear to be any affect on the growth of the bacteria as the biomass produced when TT01 was grown on 50 μM DIP was the same as the wild type and antibiotic production and pigmentation were also unaffected (Table 4.4). However, a decrease in the level of bioluminescence was observed suggesting that the physiology of the cell was affected at this concentration of

DIP. Symbiosis assays were also performed with bacteria grown on lipid agar containing 25 μM DIP and it was observed that IJ nematode recovery to hermaphrodite was reduced from 51 % without treatment to 32 % with 25 μM DIP. However, following recovery the nematodes appeared unaffected in growth and development and were able to produce IJs on the lids of symbiosis assays at 21 days. As a control, an alternative chelator of metal ions, EDTA, was used to supplement lipid agar at concentrations ranging from 0.01 to 10 mM. A concentration of 10 mM EDTA caused bacterial growth arrest, however nematode growth and development appeared to be unaffected at any of the EDTA concentrations from 0.01 to 1 mM (data not shown).

**Table 4.4.** Phenotypes of *P. luminescens* TT01 with DIP treatment

| | 2,2'-dipyridyl added to media | |
|---|---|---|
| TT01 Phenotypes | 0 μM | 50 μM |
| Pigmentation | +++ | +++ |
| Bioluminescence | +++ | ++ |
| Antibiotic Production | +++ | +++ |
| Biomass (Mg dry weight) | 126 mg +/- 4 mg | 114 mg +/- 9 mg |
| IJ Recovery to Hermaphrodite | +++ | - |

4.2.15 Proteomic analysis of DIP treated *Photorhabdus*

The striking deficiency in symbiosis observed when 50 μM DIP was added to lipid agar plates was unexpected. It seems likely that specific changes in gene expression, induced by the low levels of DIP, might be responsible for the inability of the bacteria to support nematode growth and development under these conditions. Therefore, in order to identify differences in protein production that may explain the defect in symbiotic ability 2D SDS-PAGE gel analysis was performed with total protein extracts obtained from TT01 grown on lipid agar in the presence or absence of DIP. The samples were processed by Ursula Gerike (University of Bath). In two separate sample replicates 120 μg of *Photorhabdus* protein was run on pH 4-7 IEF strips followed by separation on the second dimension by 12.5 % homogenous SDS-PAGE. The gels were stained with

Coomassie Blue and were analysed by eye. It was immediately obvious that there appeared to be very little differences in the proteomes under the 2 conditions being tested. Careful examination revealed 8 protein spots that, in both gels, appeared to have increased intensities in the samples treated with DIP (Fig. 4.14.). No spots with decreased intensities after DIP treatment were observed. These protein spots were cut out from the gels and sent to Jenna Slinn (University of the West of England, Bristol) for processing. The spots were digested using Tyrpsin and were submitted for MALDI-TOF analysis. Peptide Mass Fingerprints (PMF's) were analysed using the ProteinLynx search tool, resulting in positive protein identifications for 9 of the 10 proteins under analysis (Fig. 4.14). The most interesting proteins appeared to be spot 8 and spot 9, both spots exhibiting a significant induction upon DIP treatment from an extremely low level in the untreated bacteria. Spot 8 was identified as a protein predicted to be encoded by *plu1840.* This protein did not have any known homologues when analysed with blastp. Unfortunately spot 9 was the only protein not to be identified by this analysis. Spot 1 was identified as a probable haemin/siderophore ABC transporter encoded by *plu2853* and this protein would be expected to be up-regulated under conditions of iron restriction. Spots 6 and 7 were both identified as proteins with putative roles in virulence whilst spots 4 and 5 were both identified as the GroES chaperonin. Spot 2 (encoded by *plu1561*) was identified as a protein with homology to the slime mould calcium dependent adhesion molecule that are utilised in cell to cell adhesion during the early stage of development (Wong *et al.*, 1996). Two additional proteins that were analysed independently of altered expression levels. Spot 3 was selected based on the size of the protein being similar to Fur, however this spot was identified as CipA, the crystalline inclusion protein which is known to be essential to support nematode growth and reproduction (Bintrim and Ensign, 1998). Importantly the level of CipA appears to be the same in treated and untreated *Photorhabdus*, therefore the symbiosis defect observed was not due to a decrease in CipA. Spot 10 was analysed as the most abundant protein observed on the gel and was identified as having weak similarity to the Type III secretion system of *P. luminescens* W14 and this is encoded for by *plu3795*. The fact that all of the proteins identified were induced with DIP treatment suggests that at least one of these proteins may be inhibiting symbiosis.

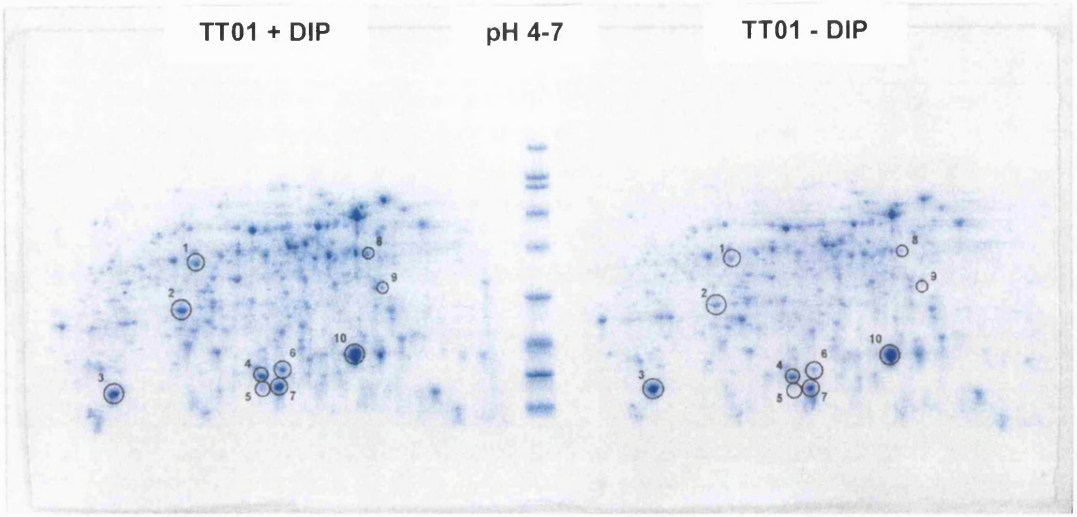


| No. | FC | + DIP | | | | - DIP | | | |
|---|---|---|---|---|---|---|---|---|---|
| | | Spot ID | Sc / Cov | PH | Function | Spot ID | Sc / Cov | PH | Function |
| 1 | + 3 | Plu2853 | 8.4 44.1 | 15 | Probable Hemin/Siderophore ABC transporter | no match | - | - | no match |
| 2 | + 4 | Plu1561 | 8.4 38.8 | 8 | Similar to *Dictyosdelium* calcium dependent adhesion molecule | Plu1561 | 8.4 37.9 | 7 | Similar to *Dictyosdelium* calcium dependent adhesion molecule |
| 3 | - | CipA | 8.3 36.5 | 8 | Crystalline inclusion protein CipA | CipA | 8.4 36.5 | 10 | Crystalline inclusion protein CipA |
| 4 | + 2 | GroES | 10.4 48.5 | 5 | 10 kDa chaperonin (Protein CPN10) (Protein GROES) | no data | - | - | no data |
| 5 | + 2 | GroES | 6.6 34.0 | 3 | 10 kDa chaperonin (Protein CPN10) (Protein GROES) | no data | - | - | no data |
| 6 | + 3 | Plu4093 | 8.4 51.9 | 6 | PirA insect toxin | Plu4093 | 8.4 69.2 | 7 | PirA insect toxin |
| 7 | + 3 | Plu0947 | 8.4 41.5 | 6 | orf 63 *P.luminescens* W14 Path island 1. *Burkholdaria* antibiotic monooxygenase | Plu0947 | 8.4 41.5 | 6 | orf 63 *P.luminescens* W14 Path island 1. *Burkholdaria* antibiotic monooxygenase |
| 8 | + 5 | Plu1840 | 8.4 34.9 | 10 | Unknown | no data | - | - | no data |
| 9 | + 5 | no data | - | - | no data | no data | - | - | no data |
| 10 | - | Plu3795 | 8.4 60.4 | 9 | Similar to TypeIII secretion system of *P.luminescens* W14 | Plu3795 | 8.4 60.4 | 9 | Similar to TypeIII secretion system of *P.luminescens* W14 |

**Figure 4.14.** Protein analysis from 2D SDS PAGE gels of TT01 WT treated with DIP. Protein spot identification was performed using the ProteinLynx software to analyse the PMF data to match to the Swissprot database. Sc= Score. Cov = Coverage. PH = Number of peptide hits. FC= Fold Change +/- DIP.

**Table 4.5.** Symbiosis of *H. downesi* nematodes on TT01 bacteria

| Strain | % Nematode Recovery | IJs produced at 21 days |
|---|---|---|
| TT01 | 50 | + |
| Δ*exbD* (BMM430) | 57 | - |
| Δ*yfeABCD* (BMM431) | 84 | + |
| Δ*feoAB* (BMM432) | 64 | + |
| Δ*ppxAB* (BMM438) | 88 | + |
| Δ*plu4231* (BMM439) | 74 | + |
| Δ*ftnA* (BMM437) | 78 | + |
| Δ*exbD yfeABCD* (BMM433) | 86 | - |
| Δ*exbD feoAB* (BMM434) | 76 | - |
| Δ*yfeABCD feoAB* (BMM435) | 60 | + |
| Δ*ppxAB plu4231* (BMM440) | 86 | + |
| Δ*exbD yfeABCD feoAB* (BMM436) | 79 | - |

### 4.2.16 Nematode crossfeeding

In contrast to *P. temperata* K122 none of the mutations in iron-associated genes constructed in *P. luminescens* TT01 appeared to show any defect in their ability to support nematode growth and development. One possible explanation of this is that the nematode partner of TT01, *H. bacteriophora* was less sensitive to perturbations in bacterial iron levels than the nematode partner of K122, *H. downesi.* To explore this idea 50 *H. downesi* IJs were added to lipid agar plates inoculated with the different TT01 mutant strains and the plates were observed for nematode recovery. All of the TT01 strains were able to support *H. downesi* nematode recovery to greater than 50 % and nematode growth and development

**Table 4.6.** Nematode growth and development after 14 days.

| | Nematode Strain | |
|---|---|---|
| *Photorhabdus* strain | *H. downesi* (K122) | *H. bacteriophora* (TT01) |
| *P. temperata* K122 | +++++ | +++++ |
| BMM417 (K122) | + | +++++ |
| *P. luminescens* TT01 | +++++ | +++++ |
| BMM430 (TT01) | +++++ | +++++ |

was also observed on all strains (Table 4.5). However, at 21 days post-inoculation no IJs developed on plates inoculated with the TT01 Δ*exbD* strain, and the double and triple mutants containing the Δ*exbD* allele (Table 4.5.). In fact it took a further 7 days for any IJs to be observed on the lids of these plates. Therefore the *H. downesi* nematodes did reveal a symbiosis defect in the TT01 Δ*exbD* strains i.e. delayed IJ production. Remarkably, when *H. bacteriophora* nematodes were grown on the *P. temperata* K122 mutant, BMM417 nematode growth and development was indistinguishable from the wild type (Table 4.6). This further suggests that the *exbD* mediated defect in *P. temperata* K122 is related to its association with *H. downesi* nematodes.

## 4.3 Discussion

### 4.3.1 The *exbD* mutation in *P. luminescens*

In Chapter 3 it was shown that the *exbD::Km* mutation in *P. temperata* K122 (BMM417) resulted in a decrease in virulence towards *Galleria mellonella* larvae and also had a striking affect on the ability of the bacteria to support nematode growth and development. The nematodes could recover from IJ to hermaphrodites on lipid agar seeded with BMM417, however symbiosis could not proceed beyond that stage. In order to identify the exact reasons for this defect an Δ*exbD* mutation was constructed in the sequenced *Photorhabdus* strain, *Photorhabdus luminescens* TT01 (Duchaud *et al.*, 2003). Pathogenicity assays revealed the TT01 Δ*exbD* mutant, BMM430, to be completely avirulent in *G. mellonella* larvae, when injected at a dose of 100 cfu per insect. This observation is consistent with previous studies where TonB has been shown to play a key role in the pathogenicity of many bacterial pathogens (Beddek *et al.*, 2004; Bosch *et al.*, 2002; Jarosik *et al.*, 1994; Pradel *et al.*, 2000; Reeves *et al.*, 2000; Seliger *et al.*, 2001; Torres *et al.*, 2001; Tsolis *et al.*, 1996). Therefore, in contrast to K122, the TT01 Δ*exbD* mutant (BMM430) does not appear to be able to grow at all in the insect environment. Growth of the BMM430 mutant was also affected when presented with an iron-limited environment either in LB media supplemented with dip chelator (Fig. 4.5) or when grown in Graces insect media (Fig. 4.4). Surprisingly, the siderophore overproduction phenotype observed in BMM417 was not evident in the TT01 Δ*exbD* mutant. The major siderophore produced by K122 and presumably overproduced in BMM417 is photobactin and subsequent analysis of the TT01 genome revealed that no operon for the production of the photobactin siderophore was present. Photobactin is not required for virulence in K122 suggesting that another TonB-dependent iron transporter is required for virulence in both K122 and TT01.

BMM430 (TT01 Δ*exbD*) did not show any defect in its ability to support nematode growth and development or IJ yield (Fig. 4.7). This is in contrast to what was previously observed with the K122 mutant, BMM417. One possible

explanation for this may be related to the presence or absence of the photobactin siderophore. In *P. aeruginosa* the pyoverdine siderophore has been shown to act as signalling molecule (Lamont *et al.*, 2002) regulating the transcription of genes involved not only in iron acquisition but also virulence. It is possible that in BMM417 (K122 *exbD::Km*) the high external concentration of photobactin siderophore causes hyper stimulation of a signalling cascade causing the symbiosis-minus phenotype observed. This hyper-stimulation is not happening in BMM430 (TT01 Δ*exbD*) as photobactin is not produced. An alternative explanation is that the mutation in the *exbD* gene may not have completely rendered the TonB system unable to function. There are known homologues to the *exbB* and *exbD* genes, *tolQ* and *tolR* and these have been shown to partially complement the function of *exbBD* in *E. coli* (Braun and Herrmann, 1993). The genome of *P. luminescens* TT01 is predicted to encode the *tolQR* genes, and it is therefore possible that low level expression of the TonB system may be occurring which may be sufficient to support nematode growth and development in the TT01 background. It is not known if these homologues are present in the K122 genome.

### 4.3.2 Alternative iron uptake systems *feoAB* and *yfeABCD*

TonB (and *exbD*)-dependent iron transport is the major mechanism for ferric ($Fe^{3+}$) iron transport but is not the only method for iron acquisition in bacteria. An alternative is the transport of ferrous ($Fe^{2+}$) iron and several ferrous iron transport systems have been characterised. Indeed an *E. coli* K-12 mutant lacking the *feoAB* ferrous ($Fe^{2+}$) uptake system was unable to colonise the mouse intestine in the streptomycin-treated mouse colonisation model (Stojiljkovic *et al.*, 1993). This was probably due to the low oxygen conditions found in the gut, as anaerobic conditions result in the increased solubility of ferrous iron. However, the role of the *feoAB* system in *Salmonella* is not so clear. One study showed a *feoB* mutant to be unaffected in systemic infection although mouse intestine colonisation was affected (Tsolis *et al.*, 1996). Another study has shown *feoB* to be required for full virulence when injected intravenously into Nramp1 mice, where a mutation in *feoB* resulted in a median survival time of 24 days

compared to 7 days for the wild type (Boyer *et al.*, 2002). Interestingly a similar decrease in virulence was also observed with a *sitABCD* mutant, suggesting that both ferrous uptake systems are essential for full virulence. In fact a double mutant in *Salmonella* (*feoAB sitABCD*) was shown to be completely avirulent (Boyer *et al.*, 2002). In *Y. pestis* the *yfeABCD* ferrous iron transport system (analogous to the *sitABCD* system in *Salmonella*) was identified as essential for full virulence and mutations in this system resulted in an approximately 100-fold decrease in the $LT_{50}$ when the bacteria were infected subcutaneously. When combined with a yersiniabactin mutant (*ybt*) which is avirulent via the subcutaneous route but is fully virulent by intravenous injection, the double mutant became avirulent (Bearden and Perry, 1999). This data implies that these two systems may be used during different stages of the disease, perhaps yersiniabactin is required for dissemination from the site of the flea bite and the *yfeABCD* system is required in the latter stages of the disease. Extracellular ferric reductases have been identified in some bacteria and can contribute to the acquisition of iron in those strains by reducing ferric ($Fe^{3+}$) iron to ferrous ($Fe^{2+}$) iron by the action of flavin reductase (Schroder *et al.*, 2003). Indeed a ferric reductase gene is predicted in the *P. luminescens* TT01 genome as the *fre* gene (*plu4404*). Therefore ferrous iron acquisition and its subsequent uptake may play an important role in *Photorhabdus* iron assimilation. During insect infection and nematode colonisation it might be expected that *Photorhabdus* will experience conditions where oxygen availability is low, especially during the latter stages of infection when microbial respiration is high and this should result in a greater solubility of ferrous iron. *P. luminescens* is predicted to encode both the *yfeABCD* system and the *feoAB* system. As expected BMM433 (Δ*exbD* Δ*yfeABCD*) and BMM434 (Δ*exbD* Δ*feoAB*) showed a reduced ability to grow on LB media supplemented with DIP (Fig. 4.6). Interestingly the BMM432 (Δ*feoAB*) mutant alone did not seem to be affected at all, whereas the BMM431 (Δ*yfeABCD*) mutant was restricted for growth, suggesting an increased importance of the *yfeABCD* locus under conditions of iron restriction even in the presence of a functional TonB system. The BMM430 (Δ*exbD*) mutant was moderately affected as would have been predicted and the triple knock out, BMM436 (Δ*exbD* Δ*yfeABCD* Δ*feoAB*), was most severely affected suggesting

the mutant was experiencing severe iron restriction. However the fact this mutant was able to grow at all suggests that at least one further iron acquisition mechanism is present in TT01. AfuABC is an ABC transporter of the oral pathogen *Actinobacillus pleuropneumoniae* and has been shown to stimulate growth of an *E. coli* siderophore mutant in the presence of iron chelator (Chin *et al.*, 1996) and this operon appears to be present in the *P. luminescens* TT01 genome (encoded by *plu0810-0812*). Therefore this locus may be important for the residual level of iron transport allowing growth.

No pathogenicity defects were detected with the single ferrous uptake mutants (Table 4.3). This was predicted as either system would have been expected to complement for the other. However, even the double knock out, BMM435, was able to kill insect larvae in the same time as wild type suggesting these iron acquisition pathways are dispensable for pathogenicity (Table 4.3). The ability of the ferrous mutants to support nematode growth and reproduction was determined to identify any defects caused by decreased iron transport. However in all cases the deletion mutants were able to support nematode growth and development to the same level as wild type. Even when the ferrous uptake mutants were combined with the *exbD* mutation nematode growth and development remained unaffected which was surprising. It was expected that increasing the number of mutations involved in iron acquisition would eventually result in a strain that would be unable to meet the nutritional demands of the nematodes feeding on it. However even the triple mutant strain, BMM436, was fully able to support nematode growth and development despite being crippled for growth on iron chelated media. This strongly suggests that the iron requirements of the *H. bacteriophora* nematode are easily met by *Photorhabdus* containing the level of iron required for essential bacterial processes.

The final stage of the symbiotic process requires the *Photorhabdus* bacteria to recolonise the gut of the infective juvenile nematode. All of the iron uptake mutants were assayed for their ability to recolonise IJ nematodes by crushing the individual IJ nematodes collected from symbiosis assays following surface sterilisation and counting the number of colonies that appeared after several days growth on LB agar. The results appeared to suggest a severe defect in IJ

colonisation with BMM431 (Δ*yfeABCD*). Further analysis suggested that this defect was in fact an artefact due to increased sensitivity of the Δ*yfeABCD* bacteria to $H_2O_2$ generated in the LB agar during exposure to fluorescent light. A set of genes homologous to *yfeABCD* have been identified as important for both manganese and iron transport and resistance to hydrogen peroxide (Sabri *et al.*, 2006). The *sitABCD* operon was identified in an avian pathogenic *E. coli* strain and this operon is able to confer $H_2O_2$ resistance in a strain carrying a mutation in the high-affinity manganese transporter encoded for by *mntH* (Sabri *et al.*, 2006). Interestingly TT01 does not contain a homologue of *mntH*, suggesting that the *yfeABCD* (*sitABCD*) operon may be the only mechanism for manganese uptake in these bacteria. In addition *in silico* analysis reveals that the only superoxide dismutase enzyme present in the TT01 genome (SodA) is predicted to require manganese as a co-factor. SOD is required for the detoxification of superoxide radicals and the absence of this activity would increase the sensitivity of cells to oxidants such as $H_2O_2$.

### 4.3.3 Iron storage proteins

*Heterorhabditis* nematodes acquire the nutrients they need to grow and develop by feeding on the *Photorhabdus* bacteria. Therefore, depleting the ability of the bacteria to store iron in various iron storage proteins might have been expected to reduce the ability of these mutants to support nematode growth and development. The photopexin operon appeared to be particularly interesting due to the presence of haemopexin like motifs in the two proteins PpxA and PpxB. The haemopexin motifs are characteristic of the eukaryotic haemopexin iron haem transport proteins (Crennell *et al.*, 2000). However there does not appear to be a role for the photopexins in the symbiotic interaction of *Photorhabdus* with *Heterorhabditis*. Moreover pathogenicity was also unaffected in these photopexin mutants suggesting that these proteins are not required for iron acquisition from the host nor are they required as an essential iron store or for protection against reactive oxygen species. Further iron storage proteins were identified in the *P. luminescens* TT01 genome sequence and were identified as ferritin (*ftnA*) and bacterioferritin (*bfr*). Both of these storage proteins are found

widespread in bacteria and are responsible for the storage of iron required for essential bacterial processes when environmental iron is low or act to store iron in iron replete conditions (Andrews, 1998). The ability for the bacterium to store excess iron is particularly important as free excess iron can cause oxidative damage via the Fenton reaction (Ratledge and Dover, 2000). The *ftnA* mutant BMM437 did not show any symbiosis defects suggesting that the ferritin protein plays no role in iron delivery to the nematodes, although it is possible that bacterioferritin can compensate for the loss of ferritin.

### 4.3.4 Phenocopying Fur

Iron homeostasis is controlled by the Fur regulator and because it was not possible to construct a *fur* deletion mutant it was decided to phenocopy this mutation using DIP. Interestingly nematode recovery from IJ to hermaphrodite was completely abolished at a concentration of DIP at least 4 times lower than that which is required to prevent *Photorhabdus* growth. This suggests two possibilities; a) the *Photorhabdus* gene expression has been altered by the action of the DIP such that signals normally produced by the *Photorhabdus* which are essential to initiate nematode recovery are not present or inhibitors have been induced; b) the DIP chelator may be acting directly on receptors within the nematode to block recovery. To define the changes in *Photorhabdus* physiology that could explain the nematode recovery defect, the proteome was compared between the wild type strain grown in the presence or absence of DIP and eight proteins with increased abundance in the DIP treated samples were identified. Interestingly several of these proteins were previously identified as being up-regulated in the proteome of the (non-symbiotic) secondary variant of TT01 i.e. spot 7 (encoded by *plu0947*) and spot 8 (encoded by *plu1840*) (Turlin *et al.*, 2006). Therefore it is possible that DIP treatment is upregulating the production of some proteins resulting in a block in symbiosis.

### 4.3.5 *H. downesi* nematodes reveal *exbD* mediated symbiosis defects

None of the TT01 mutants produced the same defect in nematode growth and development as that observed with BMM417. This led to the hypothesis that the

*H. bacteriophora* nematodes may be less sensitive to perturbations in *Photorhabdus* iron content than the *H. downesi* nematodes. This was confirmed by cross-feeding different nematodes with the different bacteria. *H. downesi* will grow and develop on TT01 bacteria but the bacteria cannot colonise the *H. downesi* IJs. In the same way *H. bacteriophora* will grow and develop on K122 but the IJs cannot be colonised. Therefore, when *H. bacteriophora* nematodes were grown on BMM417 there was no defect in nematode growth and development. Similarly the *H. downesi* nematode did not grow normally on the TT01 Δ*exbD* mutant suggesting that *H. downesi* are much more sensitive to this mutation than *H. bacteriophora*. Interestingly all of the *H. downesi* nematodes growing on TT01 containing the Δ*exbD* allele did not produce any IJs until 7 days later than normal. This result suggests a defect in the ability of these mutant strains to support the normal level of symbiosis with *H. downesi*, although the defect was much more subtle than observed when these nematodes were grown on BMM417 and the defect appeared at a later stage of symbiosis. This evidence may suggest evolutionary differences between the two nematodes and suggests that *H. downesi* may use iron as an important signal to ensure the correct symbiotic partnership. This is interesting as it highlights that there are differences in the requirements of the nematodes from their bacterial symbionts. This also hints at a possible mechanism for the strong "nutritionally-based" specificity that is observed in the interactions between *Photorhabdus* and *Heterorhabditis*.

# Chapter 5

# Stationary phase growth

## 5.1 Introduction

Once the *Photorhabdus* has been regurgitated from the nematode into the insect hemolymph the bacteria rapidly grow and kill the insect within 48-72 h. At this point *Photorhabdus* has attained a high cell density within the cadaver and the bacteria enter the stationary phase of growth (Daborn *et al.*, 2001). The nematodes then feed and develop on the stationary phase *Photorhabdus* before emerging from the insect cadaver some 14-21 days later having been colonised by *Photorhabdus* bacteria. Therefore the stationary phase of growth of *Photorhabdus* appears to play a very important role in the interaction between the bacteria and the nematode.

In support of this it has been observed that many of the phenotypes associated with the primary phenotypic variant of *Photorhabdus* are expressed during the stationary phase of growth. Moreover, accumulating evidence suggests that these activities are important for symbiosis with the nematode and collectively they have been called 'symbiosis factors' (ffrench-Constant *et al.*, 2003). It has been shown that the expression of the symbiosis factors is co-ordinately repressed by a LysR-type transcriptional regulator called HexA (Joyce and Clarke, 2003). Therefore a deletion of *hexA* results in an increase in the expression of the symbiosis factors and an increased ability to support nematode growth and development (Joyce and Clarke, 2003 and Joyce, unpublished data). HexA has been shown to negatively regulate the level of the alternative sigma factor, $\sigma^S$ (Joyce and Clarke, 2003) and interestingly the iron storage protein bacterioferritin has been shown to be dependent on $\sigma^S$ (Lacour and Landini, 2004; Weber *et al.*, 2005).

Bacterial sigma factors are subunits of the RNA polymerase that confer promoter specificity to the core RNA polymerase for the initiation of transcription (Wosten, 1998) and it is the pool of these different sigma factors within the cell

that plays a major role in determining which genes are targeted for transcription at a particular cell condition or time point (Ishihama, 2000). *E. coli* possesses seven such sigma factors (Ishihama, 2000) and the *P. luminescens* TT01 genome is predicted to encode all of these sigma factors (Duchaud *et al.*, 2003)

The sigma factor $\sigma^S$ has been shown to be important for expression of genes during stationary phase growth with particular emphasis in stress response and survival (Hengge-Aronis, 2002). Therefore, the objective of this chapter was to analyse the role of $\sigma^S$ during symbiosis and the stationary phase of growth of *Photorhabdus*.

## 5.2 Results

### 5.2.1 Directed KO of *rpoS*

In order to determine the effects of $\sigma^S$ on the lifecycle of *Photorhabdus* the entire *rpoS* gene was deleted from the genome of *P. luminescens* TT01. The *rpoS* locus in TT01 is similar to the *E. coli rpoS* locus with the lipoprotein gene *nlpD* immediately upstream of *rpoS* (see Fig. 5.1). Moreover the major stationary phase-induced promoter, *rpoS*p, can be predicted in *Photorhabdus* based on sequence similarity to *E. coli* (Fig. 5.2). The *rpoS* deletion mutant was constructed by Yan Wei during her M.Res project within the Clarke laboratory. In order to confirm the knock out allele, colony PCR was performed on the Δ*rpoS* mutant. Primers rpoS KO1 (located 564-545bp upstream of *rpoS*) and rpoS KO4 (located 571-590bp downstream of *rpoS*) were used which result in a 1159bp fragment if the deletion has been successful or a 1986bp fragment for wild type. In this way the *rpoS* deletion was confirmed (see Fig. 5.3) and the mutant was designated BMM429.

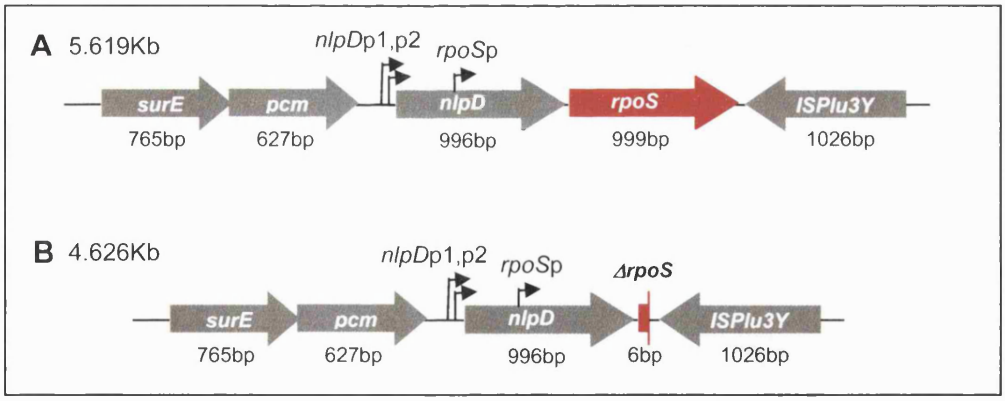


**Figure 5.1.** A. Genetic region surrounding the *rpoS* gene in *P. luminescens* TT01. Transcriptional control of *rpoS* by the promoters *nlpD*p1 and *nlpD*p2 which contribute to the basal expression of *rpoS*. These promoters are not upregulated by growth rate or growth phase in *E. coli* (Lange and Hengge-Aronis, 1994). The major promoter of *rpoS* is *rpoS*p and is subject to stationary phase induction when *E. coli* is grown on rich medium (Lange *et al.*, 1995). B. Genetic region following the directed knock out of *rpoS*.

| | -35 | -10 |
|---|---|---|
| *E. coli* | TTGCGT CGCAACGCACAATTACG | TATTCT |
| *P. luminescens* | GTTTAT AACCGTGATTATGACAG | TATTCC |

**Figure 5.2.** The major *rpoS*p promoter from *E. coli* and the equivalent in *P. luminescens* TT01. The -35 sequence is 753bp from the end of the *nlpD* gene.

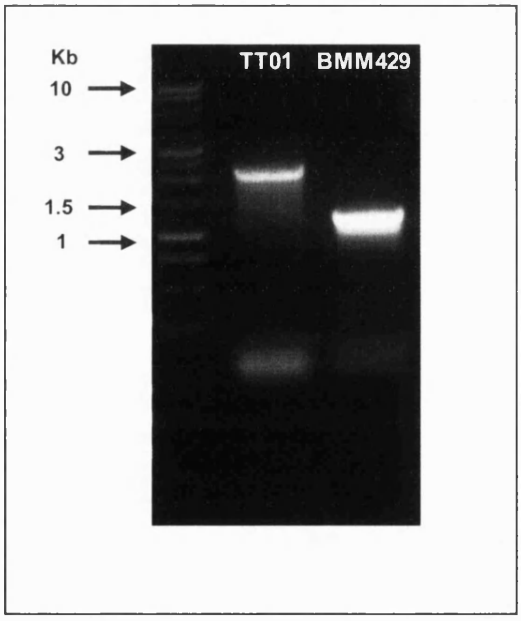


**Figure 5.3.** 1% Agarose gel of PCR products to detect the *rpoS* deletion allele. On the left is wild-type TT01 and on the right is BMM429. Colony PCR was performed with primers rpoSKO1 and rpoSKO4.

### 5.2.2 Phenotypic analysis of BMM429

The deletion of *rpoS* does not affect the growth of BMM429 in LB media (Fig. 5.4). To assess whether the deletion of *rpoS* may have pleiotropic effects on any of the primary phase characteristics phenotypic tests were undertaken. BMM429 was identical to the wild type in all of the tests with the exception of a qualitative reduction in catalase activity, as detected by a reduced rate of bubble production (catalase) when cells were immersed in 3 % (w/v) $H_2O_2$ (Table 5.1). The reduction in catalase production was confirmed by semi-quantitative tests using 13 mm Whatman filter discs that were impregnated with 50 µl of 30 % $H_2O_2$ and placed on top of an LB agar plate which had been overlaid with a mixture of 20 ml soft agar containing 0.2 ml of an overnight culture standardised to an OD of 4. These plates were incubated for 48 h before the size of the halos of growth inhibition were measured. A larger halo around the filter disc would imply an increased sensitivity to $H_2O_2$. As expected BMM429 displayed a bigger halo (49 mm +/- 1 mm compared to 24 mm +/- 1 mm for wild type) surrounding the disc suggesting that hydrogen peroxide resistance is indeed reduced in this mutant (Fig. 5.5).

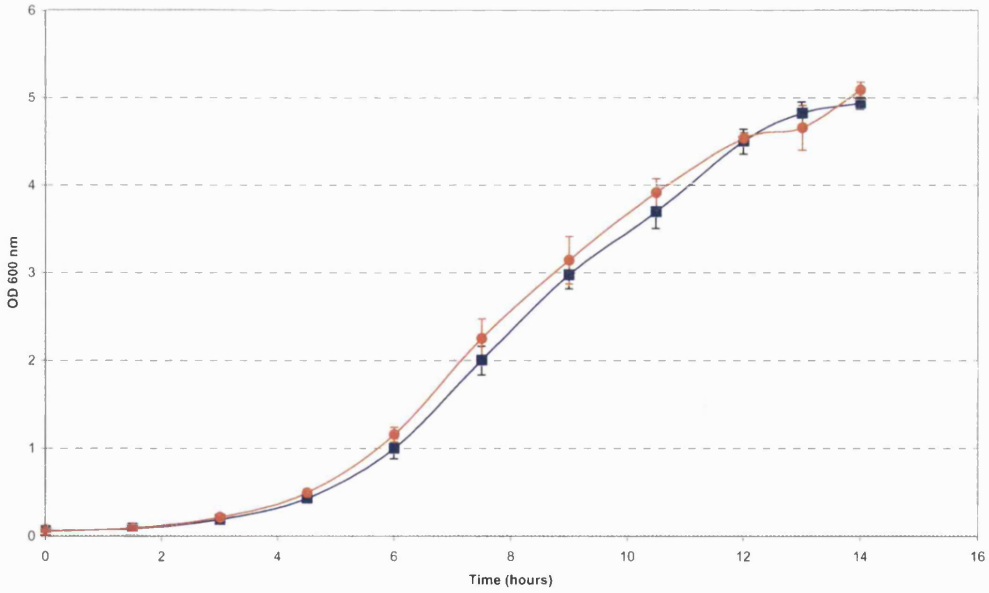


**Figure 5.4.** Growth of BMM429 (orange circles) and TT01 WT (blue squares) in LB media at 30°C 200rpm. Values are an average of 3 cultures. Error bars represent standard deviation.

**Table 5.1.** Phenotypic tests on BMM429 and WT TT01

| Test | | **TT01** | **BMM429 (Δ*rpoS*)** |
|---|---|---|---|
| Pigmentation | | Orange | Orange |
| Colony Morphology | | Convex, mucoid | Convex, mucoid |
| Bioluminescence | | +++ | +++ |
| Antibiotics | | +++ | +++ |
| Siderophore production (CAS) | | +++ | +++ |
| Lipase | | +++ | +++ |
| Motility | | +++ | +++ |
| Catalase | | +++ | + |
| Dye Uptake | EMB | Purple | Purple |
| | NBTA | Purple | Purple |
| | MacConkey | Red | Red |

5.2.3 BMM429 is unaffected in pathogenicity

Several *rpoS* mutant alleles have been shown to affect virulence in *Salmonella* (Chen *et al.*, 1995; Coynault and Norel, 1999; Kowarz *et al.*, 1994; Nickerson and Curtiss, 1997) and persistence in mice spleens (Kowarz *et al.*, 1994). Therefore 10 *Galleria mellonella* insect larvae were injected with 100 cfu of wild type TT01 and BMM429 in triplicate. After 48 h insect mortality was 100 % and 97 % when infected with wild type and BMM429 respectively suggesting that *rpoS* was not required for pathogenicity of *Photorhabdus* (data not shown).

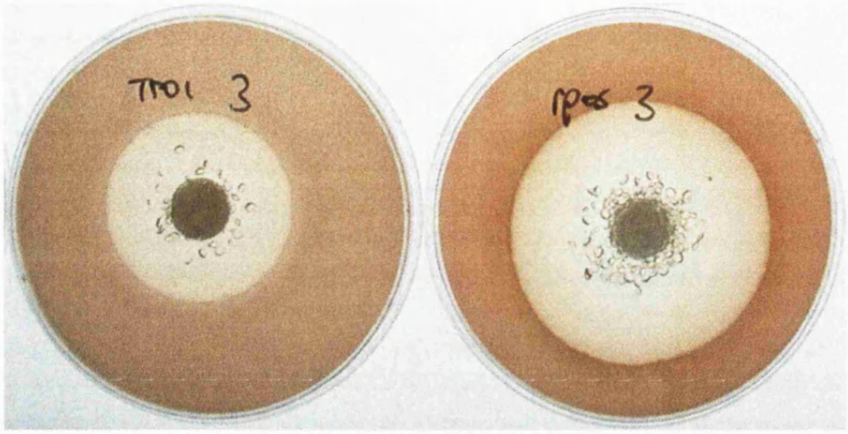


**Figure 5.5.** Hydrogen peroxide sensitivity of TT01 (left) and BMM429 (right). 50 µl 30 % H2O2 added to each 13 mm Whatman filter disc and a halo of non-growth was measured following 48 h incubation at 30°C.

### 5.2.4 BMM429 is able to support nematode growth and development

The level of $\sigma^S$ has been shown to increase during stationary phase growth in several enteric bacteria and this sigma factor is responsible for the expression of many genes involved in bacterial survival during starvation and other stresses (Hengge-Aronis, 2002). As nematode growth and development occurs during the stationary phase of growth of *Photorhabdus* it might be expected that the deletion of *rpoS* would alter the ability of BMM429 to support nematode symbiosis. However, the deletion of *rpoS* did not affect the production of many of the symbiosis factors implying that *rpoS* may not have a role in the interaction with the nematode (Table 5.1). Therefore, in order to test the ability of BMM429 to support nematode growth and development, symbiosis assays were performed on lipid agar plates. The plates were monitored for all stages of nematode growth and development over 21 days. Visual inspection of the symbiosis plates revealed no differences in the temporal development of nematode populations growing on either TT01 or BMM429 and the IJ yield was unaffected at the end of the symbiosis assay (Fig. 5.6). Therefore a deletion of *rpoS* does not affect the ability of *Photorhabdus* to support the growth and development of *Heterorhabditis* nematodes.

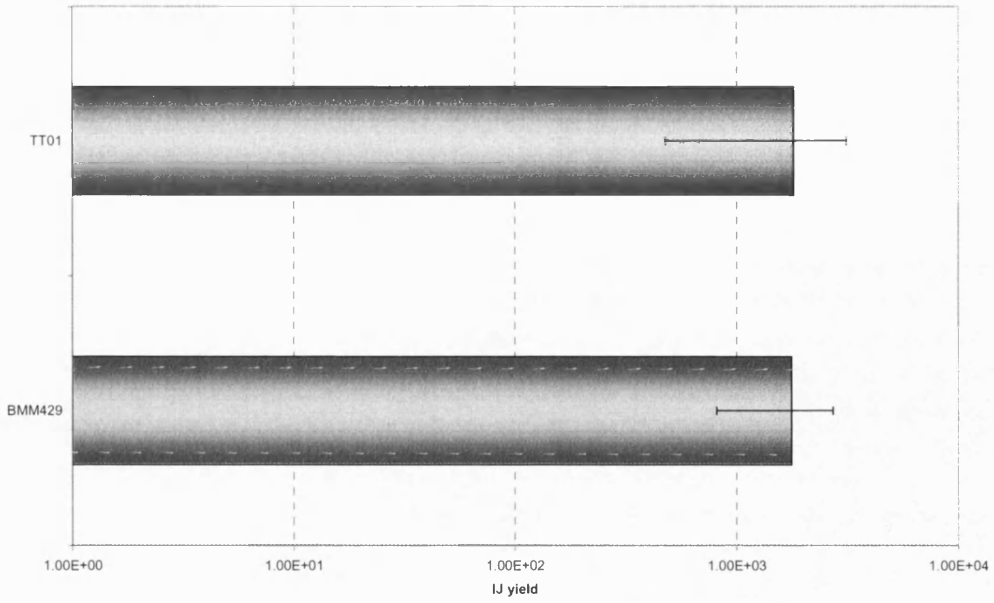


**Figure 5.6.** IJ yields of nematodes grown on TT01 or BMM429 bacteria. Error bars represent +/- standard deviation. Data is the average of 5 symbiosis plates.

### 5.2.5 Nematodes grown on BMM429 cannot infect insects

To ensure that the successful colonisation of the IJ nematodes by BMM429 had taken place, the IJ nematodes recovered from the lids of the symbiosis assays were used to infect *Galleria mellonella* insect larvae. Therefore, 1000 surface sterilised IJs were incubated with 10 insects (as described in Materials and Methods) and insect death was monitored over several days. Nematodes grown on wild type TT01 bacteria normally kill all of the insects within 72 h. Remarkably even after 5 days the insects infected with IJ nematodes reared on BMM429 were all still alive (see Fig. 5.7).

### 5.2.6 BMM429 IJs appear non-colonised

The fact that IJ nematodes reared on BMM429 bacteria could not infect insect larvae suggests that either the mutant is non-virulent or that the mutant does not colonise the IJ. It has already been shown that BMM429 is as virulent to insect larvae as wild type TT01 suggesting that the defect was in the ability of

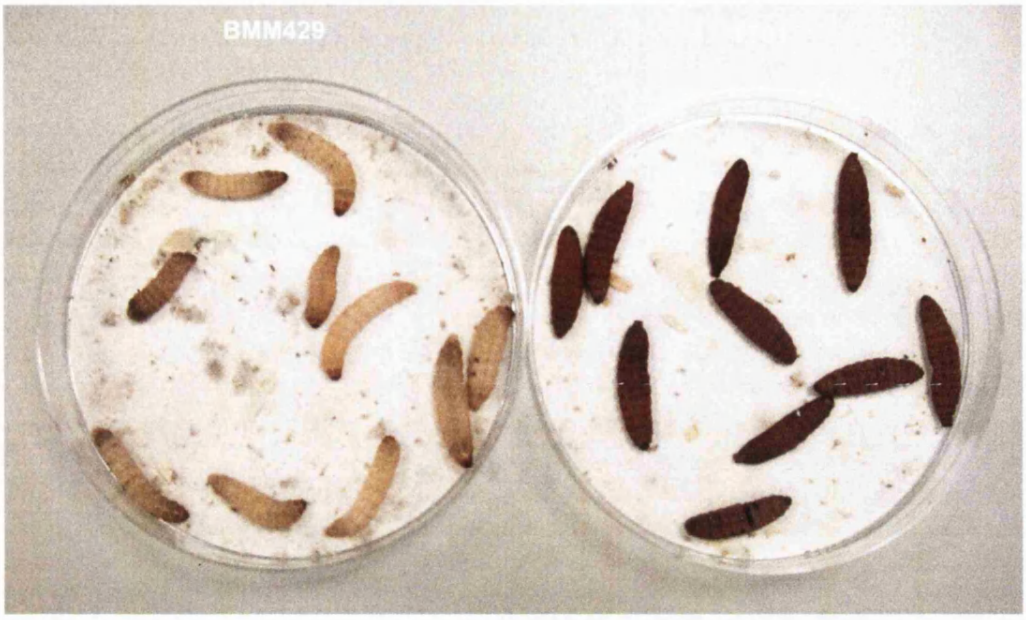


**Figure 5.7.** *Galleria mellonella* insect larvae following 5 days exposure to 1000 IJ nematodes at 25°C grown on either BMM429 or TT01 *Photorhabdus*.

the mutant bacteria to re-colonise the IJ. In order to quantify the level of colonisation of the nematode gut 10 IJ nematodes, grown on either wild type or BMM429, were crushed and the lysate was plated onto LB agar + 0.1 % (w/v) pyruvate. None of the IJs reared on BMM429 yielded any colonies, compared to a normal level of colonisation with the wild type bacteria (wild type median value 94 cfu per IJ) (Fig. 5.8). This suggested the BMM429 mutant was unable to colonise IJ nematodes.

### 5.2.7 Viability of *Photorhabdus* at the time of IJ formation

The IJ nematode generation appears approximately 21 days after the addition of nematodes to the bacterial lawn. Therefore, it is expected that, in order to be able to colonise the IJ, the bacteria will have to remain viable during an extended period of stationary phase. Therefore, the inability of BMM429 to colonise the IJ gut could be due simply to the absence of any viable bacteria after more than three weeks on lipid agar. To test the level of viability of BMM429 compared to wild type *Photorhabdus* the bacterial biomass was removed from lipid agar plates at 3 days and 24 days post-inoculation. The bacterial biomass was then

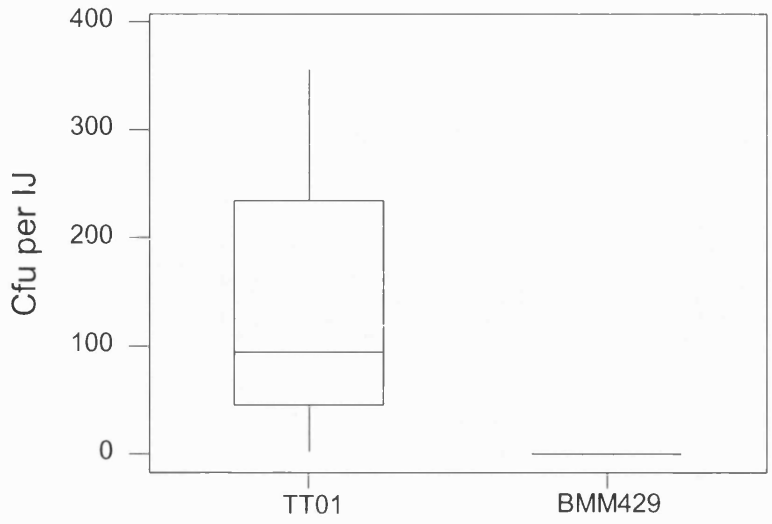


**Figure 5.8.** *Photorhabdus* bacteria recovered from single IJ crushing of nematodes grown on TT01 *Photorhabdus* or BMM429 mutant. Values are from 10 individual IJs presented as a boxplot. The line within the box represents the mean value. The box extends to the first and third quartiles. The whiskers indicate the upper and lower limits.

resuspended in PBS and the mixture serial diluted and plated onto LB agar + 0.1 % (w/v) pyruvate. The remaining biomass was then dried in an oven until the weight did not change any further. This analysis revealed that, after 24 days, the viability of both wild type and BMM429 decreased to < 10 % of the original viability measured at 3 days. The wild type retains 9 % of its original viability whereas BMM429 retains 3 % of its original viability (see Fig. 5.9). However, statistical analysis has revealed no significant difference in the number of viable cells in wild type and BMM429 cultures (approximately $3x10^7$ cfu/mg dry weight for TT01 and $1x10^7$ cfu/mg dry weight for BMM429. Mann-Whitney P = 0.3827). This suggests that both TT01 and BMM429 have a similar ability to survive extended periods of stationary phase on lipid agar and sufficient numbers of viable BMM429 would be present for nematode colonisation. Therefore it seems likely that *rpoS* is required for colonisation of the nematode by *Photorhabdus*.

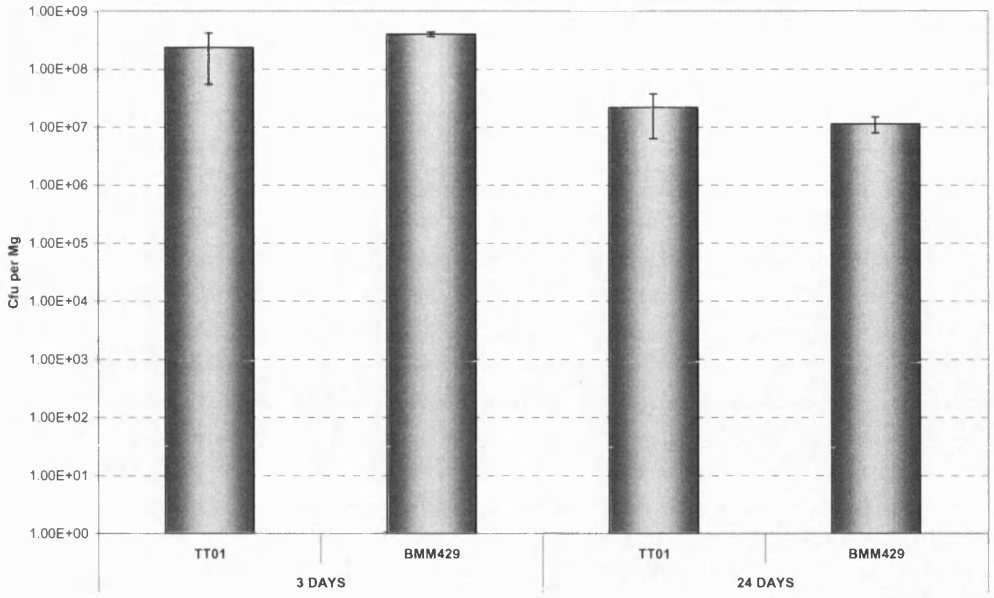


**Figure 5.9.** Viability of *Photorhabdus* removed from lipid agar plates following 3 days and 24 days incubation. Values are cfu per mg dry weight of bacteria isolated from 3 individual lipid agar plates. Error bars represent +/- standard deviation.

### 5.2.8 GFP labelling of BMM429

One advantage of using the *Photorhabdus-Heterorhabditis* model is that the nematode is completely transparent, thus facilitating the direct visualisation of the bacteria colonising the nematode gut. Therefore TT01 and BMM429 were transformed with pSU2007, a low-copy number plasmid that constitutively produces GFP (Martinez and de la Cruz, 1988). Illumination of colonies carrying pSU2007 with UV light confirmed that GFP is produced and active in *Photorhabdus* (see Fig. 5.10). Symbiosis assays were performed with wild-type and BMM429 carrying pSU2007 and the IJ nematodes were collected at the end of the assay. Colonisation analysis was performed by placing approximately 50 IJ nematodes into 100 µl PBS in each well of a 96 well flat-bottomed polystyrene plate. The IJs were then examined for the presence of bacteria using a Lecia DMIRB inverted light microscope to look for fluorescence (i.e. GFP expression) when the nematodes were exposed to a light at 450 nm. Successful colonisation was scored as the presence of a green glowing package in the gut region of the IJ (Fig. 5.11). As expected wild type *Photorhabdus* was found in the IJ gut at a

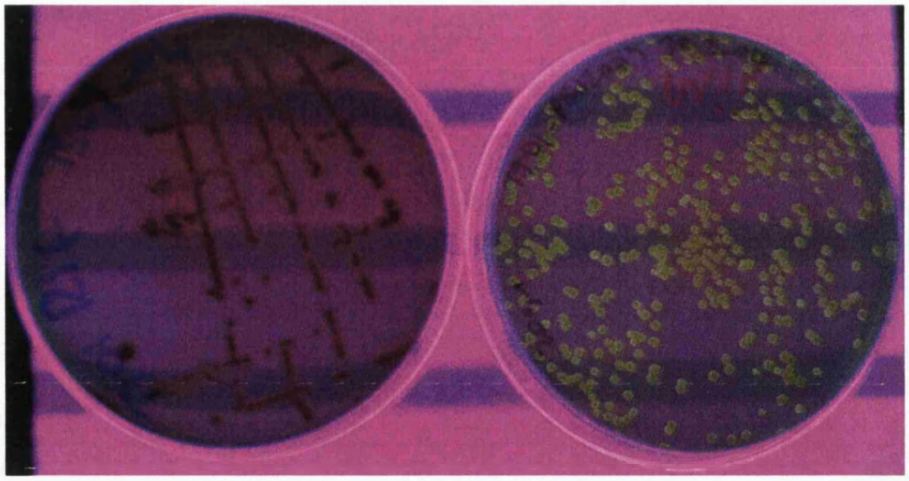

**Figure 5.10.** *P. luminescens* TT01 without pSU2007 (left) or with pSU2007-GFP (right) exposed to UV light.

frequency of approximately 80-90 %. This also confirms the plasmid is retained at high levels in the population of *Photorhabdus* throughout the duration of the symbiosis assay. However, BMM429 was observed in only 5 out of approximately 4800 IJ nematodes examined, indicating that BMM429 has a colonisation frequency of approximately 0.1 %.

### 5.2.9 Complementation of the Δ*rpoS* mutation

#### 5.2.9.1 Plasmid complementation

In *trans* expression of the *rpoS* gene in BMM429 is essential to confirm the phenotypes observed in BMM429 were due to the deletion of the *rpoS* gene. In *E. coli* the expression of the *rpoS* gene is controlled by at least 3 promoters situated within and upstream of the *nlpD* gene (Fig 5.1). Two of these promoters (*nlpD*p1 and *nlpD*p2) are required for basal levels of *rpoS* expression and are not involved in the upregulation of *rpoS* observed upon entry into stationary phase (Lange and Hengge-Aronis, 1994). The major promoter appears to be the promoter *rpoS*p, which is located within *nlpD* (Fig. 5.1). In *E. coli* this promoter has been shown to be essential for the stationary phase dependent expression of the *rpoS* gene (Lange *et al.*, 1995). Therefore, a 1860 bp

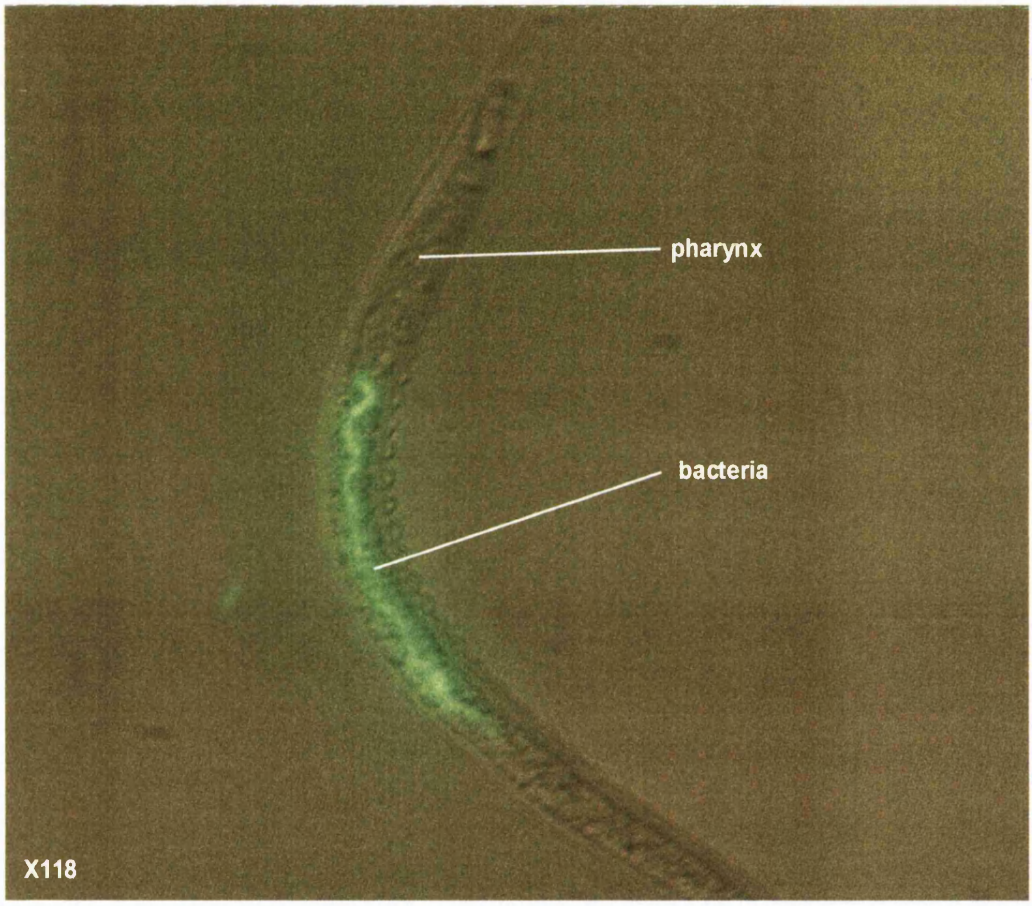


**Figure 5.11.** An IJ nematode grown on TT01 bacteria containing the plasmid pSU2007-GFP observed using fluorescence microscopy.

fragment of DNA, which includes *rpoS* and 793 bp of the 996 bp *nlpD* gene (containing *rpoS*p) was amplified from the chromosome of TT01 using primers RJW190 and RJW191 and the fragment was digested with HindIII and cloned into HindIII-digested pBR322. This construct was named pBMM4291.8. (Fig. 5.12). The plasmid was transformed into BMM429 by electroporation (see Materials and Methods) and ampicillin resistant colonies were selected for further analysis.

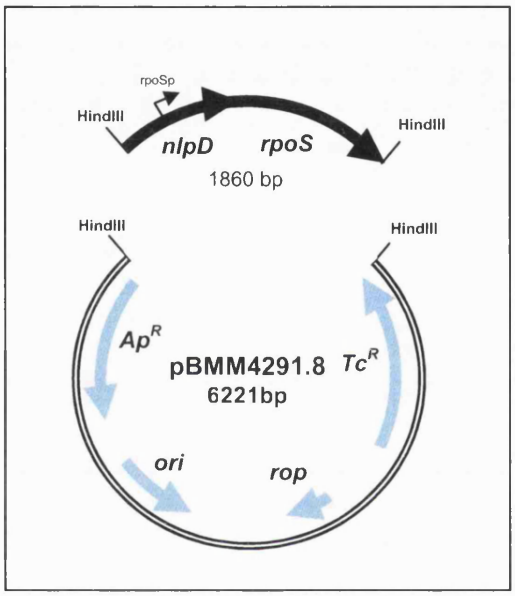


**Figure 5.12.** Complementation of BMM429 using pBR322 with a 1.8Kb fragment of *rpoS* and *nlpD* including the *rpoS*p promoter.

In the first instance the ability of the pBMM4291.8 plasmid to complement for the loss of *rpoS* from the genome was assayed by its ability to restore wild type levels of hydrogen peroxide resistance using the disc assay. As can bee seen in Fig. 5.13 the presence of pBMM4291.8 increased the resistance of BMM429 towards wild type levels. The complemented strain was also subjected to symbiosis assays. Nematode growth and development appeared similar for all strains (data not shown) and following 21 days symbiosis IJ nematodes were washed off the lids of the symbiosis plates. Statistical analysis revealed no

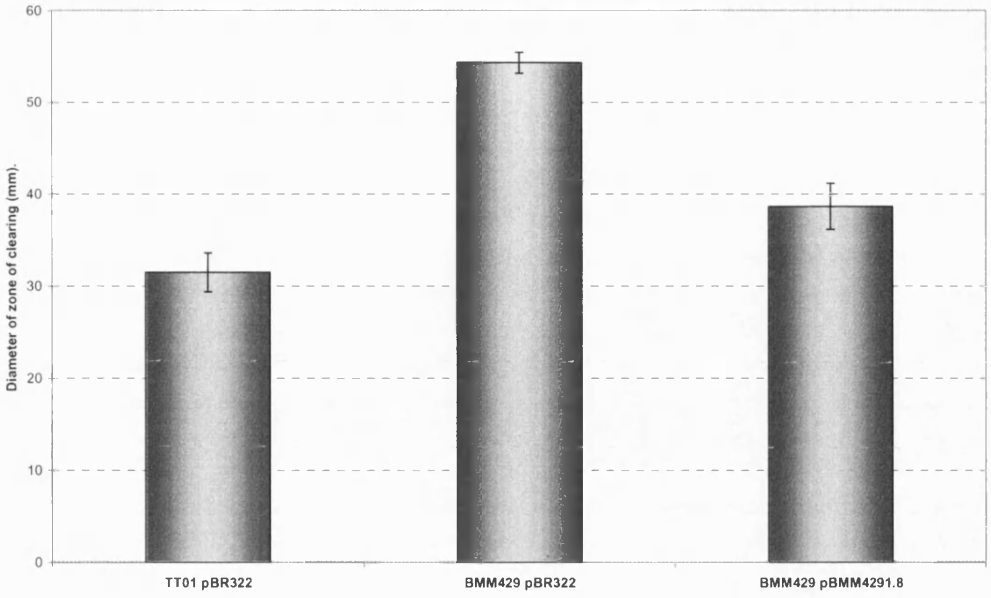


**Figure 5.13.** Diameter of *Photorhabdus* growth inhibition surrounding 13 mm Whatman filter discs soaked with 50 µl 30 % hydrogen peroxide after 48 h at 30°C. Average of 3 plates. Error bars represent +/- standard deviation.

significant difference between the IJ yields of all strains (ANOVA DF = 2, F = 1.4, P = 0.284) suggesting no defect in the ability of the bacteria to support nematode growth and development (see Fig. 5.14). The IJs recovered were surface sterilised and crushed and the lysate plated onto LB agar + 0.1 % (w/v) pyruvate. Surprisingly, pBMM4291.8 was unable to restore colonisation to BMM429 and colonisation still appeared to be completely absent (Fig. 5.15). *In vivo* infection assays were also performed with the recovered IJs. 1000 IJs resuspended in 1 ml PBS were applied to filter discs in Petri dishes and 10 *G. mellonella* insect larvae were added. After 72 h insect death was monitored which revealed 100 % insect mortality for insects infected with IJs grown on TT01/pBR322 bacteria. However all of the insects infected with IJs raised on BMM429/pBR322 or BMM429/pBMM4291.8 were all still alive. Plasmid loss over the 3 weeks of culture may have contributed to the lack of complementation and analysis of the bacteria from 24 days culture on lipid agar revealed that only 3 % of the colonies recovered maintained ampicillin resistance. Therefore an alternative method for complementation was employed.

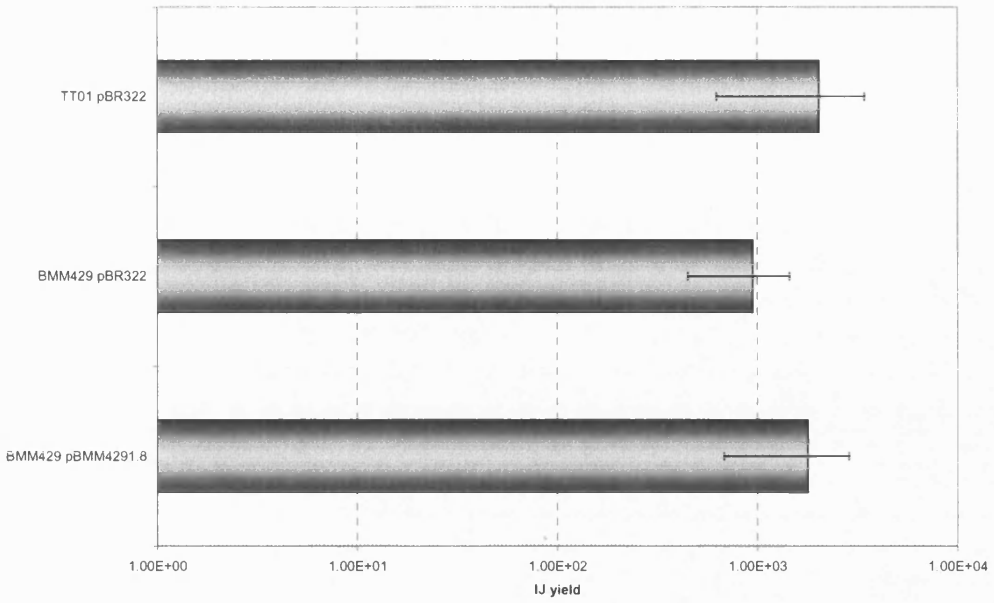


**Figure 5.14.** IJ yields after 21 days symbiosis with TT01/pBR322, BMM429/pBR322 and BMM429/pBMM4291.8. Nematodes were washed from the lids and counted from 5 individual symbiosis plates. Error bars represent +/- standard deviation

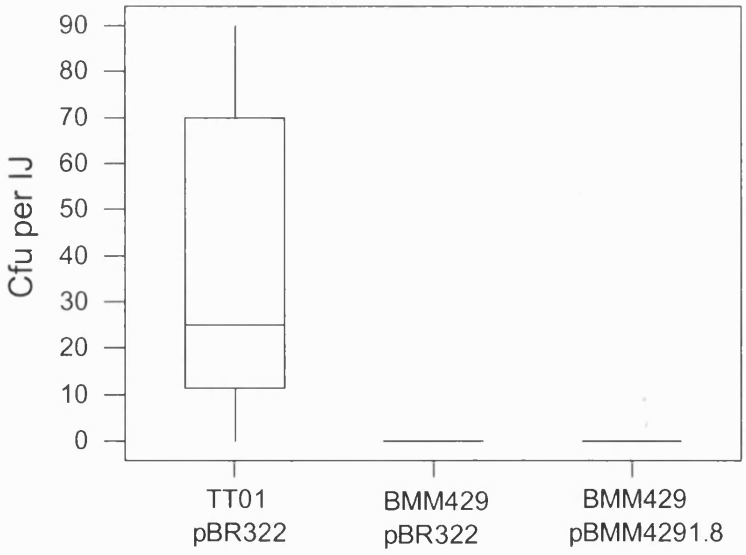


**Figure 5.15.** Colonisation of IJ nematodes by TT01 wild type carrying pBR322, BMM429 carrying pBR322 or BMM429 complemented with pBMM4291.8. Values are from 10 individual IJ nematodes. The line within the box represents the mean value. The box extends to the first and third quartiles. The whiskers indicate the upper and lower limits.

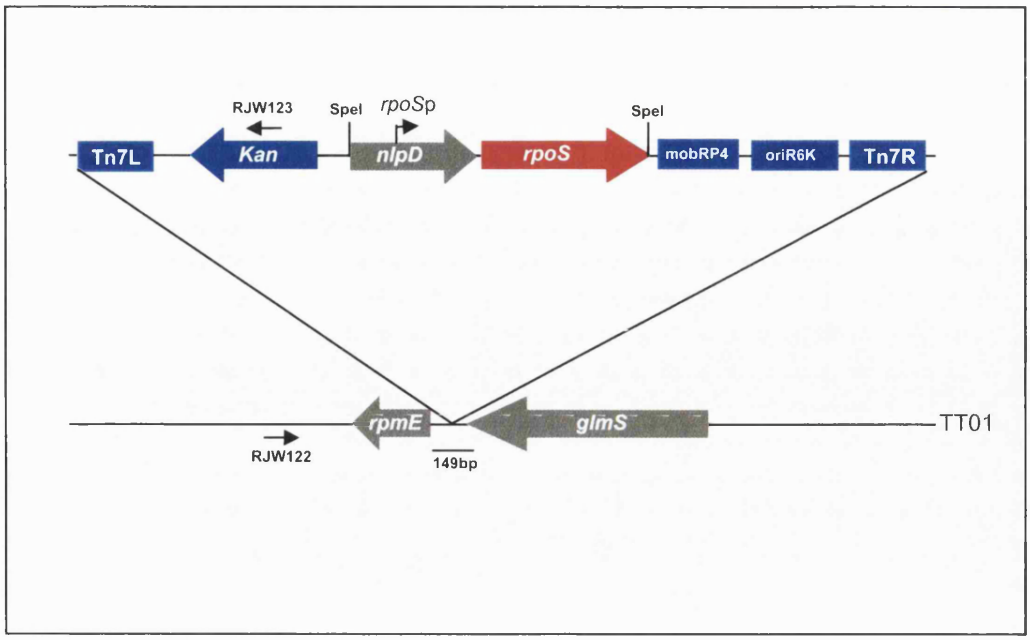


**Figure 5.16.** Complementation of BMM429 with the Tn7 transposon from pCIITn7K-a containing a 1.8 Kb *rpoS* gene fragment. Specific integration occurs between the *rpmE* and *glmS* genes. Blue colour indicates genes from the transposon.

### 5.2.9.2 Tn*7* transposon complementation

The integration of a single gene into the chromosome at a specific location avoids the issue of copy number or plasmid loss. The Tn*7* transposon has been shown to insert into the genome of a number of enteric bacteria at a specific site, attTn7, located immediately downstream from the *glmS* gene (Bao *et al.*, 1991). This is predicted to be a neutral site and in *P. luminescens* TT01 this site is located within the 149 bp DNA sequence between *glmS* and the *rpmE* gene (Fig. 5.16). Therefore, Tn*7* was selected for delivery of the 1860bp DNA fragment encoding *rpoS* and 793 bp of *nlpD* and including the *rpoS*p promoter into the genome of BMM429 (see Materials and Methods). The fragment was amplified using RJW205 and RJW206 primers to produce a fragment which was identical to the one used for the pBR322 complementation except that the restriction ends were changed to SacI sites. Following successful cloning of the fragment into pCIITn7K-a the Tn*7* transposon was introduced from the pCIITn7K-a vector via a triparental mating procedure (see Materials and Methods). Successful

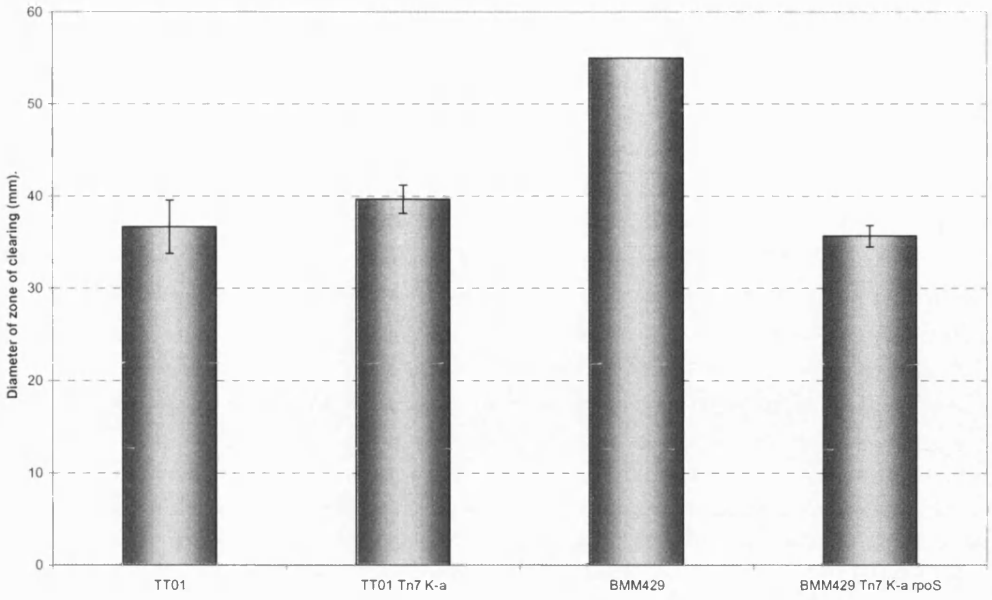


**Figure 5.17.** Hydrogen peroxide disc assay with TT01, TT01 with empty Tn7 vector, BMM429 and BMM429 with Tn7 containing a 1.8 Kb fragment consisting of *rpoS* and 793 bp of *nlpD*. Each 13 mm Whatman filter disc was impregnated with 50 µl 30 % $H_2O_2$. Data is an average of 3 plates +/- standard deviation.

integration into the genome was confirmed by PCR using primers RJW122 and RJW123 and conversion of the strain to kanamycin resistance. Primer RJW122 was designed upstream of the *glmS* gene and RJW123 was designed in the kanamycin resistance cassette of the Tn7 transposon carried by pCIITn7K-a. Therefore, only kanamycin resistant clones with the correct Tn7 insertion are able to produce a 1.5 Kb fragment after PCR. On this basis a potential clone was selected and was analysed for its resistance to $H_2O_2$ using the disc assay previously described. As can be seen in Fig. 5.17 BMM429 Tn7 K-a/*rpoS* has been restored to wild type levels of $H_2O_2$ resistance, confirming the *rpoS* gene was being expressed. These strains were also used to set up symbiosis assays and after 21 days the IJs present on the lids of the symbiosis plates were washed off and were prepared for IJ crushing. The results from the IJ crushing revealed no colonisation for BMM429 or BMM429 Tn7 K-a/*rpoS* transposon (Fig. 5.18). Most importantly the Tn7 transposon does not appear to affect wild type TT01 levels of colonisation. Therefore the integration of a single copy of *rpoS* with 793 bp of the *nlpD* gene DNA upstream was unable to complement the colonisation defect.

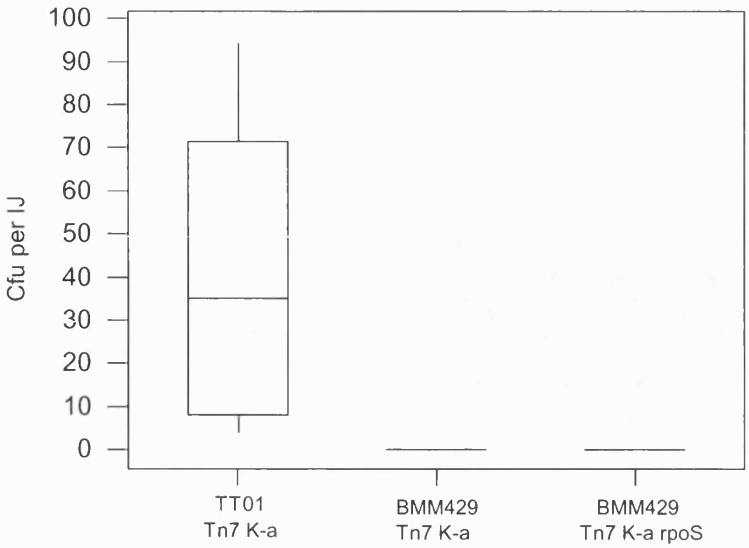


**Figure 5.18.** Colonisation of IJ nematodes by wild type TT01 *Photorhabdus* carrying an empty Tn*7* transposon, BMM429 carrying an empty Tn*7* transposon and BMM419 carrying a Tn7 transposon with a 1.8 Kb *rpoS* fragment. The line within the box represents the mean value. The box extends to the first and third quartiles. The whiskers indicate the upper and lower limits.

5.2.9.3 Directed knock-in complementation

The previous complementation attempts were unsuccessful, and may be due to a number of reasons. Plasmids can be lost unless selection pressure is maintained. The location of the DNA within the chromosome may also be crucial to its efficient expression due to the presence of promoters and inhibitors. Therefore, perhaps the definitive method to establish whether the deletion of genetic material from a region has affected the expression of a phenotype is to restore the genetic region to the way is was before deletion. This method of reintroduction of the genetic material alleviates the previous complication of plasmid loss or potential expression differences as the DNA has been restored to its native sequence. Therefore, the pDS132 plasmid was used as the delivery vector to knock-in the intact gene into the genome of the mutant strain. A DNA fragment

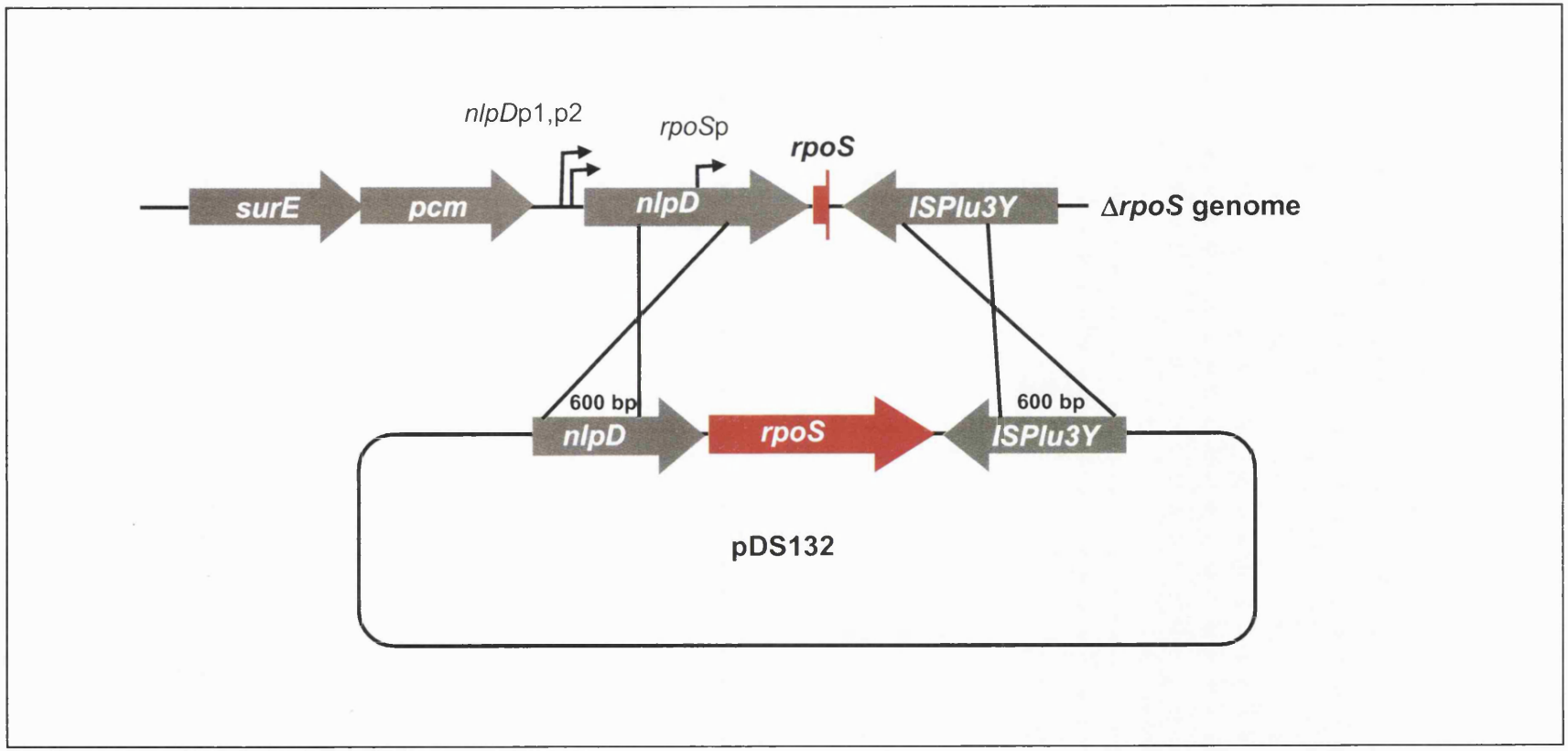


**Figure 5.19.** Schematic of the directed knock-in procedure for BMM429. Homologous recombination occurs with the 600 bp flanking regions either side of the gene of interest and the DNA from the pDS132 vector integrates into the genome.

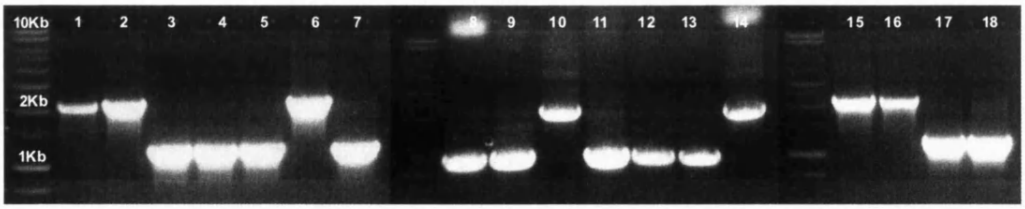


**Figure 5.20.** PCR analysis of BMM429 Knock In strains. Lanes 1+2 are TT01 wild type controls. Lanes 3-6 are BMM429 KI #2-3 Colonies 1-4, Lanes 7-10 are BMM429 KI #2-4 Colonies 1-4, Lanes 11-14 are BMM429 KI #4-3 Colonies 1-4, Lanes 15-18 are BMM429 KI #4-5 Colonies 1-4. Marker is Promega 1 Kb DNA ladder on a 1 % agarose gel.

encompassing the *rpoS* gene and 600 bp either side was amplified from the genome of TT01 using primers RJW207 and RJW208. These primers contain XbaI and SphI restriction sites respectively, facilitating the cloning of this fragment into pDS132. This plasmid was conjugated into BMM429 and $Cm^S$ $Suc^R$ exconjugants were screened by PCR, to identify strains in which the wild type *rpoS* allele had been restored (i.e. the wild type allele will give a PCR fragment of 2.1Kb compared to 1.1Kb for the deletion mutant (see Fig. 5.19 and 5.20). This method restored the wild type *rpoS* allele to Δ*rpoS* strains with a frequency of approximately 31 % (Fig. 5.20). Hydrogen peroxide sensitivity was restored to wild type levels in the knock-in strains analysed suggesting that a functional *rpoS* gene had indeed been reintroduced to the Δ*rpoS* strain (Fig. 5.21). The knock in strains KI *rpoS* 2-3-4, KI *rpoS* 2-4-4, KI *rpoS* 4-3-4, KI *rpoS* 4-5-1 and KI *rpoS* 4-5-2 were also assayed for their ability to colonise IJ nematodes following symbiosis assays. IJ nematodes were removed and surface sterilised from symbiosis assays following 21 days of incubation and 5 individual nematodes were pooled for crushing and 5 samples were processed for each strain. Surprisingly none of the knock in strains were able to colonise the nematodes (Fig. 5.22). Moreover, none of the insect larvae were killed by any of the IJ nematodes grown on the knock in strains (Table 5.2). Therefore, all of the complementation data suggest that there is a secondary mutation that has occurred in BMM429 and this unidentified mutation is responsible for the colonisation-deficient phenotype of this strain.

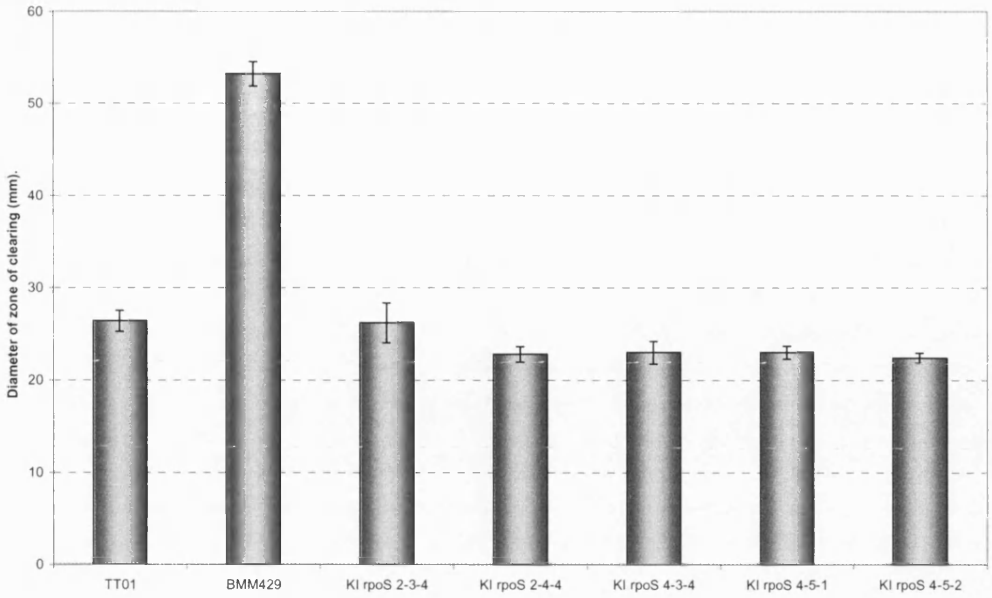


**Figure 5.21.** Resistance to hydrogen peroxide by BMM429 knock in strains. 13 mm Whatman filter discs were impregnated with 50 µL $H_2O_2$ and were placed atop soft agar containing 100 µl per 10 ml of an $OD_{600}$ = 4 overnight culture. Zones of growth inhibition were measured after 48 h incubation at 30°C. Error bars represent the standard deviation from a total of 5 plates.

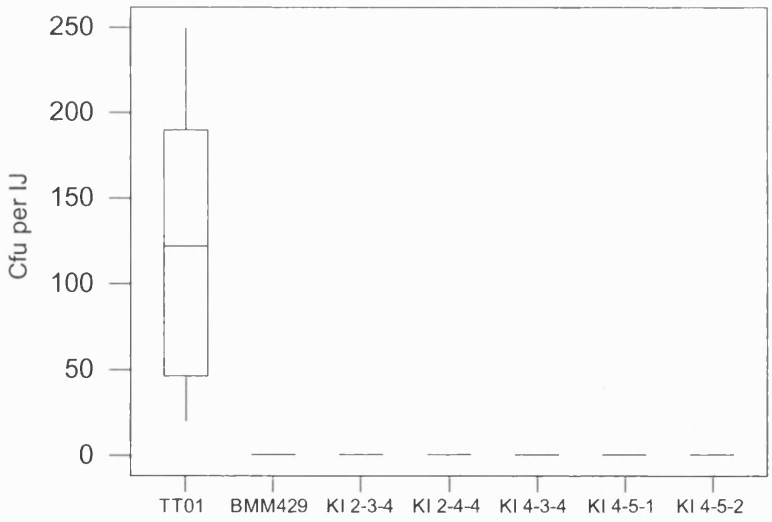


**Figure 5.22.** Colonisation of IJ nematodes with *Photorhabdus* bacteria from knock-in complementation symbiosis assays. 5 groups of 5 pooled IJs were crushed and the lysate spread onto LB pyruvate agar plates. Data is presented as a boxplot. The line within the box represents the mean value. The box extends to the first and third quartiles. The whiskers indicate the upper and lower limits.

**Table 5.2.** Insect death following infection of 10 *G. mellonella* insect larvae with 1000 IJ nematodes raised on *Photorhabdus* strains.

| | Insect mortality after 72 h infection with IJ nematodes | | |
|---|---|---|---|
| Nematodes raised on: | Set 1 | Set 2 | Set 3 |
| TT01 wild type | 100% | 100% | 90% |
| BMM429 | 0% | 0% | 0% |
| KI *rpoS* 2-3-4 | 0% | 0% | 0% |
| KI *rpoS* 2-4-4 | 0% | 0% | 0% |
| KI *rpoS* 4-3-4 | 0% | 0% | 0% |
| KI *rpoS* 4-5-1 | 0% | 0% | 0% |
| KI *rpoS* 4-5-2 | 0% | 0% | 0% |

### 5.2.10 Construction of a new Δ*rpoS* mutant strain

The strain BMM429 was originally constructed by Yan Wei and there is no clear record of how this strain was handled before glycerol stocks were prepared. Therefore, it is possible that this strain was subjected to an, albeit unintentional, environmental pressure that resulted in the selection of cells with a particular secondary mutation. Given the nature of the gene being studied this could simply be a slightly prolonged incubation on an agar plate. To confirm that *rpoS* was not involved in symbiosis it was decided to reconstruct the mutation this time taking care to minimise the exposure of the mutant to any period of prolonged growth or repeated growth steps. Moreover, BMM429 was shown to have increased sensitivity to $H_2O_2$ and therefore all manipulations were performed on LB agar kept in the dark or supplemented with 0.1 % (w/v) pyruvate to eliminate possible $H_2O_2$ stress. Furthermore to reduce the chance of selecting a single mutant with a secondary mutation 8 independent knock out mutants were selected based on PCR fragment size differences (Fig. 5.23). These strains were immediately frozen in glycerol at -80°C to prevent any further exposure to environmental stresses. Following PCR confirmation of the KO's the knock-in procedure was performed independently with each of the knock out strains. Performing multiple knock out and knock in reactions to create the same mutation would identify if

the secondary mutation was happening at a high frequency. This procedure generated 8 independent knock-in strains that were confirmed by colony PCR (Fig. 5.23).

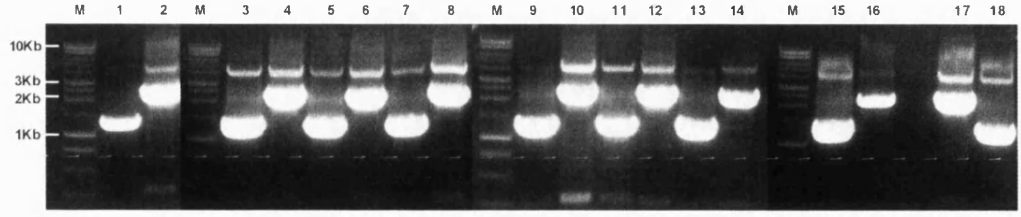


**Figure 5.23.** Agarose gel analysis of eight successful *rpoS* deletion strains and their subsequent knock-ins. Lanes 1,3,5,7,9,11,13 and 15 are Δ*rpoS* strains 2,9,10,12,14,17,19 and 33 respectively. Lanes 2,4,6,8,10,12,14 and 16 are their respective successful knock-in strains. Lane 17 is a TT01 wild type control and Lane 18 is the BMM429 mutant.

Symbiosis assays were performed with each of the 16 strains i.e. 8 Δ*rpoS* knock outs and their corresponding knock-ins. Nematode growth and development was monitored, and as expected was unchanged from the wild type. Following 21 days IJ nematodes were washed from the lids of the lipid agar plates and surface sterilised before 5 IJs were pooled for crushing and insect infections were performed. All of the Δ*rpoS* strains (and their corresponding knock-ins) were fully able to colonise the IJ nematodes (Fig. 5.24). On the other hand, BMM429, which was included as a control, was unable to colonise IJ nematodes. Furthermore, 1000 IJs that were recovered from the lids of the symbiosis assays were used to infect *G. mellonella* larvae to ensure that the different *rpoS* mutants were virulent. In all cases the *ΔrpoS* strains and their corresponding knock-in strains were able to kill these insect larvae as well as wild type (see Table 5.3). Therefore, although *rpoS* is required for the stationary phase-dependent expression of catalase activity (and therefore presumably resistance to $H_2O_2$) this gene is not required for any aspect of the symbiosis between *Photorhabdus* and the nematode.

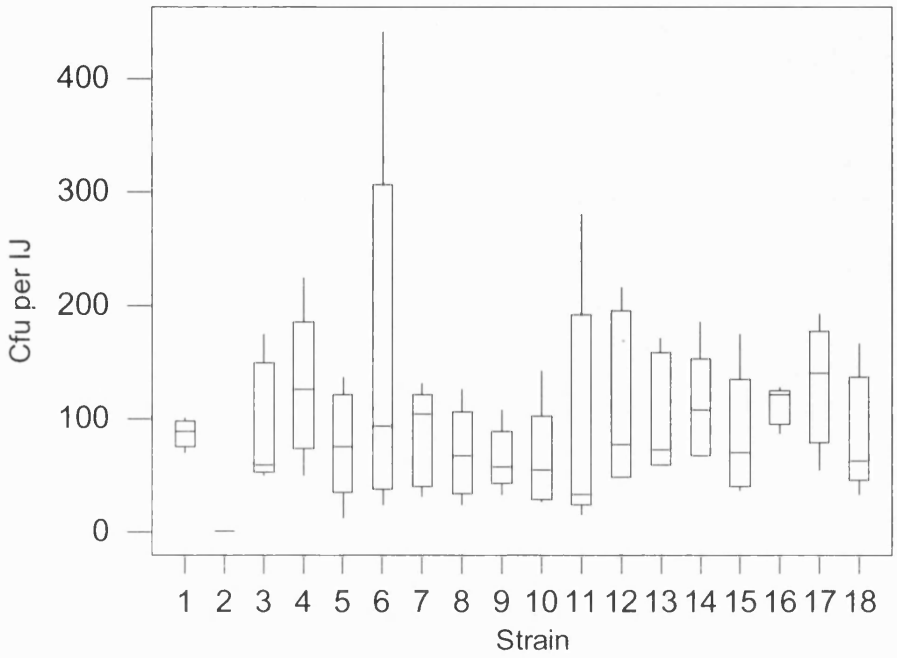


**Figure 5.24.** Colonisation of IJ nematodes by new Δ*rpoS* strains. Strain 1 is TT01 wild type. Strain 2 is BMM429. Strains 3,5,7,9,11,13,15 and 17 to 18 are Δ*rpoS* strains 2,9,10,12,14,17,19 and 33 respectively. Strains 4,6,8,10,12,14,16 and 18 are their respective knock-in strains. Values are cfu per IJ derived from crushing 5 groups of 5 pooled IJs. Data is presented as a boxplot. The line within the box represents the mean value. The box extends to the first and third quartiles. The whiskers indicate the upper and lower limits.

**Table 5.3.** Insect mortality following infection with IJs recovered from Δ*rpoS* KO and KI symbiosis assays.

| | **Insect mortality after 72h infection with IJ nematodes** | |
|---|---|---|
| **Strain** | **Set 1** | **Set 2** |
| TT01 | 100% | 100% |
| BMM429 | 0% | 0% |
| Δ*rpoS* #2 | 100% | 90% |
| KI *rpoS* #2-6 | 100% | 100% |
| Δ*rpoS* #9 | 100% | 100% |
| KI *rpoS* #9-31 | 100% | 100% |
| Δ*rpoS* #10 | 100% | 100% |
| KI *rpoS* #10-43 | 100% | 100% |
| Δ*rpoS* #12 | 100% | 100% |
| KI *rpoS* #12-54 | 100% | 100% |
| Δ*rpoS* #14 | 100% | 100% |
| KI *rpoS* #14-69 | 100% | 100% |
| Δ*rpoS* #17 | 100% | 100% |
| KI *rpoS* #17-79 | 100% | 100% |
| Δ*rpoS* #19 | 100% | 100% |
| KI *rpoS* #19-90 | 100% | 100% |
| Δ*rpoS* #33 | 100% | 100% |
| KI *rpoS* #33-92 | 100% | 100% |

## 5.3 Discussion

Nematode growth and development, both in the insect and on lipid agar plates occurs within a community of *Photorhabdus* that have reached the stationary phase of growth. In closely related bacteria such as *E. coli* and *Salmonella* spp. stationary phase physiology is controlled by an alternative sigma factor, $\sigma^S$, encoded by the *rpoS* gene. Indeed $\sigma^S$ has been shown to be responsible for the control of up to 10 % of genes in the *E. coli* genome during transition from exponential phase growth to stationary phase including the iron storage protein bacterioferritin (Lacour and Landini, 2004; Weber *et al.*, 2005). Therefore, in this study it was decided to investigate the role of *rpoS* during the stationary phase of *Photorhabdus* growth and during the interaction between *Photorhabdus* and the nematode.

In agreement with studies in other bacteria this chapter has shown that $\sigma^S$ in *Photorhabdus* regulates the production of catalase during stationary phase. Catalase is required for the enzymatic degradation of $H_2O_2$ to $H_2O$ and $O_2$ and this study has shown that the deletion of the *rpoS* gene results in reduced catalase production and increased sensitivity to hydrogen peroxide. This reduced catalase production and increased sensitivity to $H_2O_2$ was shown to be dependent on *rpoS* through complementation studies. In *E. coli* RpoS regulates both a bifunctional catalase hydroperoxidase I (HP-I) encoded by the *katG* gene and the monofunctional catalase hydroperoxidase II encoded by the *katE* gene (GonzalezFlecha and Demple, 1997). Genomic analysis of the *Photorhabdus* genome identified a homologue of KatE but no homologue of KatG suggesting the increased sensitivity of BMM429 to hydrogen peroxide was due to reduced expression of the *katE* gene.

Several studies have identified a role for $\sigma^S$ in virulence. In *Salmonella typhimurium* $\sigma^S$ controls the expression of the plasmid-encoded *spv* genes. The *spvRABCD* gene cluster is required for systemic infection and bacteraemia in animals and humans by controlling growth in deep organs (Gulig *et al.*, 1993). An insect toxin from *Serratia entomophila* has also been shown to be dependent

on $\sigma^S$ for its expression (Giddens *et al.*, 2000). However, *rpoS* was not required for the virulence of *P. luminescens* to infect and kill *G. mellonella* insect larvae and the same phenotype was seen in the closely related *Xenorhabdus nematophila* (Vivas and Goodrich-Blair, 2001).

Strains carrying a deletion of the *rpoS* gene were indistinguishable from the wild type in their ability to support nematode growth and reproduction. This is in agreement with a previous study where a mutation in the *hexA* gene caused a lower level of $\sigma^S$ production, but this mutant was unaffected in its ability to support nematode growth and development (Joyce and Clarke, 2003). Moreover, in this chapter, *rpoS* was not required for the colonisation of the nematode by *Photorhabdus*, although this is in contrast to what was reported in *X. nematophila* where *rpoS* mutants are unable to colonise their nematode partner (Vivas and Goodrich-Blair, 2001). Intriguingly an *E. coli* Δ*rpoS* mutant has been shown to be fully able to colonise the mouse intestine (Krogfelt *et al.*, 2000). Remarkably this mutant was even able to out-compete a wild type strain during a mixed infection suggesting that *rpoS* gene function is a disadvantage during mouse colonisation. Indeed a further study of *E. coli* in continuous culture has revealed that in the chemostat culture *rpoS*$^-$ mutants arise which rapidly eliminate the wild type *rpoS*$^+$ population, again suggesting that $\sigma^S$ is a disadvantage under conditions of rapid growth (Maharjan *et al.*, 2006). *V. cholerae* has also shown no requirement for $\sigma^S$ during survival when introduced directly into the intestines of mice (Yildiz and Schoolnik, 1998).

However, it is possible that the *rpoS* gene is required to maintain the fitness of the bacteria during periods of environmental stress and, therefore, questions still remain over the ability of the Δ*rpoS* strains to maintain a stable lifecycle over the long-term. For example, *Photorhabdus* need to be able to persist in the unique environment of the IJ gut for a prolonged period of time whilst in the soil, up to several months, before a new insect host is infected. Indeed, IJ nematodes can be stored in saline at 4°C in the laboratory and maintain virulence when presented with insect larvae for up to 12 months. Certainly carbon starvation has been shown to affect viability over time for both *V. cholerae* and *Burkholderia*

*pseudomallei* (Subsin *et al.*, 2003; Yildiz and Schoolnik, 1998). Experiments to determine any long-term fitness costs associated with the *rpoS* deletion could reveal a difference between the *rpoS* mutant and wild type.

With the exception of the *rpoS*-dependent decrease in catalase production, wild type and BMM429 were identical for all other phenotypes tested. However, BMM429 is unable to colonise IJ nematodes for a reason that is not yet clear. It might, therefore, be interesting to analyse this mutant further. Assuming the secondary mutation results in a loss-of-function of a gene, one approach would be to introduce fragments of the TT01 genome carried on cosmids into BMM429 Tn7 K-a/rpoS pSU2007 and to assess for colonisation using the GFP marker. In addition, comparative approaches e.g. transcriptomics and comparative 2D-electrophoresis may also identify genes and/or proteins that have altered expression levels. A proteomic approach has been used previously to identify differences in the proteins produced by primary and secondary variants of *Photorhabdus* (Turlin *et al.*, 2006). These approaches may identify a novel genetic region required by *Photorhabdus* for the colonisation of nematodes.

# Chapter 6

# General Discussion

Entomopathogenic nematodes of the family *Heterorhabditis* have a mutualistic relationship with bacteria from the family *Photorhabdus* where the bacteria colonise the gut of the IJ stage of the nematode. The bacteria-nematode interaction forms a highly effective pathogenic complex that targets a wide variety of soil-dwelling insect larvae. From the bacterial point of view the nematodes serve as a vector, carrying *Photorhabdus* from insect to insect whilst also protecting the bacteria from the adverse conditions found in the soil. On the other hand, the nematodes use the high bacterial cell density generated in the insect during pathogenicity as a food source for growth and development. It is well established that the requirement of the nematode for *Photorhabdus* is both obligate and highly specific. However, the genetic basis of this interaction is largely unknown. Iron is a key nutrient for nearly all living organisms and the genome sequence of *P. luminescens* TT01 has revealed a large number of potential iron acquisition systems. The fact that *Photorhabdus* has a varied lifecycle suggests that these different iron acquisition systems may be required for the interactions of *Photorhabdus* with different eukaryotes. The aim of this study was to identify the role of these iron homeostasis systems in the pathogenic and symbiotic interactions of *Photorhabdus* to identify which aspects of iron homeostasis were involved in pathogenicity, mutualism or both interactions.

This question was approached by creating random transposon mutants of *P. temperata* K122 and screening for an altered level of siderophore production indicating a disruption to the iron homeostasis machinery. Five mutants were identified, three of which were identified in the photobactin siderophore operon and one further mutant involved in the production of molecules for siderophore synthesis. These four mutants were unaffected in any of the interactions studied in the laboratory, however it is possible that the photobactin siderophore has a role in protecting the insect cadaver in the soil from invading microbes. Pyochelin and pyoverdine siderophores produced by *Pseudomonas aeruginosa* have been shown to protect tomato plants from pathogenic *Pythium* fungi,

probably by the competitive exclusion of available iron for the fungus (Buysens *et al.*, 1996). Therefore, it would be interesting to test the photobactin non-producing mutant, BMM401 for its antifungal properties *in vitro*.

The fourth mutant identified was attenuated in both pathogenicity and mutualism. BMM417 was identified as possessing an insertion in the *exbD* gene, a component of the TonB energy-transducing complex that is known to play an important role in ferric iron acquisition. Both the pathogenicity and symbiosis deficiencies could be complemented by the addition of exogenous iron revealing these effects to be due to iron limitation. The pathogenicity defect was attributed to a slower growth rate *in vivo*, and the importance of *exbD* (TonB) mediated iron acquisition has been seen for a number of pathogens including *Actinobacillus pleuropneumoniae*, *Pasteurella multocida*, *Haemophilus influenzae* type b, *Bordetella pertussis*, *Shigella dysenteriae*, *Vibrio anguillarum*, *E. coli* and *S. typhimurium* (Beddek *et al.*, 2004; Bosch *et al.*, 2002; Jarosik *et al.*, 1994; Pradel *et al.*, 2000; Reeves *et al.*, 2000; Stork *et al.*, 2004; Torres *et al.*, 2001; Tsolis *et al.*, 1996). However, very little is known about the role of *exbD* mediated iron acquisition during mutualistic associations. The most obvious reason for the inability of BMM417 to support nematode growth and development would have been due to a reduced iron content of the *Photorhabdus* which was unable to meet the nutritional needs of the developing nematodes. However, this does not seem to be the case as another mutant, BMM401, which contains the same reduced level of total iron is fully able to support nematode growth and development. Although the total level of iron may not be important, the distribution of the iron within the cell may be essential. Therefore, BMM417 may be unable to support nematode growth and development as the iron within the cell has not been converted into a source which the nematodes can utilise. Analysis of the subcellular location of the iron stored within BMM417 may reveal differences in the iron storage profile compared to the wild type which may explain the symbiosis defect. It is also possible that the high concentrations of photobactin secreted by BMM417 is causing the symbiosis defect although this scenario seems unlikely given that both BMM415 and BMM416 hyper-secrete photobactin and are fully able to support nematode growth and development. However, this question could be addressed by creating a *phbC*

isochorismate synthase deletion in the BMM417 mutant which would result in no photobactin being produced, therefore allowing hyper-secretion of photobactin to be ruled out as a factor in the symbiosis deficient phenotype. As the *exbD* mutation is expected to affect all TonB mediated systems, a targeted deletion of each of these uptake pathways could help to identify which aspect of *exbD* mediated iron acquisition is important for nematode growth and development. However, the lack of a *P. temperata* K122 genome sequence would make further study of the distinct pathways involved extremely difficult.

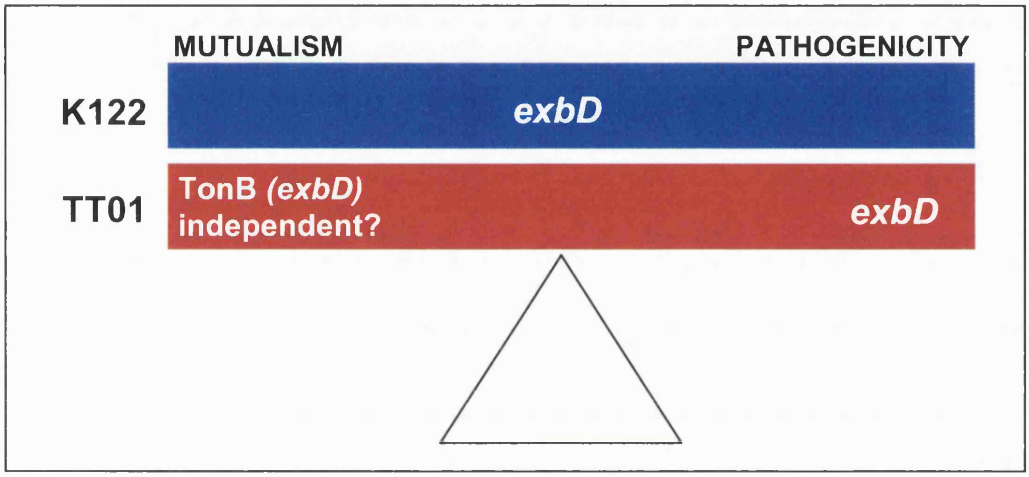


**Figure 6.1.** The influence of *exbD* mediated iron acquisition in the interactions of K122 and TT01 bacteria in mutualism or pathogenicity.

The nature of the symbiosis defect was clearly identified as iron related in the *P. temperata* K122 *exbD* mutant but the exact reason for the defect was not resolved in the first chapter. To elucidate the role of *exbD* mediated iron acquisition in the interaction with the nematode the mutation was moved into the *P. luminescens* TT01 strain where the genome had been sequenced (Duchaud *et al.*, 2003). This was achieved by developing a directed knock out technique to create targeted deletions of *Photorhabdus* genes. The pathogenicity defect was more acute in the TT01 Δ*exbD* mutant, with 100 cfu of BMM430 unable to kill any insect larvae. Remarkably, despite this severe pathogenicity defect, BMM430 was fully able to support nematode growth and development and BMM430 was also able to fully colonise the nematode. This result suggests that

TT01 has a greater dependence on *exbD* mediated iron acquisition for pathogenicity compared to K122, and that TonB-independent uptake systems may be involved in the symbiotic interaction of *Photorhabdus* with the nematode in TT01 (Fig. 6.1). To that end several TonB-independent ferrous transport mutants were created but these mutants were fully able to support symbiosis and were fully virulent. *Photorhabdus* iron storage was identified as a potential area of interaction with the nematode, however mutants in genes encoding predicted iron storage proteins did not affect any aspect of the lifecycle (although it was not possible to examine the role of bacterioferritin). The Fur protein has been shown to be a major regulator of iron responsive genes in Gram-negative bacteria (Lee and Helmann, 2007). The addition of the ferrous iron chelator DIP, which has shown to alter expression of Fur regulated genes in *B. subtilis* and *Y. pestis* (Baichoo *et al.*, 2002; Zhou *et al.*, 2006) caused a complete abolition of the symbiotic ability of the *Photorhabdus* to support nematode growth and development. The level of DIP required for the symbiosis defect was far lower than the concentration that prevented *Photorhabdus* growth and subsequent analysis of the proteins produced by *Photorhabdus* with DIP treatment has revealed eight proteins to have increased abundance, two of these proteins Plu0947 and Plu1840 have been identified in a previous study into the differences between the symbiosis proficient primary variant and the symbiosis deficient secondary variant of *Photorhabdus* (Turlin *et al.*, 2006). The signals that are required for initiation of nematode symbiosis still remain largely unknown and this study has identified these two proteins, Plu0947 and Plu1840 worthy of further investigation. Deletion of these proteins and re-analysis of the symbiosis phenotype under DIP treatment or over-expression of these proteins in the *Photorhabdus* primary variant may reveal the importance of these proteins in symbiosis control.

The addition of DIP to the medium means that the iron chelator may be interacting directly with the *Heterorhabditis* nematodes. Further work to create a Fur mutant and a comparison of both the proteome and transcriptome of this mutant compared to DIP treated cells would elucidate if the DIP was indeed causing a Fur mediated change in protein and gene expression. Furthermore, if proved to be similar, the Fur mutant could be subject to symbiosis assays without

the complication of the presence of DIP. However, if this analysis proved the block of nematode growth and development was actually due to the presence of DIP in the media this discovery could have an impact on a wide range of nematodes. Human gastrointestinal nematodes pose a global health threat and the drugs that treat them are increasingly ineffective (Stepek *et al.*, 2006). Therefore, novel therapeutics are required. *C. elegans* would be an excellent model on to which to test this hypothesis as it has been the most well studied of all nematodes. If the mechanism of DIP was indeed found to disable the growth and development of *C. elegans* and other nematodes the use of metal chelators may present a novel mechanism of treating nematode infections.

The K122 and TT01 strains of *Photorhabdus* have been shown in this study to possess differences in their *exbD* iron mediated pathogenicity and symbiosis defects. However, the nematode must also be considered in this interaction. When *H. downesi* IJs (the cognate partner of K122) were grown on all of the TT01 mutants it was interesting to observe that any strain carrying Δ*exbD* allele was delayed in its ability to support IJ production at the end of the assay. Conversely *H. bacteriophora* IJs (the cognate partner of TT01) were able to grow and reproduce on BMM417, something that could not be achieved with the *H. downesi* nematodes. Therefore, the nematodes clearly have different sensitivities to the *exbD* mutation. The genome sequences of both of these nematodes are not yet available although sequencing of *H. bacteriophora* is in progress. A comparison of both of these nematode genomes could reveal the reasons for the dependence of the *H. downesi* nematode for *exbD* mediated iron uptake compared to *H. bacteriophora.* Interestingly, *C. elegans* has been identified as a rare free living eukaryote that cannot synthesise its own haem *de novo* (Rao *et al.*, 2005). It would be tempting to speculate that *H. bacteriophora* can synthesis its own haem but that *H. downesi* cannot. Bacterial haem acquisition has been shown to be *exbD* (TonB) dependent, therefore the inability of BMM417 to support *H. downesi* nematode growth and development could be due the inability of BMM417 to supply enough environmentally acquired haem to the *H. downesi* nematodes. The difference identified between these two nematode species may suggest that iron (haem) is the environmental trigger that

controls *H. downesi* growth and development and that *H. bacteriophora* has evolved a different control mechanism. Further study of the genomes of these two nematodes and other nematode species may begin to address these questions.

Several studies have shown no role for TonB-mediated iron acquisition during beneficial interactions between eukaryotes and bacteria, but many have shown that TonB is required for pathogenicity. Therefore, if TonB mediated iron uptake is shown to be more prevalent for pathogens, novel chemotherapeutics could be developed to target the TonB system. The major advantage would be that the majority of beneficial microbe colonisers would be unaffected by this treatment, unlike current antibiotic treatments which cannot discriminate between beneficial and harmful microbes. Further study of TonB mutants in pathogenic and beneficial interactions may reveal how widespread this phenomenon is and whether it could be a useful avenue to explore.

The majority of the interactions between *Photorhabdus* and *Heterorhabditis* take place when *Photorhabdus* is in the stationary phase of growth. It is during stationary phase that *Photorhabdus* produces the characteristic primary phase phenotypes such as pigmentation, antibiotics lipase, protease etc. Therefore, to characterise important aspects of stationary phase growth in maintaining the symbiotic ability with the nematode the stationary phase induced sigma factor $\sigma^S$ was deleted from *Photorhabdus*. This Δ*rpoS* mutant was more sensitive to hydrogen peroxide stress but no deficiency was observed in pathogenicity or the ability of the mutant to support nematode growth and development and nematode colonisation. The production and release of reactive oxygen species (ROS) has been used by legume hosts to eliminate microbes which are not part of the symbiotic partnership (Tavares *et al.*, 2007). The data obtained in this study suggests that *H. bacteriophora* nematodes do not exhibit this oxidative burst, otherwise it would have been expected that the *P. luminescens* TT01 Δ*rpoS* mutant would have been eliminated from the nematode gut due to its inability to resist oxidative stress. Interestingly, although no role could be identified for $\sigma^S$ during the pathogenicity or symbiosis assays within the laboratory, it is possible that in the environment the Δ*rpoS* mutant would not be successful. The mutant

would have to survive extended periods of stationary phase in the nematode gut and would probably be exposed to nutrient limitation and temperature flux. Further investigation of IJ nematodes colonised with the Δ*rpoS* mutant may indeed reveal a role for *rpoS* in *Photorhabdus*. During the course of this study, mutant BMM429 was identified which showed an inability to colonise nematodes. This mutant was constructed as a directed deletion of the *rpoS* gene, however restoration of the *rpoS* gene into its native position could not restore the colonisation defect. The mutant appeared to be indistinguishable from the primary variant wild type, which suggests that an unknown genetic locus has been affected for its ability to colonise the nematode gut and further characterisation of this mutant is required. Complementation of BMM429 with the TT01 cosmid library may allow the identification of the locus responsible for the colonisation defect.

This study set out to identify the role of iron within the pathogenic and symbiotic interactions of *Photorhabdus*. To that end it has been successful in identifying the *exbD* gene as important for both interactions in K122 and for pathogenicity in TT01. Moreover several iron regulated proteins have been identified that were overproduced by the presence of DIP. Some of these proteins were also identified in a previous study and are likely to be involved in the control of nematode symbiosis. Interestingly the two closely related nematode species studied showed different sensitivities to the *Photorhabdus exbD* mutation which suggests that the nematodes have evolved differently and that iron may be an important nutritional signal in *H. downesi*. In addition this study has shown that the stationary phase sigma factor, $\sigma^S$, is not involved in the control of symbiosis with the nematode suggesting that there is another, $\sigma^S$-independent regulon in the post-exponential phase of *Photorhabdus* that is required for the interaction with the nematode.

## Bibliography

Akhurst, R.J., Boemare, N.E., Janssen, P.H., Peel, M.M., Alfredson, D.A., and Beard, C.E. (2004) Taxonomy of Australian clinical isolates of the genus *Photorhabdus* and proposal of *Photorhabdus asymbiotica* subsp. *asymbiotica* subsp. *nov.* and *P. asymbiotica* subsp. australis subsp. nov. *Int J Syst Evol Microbiol* **54**: 1301-1310.

Andrews, S.C. (1998) Iron storage in bacteria. *Adv Microb Physiol* **40**: 281-351.

Andrews, S.C., Robinson, A.K., and Rodriguez-Quinones, F. (2003) Bacterial iron homeostasis. *FEMS Microbiol Rev* **27**: 215-237.

Ashton, F.T., Zhu, X.D., Lok, J.B., and Schad, G.A. (2007) *Strongyloides stercoralis*: Amphidial neuron pair ASJ triggers significant resumption of development by infective larvae under host-mimicking *in vitro* conditions. *Exp Parasitol* **115**: 92-97.

Aumann, J., and Ehlers, R.U. (2001) Physico-chemical properties and mode of action of a signal from the symbiotic bacterium *Photorhabdus luminescens* inducing dauer juvenile recovery in the entomopathogenic nematode *Heterorhabditis bacteriophora*. *Nematology* **3**: 849-853.

Bagg, A., and Neilands, J.B. (1987) Molecular mechanism of regulation of siderophore-mediated iron assimilation. *Microbiol Rev* **51**: 509-518.

Baichoo, N., Wang, T., Ye, R., and Helmann, J.D. (2002) Global analysis of the *Bacillus subtilis* Fur regulon and the iron starvation stimulon. *Mol Microbiol* **45**: 1613-1629.

Bao, Y., Lies, D.P., Fu, H., and Roberts, G.P. (1991) An improved Tn7-based system for the single-copy insertion of cloned genes into chromosomes of Gram-negative bacteria. *Gene* **109**: 167-168.

Bargmann, C.I., and Horvitz, H.R. (1991) Control of larval development by chemosensory neurons in *Caenorhabditis elegans*. *Science* **251**: 1243-1246.

Barnard, T.J., Watson, M.E., Jr., and McIntosh, M.A. (2001) Mutations in the *Escherichia coli* receptor FepA reveal residues involved in ligand binding and transport. *Mol Microbiol* **41**: 527-536.

Bearden, S.W., Fetherston, J.D., and Perry, R.D. (1997) Genetic organization of the yersiniabactin biosynthetic region and construction of avirulent mutants in *Yersinia pestis*. *Infect Immun* **65**: 1659-1668.

Bearden, S.W., Staggs, T.M., and Perry, R.D. (1998) An ABC transporter system of *Yersinia pestis* allows utilization of chelated iron by *Escherichia coli* SAB11. *J Bacteriol* **180**: 1135-1147.

Bearden, S.W., and Perry, R.D. (1999) The Yfe system of *Yersinia pestis* transports iron and manganese and is required for full virulence of plague. *Mol Microbiol* **32**: 403-414.

Beddek, A.J., Sheehan, B.J., Bosse, J.T., Rycroft, A.N., Kroll, J.S., and Langford, P.R. (2004) Two TonB systems in *Actinobacillus pleuropneumoniae*: their roles in iron acquisition and virulence. *Infect Immun* **72**: 701-708.

Bennett, H.P., and Clarke, D.J. (2005) The *pbgPE* operon in *Photorhabdus luminescens* is required for pathogenicity and symbiosis. *J Bacteriol* **187**: 77-84.

Bintrim, S.B., and Ensign, J.C. (1998) Insertional inactivation of genes encoding the crystalline inclusion proteins of *Photorhabdus luminescens* results in mutants with pleiotropic phenotypes. *J Bacteriol* **180**: 1261-1269.

Blackburn, M., Golubeva, E., Bowen, D., and ffrench-Constant, R.H. (1998) A novel insecticidal toxin from *Photorhabdus luminescens*, toxin complex a (Tca), and its histopathological effects on the midgut of *Manduca sexta*. *Appl Environ Microbiol* **64**: 3036-3041.

Blanvillain, S., Meyer, D., Boulanger, A., Lautier, M., Guynet, C., Denance, N., Vasse, J., Lauber, E., and Arlat, M. (2007) Plant carbohydrate scavenging through TonB-dependent receptors: A feature shared by phytopathogenic and aquatic bacteria. *PLoS ONE* **2**: e224.

Bleakley, B., and Nealson, K.H. (1988) Characterization of primary and secondary forms of *Xenorhabdus luminescens* strain Hm. *FEMS Microbiol Ecol* **53**: 241-249.

Boemare, N.E., and Akhurst, R.J. (1988) Biochemical and physiological characterization of colony form variants in *Xenorhabdus* spp. (*Enterobacteriaceae*). *J Gen Microbiol* **134**: 751-761.

Bonnah, R.A., and Schryvers, A.B. (1998) Preparation and characterization of *Neisseria meningitidis* mutants deficient in production of the human lactoferrin-binding proteins LbpA and LbpB. *J Bacteriol* **180**: 3080-3090.

Bosch, M., Garrido, E., Llagostera, M., Perez de Rozas, A.M., Badiola, I., and Barbe, J. (2002) *Pasteurella multocida exbB*, *exbD* and *tonB* genes are physically linked but independently transcribed. *FEMS Microbiol Lett* **210**: 201-208.

Bou-Abdallah, F., Lewin, A.C., Le Brun, N.E., Moore, G.R., and Chasteen, N.D. (2002) Iron detoxification properties of *Escherichia coli* bacterioferritin. Attenuation of oxyradical chemistry. *J Biol Chem* **277**: 37064-37069.

Bowen, D.J., and Ensign, J.C. (2001) Isolation and characterization of intracellular protein inclusions produced by the entomopathogenic bacterium *Photorhabdus luminescens*. *Appl Environ Microbiol* **67**: 4834-4841.

Bowen, D.J., Rocheleau, T.A., Grutzmacher, C.K., Meslet, L., Valens, M., Marble, D., Dowling, A., ffrench-Constant, R., and Blight, M.A. (2003) Genetic and biochemical characterization of PrtA, an RTX-like metalloprotease from *Photorhabdus*. *Microbiology* **149**: 1581-1591.

Boyer, E., Bergevin, I., Malo, D., Gros, P., and Cellier, M.F. (2002) Acquisition of Mn(II) in addition to Fe(II) is required for full virulence of *Salmonella enterica* serovar Typhimurium. *Infect Immun* **70**: 6032-6042.

Braun, V., and Herrmann, C. (1993) Evolutionary relationship of uptake systems for biopolymers in *Escherichia coli*: cross-complementation between the TonB-ExbB-ExbD and the TolA-TolQ-TolR proteins. *Mol Microbiol* **8**: 261-268.

Braun, V., Braun, M., and Killmann, H. (2004) *Ferrichrome- and citrate-mediated iron transport. In: Crosa, J.H. et al (ed) Iron transport in Bacteria. p158-184.* Washington D.C.: ASM Press.

Brillard, J., Duchaud, E., Boemare, N., Kunst, F., and Givaudan, A. (2002) The PhlA hemolysin from the entomopathogenic bacterium *Photorhabdus luminescens* belongs to the two-partner secretion family of hemolysins. *J Bacteriol* **184**: 3871-3878.

Brown, S.E., Cao, A.T., Dobson, P., Hines, E.R., Akhurst, R.J., and East, P.D. (2006) Txp40, a ubiquitous insecticidal toxin protein from *Xenorhabdus* and *Photorhabdus* bacteria. *Appl Environ Microbiol* **72**: 1653-1662.

Brugirard-Ricaud, K., Duchaud, E., Givaudan, A., Girard, P.A., Kunst, F., Boemare, N., Brehelin, M., and Zumbihl, R. (2005) Site-specific antiphagocytic function of the *Photorhabdus luminescens* type III secretion system during insect colonization. *Cell Microbiol* **7**: 363-371.

Buchanan, S.K., Smith, B.S., Venkatramani, L., Xia, D., Esser, L., Palnitkar, M., Chakraborty, R., van der Helm, D., and Deisenhofer, J. (1999) Crystal structure of the outer membrane active transporter FepA from *Escherichia coli*. *Nat Struct Biol* **6**: 56-63.

Buell, C.R., Joardar, V., Lindeberg, M., Selengut, J., Paulsen, I.T., Gwinn, M.L., Dodson, R.J., Deboy, R.T., Durkin, A.S., Kolonay, J.F., Madupu, R., Daugherty, S., Brinkac, L., Beanan, M.J., Haft, D.H., Nelson, W.C., Davidsen, T., Zafar, N., Zhou, L., Liu, J., Yuan, Q., Khouri, H., Fedorova, N., Tran, B., Russell, D., Berry, K., Utterback, T., Van Aken, S.E., Feldblyum, T.V., D'Ascenzo, M., Deng, W.L., Ramos, A.R., Alfano, J.R., Cartinhour, S., Chatterjee, A.K., Delaney, T.P., Lazarowitz, S.G., Martin, G.B., Schneider, D.J., Tang, X., Bender, C.L., White, O., Fraser, C.M., and Collmer, A. (2003) The complete genome sequence of the *Arabidopsis* and tomato pathogen *Pseudomonas syringae* pv. tomato DC3000. *Proc Natl Acad Sci U S A* **100**: 10181-10186.

Buysens, S., Huengens, K., Poppe, J., and Hofte, M. (1996) Involvement of pyochelin and pyoverdin in suppression of *Pythium*-induced damping-off of tomato by *Pseudomonas aeruginosa* 7NSK2. *Appl Environ Microbiol* **62**: 865-871.

Cadieux, N., Bradbeer, C., and Kadner, R.J. (2000) Sequence changes in the Ton box region of BtuB affect its transport activities and interaction with TonB protein. *J Bacteriol* **182**: 5954-5961.

Cartron, M.L., Maddocks, S., Gillingham, P., Craven, C.J., and Andrews, S.C. (2006) Feo-transport of ferrous iron into bacteria. *Biometals* **19**: 143-157.

Cascales, E., Buchanan, S.K., Duche, D., Kleanthous, C., Lloubes, R., Postle, K., Riley, M., Slatin, S., and Cavard, D. (2007) Colicin biology. *Microbiol Molec Biol Rev* **71**: 158-229.

Chen, C.Y., Buchmeier, N.A., Libby, S., Fang, F.C., Krause, M., and Guiney, D.G. (1995) Central regulatory role for the RpoS sigma-factor in expression of *Salmonella dublin* plasmid virulence genes. *J Bacteriol* **177**: 5303-5309.

Chin, N., Frey, J., Chang, C.F., and Chang, Y.F. (1996) Identification of a locus involved in the utilization of iron by *Actinobacillus pleuropneumoniae. FEMS Microbiol Lett* **143**: 1-6.

Chipperfield, J.R., and Ratledge, C. (2000) Salicylic acid is not a bacterial siderophore: a theoretical study. *Biometals* **13**: 165-168.

Ciche, T.A., Bintrim, S.B., Horswill, A.R., and Ensign, J.C. (2001) A phosphopantetheinyl transferase homolog is essential for *Photorhabdus luminescens* to support growth and reproduction of the entomopathogenic nematode *Heterorhabditis bacteriophora. J Bacteriol* **183**: 3117-3126.

Ciche, T.A., Blackburn, M., Carney, J.R., and Ensign, J.C. (2003) Photobactin: a catechol siderophore produced by *Photorhabdus luminescens*, an entomopathogen mutually associated with *Heterorhabditis bacteriophora* NC1 nematodes. *Appl Environ Microbiol* **69**: 4706-4713.

Ciche, T.A., and Ensign, J.C. (2003) For the insect pathogen *Photorhabdus luminescens*, which end of a nematode is out? *Appl Environ Microbiol* **69**: 1890-1897.

Clarke, D., J. (1993) An investigation into cold activity in the insect pathogenic bacterium *Xenorhabdus luminescens* PhD thesis.: National University of Ireland, Maynooth.

Clarke, D.J., and Dowds, B.C.A. (1995) Virulence mechanisms of *Photorhabdus* sp strain K122 toward Wax Moth larvae. *J Invert Pathol* **66**: 149-155.

Clarke, T.E., Tari, L.W., and Vogel, H.J. (2001) Structural biology of bacterial iron uptake systems. *Curr Top Med Chem* **1**: 7-30.

Cobessi, D., Celia, H., and Pattus, F. (2005) Crystal structure at high resolution of ferric-pyochelin and its membrane receptor FptA from *Pseudomonas aeruginosa. J Mol Biol* **352**: 893-904.

Cornelissen, C.N., Kelley, M., Hobbs, M.M., Anderson, J.E., Cannon, J.G., Cohen, M.S., and Sparling, P.F. (1998) The transferrin receptor expressed by gonococcal strain FA1090 is required for the experimental infection of human male volunteers. *Mol Microbiol* **27**: 611-616.

Coynault, C., and Norel, F. (1999) Comparison of the abilities of *Salmonella typhimurium rpoS, aroA and rpoS aroA* strains to elicit humoral immune responses in BALB c mice and to cause lethal infection in athymic BALB c mice. *Microb Path* **26**: 299-305.

Crennell, S.J., Tickler, P.M., Bowen, D.J., and ffrench-Constant, R.H. (2000) The predicted structure of photopexin from *Photorhabdus* shows the first haemopexin-like motif in prokaryotes. *FEMS Microbiol Lett* **191**: 139-144.

Crosa, J.H. (1997) Signal transduction and transcriptional and posttranscriptional control of iron-regulated genes in bacteria. *Microbiol Mol Biol Rev* **61**: 319-336.

Daborn, P.J., Waterfield, N., Blight, M.A., and ffrench-Constant, R.H. (2001) Measuring virulence factor expression by the pathogenic bacterium *Photorhabdus luminescens* in culture and during insect infection. *J Bacteriol* **183**: 5834-5839.

Daborn, P.J., Waterfield, N., Silva, C.P., Au, C.P., Sharma, S., and ffrench-Constant, R.H. (2002) A single *Photorhabdus* gene, makes caterpillars floppy (mcf), allows *Escherichia coli* to persist within and kill insects. *Proc Natl Acad Sci U S A* **99**: 10742-10747.

Davies, B.W., and Walker, G.C. (2007) Disruption of *sitA* compromises *Sinorhizobium meliloti* for manganese uptake required for protection against oxidative stress. *J Bacteriol* **189**: 2101-2109.

de Lorenzo, V., Perez-Martin, J., Escolar, L., Pesole, G., and Bertoni, G. (2004) *Mode of binding of the Fur protein to target DNA: Negative regulation if iron-controlled gene expression In: Crosa, J.H. et al (ed) Iron transport in Bacteria. p185-196.* Washington D.C.: ASM Press.

DeRocco, A.J., and Cornelissen, C.N. (2007) Identification of transferrin-binding domains in TbpB expressed by *Neisseria gonorrhoeae. Infect Immun* **75**: 3220-3232.

Derzelle, S., Ngo, S., Turlin, E., Duchaud, E., Namane, A., Kunst, F., Danchin, A., Bertin, P., and Charles, J.F. (2004a) AstR-AstS, a new two-component signal transduction system, mediates swarming, adaptation to stationary phase and phenotypic variation in *Photorhabdus luminescens*. *Microbiology* **150**: 897-910.

Derzelle, S., Turlin, E., Duchaud, E., Pages, S., Kunst, F., Givaudan, A., and Danchin, A. (2004b) The PhoP-PhoQ two-component regulatory system of *Photorhabdus luminescens* is essential for virulence in insects. *J Bacteriol* **186**: 1270-1279.

Dowling, A.J., Daborn, P.J., Waterfield, N.R., Wang, P., Streuli, C.H., and ffrench-Constant, R.H. (2004) The insecticidal toxin Makes caterpillars floppy (Mcf) promotes apoptosis in mammalian cells. *Cell Microbiol* **6**: 345-353.

Dowling, A.J., Waterfield, N.R., Hares, M.C., Le Goff, G., Streuli, C.H., and ffrench-Constant, R.H. (2007) The Mcf1 toxin induces apoptosis via the mitochondrial pathway and apoptosis is attenuated by mutation of the BH3-like domain. *Cell Microbiol* **9**: 2470-2484.

Duchaud, E., Rusniok, C., Frangeul, L., Buchrieser, C., Givaudan, A., Taourit, S., Bocs, S., Boursaux-Eude, C., Chandler, M., Charles, J.F., Dassa, E., Derose, R., Derzelle, S., Freyssinet, G., Gaudriault, S., Medigue, C., Lanois, A., Powell, K., Siguier, P., Vincent, R., Wingate, V., Zouine, M., Glaser, P., Boemare, N., Danchin, A., and Kunst, F. (2003) The genome sequence of the entomopathogenic bacterium *Photorhabdus luminescens*. *Nat Biotechnol* **21**: 1307-1313.

Eleftherianos, I., Millichap, P.J., ffrench-Constant, R.H., and Reynolds, S.E. (2006) RNAi suppression of recognition protein mediated immune responses in the tobacco hornworm *Manduca sexta* causes increased susceptibility to the insect pathogen *Photorhabdus*. *Dev Comp Immunol* **30**: 1099-1107.

Eleftherianos, I., Boundy, S., Joyce, S.A., Aslam, S., Marshall, J.W., Cox, R.J., Simpson, T.J., Clarke, D.J., ffrench-Constant, R.H., and Reynolds, S.E. (2007) An antibiotic produced by an insect-pathogenic bacterium suppresses host defenses through phenoloxidase inhibition. *Proc Natl Acad Sci U S A* **104**: 2419-2424.

Escolar, L., Perez-Martin, J., and De Lorenzo, V. (1999) Opening the iron box: Transcriptional metalloregulation by the Fur protein. *J Bacteriol* **181**: 6223-6229.

Farmer, J.J., 3rd, Jorgensen, J.H., Grimont, P.A., Akhurst, R.J., Poinar, G.O., Jr., Ageron, E., Pierce, G.V., Smith, J.A., Carter, G.P., Wilson, K.L., and et al. (1989) *Xenorhabdus luminescens* (DNA hybridization group 5) from human clinical specimens. *J Clin Microbiol* **27**: 1594-1600.

Ferguson, A.D., Hofmann, E., Coulton, J.W., Diederichs, K., and Welte, W. (1998) Siderophore-mediated iron transport: crystal structure of FhuA with bound lipopolysaccharide. *Science* **282**: 2215-2220.

Ferguson, A.D., Chakraborty, R., Smith, B.S., Esser, L., van der Helm, D., and Deisenhofer, J. (2002) Structural basis of gating by the outer membrane transporter FecA. *Science* **295**: 1715-1719.

Ferrieres, L., Francez-Charlot, A., Gouzy, J., Rouille, S., and Kahn, D. (2004) FixJ-regulated genes evolved through promoter duplication in *Sinorhizobium meliloti*. *Microbiology* **150**: 2335-2345.

ffrench-Constant, R., Waterfield, N., Daborn, P., Joyce, S., Bennett, H., Au, C., Dowling, A., Boundy, S., Reynolds, S., and Clarke, D. (2003) *Photorhabdus*: towards a functional genomic analysis of a symbiont and pathogen. *FEMS Microbiol Rev* **26**: 433-456.

Fischbach, M.A., Lin, H., Liu, D.R., and Walsh, C.T. (2006) How pathogenic bacteria evade mammalian sabotage in the battle for iron. *Nat Chem Biol* **2**: 132-138.

Fischer-Le Saux, M., Viallard, V., Brunel, B., Normand, P., and Boemare, N.E. (1999) Polyphasic classification of the genus *Photorhabdus* and proposal of new taxa: *P. luminescens* subsp. luminescens subsp. nov., *P. luminescens* subsp. akhurstii subsp. nov., *P. luminescens* subsp. laumondii subsp. nov., *P. temperata* sp. nov., *P. temperata* subsp. temperata subsp. nov. and *P. asymbiotica* sp. nov. *Int J Syst Bacteriol* **49 Pt 4**: 1645-1656.

Gaudriault, S., Duchaud, E., Lanois, A., Canoy, A.S., Bourot, S., Derose, R., Kunst, F., Boemare, N., and Givaudan, A. (2006) Whole-genome comparison between *Photorhabdus* strains to identify genomic regions involved in the specificity of nematode interaction. *J Bacteriol* **188**: 809-814.

Gehring, A.M., Bradley, K.A., and Walsh, C.T. (1997) Enterobactin biosynthesis in *Escherichia coli*: isochorismate lyase (EntB) is a bifunctional enzyme

that is phosphopantetheinylated by EntD and then acylated by EntE using ATP and 2,3-dihydroxybenzoate. *Biochemistry* **36**: 8495-8503.

Gerrard, J., Waterfield, N., Vohra, R., and ffrench-Constant, R. (2004) Human infection with *Photorhabdus asymbiotica*: an emerging bacterial pathogen. *Microbes Infect* **6**: 229-237.

Gerrard, J.G., Joyce, S.A., Clarke, D.J., ffrench-Constant, R.H., Nimmo, G.R., Looke, D.F.M., Feil, E.J., Pearce, L., and Waterfield, N.R. (2006) Nematode symbiont for *Photorhabdus asymbiotica*. *Emerg Infect Dis* **12**: 1562-1564.

Gerritsen, L.J.M., and Smits, P.H. (1997) The influence of *Photorhabdus luminescens* strains and form variants on the reproduction and bacterial retention of *Heterorhabditis megidis*. *Fund Appl Nemat* **20**: 317-322.

Gerritsen, L.J.M., Wiegers, G.L., and Smits, P.H. (1998) Pathogenicity of new combinations of *Heterorhabditis* spp. and *Photorhabdus luminescens* against *Galleria mellonella* and *Tipula oleracea*. *Bio Cont* **13**: 9-15.

Giddens, S.R., Tormo, A., and Mahanty, H.K. (2000) Expression of the antifeeding gene *anfA1* in *Serratia entomophila* requires *rpoS*. *Appl Environ Microbiol* **66**: 1711-1714.

GonzalezFlecha, B., and Demple, B. (1997) Homeostatic regulation of intracellular hydrogen peroxide concentration in aerobically growing *Escherichia coli*. *J Bacteriol* **179**: 382-388.

Goodrich-Blair, H., and Clarke, D.J. (2007) Mutualism and pathogenesis in *Xenorhabdus* and *Photorhabdus*: two roads to the same destination. *Mol Microbiol* **64**: 260-268.

Graf, J., and Ruby, E.G. (2000) Novel effects of a transposon insertion in the *Vibrio fischeri glnD* gene: defects in iron uptake and symbiotic persistence in addition to nitrogen utilization. *Mol Microbiol* **37**: 168-179.

Grass, G. (2006) Iron transport in *Escherichia coli*: all has not been said and done. *Biometals* **19**: 159-172.

Griffiths, E. (1999) *Iron and Infection: Molecular, Physiological and Clinical Aspects*: Wiley Press.

Gudmundsdottir, A., Bell, P.E., Lundrigan, M.D., Bradbeer, C., and Kadner, R.J. (1989) Point mutations in a conserved region (TonB box) of *Escherichia*

*coli* outer membrane protein BtuB affect vitamin $B_{12}$ transport. *J Bacteriol* **171**: 6526-6533.

Gulig, P.A., Danbara, H., Guiney, D.G., Lax, A.J., Norel, F., and Rhen, M. (1993) Molecular analysis of *spv* virulence genes of the *Salmonella virulence* plasmids. *Mol Microbiol* **7**: 825-830.

Gumbart, J., Wiener, M.C., and Tajkhorshid, E. (2007) Mechanics of force propagation in TonB-dependent outer membrane transport. *Biophys J* **93**: 496-504.

Guzman, L.M., Belin, D., Carson, M.J., and Beckwith, J. (1995) Tight regulation, modulation, and high-level expression by vectors containing the arabinose pBAD promoter. *J Bacteriol* **177**: 4121-4130.

Hallem, E.A., Rengarajan, M., Ciche, T.A., and Sternberg, P.W. (2007) Nematodes, bacteria, and flies: A tripartite model for nematode parasitism. *Curr Biol* **17**: 898-904.

Han, R., and Ehlers, R.U. (2000) Pathogenicity, development, and reproduction of *Heterorhabditis bacteriophora* and *Steinernema carpocapsae* under axenic *in vivo* conditions. *J Invertebr Pathol* **75**: 55-58.

Han, R.C., and Ehlers, R.U. (1998) Cultivation of axenic *Heterorhabditis* spp. dauer juveniles and their response to non-specific *Photorhabdus luminescens* food signals. *Nematologica* **44**: 425-435.

Hantke, K. (1987) Selection procedure for deregulated iron transport mutants (fur) in *Escherichia coli* K12: fur not only affects iron metabolism. *Mol Gen Genet* **210**: 135-139.

Heller, K.J., Kadner, R.J., and Gunther, K. (1988) Suppression of the btuB451 mutation by mutations in the *tonB* gene suggests a direct interaction between TonB and TonB-dependent receptor proteins in the outer membrane of *Escherichia coli*. *Gene* **64**: 147-153.

Hengge-Aronis, R. (2002) Signal transduction and regulatory mechanisms involved in control of the sigma(S) (RpoS) subunit of RNA polymerase. *Microbiol Mol Biol Rev* **66**: 373-395.

Herrero, M., de Lorenzo, V., and Timmis, K.N. (1990) Transposon vectors containing non-antibiotic resistance selection markers for cloning and stable chromosomal insertion of foreign genes in Gram-negative bacteria. *J Bacteriol* **172**: 6557-6567.

Higgs, P.I., Larsen, R.A., and Postle, K. (2002) Quantification of known components of the *Escherichia coli* TonB energy transduction system: TonB, ExbB, ExbD and FepA. *Mol Microbiol* **44**: 271-281.

Hufton, S.E., Ward, R.J., Bunce, N.A., Armstrong, J.T., Fletcher, A.J., and Glass, R.E. (1995) Structure-function analysis of the vitamin $B_{12}$ receptor of *Escherichia coli* by means of informational suppression. *Mol Microbiol* **15**: 381-393.

Imler, J.L., and Bulet, P. (2005) Antimicrobial peptides in *Drosophila*: structures, activities and gene regulation. *Chem Immunol Allergy* **86**: 1-21.

Ishihama, A. (2000) Functional modulation of *Escherichia coli* RNA polymerase. *Annu Rev Microbiol* **54**: 499-518.

Jakubovics, N.S., and Jenkinson, H.F. (2001) Out of the iron age: new insights into the critical role of manganese homeostasis in bacteria. *Microbiology* **147**: 1709-1718.

Janakiraman, A., and Slauch, J.M. (2000) The putative iron transport system SitABCD encoded on SPI1 is required for full virulence of *Salmonella typhimurium*. *Mol Microbiol* **35**: 1146-1155.

Jarosik, G.P., Sanders, J.D., Cope, L.D., Muller-Eberhard, U., and Hansen, E.J. (1994) A functional *tonB* gene is required for both utilization of haem and virulence expression by *Haemophilus influenzae* type b. *Infect Immun* **62**: 2470-2477.

Joyce, S.A., and Clarke, D.J. (2003) A *hexA* homologue from *Photorhabdus* regulates pathogenicity, symbiosis and phenotypic variation. *Mol Microbiol* **47**: 1445-1457.

Joyce, S.A., Watson, R.J., and Clarke, D.J. (2006) The regulation of pathogenicity and mutualism in *Photorhabdus*. *Curr Opin Microbiol* **9**: 127-132.

Kadner, R.J., and Heller, K.J. (1995) Mutual inhibition of cobalamin and siderophore uptake systems suggests their competition for TonB function. *J Bacteriol* **177**: 4829-4835.

Kanost, M.R., Jiang, H.B., and Yu, X.Q. (2004) Innate immune responses of a lepidopteran insect, *Manduca sexta*. *Immun Rev* **198**: 97-105.

Koebnik, R. (2005) TonB-dependent trans-envelope signalling: the exception or the rule? *Trends Microbiol* **13**: 343-347.

Kohanski, M.A., Dwyer, D.J., Hayete, B., Lawrence, C.A., and Collins, J.J. (2007) A common mechanism of cellular death induced by bactericidal antibiotics. *Cell* **130**: 797-810.

Koster, W. (2001) ABC transporter-mediated uptake of iron, siderophores, haem and vitamin $B_{12}$. *Res Microbiol* **152**: 291-301.

Kowarz, L., Coynault, C., Robbesaule, V., and Norel, F. (1994) The *Salmonella typhimurium katF* (*rpoS*) gene - Cloning, nucleotide-sequence, and regulation of *spvR* and *spvABCD* virulence plasmid genes. *J Bacteriol* **176**: 6852-6860.

Krin, E., Chakroun, N., Turlin, E., Givaudan, A., Gaboriau, F., Bonne, I., Rousselle, J.C., Frangeul, L., Lacroix, C., Hullo, M.F., Marisa, L., Danchin, A., and Derzelle, S. (2006) Pleiotropic role of quorum-sensing autoinducer 2 in *Photorhabdus luminescens*. *Appl Environ Microbiol* **72**: 6439-6451.

Krogfelt, K.A., Hjulgaard, M., Sorensen, K., Cohen, P.S., and Givskov, M. (2000) *rpoS* gene function is a disadvantage for *Escherichia coli* BJ4 during competitive colonization of the mouse large intestine. *Infect Immun* **68**: 2518-2524.

Lacour, S., and Landini, P. (2004) SigmaS-dependent gene expression at the onset of stationary phase in *Escherichia coli*: function of sigmaS-dependent genes and identification of their promoter sequences. *J Bacteriol* **186**: 7186-7195.

Lamont, I.L., Beare, P.A., Ochsner, U., Vasil, A.I., and Vasil, M.L. (2002) Siderophore-mediated signaling regulates virulence factor production in *Pseudomonas aeruginosa*. *Proc Natl Acad Sci U S A* **99**: 7072-7077.

Lange, R., and Hengge-Aronis, R. (1994) The *nlpD* gene is located in an operon with *rpoS* on the *Escherichia coli* chromosome and encodes a novel lipoprotein with a potential function in cell wall formation. *Mol Microbiol* **13**: 733-743.

Lange, R., Fischer, D., and Hengge-Aronis, R. (1995) Identification of transcriptional start sites and the role of ppGpp in the expression of *rpoS*, the structural gene for the sigma S subunit of RNA polymerase in *Escherichia coli*. *J Bacteriol* **177**: 4676-4680.

Larsen, R.A., Letain, T.E., and Postle, K. (2003) *In vivo* evidence of TonB shuttling between the cytoplasmic and outer membrane in *Escherichia coli*. *Mol Microbiol* **49**: 211-218.

Lazdunski, C.J., Bouveret, E., Rigal, A., Journet, L., Lloubes, R., and Benedetti, H. (1998) Colicin import into *Escherichia coli* cells. *J Bacteriol* **180**: 4993-5002.

Lee, J.W., and Helmann, J.D. (2007) Functional specialization within the Fur family of metalloregulators. *Biometals* **20**: 485-499.

Lemaitre, B., and Hoffmann, J. (2007) The host defense of *Drosophila melanogaster*. *Annu Rev Immunol* **25**: 697-743.

Litwin, C.M., Rayback, T.W., and Skinner, J. (1996) Role of catechol siderophore synthesis in *Vibrio vulnificus* virulence. *Infect Immun* **64**: 2834-2838.

Locher, K.P., Rees, B., Koebnik, R., Mitschler, A., Moulinier, L., Rosenbusch, J.P., and Moras, D. (1998) Transmembrane signaling across the ligand-gated FhuA receptor: crystal structures of free and ferrichrome-bound states reveal allosteric changes. *Cell* **95**: 771-778.

Locke, M., and Nichol, H. (1992) Iron economy in insects - Transport, metabolism, and storage. *Ann Rev Entomol* **37**: 195-215.

Loprasert, S., Sallabhan, R., Whangsuk, W., and Mongkolsuk, S. (2000) Characterization and mutagenesis of *fur* gene from *Burkholderia pseudomallei*. *Gene* **254**: 129-137.

Maharjan, R., Seeto, S., Notley-McRobb, L., and Ferenci, T. (2006) Clonal adaptive radiation in a constant environment. *Science* **313**: 514-517.

Martens, E.C., Russell, F.M., and Goodrich-Blair, H. (2005) Analysis of *Xenorhabdus nematophila* metabolic mutants yields insight into stages of *Steinernema carpocapsae* nematode intestinal colonization. *Mol Microbiol* **58**: 28-45.

Martinez, E., and de la Cruz, F. (1988) Transposon Tn21 encodes a RecA-independent site-specific integration system. *Mol Gen Genet* **211**: 320-325.

Masse, E., and Gottesman, S. (2002) A small RNA regulates the expression of genes involved in iron metabolism in *Escherichia coli*. *Proc Natl Acad Sci U S A* **99**: 4620-4625.

Meyer, J.M., Neely, A., Stintzi, A., Georges, C., and Holder, I.A. (1996) Pyoverdin is essential for virulence of *Pseudomonas aeruginosa*. *Infect Immun* **64**: 518-523.

Nappi, A.J., and Ottaviani, E. (2000) Cytotoxicity and cytotoxic molecules in invertebrates. *Bioessays* **22**: 469-480.

Neilands, J.B. (1995) Siderophores: structure and function of microbial iron transport compounds. *J Biol Chem* **270**: 26723-26726.

Nickerson, C.A., and Curtiss, R. (1997) Role of sigma factor RpoS in initial stages of *Salmonella typhimurium* infection. *Infect Immun* **65**: 1814-1823.

Nikaido, H. (1994) Porins and specific diffusion channels in bacterial outer membranes. *J Biol Chem* **269**: 3905-3908.

O'Neill, K.H., Roche, D.M., Clarke, D.J., and Dowds, B.C. (2002) The *ner* gene of *Photorhabdus*: effects on primary-form-specific phenotypes and outer membrane protein composition. *J Bacteriol* **184**: 3096-3105.

Occhino, D.A., Wyckoff, E.E., Henderson, D.P., Wrona, T.J., and Payne, S.M. (1998) *Vibrio cholerae* iron transport: haem transport genes are linked to one of two sets of *tonB*, *exbB*, *exbD* genes. *Mol Microbiol* **29**: 1493-1507.

Pawelek, P.D., Croteau, N., Ng-Thow-Hing, C., Khursigara, C.M., Moiseeva, N., Allaire, M., and Coulton, J.W. (2006) Structure of TonB in complex with FhuA, *E.coli* outer membrane receptor. *Science* **312**: 1399-1402.

Payne, S.M. (1993) Iron acquisition in microbial pathogenesis. *Trends Microbiol* **1**: 66-69.

Pendrak, M.L., and Perry, R.D. (1993) Proteins essential for expression of the Hms+ phenotype of *Yersinia pestis*. *Mol Microbiol* **8**: 857-864.

Perkins-Balding, D., Ratliff-Griffin, M., and Stojiljkovic, I. (2004) Iron transport systems in *Neisseria meningitidis*. *Microbiol Mol Biol Rev* **68**: 154-171.

Perry, R.D., Pendrak, M.L., and Schuetze, P. (1990) Identification and cloning of a hemin storage locus involved in the pigmentation phenotype of *Yersinia pestis*. *J Bacteriol* **172**: 5929-5937.

Perry, R.D., Shah, J., Bearden, S.W., Thompson, J.M., and Fetherston, J.D. (2003) *Yersinia pestis* TonB: role in iron, haem, and hemoprotein utilization. *Infect Immun* **71**: 4159-4162.

Perry, R.D., Mier, I., Jr., and Fetherston, J.D. (2007) Roles of the Yfe and Feo transporters of *Yersinia pestis* in iron uptake and intracellular growth. *Biometals* **20**: 699-703.

Philippe, N., Alcaraz, J.P., Coursange, E., Geiselmann, J., and Schneider, D. (2004) Improvement of pCVD442, a suicide plasmid for gene allele exchange in bacteria. *Plasmid* **51**: 246-255.

Poinar, G.O., Thomas, G., Haygood, M., and Nealson, K.H. (1980) Growth and luminescence of the symbiotic bacteria associated with the terrestrial nematode, *Heterorhabditis bacteriophora*. *Soil Biol Biochem* **12**: 5-10.

Postle, K., and Kadner, R.J. (2003) Touch and go: tying TonB to transport. *Mol Microbiol* **49**: 869-882.

Postle, K., and Larsen, R.A. (2004) *The TonB, ExbB and ExbD proteins In: Crosa, J.H. et al (ed) Iron transport in Bacteria. p96-112.* Washington D.C.: ASM Press.

Postle, K., and Larsen, R.A. (2007) TonB-dependent energy transduction between outer and cytoplasmic membranes. *Biometals* **20**: 453-465.

Pradel, E., Guiso, N., Menozzi, F.D., and Locht, C. (2000) *Bordetella pertussis* TonB, a Bvg-independent virulence determinant. *Infect Immun* **68**: 1919-1927.

Rao, A.U., Carta, L.K., Lesuisse, E., and Hamza, I. (2005) Lack of haem synthesis in a free-living eukaryote. *Proc Natl Acad Sci U S A* **102**: 4270-4275.

Ratledge, C., and Dover, L.G. (2000) Iron metabolism in pathogenic bacteria. *Annu Rev Microbiol* **54**: 881-941.

Raymond, K.M., and Dertz, E.A. (2004) *Biochemical and physical properties of siderophores. In: Crosa, J.H. et al (ed) Iron transport in Bacteria. p3-37.* Washington D.C.: ASM Press.

Raymond, K.N., Dertz, E.A., and Kim, S.S. (2003) Enterobactin: an archetype for microbial iron transport. *Proc Natl Acad Sci U S A* **100**: 3584-3588.

Redford, P., and Welch, R.A. (2006) Role of sigma E-regulated genes in *Escherichia coli* uropathogenesis. *Infect Immun* **74**: 4030-4038.

Reeves, S.A., Torres, A.G., and Payne, S.M. (2000) TonB is required for intracellular growth and virulence of *Shigella dysenteriae*. *Infect Immun* **68**: 6329-6336.

Reichard, P. (1993) The anaerobic ribonucleotide reductase from *Escherichia coli*. *J Biol Chem* **268**: 8383-8386.

Runyen-Janecky, L., Dazenski, E., Hawkins, S., and Warner, L. (2006) Role and regulation of the *Shigella flexneri* Sit and MntH systems. *Infect Immun* **74**: 4666-4672.

Sabri, M., Leveille, S., and Dozois, C.M. (2006) A SitABCD homologue from an avian pathogenic *Escherichia coli* strain mediates transport of iron and manganese and resistance to hydrogen peroxide. *Microbiology* **152**: 745-758.

Sambrook, J.E., Fritsch, E.F., and Maniatis, T. (1989) *Molecular Cloning: A Laboratory Manual, 2nd ed.* Cold Spring Harbor N.Y.: Cold Spring Harbor Laboratory Press.

Schauer, K., Gouget, B., Carriere, M., Labigne, A., and de Reuse, H. (2007) Novel nickel transport mechanism across the bacterial outer membrane energized by the TonB/ExbB/ExbD machinery. *Mol Microbiol* **63**: 1054-1068.

Schroder, I., Johnson, E., and de Vries, S. (2003) Microbial ferric iron reductases. *FEMS Microbiol Rev* **27**: 427-447.

Schwyn, B., and Neilands, J.B. (1987) Universal chemical assay for the detection and determination of siderophores. *Anal Biochem* **160**: 47-56.

Seliger, S.S., Mey, A.R., Valle, A.M., and Payne, S.M. (2001) The two TonB systems of *Vibrio cholerae*: redundant and specific functions. *Mol Microbiol* **39**: 801-812.

Shultis, D.D., Purdy, M.D., Banchs, C.N., and Wiener, M.C. (2006) Outer membrane active transport: structure of the BtuB:TonB complex. *Science* **312**: 1396-1399.

Smigielski, A.J., Akhurst, R.J., and Boemare, N.E. (1994) Phase variation in *Xenorhabdus nematophilus* and *Photorhabdus luminescens*: Differences in respiratory activity and membrane energization. *Appl Environ Microbiol* **60**: 120-125.

Spencer, G., V. (2001) The role of siderophores in the pathogenicity and symbiosis of *Photorhabdus luminescens*. In *Biology and Biochemistry Final Year Report*: University of Bath.

Stepek, G., Buttle, D.J., Duce, I.R., and Behnke, J.M. (2006) Human gastrointestinal nematode infections: are new control methods required? *Int J Exp Path* **87**: 325-341.

Stock, S.P., Griffin, C.T., and Burnell, A.M. (2002) Morphological characterisation of three isolates of *Heterorhabditis poinar*, 1976 from the 'Irish group' (*Nematoda: Rhabditida: Heterorhabditidae*) and additional evidence supporting their recognition as a distinct species, *H. downesi* n.sp. *Syst Parasitol* **51**: 95-106.

Stojiljkovic, I., Cobeljic, M., and Hantke, K. (1993) *Escherichia coli* K-12 ferrous iron uptake mutants are impaired in their ability to colonize the mouse intestine. *FEMS Microbiol Lett* **108**: 111-115.

Stoltzfus, R.J. (2003) Iron deficiency: global prevalence and consequences. *Food Nutr Bull* **24**: S99-103.

Stork, M., Di Lorenzo, M., Mourino, S., Osorio, C.R., Lemos, M.L., and Crosa, J.H. (2004) Two *tonB* systems function in iron transport in *Vibrio anguillarum*, but only one is essential for virulence. *Infect Immun* **72**: 7326-7329.

Strauch, O., and Ehlers, R.U. (1998) Food signal production of *Photorhabdus luminescens* inducing the recovery of entomopathogenic nematodes *Heterorhabditis* spp. in liquid culture. *Appl Microbiol Biotech* **50**: 369-374.

Subsin, B., Thomas, M.S., Katzenmeier, G., Shaw, J.G., Tungpradabkul, S., and Kunakorn, M. (2003) Role of the stationary growth phase sigma factor RpoS of *Burkholderia pseudomallei* in response to physiological stress conditions. *J Bacteriol* **185**: 7008-7014.

Tavares, F., Santos, C.L., and Sellstedt, A. (2007) Reactive oxygen species in legume and actinorhizal nitrogen-fixing symbioses: the microsymbiont's responses to an unfriendly reception. *Physiol Planta* **130**: 344-356.

Torres, A.G., Redford, P., Welch, R.A., and Payne, S.M. (2001) TonB-dependent systems of uropathogenic *Escherichia coli*: aerobactin and haem transport and TonB are required for virulence in the mouse. *Infect Immun* **69**: 6179-6185.

Trousseau, A. (1872) *Lectures on clinical medicine, delivered at the Hôtel-Dieu, Paris.* London.

Tsolis, R.M., Baumler, A.J., Heffron, F., and Stojiljkovic, I. (1996) Contribution of TonB- and Feo-mediated iron uptake to growth of *Salmonella typhimurium* in the mouse. *Infect Immun* **64**: 4549-4556.

Turlin, E., Pascal, G., Rousselle, J.C., Lenormand, P., Ngo, S., Danchin, A., and Derzelle, S. (2006) Proteome analysis of the phenotypic variation process in *Photorhabdus luminescens*. *Proteomics* **6**: 2705-2725.

Vakharia-Rao, H., Kastead, K.A., Savenkova, M.I., Bulathsinghala, C.M., and Postle, K. (2007) Deletion and substitution analysis of the *Escherichia coli* TonB q160 region. *J Bacteriol* **189**: 4662-4670.

Valdebenito, M., Bister, B., Reissbrodt, R., Hantke, K., and Winkelmann, G. (2005) The detection of salmochelin and yersiniabactin in uropathogenic *Escherichia coli* strains by a novel hydrolysis-fluorescence-detection (HFD) method. *Int J Med Microbiol* **295**: 99-107.

Vasil, M.L. (2007) How we learnt about iron acquisition in *Pseudomonas aeruginosa*: a series of very fortunate events. *Biometals* **20**: 587-601.

Vivas, E.I., and Goodrich-Blair, H. (2001) *Xenorhabdus nematophilus* as a model for host-bacterium interactions: *rpoS* is necessary for mutualism with nematodes. *J Bacteriol* **183**: 4687-4693.

Walters, M., Sircili, M.P., and Sperandio, V. (2006) AI-3 synthesis is not dependent on *luxS* in *Escherichia coli*. *J Bacteriol* **188**: 5668-5681.

Wandersman, C., and Delepelaire, P. (2004) Bacterial iron sources: from siderophores to hemophores. *Annu Rev Microbiol* **58**: 611-647.

Waterfield, N., Dowling, A., Sharma, S., Daborn, P.J., Potter, U., and ffrench-Constant, R.H. (2001) Oral toxicity of *Photorhabdus luminescens* W14 toxin complexes in *Escherichia coli*. *Appl Environ Microbiol* **67**: 5017-5024.

Waterfield, N., Kamita, S.G., Hammock, B.D., and ffrench-Constant, R. (2005) The *Photorhabdus* Pir toxins are similar to a developmentally regulated insect protein but show no juvenile hormone esterase activity. *FEMS Microbiol Lett* **245**: 47-52.

Waterfield, N.R., Daborn, P.J., Dowling, A.J., Yang, G., Hares, M., and ffrench-Constant, R.H. (2003) The insecticidal toxin makes caterpillars floppy 2 (Mcf2) shows similarity to HrmA, an avirulence protein from a plant pathogen. *FEMS Microbiol Lett* **229**: 265-270.

Weber, H., Polen, T., Heuveling, J., Wendisch, V.F., and Hengge, R. (2005) Genome-wide analysis of the general stress response network in *Escherichia coli*: sigmaS-dependent genes, promoters, and sigma factor selectivity. *J Bacteriol* **187**: 1591-1603.

Weinberg, E.D. (1993) The development of awareness of iron-withholding defense. *Perspect Biol Med* **36**: 215-221.

Weissfeld, A.S., Halliday, R.J., Simmons, D.E., Trevino, E.A., Vance, P.H., O'Hara, C.M., Sowers, E.G., Kern, R., Koy, R.D., Hodde, K., Bing, M., Lo, C., Gerrard, J., Vohra, R., and Harper, J. (2005) *Photorhabdus asymbiotica*, a pathogen emerging on two continents that proves that there is no substitute for a well-trained clinical microbiologist. *J Clin Microbiol* **43**: 4152-4155.

Wexler, M., Yeoman, K.H., Stevens, J.B., de Luca, N.G., Sawers, G., and Johnston, A.W. (2001) The *Rhizobium leguminosarum tonB* gene is required for the uptake of siderophore and haem as sources of iron. *Mol Microbiol* **41**: 801-816.

White, G.F. (1927) A method for obtaining infective nematode larvae from cultures. *Science* **66**: 302-303.

Wilson, K. (1992) *Preparation of genomic DNA from bacteria, p.2-10 - 2-12. In: Ausubel, F.M., Brent, R., Kingston, R.E., Moore, D.D., Seidman, J.G., Smith, J. A., Struhl, K. (ed.) Short protocols in molecular biology, 2nd ed.*: John Wiley & Sons, New York.

Wirth, C., Meyer-Klaucke, W., Pattus, F., and Cobessi, D. (2007) From the periplasmic signaling domain to the extracellular face of an outer membrane signal transducer of *Pseudomonas aeruginosa*: crystal structure of the ferric pyoverdine outer membrane receptor. *J Mol Biol* **368**: 398-406.

Wong, E.F., Brar, S.K., Sesaki, H., Yang, C., and Siu, C.H. (1996) Molecular cloning and characterization of DdCAD-1, a Ca2+-dependent cell-cell adhesion molecule, in *Dictyostelium discoideum*. *J Biol Chem* **271**: 16399-16408.

Wosten, M.M. (1998) Eubacterial sigma-factors. *FEMS Microbiol Rev* **22**: 127-150.

Xu, J., and Hurlbert, R.E. (1990) Toxicity of irradiated media for *Xenorhabdus* spp. *Appl Environ Microbiol* **56**: 815-818.

Yeowell, H.N., and White, J.R. (1982) Iron requirement in the bactericidal mechanism of streptonigrin. *Antimicrob Agents Chemother* **22**: 961-968.

Yildiz, F.H., and Schoolnik, G.K. (1998) Role of *rpoS* in stress survival and virulence of *Vibrio cholerae*. *J Bacteriol* **180**: 773-784.

You, J., Liang, S., Cao, L., Liu, X., and Han, R. (2006) Nutritive significance of crystalline inclusion proteins of *Photorhabdus luminescens* in *Steinernema nematodes*. *FEMS Microbiol Ecol* **55**: 178-185.

Yue, W.W., Grizot, S., and Buchanan, S.K. (2003) Structural evidence for iron-free citrate and ferric citrate binding to the TonB-dependent outer membrane transporter FecA. *J Mol Biol* **332**: 353-368.

Zahran, H.H. (1999) *Rhizobium*-legume symbiosis and nitrogen fixation under severe conditions and in an arid climate. *Microbiol Mol Biol Rev* **63**: 968-989, table of contents.

Zhai, Y.F., Heijne, W., and Saier, M.H., Jr. (2003) Molecular modeling of the bacterial outer membrane receptor energizer, ExbBD/TonB, based on homology with the flagellar motor, MotAB. *Biochim Biophys Acta* **1614**: 201-210.

Zhao, G., Ceci, P., Ilari, A., Giangiacomo, L., Laue, T.M., Chiancone, E., and Chasteen, N.D. (2002) Iron and hydrogen peroxide detoxification properties of DNA-binding protein from starved cells. A ferritin-like DNA-binding protein of *Escherichia coli*. *J Biol Chem* **277**: 27689-27696.

Zhao, Q., and Poole, K. (2000) A second *tonB* gene in *Pseudomonas aeruginosa* is linked to the *exbB* and *exbD* genes. *FEMS Microbiol Lett* **184**: 127-132.

Zhou, D., Qin, L., Han, Y., Qiu, J., Chen, Z., Li, B., Song, Y., Wang, J., Guo, Z., Zhai, J., Du, Z., Wang, X., and Yang, R. (2006) Global analysis of iron assimilation and *fur* regulation in *Yersinia pestis*. *FEMS Microbiol Lett* **258**: 9-17.

Zhu, W., Arceneaux, J.E., Beggs, M.L., Byers, B.R., Eisenach, K.D., and Lundrigan, M.D. (1998) Exochelin genes in *Mycobacterium smegmatis*: identification of an ABC transporter and two non-ribosomal peptide synthetase genes. *Mol Microbiol* **29**: 629-639.